UNIVERSITY OF OKLAHOMA

GRADUATE COLLEGE

HARNESSING METAL CARBENOIDS TO ASSEMBLE SPIROCYCLES AND GLYCANS

A DISSERTATION

SUBMITTED TO THE GRADUATE FACULTY

in partial fulfillment of the requirements for the

Degree of

DOCTOR OF PHILOSOPHY

By

ANAE I. BAIN
Norman, Oklahoma
2022

HARNESSING METAL CARBENOIDS TO ASSEMBLE SPIROCYCLES AND GLYCANS

A DISSERTATION APPROVED FOR THE
DEPARTMENT OF CHEMISTRY AND BIOCHEMISTRY

BY THE COMMITTEE CONSISTING OF

Dr. Indrajeet Sharma, Chair

Dr. Shanteri Singh

Dr. Si Wu

Dr. Steven P. Crossley

© Copyright by ANAE BAIN 2022
All Rights Reserved.

DEDICATION

I dedicate this dissertation to my mother, Anita Margie Bain. You have been my inspiration always.

ABSTRACT

Within the realm of drug discovery more intricate, rigid small molecules exhibit higher potencies as drug leads and candidates. This is because molecules with three-dimensional features such as stereochemistry and bond saturation have increased binding specificities, decreased toxicological liabilities, and favorable pharmacological properties. Natural products, due to their structural complexity, have historically established the blueprint for drug discovery, inspiring the cores or complete scaffolds for most pharmaceuticals available today. As a result, over 50% of available drugs are either natural products or their derivatives. While natural products have historically served as trailblazers for the pharmaceutical industry, in the past twenty years drug-discovery programs have de-emphasized natural products in favor of high-throughput screening of synthetic chemical libraries. This shift has been met with diminishing returns, as these changes have led to an average 'hit rate' of >0.001% for pharmaceutical screenings of synthetic chemical libraries. Resultantly, there has been a resurgence in the belief that natural product-based drug design is the most practical model for future drug discovery efforts. Therefore, there is a need for convergent methods to access complex cores to sustain these early discovery programs, as often trivial differences in substrates lead to vast differences in site-binding and drug efficacy.

There are several challenges associated with natural product-based drug design, however, the most glaring is the lack of low-cost, efficient methodologies to access privileged natural product-like cores. This dissertation addresses these issues with two primary foci: 1. The implementation of carbenoid-initiated reactions to form complex,

natural product-like cores in efficient transformations; and 2. the utilization of metal catalysts for highly specific transformations. While my preliminary studies feature precious metal catalysts, the continuation of my research features Earth-abundant catalysts.

These focuses have converged for the development of methodologies surrounding two small-molecule frameworks: spirocycles and carbohydrates. Through the implementation of metal-carbenoids, we have developed stereoselective protocols to access these privileged frameworks readily in tandem or cascade strategies. Cascade reactions are multiple synthetic transformations that can occur in a single reaction pot, thereby truncating long reaction sequences into a single step. These reactions reduce the number of overall steps necessary to synthesize the desired compound while facilitating the rapid generation of structural complexity from simple starting materials. Likewise, multiple reactions can be completed in a single flask, which negates the need for the isolation of intermediates, thereby reducing the total cost of synthesis. The work herein details cascade sequences that can be utilized to access both scaffolds.

ACKNOWLEDGMENTS

First, I wish to express my gratitude toward my family. My parents, John Bain and Anita Bain, your sacrifices and prayers have shaped me into the woman I am today. My sister, Summer-Mia Bain thank you for your daily affirmations and assurance. Thank you to my siblings, family, friends, and everyone who has shared this experience with me. I would not have been able to obtain these achievements without your love, encouragement, and support.

Secondly, I would like to thank the University of Oklahoma and the Department of Chemistry and Biochemistry for allowing me to pursue my doctoral studies. Most importantly my mentor and Ph.D. advisor, Dr. Inderjeet Sharma, thank you. You have shaped me into a scientist, and the wealth of knowledge I have gained from our conversations about science and life has shaped me as a scientist, and as an individual. You have always encouraged me throughout these five years and without your mentorship, I would not be where I am today.

I would like to thank the members of the Sharma Research Group –past and present who have guided and shaped me as a scientist. Specifically, I am indebted to my senior lab mates who mentored me –Dr. Arianne Hunter, Dr. Nicholas Massaro and Dr. Steven Schlitzer. Additionally, I thank the junior students (Adam Alder, Randell Welles) and post-doctoral researchers (Dr. Bidhan Ghosh, Dr. Prashant Mandal Dr. Kiran Chinthapally, Dr. Dhanarajan 'Arun' Arunprasah) for their guidance, commandry, and conversation. I would also like to thank the members of my graduate committee, Dr. Shanteri Singh, Dr. Sisi Wu and Dr. Steven Crossley. Additionally, I would like to thank my former committee members Dr. Adam Duerfeldt and Dr. George Richter-Addo.

Lastly, I would like to thank my undergraduate professors, Dr. Patricia Stan, Dr. Dan Hammond, and Dr. Daniel King. Thank you for facilitating my love of chemistry and inquisitiveness.

LIST OF FIGURES

Chapter 1: *Bioactive Motifs in Drug Discovery*

Figure 1.1: Pharmaceuticals inspired by natural products; [a] Not a direct synthesis 3
Figure 1.2: Spirocycles in pharmaceuticals and bioactive molecules 5
Figure 1.3: Traditional Access to Spirocycles 6
Figure 1.4: Formal Synthesis of –(-)cephalotaxine 7
Figure 1.5: Generation of Primary and Secondary Metabolites through Photosynthesis 8
Figure 1.6: Drugs and Bioactive Molecules Containing Carbohydrates 10
Figure 1.7: Overview of Established Carbohydrate Chemistry 11
Figure 1.8: Synthesis of medermycin featuring Fischer carbene 12
Figure 1.9: Comparison of Charged Carbon Species 13
Figure 1.10: Comparison of Fischer and Schrock Carbenes 14
Figure 1.11: Carbene-Mediated Transformations Detailed within Dissertation 15

Chapter 2: *Carbene-Initiated Spirocyclization Cascades*

Figure 2.1: Spirojunction in [6,6] ring system; Spirocyclic moieties in progesterone medications 21
Figure 2.2: Synthesis of diazo compounds via Regitz Transfer 23
Figure 2.3: Comparison of diazos compounds and their respective metal carbenoids 24
Figure 2.4: Overview of metal carbenoid generation/ X–H insertion 25
Figure 2.5: Illustration of a two-step cascade or tandem reaction 26
Figure 2.6: Overview of Spirocycle Synthesis 28
Figure 2.7: Bimetallic synergistic catalysis with diazo compounds 29
Figure 2.8: Overview of Conia-ene Cyclizations 31
Figure 2.9: Two-step protocol for the synthesis of aminoalkynes **17** 32
Figure 2.10: Two-step protocol for the synthesis of aminoalkyne **20** 32
Figure 2.11: Optimized conditions for the synthesis of Spiroalkoids 33
Figure 2.12: Representative Substrate Scope for Spiroalkoids 34
Figure 2.13: Postulated N–H Insertion/Conia-ene Mechanism 35
Figure 2.14: Double Metal Activation for Enantioselective Coniae-ene 37
Figure 2.15: Copper-catalyzed stepwise asymmetric Conia-ene reaction 38
Figure 2.16: Initial Observations for [5,5] Spirocarbocycles 39
Figure 2.17: Access to [5,6] and [5,7] Spirocarbocycles 40
Figure 2.18: Access to [5,5] Spirocarbocycles 41
Figure 2.19: Starting Material Preparation for Spirocarbocycles 42
Figure 2.20: Synthesis and Preparation of Diazo **39b** 43
Figure 2.21: Synthesis of BOX Ligands screened 46

Chapter 3: *Glycal Carbenes –A Novel Glycosyl Donor for Stereoselective Glycosylation*

Figure 3.1: Traditional Approaches to Glycosidic Bond Formation 79

Figure 3.2: Vinylogous Reactivity of Vinyl Metal Carbenoids 80
Figure 3.3: Oxy-vinylogous Carbene Literature Precedence 82
Figure 3.4: Overview of Glycosylation Strategy 83
Figure 3.5: Failed Syntheses of Glycal Diazos 84
Figure 3.6: Enynones and Enynals as Metal Carbenoid Precursors 85
Figure 3.7: Synthesis of Glycal Carbene from Enynones 86
Figure 3.8: Initial Observation with Benzyl-protected Glycal 88
Figure 3.9: Initial Observations using Triacetate System 89
Figure 3.10: Optimization Conditions for a-anomer formation 93
Figure 3.11: Glycosylation Reactions with Simple Alcohols 94
Figure 3.12: Glycosylation Attempts with Sugar Acceptor 95
Figure 3.13: Mechanistic Rationale for Glycosylation 96
Figure 3.14: Solvent and Counterion Effect on Anomeric Ratio 97
Figure 3.15: Diversification of Furan Moiety for Diverse pyranosides 98

Chapter 4: *Carbene-Mediated Glycosyl Donors*

Figure 4.1: Reported Carbene-Assisted Glycosylation Strategies 125
Figure 4.2: Early Reports of Au-Mediated Glycosylations 127
Figure 4.3: Gold-Assisted Alkyne Activations for Glycosylations 128
Figure 4.4: Liming Zhang’s oxazole based Glycosyl Donor 128
Figure 4.5: Overview of Glycosylation Strategy 130
Figure 4.6: Inspiration behind New Donor Design 132
Figure 4.7: Synthesis of Benzylidene Protected Mannose Donor 134
Figure 4.8: Plausible Mechanistic Pathway 138
Figure 4.9: Competing Intramolecular Rearrangement 139
Figure 4.10: Synthetic Route to β-Sugar Enynone 140
Figure 4.11: Access to O–Glycosides 141
Figure 4.12: Substrate Scope with Non-Oxygen Acceptors 143

LIST OF TABLES

Table 2.1: Iron Metal Screening for O–H Insertion/Aldol Cascade 45
Table 2.2: Catalyst Screening with Oxindole Diazo 47
Table 3.1: Metal Catalyst Optimization for Anomeric Stereoselectivity……………………………..………90
Table 3.2: Solvent Optimization Table………………………………………………………………………….……92
Table 4.1: Initial Catalyst Screening of System with Isopropanol 135
Table 4.2: Current Optimization with Sugar Acceptor 137

LIST OF ABBREVIATIONS

α	alpha anomer
Å	Ångstrom
Ac	acetate group
Ar	aryl group
AcOH	acetic acid
ATP	Adenosine triphosphate
A/A	acceptor/acceptor
β	beta anomer
BA_rF	tetrakis(3,5-bis(trifluoromethyl)phenyl)borate
Bn	benzyl group
Boc	tert-butyloxycarbonyl
BF_4	tetrafluoroborate
BOX	bisoxazoline
Bu	butyl
Bz	benzoyl group
ºC	degrees Celsius (centigrade)
calc’d	calculated
d	doublet
D	dextrorotatory
DBU	1,8-Diazabicyclo[5.4.0]undec-7-ene
DCE	1,2 dichloroethane
DCM	dichloromethane
dd	doublet of doublets
DMAP	4-Dimethylaminopyridine
DMB	2,4 dimethoxybenzyl
DMF	N,N-dimethylformamide
DMP	Dess-Martin periodinane
DMSO	Dimethyl sulfoxide
DTBMSegPhos	Bis[di(3,5-di-tert-butyl-4-methoxyphenyl)phosphino]-4,4’-bi-1,3-benzodioxole, [(4R)-(4,4’-bi-1,3-benzodioxole)-5,5’-diyl]bis[bis(3,5-di-tert-butyl-4-methoxyphenyl)phosphine]
DTBP	2,6-Di-tert-butylpyridine
D/A	donor/acceptor
E	electrophile
ee	enantiomeric excess
EDCI	1-Ethyl-3-(3-dimethylaminopropyl)carbodiimide
EDG	electron-donating group
esp	a,a,a’a,’-tetramethyl-1,3-benzenedipropionic acid
Et	ethyl
EtOAc	ethyl acetate
equiv	equivalent

EWG	electron-withdrawing group
g	gram
h	hour
HMPA	hexamethylphosphoramide
HPLC	high-performance liquid chromatography
$_{i}$Pr	isopropyl
IR	infrared (spectroscopy)
J	coupling constant
KHMDS	potassium bis(trimethylsilyl)amide
L	levorotatory
LG	leaving group
m	multiplet or milli
M	metal or molar
Me	methyl
MeCN	acetonitrile
MHz	megahertz
ML_n	metal catalyst with X ligands
MS	molecular sieves
m/z	mass to charge ratio
mol	mole(s)
$NaBH_4$	sodium borohydride
^{n}Bu	n-butyl
nd	not determined
NMR	Nuclear Magnetic Resonance
nr	no reaction
Nu	nucleophile
Nuc	nucleophile
o	ortho
p	para
p-ABSA	4-acetamiobenzenesulfonyl azide
PF_6	hexafluorophosphate
PG	protecting group
Ph	phenyl group
pH	hydrogen ion concentration in aqueous solution
q	quartet
R	alkyl group
R_f	retention factor
$Rh_2(OAc)_4$	rhodium (II) acetate dimer
$Rh_2(oct)_4$	rhodium (II) octanoate dimer
$Rh_2(HFB)_4$	rhodium(II) Heptafluorobutyrate Dimer
Rt	room temperature
s	singlet
sub	substrate
S_N1	nucleophilic substitution unimolecular

S_N2	nucleophilic substitution dimolecular
t	triplet
TBAF	tetra-n-butylammonium fluoride
^{t}Bu	tert-butyl
TBS	tert-butyldimethylsilyl
Tf	trifluoromethanesulfonyl (trifyl)
TFA	trifluoroacetic acid
THF	tetrahydrofuran
TLC	thin-layer chromatography
Ts	*p*-toluenesulfonyl (tosyl)
WHO	World Health Organization
X	anionic ligand or halide

TABLE OF CONTENTS

ABSTRACT v
ACKNOWLEDGMENTS vii
LIST OF FIGURES ix
LIST OF TABLES xi
LIST OF ABBREVIATIONS xii

1. CHAPTER 1 1
Bioactive Motifs in Drug Discovery 1
- **1.2 Natural Products as an Inspiration for the Synthesis of Bioactive Scaffolds** 1
  - **1.2.1 Spiro-Systems In Bioactive Molecules** 4
  - **1.2.2 Sugars in Natural Products and Pharmaceuticals** 7
  - **1.2.3 Carbenes as an Ambiphilic Synthon** 13
  - **1.2.4 Goals of Dissertation** 15
- **1.3 References for Chapter 1** 17

2. CHAPTER 2 20
Carbene-Initiated Spirocyclization Cascades 20
- **2.1 Historical Perspective of Spirosystems and Metal Carbenoids** 20
  - **2.1.1 Synthesis and Reactivity of Diazo Compounds** 22
  - **2.1.2 Metal-Carbenoid Chemistry: Scope and Traditional Transformations** 24
  - **2.1.3 Cascade/Domino/Tandem Sequences** 26
  - **2.1.4 Objective of Chapter** 27
- **2.2 Metal Catalyst Synergism** 29
- **2.3 Propargyl-Activated Conia-Ene Reports** 30
- **2.4 Access to Spiroalkoloids** 31
  - **2.4.1 Synthesis of Spiroalkaloid Precursors** 31
  - **2.4.2 N–H Insertion/Conia-Ene Cascade For Spiroalkoiods** 33
- **2.5 Access to All Carbon Spirocycles** 38
  - **2.5.1 Synthesis of Diazo Acetamides & Contributions to Work** 40
- **2.6 Access to Spiroethers: O–H Insertion/Aldol Cascade** 43
  - **2.6.1 Development Of Earth-Abundant Catalysis Strategies** 43

2.7 **Conclusions and Summaries** 48
2.8 **References for Chapter 2** 49
2.9 **Experimental Section for Chapter 2** 53
  2.9.1 **Synthesis of Spirocyclic Alkaloids** 55
  2.9.2 **Synthesis of Spirocarbocycles** 59
  2.9.3 **O–H Insertion/Aldol Cascade** 61
2.10 **Appendix 1** 68
2.11 **References for Chapter 2 Experimentals** 77

3. CHAPTER 3 78
Glycal Carbenes –A Novel Glycosyl Donor for Stereoselective Glycosylation 78
3.1 **Introduction to Stereoselective Glycosylation** 78
  3.1.1 **Vinylcarbenoids and Oxy-Vinylogous Carbenes** 80
  3.1.2 **Objective of Chapter** 82
3.2 **Design, Synthesis, and Study of Glycal Carbenes** 83
  3.2.1 **Applicable Substrate Scope** 93
  3.2.2 **Mechanistic Insights** 95
3.3 **Future Directions and Limitations** 97
3.4 **Summaries** 98
3.5 **References for Chapter 4** 100
3.6 **Experimental Section for Section 3** 103
  3.6.1 **Synthesis of Glycal Carbene** 104
  3.6.2 **Synthesis of Sugar Acceptor** 108
  3.6.3 **General Procedure for Vinylic O–H Insertion of Glycal Carbenes** 109
3.7 **Appendix 2** 112
3.8 **References for Chapter 3 Experimentals** 123

4. CHAPTER 4 124
Carbene-Mediated Glycosyl Donors 124
4.1 **Introduction to Carbene-Assisted Glycosylation** 124
  4.1.1 **Gold-Assisted Glycosylations** 126
  4.1.2 **Objectives of Chapter** 129

4.2 Design, Synthesis, and Applications of Carbene-Mediated Donor 131
4.2.1 Experimental Design 131
4.2.2 Preliminary Optimization Studies 134
4.2.3 Postulated Mechanistic Pathway 137
4.2.4 Handicap of Methodology 139
4.3 Future Directions and Conclusions 140
4.3.1 Synthesis of O–Glycosides 141
4.3.2 Applications to N– And S– Glycosides and Furanoses 142
4.3.3 Conclusions 143
4.4 References for Chapter 4 145
4.5 Experimental Section for Section 4 147
4.5.1 Synthesis of Alkynyl Donor 149
4.5.2 Synthesis of Sugar Alcohol 151
4.5.3 Glycosylation Reactions 152
4.6 Appendix 3 155
4.7 References for Chapter 4 Experimentals 159

5. CHAPTER 5 160
Summaries, Conclusions, And Future Directions 160
5.1 Synthesis of Diverse Spirocycles 160
5.2 Carbene-Assisted Access to Glycosides 161
5.3 Development Of Earth-Abundant Catalysis and Sustainable Strategies 162
5.4 Future Directions and Scope of Work 164

Autobiographical Statement 165

CHAPTER 1

Bioactive Motifs in Drug Discovery

1.1 NATURAL PRODUCTS AS AN INSPIRATION FOR THE SYNTHESIS OF BIOACTIVE SCAFFOLDS

The proverb “health is wealth” alludes to the conviction that health is one’s most valuable asset. Thus, as humans, we should prioritize health and well-being above all else. Yet, the high cost of potent therapeutics suggests that access to medications necessary to preserve one’s health is a luxury. By 2023, the global pharmaceutical market will exceed $1.5 trillion.[1] The high cost of medication can be attributed to various elements; however, the most alarming factor is the high cost of drug development.

Nature and medicine are intertwined. Due to their chemical and structural diversity and the biodiversity of flora, plants are the most dominant source of new medicines.[2] Natural products, organic molecules synthesized within living organisms, have historically served as trailblazers for the pharmaceutical industry.[3] More complex, rigid molecules exhibit higher efficacies within drug discovery as drug leads and candidates. Molecules with three-dimensional features such as chirality and bond saturation have increased binding specificities. Likewise, these molecules sustain favorable pharmacological properties and decreased toxicological liabilities.[3a] Natural products often possess many of these features, including rigid frameworks and structural complexity. As a result, these molecules have historically served as the blueprint for drug discovery. Consequently, these molecules have inspired the structural core or mimics for most pharmaceuticals available today. As a result, over 50% of available drugs are natural products or derivatives (**Figure 1.1**).[3b, 3c]

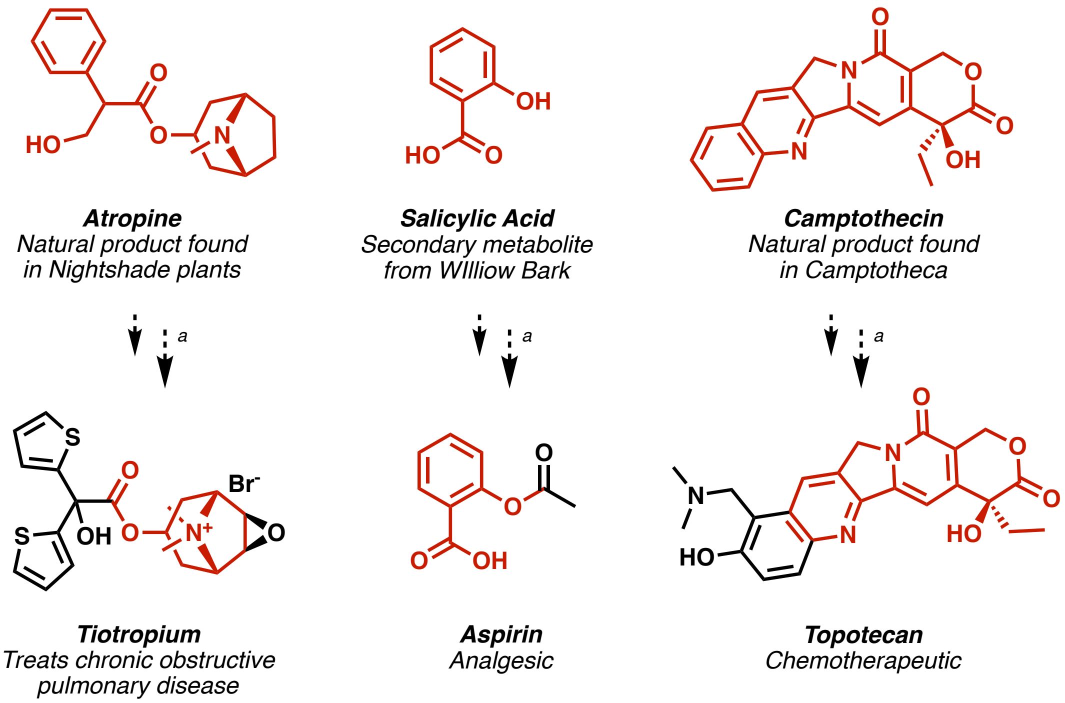
Atropine
Natural product found in Nightshade plants
Salicylic Acid
Secondary metabolite from WIlliow Bark
Camptothecin
Natural product found in Camptotheca
a
a
a
Tiotropium
Treats chronic obstructive pulmonary disease
Aspirin
Analgesic
Topotecan
Chemotherapeutic

Figure 1.1: Pharmaceuticals inspired by natural products; ^{a} Not a direct synthesis

However, drug-discovery programs have de-emphasized natural products favoring high-throughput screening of synthetic chemical libraries in the last two decades. This shift has been met with diminishing returns, as these changes have led to an average hit rate of <0.001% for pharmaceutical screenings of synthetic chemical libraries.[4] Resultantly, there has been a resurgence in the conviction that natural product-based drug design is the most practical model for future drug discovery efforts.[5]

Traditionally, terrestrial plants and microorganisms are the most significant sources of biologically active natural products.[3b-d, 6] Additionally, terrestrial and aquatic species of plants and microorganisms, especially those of marine origin,[7] have consistently yielded unique bioactive small molecules, leading to a variety of valuable therapeutics and lead structures for potential new drugs.

The extraction of some valuable natural products from their biological sources is challenging. Conventional extraction methods such as maceration, percolation, and reflux extractions offer a series of disadvantages that make extracting natural products found in low concentrations impractical.[8] These extractions typically employ long extraction times and large quantities of solvents only to obtain low yields of the desired molecule.[8b, 9] Additionally, the amounts of bioactive small molecules from these sources are typically relatively low. As a result, there is an urgent need to develop efficient methodologies to access these scaffolds in large quantities. The design of efficient synthetic methodologies to access natural product cores is thought by some to be the most practical route to access sizable quantities of candidates for drug screening programs.

Natural products typically are characterized by massive structural diversity as well as scaffold complexity. In contrast to conventional synthetic small molecules, these molecules are often rigid and contain a large fraction of sp^3 carbons. Compounds featuring a large fraction of sp^3 centers (fsp^3) have an increased likelihood of progression in drug discovery programs.[10] Additionally, increased fsp^3 character in molecules increases the range of accessible fragment growth vectors, thus enabling the structural elaboration of fragment hits in a three-dimensional manner in Fragment-Based Drug Discovery (FBDD) efforts.[11] This has led to the development of numerous 3D fragment libraries. One of the most common strategies for incorporating these features and rigidity is the introduction of quaternary stereocenters. An example of a valuable class of molecules featuring a quaternary center and high fsp^3 character is spirocycles.

1.1.1 SPIRO-SYSTEMS IN BIOACTIVE MOLECULES

Spirocycles are a class of molecules containing two or more rings fused by a single atom –i.e., its spirocore or spirocenter. Spirocycles, due to this spiro-junction, are inherently rigid molecules.[12] Additionally, the spiro-ring fusion (highlighted in red) is a valuable motif that can increase molecular complexity. These molecules are distinctly three-dimensional in nature and thus can adapt to many types of proteins as biological targets.[13] These features make the spirocyclic motif a privileged structure for drug discovery efforts (**Figure 1.2**).

Spirocyclic motifs are found abundantly in nature and natural product scaffolds.[14] Subclasses of spirocycles including spiroketals,[14] spirolactams,[15] spiroethers[16], and spiroamines[17] are prominent in natural products and bioactive small molecules.

Additionally, several drug candidates contain a spirocyclic moiety. Griseofulvin is a World Health Organization (WHO) essential antifungal treatment used to treat infections of the skin, hair, and nails.[18] Additionally, spironolactone is a small molecule medication used to treat high blood pressure and heart failure. Too, spironolactone is a diuretic and aldosterone receptor antagonist.[19]

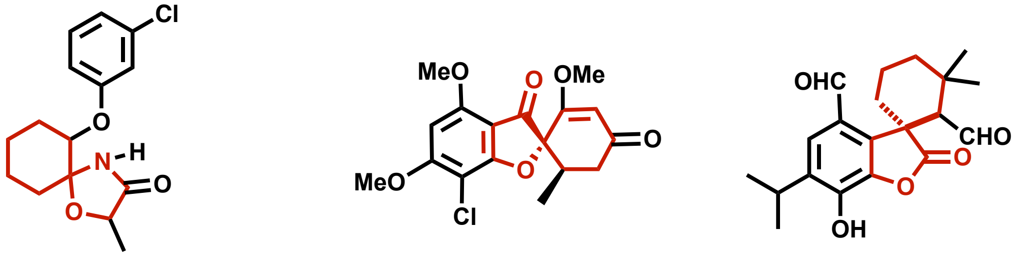

enilospirone
5-HT1A receptor agonist

griseofulvin
WHO's essential drug

rosmadial
antioxidant

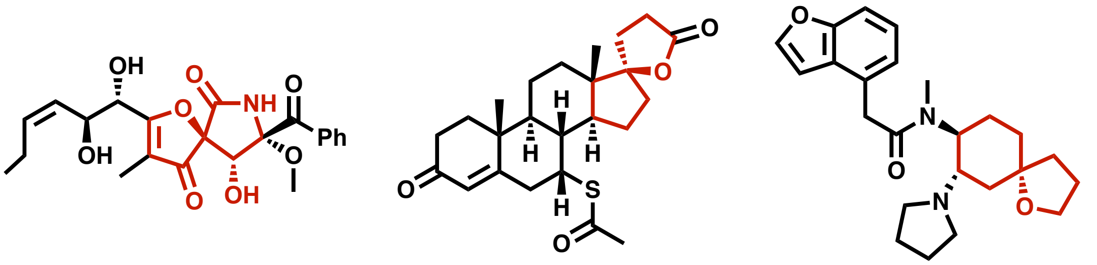

pseurotin A
chitin synthase inhibitor

spironolactone
diuretic

enadoline
κ-opioid agonist

Figure 1.2: Spirocycles in pharmaceuticals and bioactive molecules

Despite this, comparatively few spirocyclic moieties have been evaluated as drug candidates in the past decades.[12] While these compounds' structural rigidity and complexity are ideal for drug discovery programs, their limited availability in phenotypic screenings is predominately due to the challenges surrounding their synthesis. The installation of a quaternary center is one of the most challenging synthetic transformations.[20] More challenging is the installation of carbon centers with designated stereochemistry. The progress on new synthetic routes to access spiro building blocks will facilitate the incorporation of spirocyclic scaffolds into more pharmaceutically relevant molecules.

Most existing methods to access spirocycles rely heavily on intramolecular cyclization/rearrangement reactions of appropriate linear precursors. These strategies are handicapped by long starting material preparation to synthesize the appropriate precursors (**Figure 1.3**).[21]

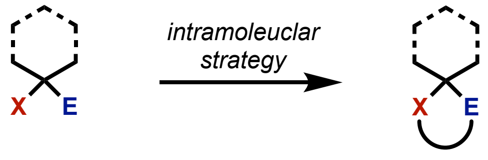

Handicap: *bridging components must be installed prior to cyclization step*

Figure 1.3: Traditional Access to Spirocycles

1.1.1.1 Formal Synthesis of (–)-Cephalotaxine Core: Spirocyclic Natural Product

Cephalotaxus harringtonia, an evergreen plum plant species native to Japan, is responsible for a potent class of alkaloids renowned for their significant antileukemic activity.[22] Hayes *et al*. completed the formal synthesis of the spirocyclic tetracyclic alkaloid core of (–)-cephalotaxine (**5**) twice, and in both syntheses, utilized an alkylidyne-derived carbene to establish a critical quaternary stereocenter (**Figure 1.4**).[23]

Both syntheses employ an alkylidene carbene cyclization precursor **1** that, once exposed to excess KHMDS (2.0 equiv.), results in the formation of the transient alkylidene carbene species **2**. Alkylidene **2** can participate in a 1,5 C–H insertion bond formation to furnish the spirocyclic alkaloid **3**. Immediately following this carbon bond-forming event, spiroalkaloid **3** is exposed to iodinating conditions to supply the aryl halide. Tetracycle **4** is then bridged together via a Heck cyclization.

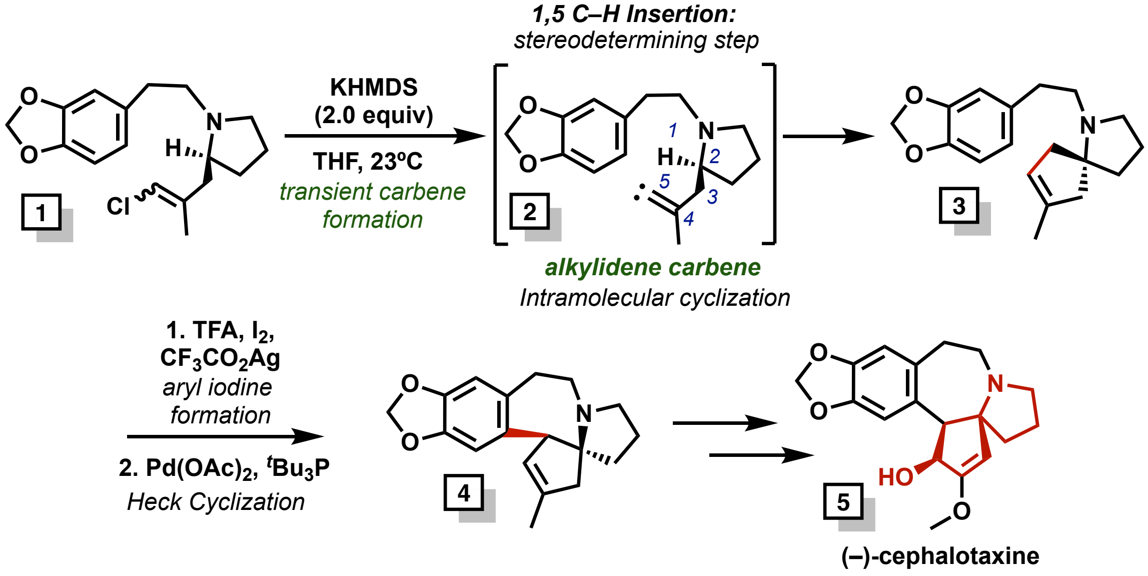
1,5 C–H Insertion:
stereodetermining step
1
KHMDS
(2.0 equiv)
THF, 23°C
transient carbene
formation
2
3
alkylidene carbene
Intramolecular cyclization
1. TFA, I2,
CF3CO2Ag
aryl iodine
formation
2. Pd(OAc)2, tBu3P
Heck Cyclization
4
5
(–)-cephalotaxine

Figure 1.4: Formal Synthesis of -(-)cephalotaxine

Spirocycles are one of the least studied fragments in drug discovery. Complementary to this work, this dissertation will detail synthetic strategies to access the most abundant natural-product framework –carbohydrates.

1.1.2 SUGARS IN NATURAL PRODUCTS AND PHARMACEUTICALS

Carbohydrates are the most abundant type of biomolecule.[24] As carbohydrates are the primary energy source for many living organisms, most often, these molecules are primarily discussed in terms of nutrition and diet. However, the biological roles of oligosaccharides are vast.[25] Carbohydrates are the most abundant natural product moiety and are responsible for various biological functions and disease processes. Likewise, glycosidic linkages are universal among all living organisms.

Plants produce carbohydrates via photosynthesis, a process that converts electromagnetic energy into chemical energy. Plants are responsible for the biosynthesis of upwards of 200,000 distinct small molecule natural products that serve as primary and secondary metabolites.[26] Primary metabolites perform essential metabolic roles that are indispensable for life. Conversely, secondary metabolites are molecules not required for growth and development; however, assist in other biological capacities. The biosynthesis of natural products as secondary metabolites, while not completely understood, is composed of networks of secondary metabolic pathways utilizing biosynthetic enzymes and CO_2 (**Figure 1.5**).[26c, 27]

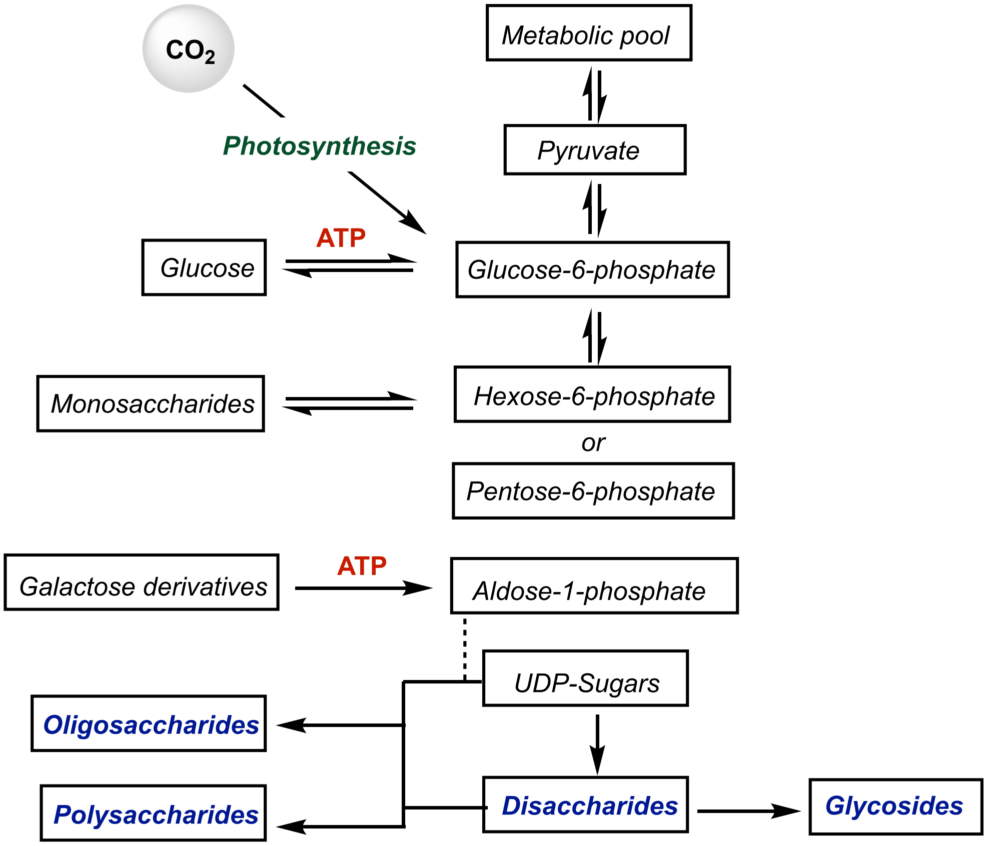
CO2
Photosynthesis
Metabolic pool
Pyruvate
Glucose
ATP
Glucose-6-phosphate
Monosaccharides
Hexose-6-phosphate
or
Pentose-6-phosphate
Galactose derivatives
ATP
Aldose-1-phosphate
UDP-Sugars
Oligosaccharides
Polysaccharides
Disaccharides
Glycosides

Figure 1.5: Generation of Primary and Secondary Metabolites through Photosynthesis

A variety of carbohydrate-containing scaffolds including glycans,[28]glycoconjugates,[29]aminoglycosides,[30] and nucleosides[31] are used abundantly as drug and vaccine candidates and pharmaceuticals (highlighted in red) (**Figure 1.6**).

Salicin is a β-glycoside in willow bark and is responsible for the tree's therapeutic properties. Likewise, salicin is the biosynthetic precursor to the analgesic salicylaldehyde –the inspiration and precursor to the analgesic medicine aspirin. Willow bark is colloquially termed "Nature's aspirin" in many cultures as it has been used for centuries as a pain reliever and anti-inflammatory.[32]

Empagliflozin and the spiroglycan tofogliflozin are treatment options for diabetic patients.[33]

Likewise, the α-glycosides idarubicin and doxorubicin are chemotherapeutic treatments. Stavudine belongs to a class of nucleoside reverse transcriptase inhibitors (NRTIs) and is an antiretroviral medication, commonly sold as Zerit, that is prescribed for the prevention and treatment of HIV and AIDS.

Additionally, aminoglycosides represent a significant class of broad-spectrum antibiotics used to treat gram-negative bacterial infections.[30, 34] A variety of aminoglycoside antibiotics are currently available today to treat a range of illnesses; clindamycin is used to treat particularly stubborn cases of acne and bacterial vaginosis.[35] Framycein is used to treat eye and ear infections.[36] Additionally, carbohydrates have been used as antiviral treatments for SARS-CoV-2 infections such as N4-hydroxycytidine and remdesivir.[37]

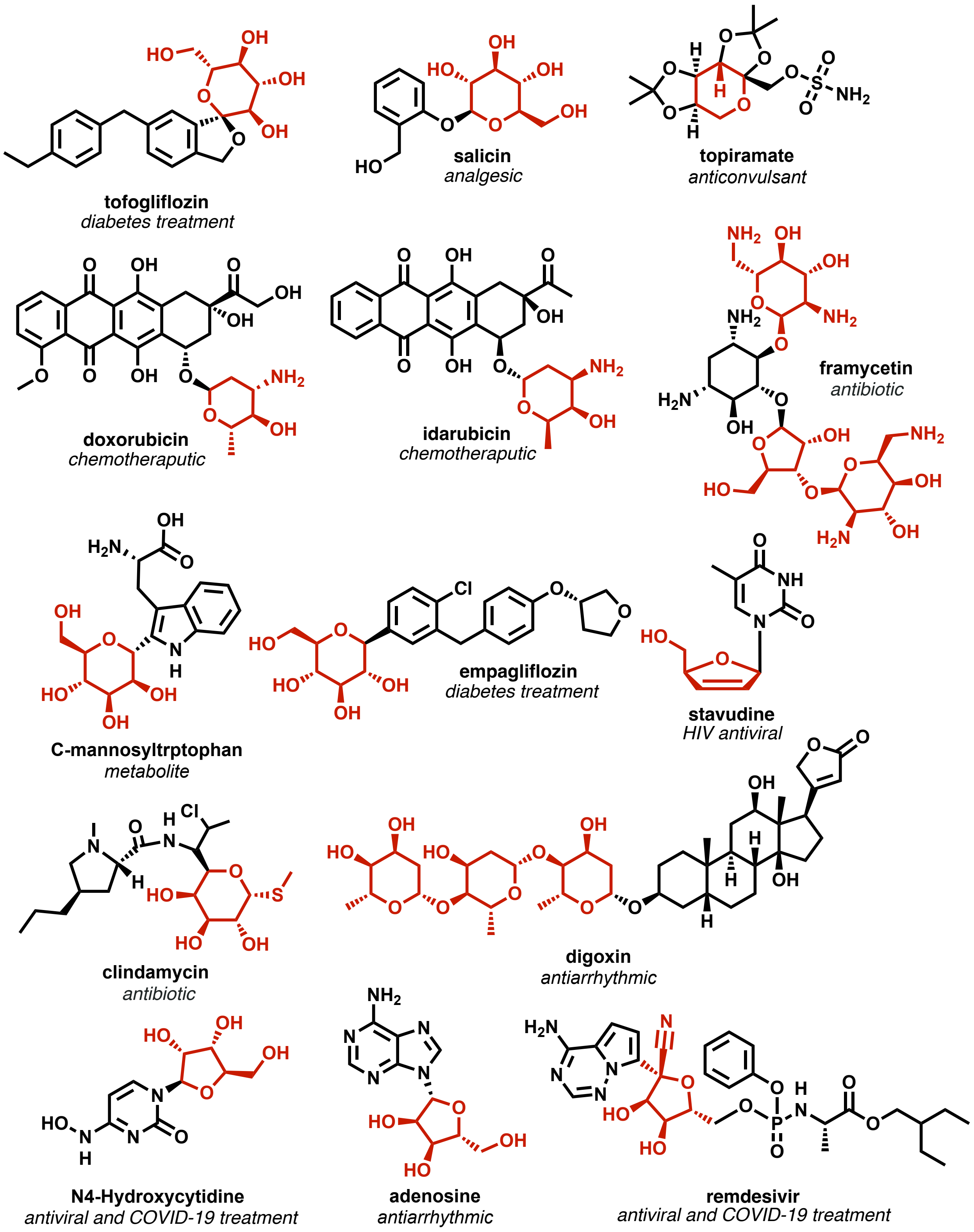

tofogliflozin
diabetes treatment

salicin
analgesic

topiramate
anticonvulsant

doxorubicin
chemotheraputic

idarubicin
chemotheraputic

framycetin
antibiotic

C-mannosyltrptophan
metabolite

empagliflozin
diabetes treatment

stavudine
HIV antiviral

clindamycin
antibiotic

digoxin
antiarrhythmic

N4-Hydroxycytidine
antiviral and COVID-19 treatment

adenosine
antiarrhythmic

remdesivir
antiviral and COVID-19 treatment

Figure 1.6: Drugs and Bioactive Molecules Containing Carbohydrates

The stereoselective synthesis of glycosidic bonds is the most prevalent challenge within carbohydrate chemistry. Most glycosylation methods proceed through either S_N1 or S_N2-type reactivity at the anomeric carbon.[38] The stereoselectivity of these reactions is typically dominated by the anomeric effect or protecting group manipulations (**Figure 1.7a**).[38a] The anomeric effect is a stereo-electronic phenomenon observed in cyclic rings containing a heteroatom, where a heteroatom-carbon bond at the anomeric position prefers the axial orientation as opposed to an equatorial configuration. This is due to a stabilizing hyperconjugation interaction where the oxygen's electrons from the non-bonding orbital can donate into the antibonding orbital of the C–X bond, stabilizing the axial position (**Figure 1.7b**).

a) Traditional Glycosylation Approaches

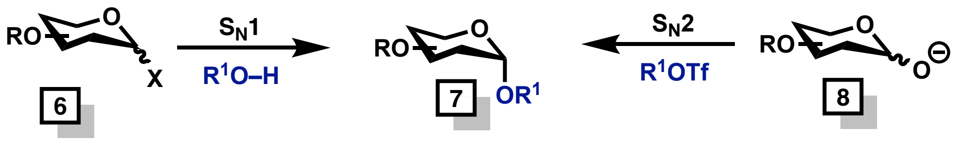
RO
O
X
6
SN1
R1O–H
RO
O
7
OR1
SN2
R1OTf
RO
O
O⊖
8

b) Anomeric Effect in Pyranoses

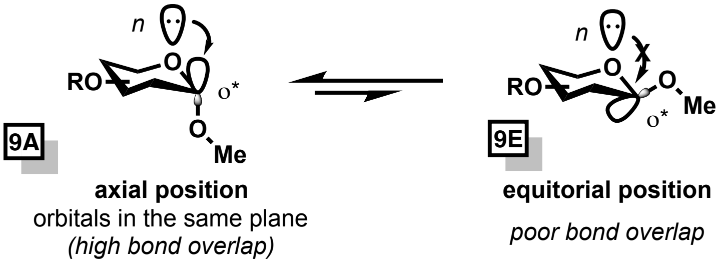
n
RO
O
σ*
O
Me
9A
axial position
orbitals in the same plane
(high bond overlap)
n
RO
O
O
Me
σ*
9E
equitorial position
poor bond overlap

Figure 1.7: Overview of Established Carbohydrate Chemistry

1.1.2.1 Synthesis of Medermycin: Carbohydrate-Based Natural Product

Medermycin is an aryl β-C-aminoglycoside first isolated from *Streptomyces sp.* in 1976.[39] Analogous to other aminoglycosides within the pyranonaphthoquinone family of antibiotics, mermycin (**15**) possesses potent activity against gram-position organisms, including species of *Staphylococcus* and *Bacillus*.[40] Early methods developed by Pulley *et al.* utilize Fischer chromium carbenes in a Wulff-Dötz annulation as the key step toward synthesizing the valuable aminoglycoside (**Figure 1.8**).[41]

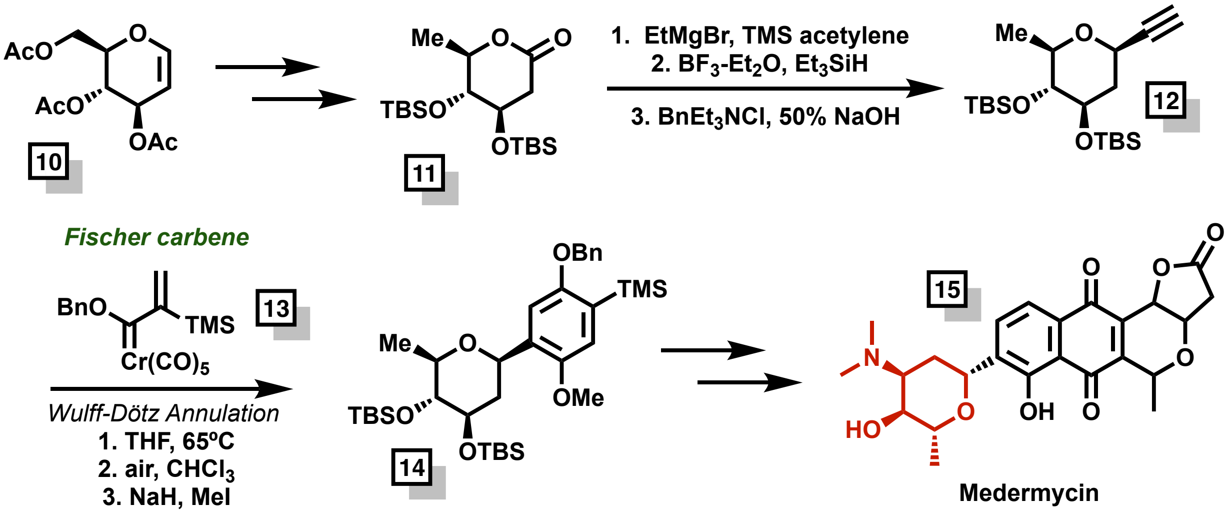
AcO
AcO
OAc
10
Me
TBSO
OTBS
11
1. EtMgBr, TMS acetylene
2. BF3-Et2O, Et3SiH
3. BnEt3NCl, 50% NaOH
Me
TBSO
OTBS
12
Fischer carbene
BnO
TMS
Cr(CO)5
13
Wulff-Dötz Annulation
1. THF, 65ºC
2. air, CHCl3
3. NaH, MeI
OBn
TMS
Me
TBSO
OTBS
OMe
14
15
N
HO
OH
Medermycin

Figure 1.8: Synthesis of Medermycin featuring Fischer Carbene

Ketopyranoside **11** was synthesized in three steps from the commercially available glucal **10**. In three steps, the propargyl moiety was stereoselectively installed at the anomeric position to furnish the propargyl pyranoside **12**. Pyranoside **12** was then exposed to the vinyl TMS carbene complex **13** to induce a Dötz benzannulation to deliver the aryl C-glycoside **14**.

1.1.3 CARBENES AS AN AMBIPHILIC SYNTHON

Ambiphilic synthons are a widely untapped resource within synthetic chemistry and, with proper design and innovation, can be used to access a broad spectrum of valuable scaffolds. These reagents bear dual reactivity, as they have both electrophilic and nucleophilic characteristics. One example of a powerful ambiphilic synthon is carbenes, which exist as an amalgam of carbocationic and carbanionic properties (**Figure 1.9**).

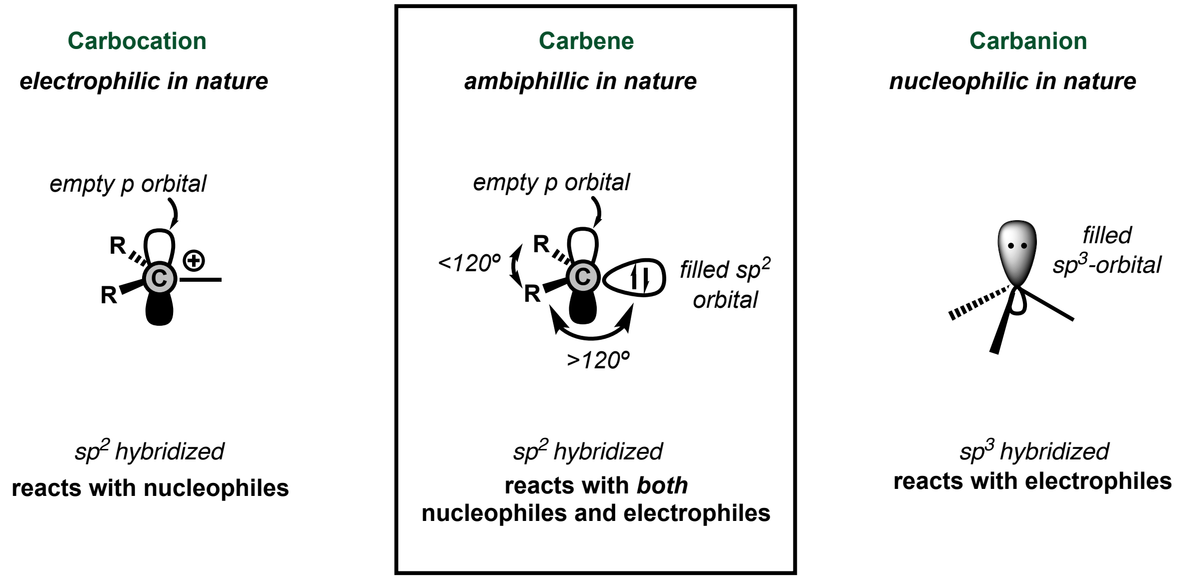
Carbocation
electrophilic in nature
empty p orbital
R
R
C
⊕
sp2 hybridized
reacts with nucleophiles
Carbene
ambiphillic in nature
empty p orbital
<120°
R
R
C
filled sp2 orbital
>120°
sp2 hybridized
reacts with both nucleophiles and electrophiles
Carbanion
nucleophilic in nature
filled sp3-orbital
sp3 hybridized
reacts with electrophiles

Figure 1.9: Comparison of Reactive Carbon Species

Carbenes are a neutral, divalent carbon species containing six electrons. Carbene generation can lead to the formation of two types of carbenes with different electron configurations. Fischer carbenes are a neutral carbon species containing six electrons, with a pair of spin paired, *singlet* electrons that occupy an *sp*^{2} orbital and an empty π orbital. These differ from Schrock carbenes, where electrons exist in a *triplet* state in two *sp* orbitals (**Figure 1.10**).

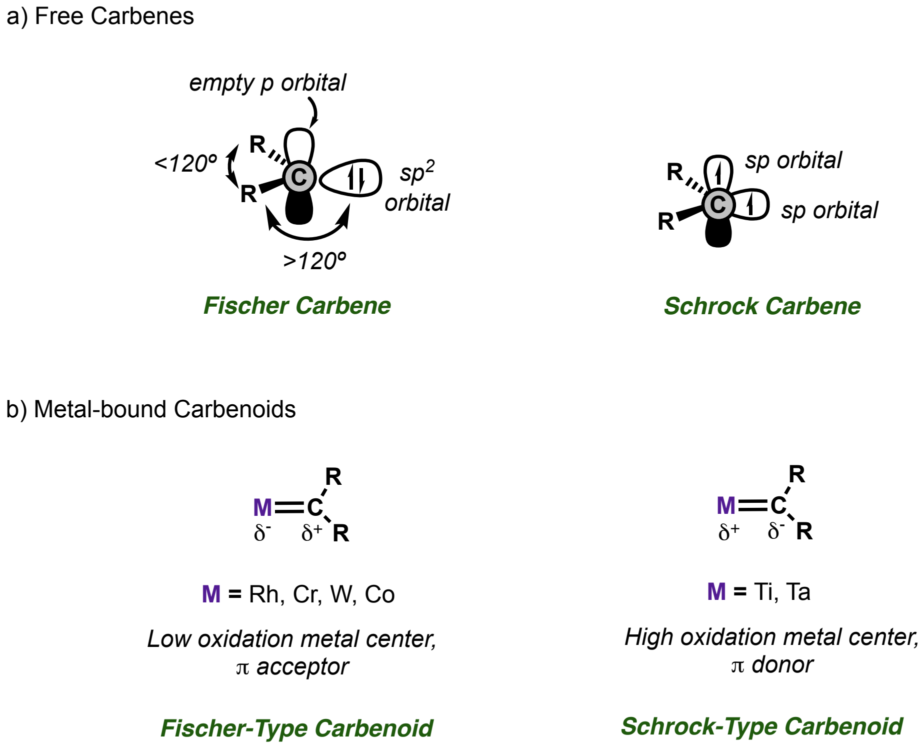
a) Free Carbenes
empty p orbital
<120º
R
R
C
sp2 orbital
>120º
Fischer Carbene
R
R
C
sp orbital
sp orbital
Schrock Carbene
b) Metal-bound Carbenoids
M=C
R
R
δ-
δ+
M = Rh, Cr, W, Co
Low oxidation metal center, π acceptor
Fischer-Type Carbenoid
M=C
R
R
δ+
δ-
M = Ti, Ta
High oxidation metal center, π donor
Schrock-Type Carbenoid

***Figure 1.10**:* Comparison of Fischer and Schrock Carbenes

Metal bound carbenes, or *carbenoids*, maintain carbene-like properties while being partially bound to a metal center. Carbenoids can exist as a Fischer-type or Schrock-type. Fischer-type carbenoids are bounded to electron-poor metals that cannot participate in large amounts of electron-back donation, making Fischer carbenes initially electrophilic. This dissertation focuses on incorporating Fischer-type metal carbenoids for the construction of privileged motifs.

As previously described, both carbenes and carbenoids have served as key intermediates in the synthesis of biologically relevant, complex natural products and potential pharmaceutical agents. The primary goal of the research efforts described within will detail the synthetic strategies used to harness the amphiphilicity of metal carbenoids for the construction of privileged motifs.

1.1.4 GOALS OF DISSERTATION

This dissertation *aims to utilize metal-bound carbenoids as synthons to construct privileged bioactive motifs*. Specifically, this dissertation details our attempts to access spirocyclic cores and glycosidic bonds. The research featured in *Chapter 2* of this dissertation details the synthesis of spirocycles (spiroalkaloids, spirocarbocycles, and spirooxindoles) using diazo-derived carbene synthons via an intermolecular strategy. This approach incorporates rhodium (II) carbenoids, which can undergo X–H insertion initiated cascade sequences, to access the desired spirosystems with a high degree of stereoselectivity (**Figure 1.11**).

Chapter 2: Spirocyclizations

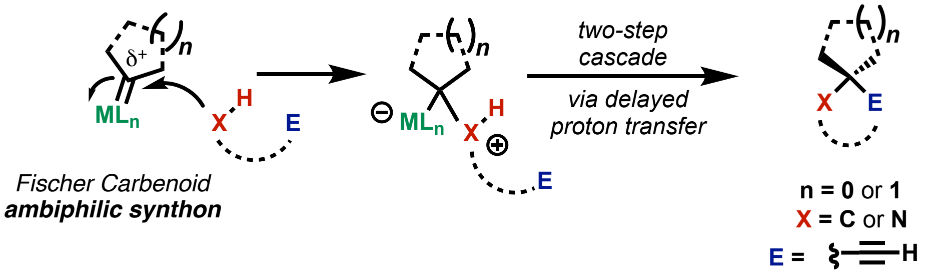
δ+
n
ML_n
H
X
E
Fischer Carbenoid
ambiphilic synthon
⊖ ML_n
n
H
X
⊕
E
two-step cascade
via delayed proton transfer
n
X
E
n = 0 or 1
X = C or N
E = ≡H

Chapters 3 and 4: Glycosylations

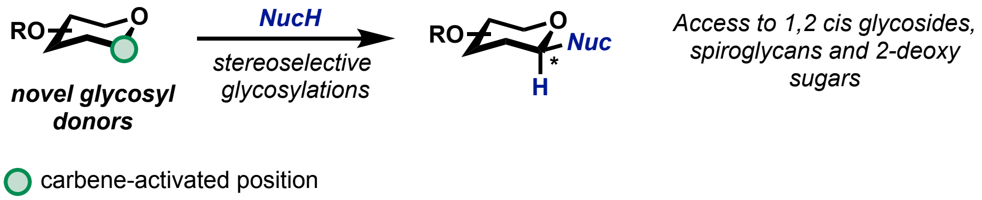
RO
O
novel glycosyl donors
NucH
stereoselective glycosylations
RO
O
Nuc
*
H
Access to 1,2 cis glycosides, spiroglycans and 2-deoxy sugars
carbene-activated position

Figure 1.11: Carbene-Mediated Transformations Detailed within Dissertation

Additionally, this dissertation will disclose the synthesis and application of enynone-derived, carbene-mediated glycosyl donors for stereoselective glycosylation. *Chapters 3* *and 4* will detail the synthesis and design of two novel carbene-assisted glycosyl donors. These chapters will describe research efforts surrounding these donors in stereoselective glycosylation reactions for the formation of *O*-glycosides (**Figure 1.11**).

In our research, we have utilized alkynes as versatile synthons to access both classes of molecules. In *Chapter 2*, we used propargyl groups as bifunctional trapping agents to access spirocyclic moieties. Then, bearing in mind these resourceful synthons, we turned to alkynes for the generation of metal carbenes to realize our glycosylation strategy, featured in *Chapters 3* and *4*.

1.2 REFERENCES FOR CHAPTER 1

[1] S. Vincent Rajkumar, *Blood Cancer Journal* **2020**, *10*, 71.

[2] S. Mathur, C. Hoskins, *Biomed Rep* **2017**, *6*, 612-614.

[3] a). I. Sharma, D. S. Tan, *Nature Chemistry* **2013**, *5*, 157-158; b). C. Veeresham, *J Adv Pharm Technol Res* **2012**, *3*, 200-201; c). D. J. Newman, G. M. Cragg, *Journal of Natural Products* **2012**, *75*, 311-335; d). D. J. Newman, G. M. Cragg, *Journal of Natural Products* **2020**, *83*, 770-803.

[4] K. J. Weissman, P. F. Leadlay, *Nature Reviews Microbiology* **2005**, *3*, 925-936.

[5] a). R. A. Bauer, J. M. Wurst, D. S. Tan, *Curr Opin Chem Biol* **2010**, *14*, 308-314; b). S. Hanessian, *Total Synthesis of Natural Products: The 'Chiron' Approach*, **1983**.

[6] a). J. A. Beutler, *Curr Protoc Pharmacol* **2009**, *46*, 9.11.11-19.11.21; b). A. G. Atanasov, S. B. Zotchev, V. M. Dirsch, I. E. Orhan, M. Banach, J. M. Rollinger, D. Barreca, W. Weckwerth, R. Bauer, E. A. Bayer, M. Majeed, A. Bishayee, V. Bochkov, G. K. Bonn, N. Braidy, F. Bucar, A. Cifuentes, G. D'Onofrio, M. Bodkin, M. Diederich, A. T. Dinkova-Kostova, T. Efferth, K. El Bairi, N. Arkells, T.-P. Fan, B. L. Fiebich, M. Freissmuth, M. I. Georgiev, S. Gibbons, K. M. Godfrey, C. W. Gruber, J. Heer, L. A. Huber, E. Ibanez, A. Kijjoa, A. K. Kiss, A. Lu, F. A. Macias, M. J. S. Miller, A. Mocan, R. Müller, F. Nicoletti, G. Perry, V. Pittalà, L. Rastrelli, M. Ristow, G. L. Russo, A. S. Silva, D. Schuster, H. Sheridan, K. Skalicka-Woźniak, L. Skaltsounis, E. Sobarzo-Sánchez, D. S. Bredt, H. Stuppner, A. Sureda, N. T. Tzvetkov, R. A. Vacca, B. B. Aggarwal, M. Battino, F. Giampieri, M. Wink, J.-L. Wolfender, J. Xiao, A. W. K. Yeung, G. Lizard, M. A. Popp, M. Heinrich, I. Berindan-Neagoe, M. Stadler, M. Daglia, R. Verpoorte, C. T. Supuran, T. the International Natural Product Sciences, *Nature Reviews Drug Discovery* **2021**, *20*, 200-216.

[7] a). R. Montaser, H. Luesch, *Future Medicinal Chemistry* **2011**, *3*, 1475-1489; b). C. Jiménez, *ACS Medicinal Chemistry Letters* **2018**, *9*, 959-961.

[8] a). R. Tambun, V. Alexander, Y. Ginting, *IOP Conference Series: Materials Science and Engineering* **2021**, *1122*, 012095; b). Q.-W. Zhang, L.-G. Lin, W.-C. Ye, *Chinese Medicine* **2018**, *13*, 20.

[9] F. B. Gerardo, *Agronomy* **2021**, *v. 11*, pp. --2021 v.2011 no.2023.

[10] A. R. Hanby, N. S. Troelsen, T. J. Osberger, S. L. Kidd, K. T. Mortensen, D. R. Spring, *Chemical Communications* **2020**, *56*, 2280-2283.

[11] C. W. Murray, D. C. Rees, *Angewandte Chemie International Edition* **2016**, *55*, 488-492.

[12] Y. Zheng, C. M. Tice, S. B. Singh, *Bioorganic & Medicinal Chemistry Letters* **2014**, *24*, 3673-3682.

[13] E. Chupakhin, O. Babich, A. Prosekov, L. Asyakina, M. Krasavin, *Molecules* **2019**, *24*, 4165.

[14] F. Perron, K. F. Albizati, *Chemical Reviews* **1989**, *89*, 1617-1661.

[15] A. J. S. Alves, N. G. Alves, C. C. Caratão, M. I. M. Esteves, D. Fontinha, I. Bártolo, M. I. L. Soares, S. M. M. Lopes, M. Prudêncio, N. Taveira, E. M. T. Pinho, *Curr Top Med Chem* **2020**, *20*, 140-152.

[16] I. Mavridis, G. Kythreoti, K. Koltsida, D. Vourloumis, *Bioorganic & Medicinal Chemistry* **2014**, *22*, 1329-1341.

[17] T. P. Culbertson, J. P. Sanchez, L. Gambino, J. A. Sesnie, *Journal of Medicinal Chemistry* **1990**, *33*, 2270-2275.

[18] *What is griseofulvin and why is it used in the treatment of fungal infections?.* https://www.chemservice.com/news/what-is-griseofulvin/ (accessed 2022-03-04)

[19] *Clindamycin.* https://medlineplus.gov/druginfo/meds/a682399.html/ (accessed 2022-02-24)

[20] E. A. Peterson, L. E. Overman, *Proceedings of the National Academy of Sciences* **2004**, *101*, 11943-11948.

[21] a). K. Fominova, T. Diachuk, D. Granat, T. Savchuk, V. Vilchynskyi, O. Svitlychnyi, V. Meliantsev, I. Kovalchuk, E. Litskan, Vadym V. Levterov, V. R. Badlo, R. I. Vaskevych, A. I. Vaskevych, A. V. Bolbut, V. V. Semeno, R. Iminov, K. Shvydenko, A. S. Kuznetsova, Y. V. Dmytriv, D. Vysochyn, V. Ripenko, A. A. Tolmachev, O. Pavlova, H. Kuznietsova, I. Pishel, P. Borysko, P. K. Mykhailiuk, *Chemical Science* **2021**, *12*, 11294-11305; b). Y. Tamaru, S.-i. Kawamura, Z.-i. Yoshida, *Tetrahedron Letters* **1985**, *26*, 2885-2888.

[22] M. A. Jalil Miah, T. Hudlicky, J. W. Reed, in *The Alkaloids: Chemistry and Biology, Vol. 51* (Ed.: G. A. Cordell), Academic Press, **1998**, pp. 199-269.

[23] a). A. Hameed, A. J. Blake, C. J. Hayes, *The Journal of Organic Chemistry* **2008**, *73*, 8045-8048; b). S. M. Worden, R. Mapitse, C. J. Hayes, *Tetrahedron Letters* **2002**, *43*, 6011-6014.

[24] V. K. Tiwari, B. B. Mishra, R. Signpost, *Opportunity, Challenge and Scope of Natural Products in Medicinal Chemistry*, **2011**.

[25] a). A. C. Weymouth-Wilson, *Natural Product Reports* **1997**, *14*, 99-110; b). A. Varki, *Glycobiology* **2017**, *27*, 3.

[26] a). J.-K. Weng, R. N. Philippe, J. P. Noel, *Science* **2012**, *336*, 1667-1670; b). G. A. Cordell, *Journal of Natural Products* **2002**, *65*, 952-952; c). G. Anarat-Cappillino, E. S. Sattely, *Current Opinion in Plant Biology* **2014**, *19*, 51-58.

[27] Pharmacognosy and Phytochemistry : Drugs Containing Carbohydrate and Derived Products.; *Biosynthesis of Carbohydrates*

[28] a). C. H. Wong, *Carbohydrate-based drug discovery*, **2006**; b). T. J. Boltje, T. Buskas, G.-J. Boons, *Nature chemistry* **2009**, *1*, 611-622; c). P. Bose, A. K. Agrahari, A. S. Singh, M. K. Jaiswal, V. K. Tiwari, in *Carbohydrates in Drug Discovery and Development* (Ed.: V. K. Tiwari), Elsevier, **2020**, pp. 213-266.

[29] S. Bhatia, M. Dimde, R. Haag, *MedChemComm* **2014**, *5*, 862-878.

[30] a). L. S. Gonzalez, 3rd, J. P. Spencer, *Am Fam Physician* **1998**, *58*, 1811-1820; b). K. M. Krause, A. W. Serio, T. R. Kane, L. E. Connolly, *Cold Spring Harb Perspect Med* **2016**, *6*, a027029.

[31] a). C. M. Galmarini, J. R. Mackey, C. Dumontet, *Leukemia* **2001**, *15*, 875-890; b). L. Eyer, R. Nencka, E. de Clercq, K. Seley-Radtke, D. Růžek, *Antiviral chemistry & chemotherapy* **2018**, *26*, 2040206618761299-2040206618761299.

[32] M. J. R. Desborough, D. M. Keeling, *British Journal of Haematology* **2017**, *177*, 674-683.

[33] Y. Ishibashi, T. Matsui, S. Yamagishi, *Horm Metab Res* **2016**, *48*, 191-195.

[34] R. Lorpitthaya, K. B. Sophy, J. L. Kuo, X. W. Liu, *Org. Biomol. Chem.* **2009**, *7*, 1284.

[35] *Clindamycin.* https://medlineplus.gov/druginfo/meds/a682399.html/ (accessed 2022-02-24)

[36] *Framycetin*. https://go.drugbank.com/drugs/DB00452/ (accessed 2022-02-28)

[37] R. Ghanbari, A. Teimoori, A. Sadeghi, A. Mohamadkhani, S. Rezasoltani, E. Asadi, A. Jouyban, S. C. Sumner, *Future Microbiology* **2020**, *15*, 1747-1758.

[38] a). P. O. Adero, H. Amarasekara, P. Wen, L. Bohé, D. Crich, *Chemical Reviews* **2018**, *118*, 8242; b). K. Le Mai Hoang, W. L. Leng, Y. J. Tan, X. W. Liu, *Selective Glycosylations: Synthetic Methods and Catalysts*, **2017**.

[39] S. Takano, K. Hasuda, A. Ito, Y. Koide, F. Ishii, *J Antibiot (Tokyo)* **1976**, *29*, 765-768.

[40] A. Nakagawa, N. Fukamachi, K. Yamaki, M. Hayashi, S. Oh-ishi, B. Kobayashi, S. Omura, *J Antibiot (Tokyo)* **1987**, *40*, 1075-1076.

[41] C. Qu, E. Tang, R. Loeppky, Z. Deng, S. R. Pulley, X. Hong, *Chirality* **2015**, *27*, 18-22.

CHAPTER 2

Carbene-Initiated Spirocyclization Cascades

2.1 HISTORICAL PERSPECTIVE OF SPIROSYSTEMS AND METAL CARBENOIDS

Spirocyclic frameworks are considered privileged structures in drug discovery. The three-dimensionality and rigidity of these scaffolds allow them to perform and adapt well to biological targets.[1] Resultantly, these motifs have been of intense interest in modern drug discovery. Nonetheless, there has been a dramatic drop in spiro-junctions found in drug leads, thought to be a result of the increased synthetic effort necessary for their installation.[2]

The popularity of spiro-junctions can, in part, be attributed to the breakthrough development of the drug spironolactone in 1957 (**Figure 2.1**).[3] Spironolactone is a mineralocorticoid receptor (MR) antagonist used to treat heart disease and hypertension. This discovery paved the way for scaffolds possessing a spirocore in medicines. Spironolactone was approved for use in 1959, and in the decades following, scientists continued the development of spironolactone antiandrogens for libraries of progesterones. Eplerenone is another MR antagonist patented in 1983 and approved for medical use in the United States in 2002.[4] Additionally, drospirenone is a progesterone medication featuring a spirolactone moiety sold as birth control since its approval in 2000.[5]

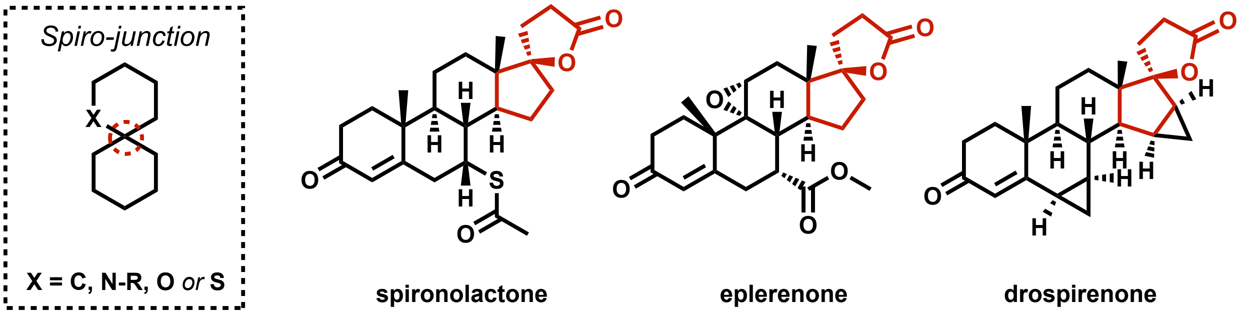

spironolactone
diuretic

eplerenone
diuretic

drospirenone
contraceptive

Figure 2.1: Spirojunction in [6,6] ring system; Spirocyclic moieties in progesterone medications

Spiro-junctions are found abundantly in natural products, and often more than one spirosystem can be found in a single natural product. These include spiro sub-classes for spiroethers (spiroacetals, spiroketals), spirocyclic alkaloids (spirolactams), and spirocarbocycles. Additionally, spiro-ring systems have been incorporated successfully into enzymes and protein-protein interaction inhibitors. The introduction of conformational restriction by ring formation, including spiro-ring formation, can modulate binding potency and specificity. Likewise, these restrictions can potentially improve bioavailability and metabolic stability. Furthermore, conformational restrictions may reduce off-target activities.[6]

In literature, spirocycles are typically formed through alkylations, rearrangements, cycloadditions, oxidative or reductive couplings, or the cleavage of bridged systems. While powerful, most of these reports lack a general strategy for synthesizing different sub-classes of spirosystems —the work presented details our attempts to combat this challenge utilizing carbenoid-initiated cascade cyclizations.

2.1.1 SYNTHESIS AND REACTIVITY OF DIAZO COMPOUNDS

Diazo compounds have a long history of synthetic applications. Originating as dyes, they quickly were applied as efficient alkylating agents. Initially feared due to their instability and potential explosive behavior,[7] synthetic efforts for their efficient and safe synthesis have made these compounds commonplace in the academic lab setting.[8]

More recently, their popularity has converged to their application as carbenoid precursors, often achieved through metal-catalyzed diazo decomposition. The most popular means of synthesizing diazos are via a Reigtz diazo transfer, formed via an amine base promoted transfer from an azide moiety (**Figure 2.2**).[9] The diazos synthesized within this chapter will be prepared using this method.

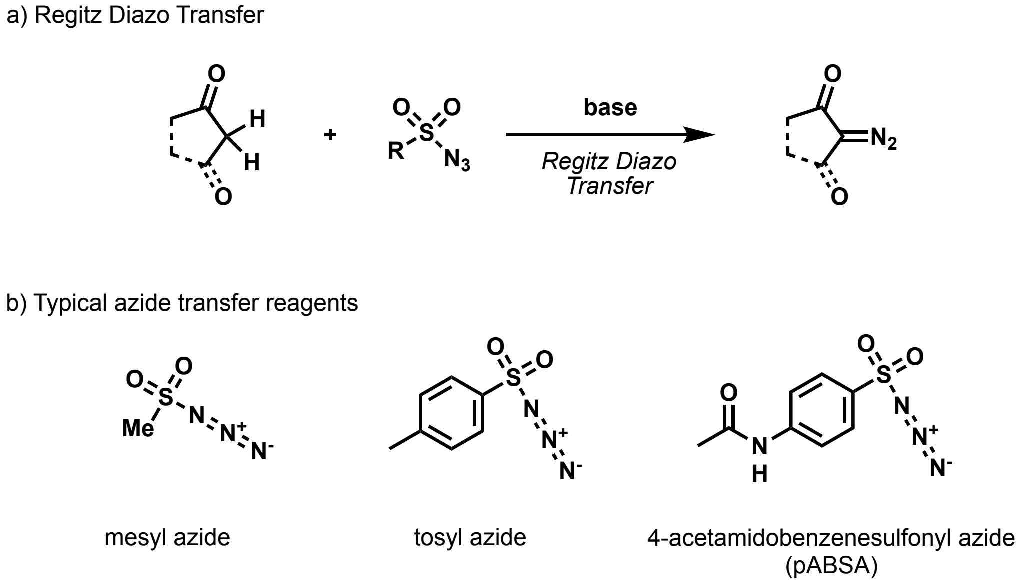
a) Regitz Diazo Transfer
O
H
H
O
+
O
O
S
R
N3
base
Regitz Diazo Transfer
O
N2
O
b) Typical azide transfer reagents
O
O
S
Me
N
N+
N-
mesyl azide
O
O
S
N
N+
N-
tosyl azide
O
N
H
O
O
S
N
N+
N-
4-acetamidobenzenesulfonyl azide (pABSA)

Figure 2.2: Synthesis of diazo compounds via Regitz Transfer

Benchtop stable diazos are divided into three categories: donor/acceptor diazos (D/A), acceptor-only diazos (A), and acceptor/acceptor (A/A) diazos.[10] Notably, while offering the most reactivity, donor/acceptor diazos are plagued with decreased stability due to the donor substituent destabilizing the diazo moiety (**Figure 2.3a**). Contrastingly, acceptor/acceptor diazos are incredibly stable; however often require high temperatures, refluxing conditions, or higher catalyst loadings to decompose the diazo. The reactivity is reversed once the diazo is decomposed to the metal carbenoid (**Figure 2.3b**).

A/A carbenes are the most reactive species due to the two electron-withdrawing substituents destabilizing the electron-deficient carbene species resulting in the most electrophilic species. D/A carbenes are the most long-lived traditional species and tend to facilitate more selective transformations. Recently, newly developed, non-diazo carbene surrogates have led to the introduction and study of donor-only (D) and donor-donor carbenes (D/D).[11]

a) Classification and reactivity profile of diazo compounds

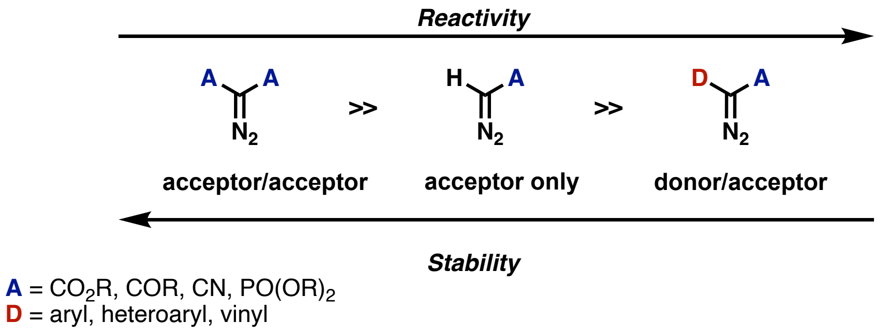
Reactivity
A A
N2
>>
H A
N2
>>
D A
N2
acceptor/acceptor
acceptor only
donor/acceptor
Stability
A = CO2R, COR, CN, PO(OR)2
D = aryl, heteroaryl, vinyl

b) Classification and reactivity profile of metal-bound carbenoids

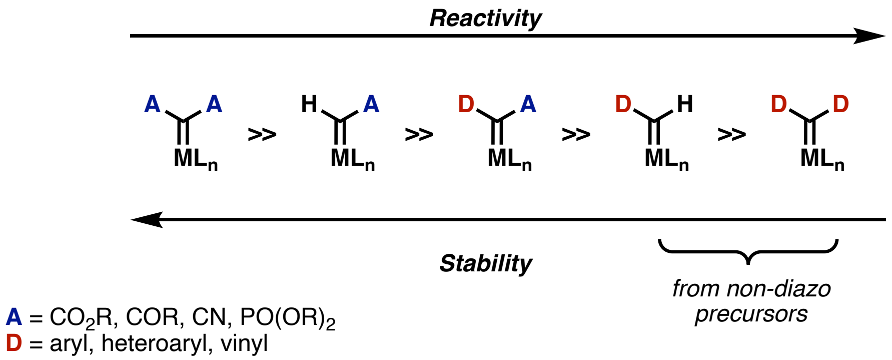
Reactivity
A A
MLn
>>
H A
MLn
>>
D A
MLn
>>
D H
MLn
>>
D D
MLn
Stability
from non-diazo precursors
A = CO2R, COR, CN, PO(OR)2
D = aryl, heteroaryl, vinyl

Figure 2.3: Comparison of diazos compounds and their respective metal carbenoids

2.1.2 METAL-CARBENOID CHEMISTRY: SCOPE AND TRADITIONAL TRANSFORMATIONS

Padwa, Doyle, and Davies devoted a great effort towards the synthesis, understanding, and applications of diazo-derived metal carbenoid systems.[12] Catalytically generated metal carbenoids have been shown as synthetically useful synthons. Mechanistically, catalytically induced diazo decomposition is initiated by the electrophilic addition of the metal salt onto the diazo carbon, prompting the loss of dinitrogen gas. This forms the electrophilic metal carbenoid species (boxed in red). As ambiphilic synthons, metal carbenoids can participate in various transformations, most notably X–H insertions (**Figure 2.4**).

Rhodium is undoubtedly the most common and most effective transition metal catalyst for diazo decomposition.[12b, 13] Often, dirhodium (II) complexes are commercially available with a wide variety of bridging carboxylate or carboxamide ligands that provide a range of reactivities. Dirhodium (II) acetate ($Rh_2(OAc)_4$) is typically regarded as the standard rhodium catalyst. Replacing the acetate ligands can influence the chemical and physical properties of the catalyst and the resulting carbenoid. For example, rhodium (II) octonate is more soluble in non-polar solvents, and rhodium (II) perfluorobutyrate results in a more electrophilic carbene. Additionally, these catalysts are exceptionally versatile and can be used at extremely low catalyst loadings, thus having remarkably high turnover numbers. Additionally, copper catalysts have been historically used for diazo decomposition.

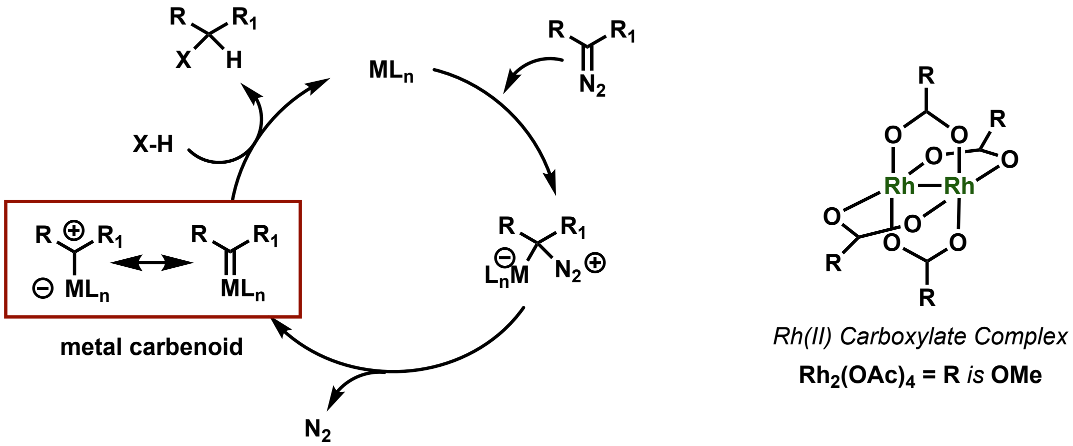

Rh(II) Carboxylate Complex

$Rh_2(OAc)_4$ = R *is* OMe

Figure 2.4: Overview of metal carbenoid generation/ X–H insertion

These carbenoids are easily generated, well studied, and engage in very reliable transformations such as cyclopropanations,[14] cyclopropenations,[15] insertion reactions (C–H, N–H, O–H, S–H, B–H, Si–H),[13a, 16] trifluoromethylations,[17] C–H functionalization,[12f, 18] dipolar additions,[19] cascades, [12a, 18a, 20] formal cycloadditions,[21] and rearrangement reactions.[22]

2.1.3 CASCADE/DOMINO/TANDEM SEQUENCES

Cascade reactions are a series of sequential chemical transformations operating in a single flask without the need for intermediary isolation. Additionally, the product(s) from the initial reaction is used as the starting material for the successive reaction. This sequence is continued until a stable product is formed that can be isolated (**Figure 2.5**).[12a, 20a, 23]

a) Traditional, step-wise approach

Two-step procedure. Involves the isolation and purification of intermediary products (B) before moving on to the final step

b) Cascade or Tandem Approach

One-pot tandem protocol. No intermediary isolation is necessary

Figure 2.5: Illustration of a two-step cascade or tandem reaction

There has been a significant increase in cascade-based method development in the past few decades, often towards target-oriented synthesis and diverted synthesis efforts. These transformations are increasingly practical and can be utilized to develop highly functionalized building blocks and other fine chemicals. Often, cascade reactions provide an efficient route to highly complex scaffolds. These reactions are typically accompanied by high stereoselectivity due to the higher-ordered transition states integral to these transformations.

Additionally, cascade sequences are synthetically ‘green’ as these reactions reduce waste generation. Likewise, these reactions save resources, time, and effort. Due to their usefulness and practicality, numerous reviews have been reported detailing cascade-based transformations involved in pericyclic and sigmatropic rearrangements,[24] radical reactions,[23a, 25] carbene/carbenoid reactions,[12a, 12d, 22, 26] and ionic reactions.[25d, 27]

Cascade reactions are frequently accessed through reactive dual-character synthons. Diazo carbonyls are reliable precursors routinely used to access a powerful ambiphilic synthon –metal carbenoids. Once decomposed, diazos are converted to electrophilic metal-bound carbenoids, which can react with an accessible nucleophile to form reactive zwitterionic intermediates.[19, 28]

2.1.4 OBJECTIVE OF CHAPTER

The research included within this chapter features a general, convergent strategy for the convenient synthesis of diverse spirocycles, featuring X–H insertion tandem intermolecular sequences (**Figure 2.6a**). These reactions function by bypassing a common limitation observed in metal-carbenoid reactions, the 1,2 proton transfer.

Towards the goal of stereoselectively synthesizing spirocycles, we have identified synergistic bimetallic conditions for synthesizing various spirosystems. Namely, we have applied these conditions towards spirocyclic alkaloids[20b] and spirocarbocyclic systems[18a] using a previously identified Rh (II)/ cationic Au(I) catalyst combination (**Figure 2.6b**).[29] Additionally, we have begun developing conditions using Earth-abundant metals for the synthesis of spiroethers.

a) General approach to diazo-trap cascade

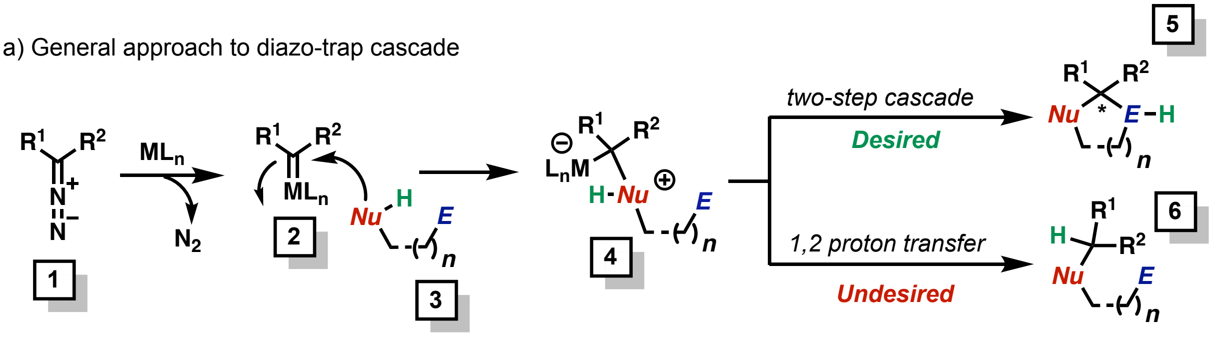
1
ML$_n$
N$_2$
2
3
4
two-step cascade
Desired
5
1,2 proton transfer
Undesired
6
R^1
R^2
Nu
E
H
n
L$_n$M

b) Goals of spircocyclization project

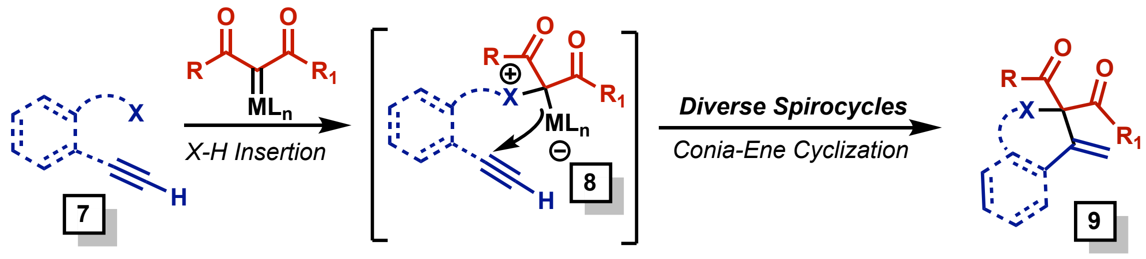
7
X-H Insertion
8
Diverse Spirocycles
Conia-Ene Cyclization
9
R
R$_1$
ML$_n$
X
H

X = sp^2 CH, sp^3 CH, OH or NHR
R = **R$_1$**, alkyl, O-alkyl
ML$_n$ = Rh$_2$L$_2$, Cu (II) Zn(OTf)$_2$

Figure 2.6: Overview of Spirocycle Synthesis

2.2 METAL CATALYST SYNERGISM

There are many facets of dual catalysis. Dual synergistic catalysis involves two catalysts that independently activate two separate substrates. This concurrent activation creates two reactive species that can rapidly react to form a new bond (**Figure 2.7**).[30] This differs from other multicatalyst systems, such as double activation catalysts, where two catalysts work cooperatively to activate a single substrate,[30-31] or cascade/relay catalyst systems that require the systematic activation of a single substrate.[32] Often, these systems are more efficient than traditional single catalysts and enable new transformations not possible with mono-catalytic systems.

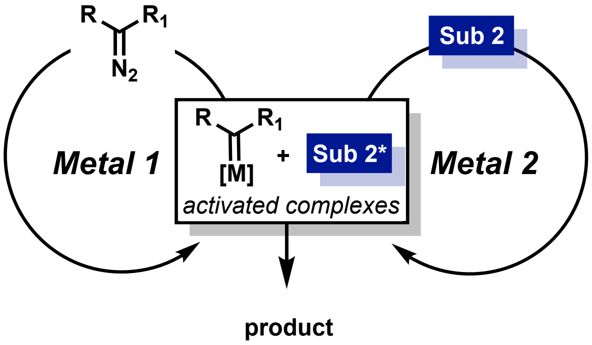

Figure 2.7: Bimetallic synergistic catalysis with diazo compounds

Our research group has had considerable success using synergistic catalysis,† specifically pertaining to rhodium (II) mediated X–H insertion/Conia-ene cascades. [18a, 20b, 29, 33] In 2016, Hunter *et al.* identified an Rh(II)/Au(I) dual catalyst system to facilitate the O–H insertion/Conia-ene tandem reaction, using a combinatory AgOTf/PPh_3AuCl system. Building upon our Rh(II)/Au(I) finding, we then expanded this methodology for trapping different bifunctional reactants to synthesize both spiroalkaloid systems and all-carbon spirocycles.

---

† This topic was a featured cover review article for European Journal of Organic Chemistry, see reference: **A. I. Bain**, K. Chinthapally, A. C. Hunter, I. Sharma, "Dual Catalysis in Rhodium(II) Carbenoid Chemistry" *Eur. J. Org. Chem.* **2022**, e202101419.

2.3 PROPARGYL-ACTIVATED CONIA-ENE REPORTS

Historically, Conia-ene cyclizations consist of a thermally induced intramolecular cyclization of an enolizable carbonyl with an olefinic or propargyl moiety (**Figure 2.8a**). The Conia-ene reaction is a widely utilized synthetic transformation that can be used to construct carbon-containing rings.[34] Implementation of a metal catalyst allows further activation of the π-system, thereby decreasing the activation energy necessary for the desired cyclization. This activation allows for milder reaction conditions and shorter reaction times. Pioneering strategies for metal-catalyzed Conia-ene reactions were developed by Toste using 1,3 dicarbonyls and cationic gold, forming a variety of cyclized products with high diastereoselectivities (**Figure 2.8b**).[35] Since then, Conia-ene reactions mediated by propargyl activations have been expanded to encompass diazo-mediated reactions and a broad range of metals.[36]

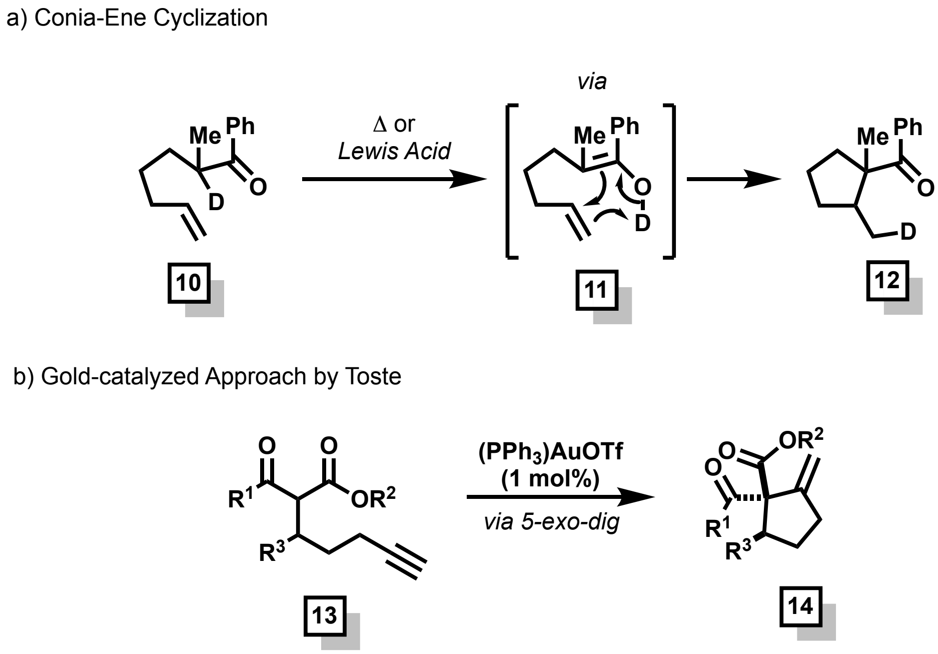
a) Conia-Ene Cyclization

b) Gold-catalyzed Approach by Toste
Me
Ph
D
O
10
Δ or
Lewis Acid
via
Me
Ph
O
D
11
Me
Ph
O
D
12
O
O
R1
OR2
R3
13
(PPh3)AuOTf
(1 mol%)
via 5-exo-dig
O
OR2
O
R1
R3
14

***Figure 2.8**:* Overview of Conia-ene Cyclizations

2.4 ACCESS TO SPIROALKOLOIDS

2.4.1 SYNTHESIS OF SPIROALKALOID PRECURSORS

To access spiroalkoloids systems, we initially synthesized propargyl amines **17** as a bifunctional nucleo- and electrophilic trapping partner via a reported two-step sequence (**Figure 2.9**).[37]

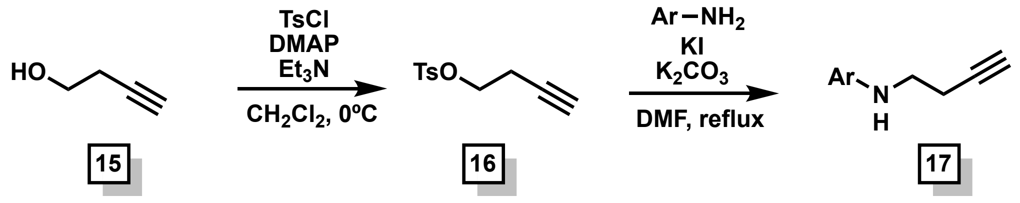
HO
TsCl
DMAP
Et_3N
CH_2Cl_2, 0ºC
TsO
Ar–NH_2
KI
K_2CO_3
DMF, reflux
Ar
N
H
15
16
17

Ar = Ph, 4OMe-Ph

Figure 2.9: Two-step protocol for the synthesis of aminoalkynes **17**

Additionally, the ethynylaniline **20** was prepared in two steps from 2-iodoaniline.[38] Ethynyltrimethylsilane was coupled at the ortho position of 2-iodoaniline via a Sonogashira coupling to yield the silyl-protected propargyl amine **19**, which was exposed to Tetra-n-butylammonium iodide (TBAF) to yield the desired propargyl amine **20** (**Figure 2.10**).

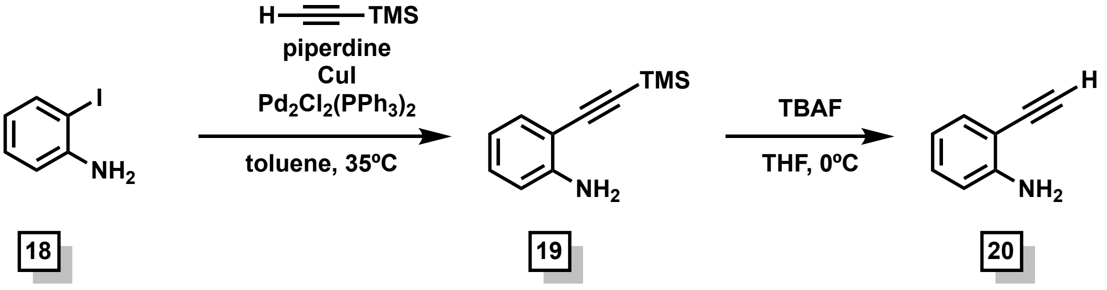
H
TMS
piperdine
CuI
$Pd_2Cl_2(PPh_3)_2$
toluene, 35ºC
I
NH_2
TMS
TBAF
THF, 0ºC
H
18
19
20

Figure 2.10: Two-step protocol for the synthesis of aminoalkyne **20**

Likewise, the diazo precursors were synthesized readily via a Reigtz diazo transfer of the corresponding 1,3 dicarbonyls to synthesize a variety of diazos readily. With a reliable synthetic route for both the diazo and aminoalkynes, the substrates were exposed to conditions previously identified by Hunter to undergo an N–H insertion/Conia-ene cascade sequence.[29]

2.4.2 N–H INSERTION/CONIA-ENE CASCADE FOR SPIROALKOIODS

After developing an Rh(II)/ cationic gold catalytic cocktail to furnish O–H/Conia-ene cascades,[33] our group furthered our own methodology to trap aminoalkynes **17** (**Figure 2.11**).[20b] This transformation employed Rh_2esp_2 (1 mol%) as a rhodium (II) source for efficient diazo decomposition, as well as the cationic gold complex PPh_3AuSbF_6 (10 mol%), which is produced *in situ* from PPh_3AuCl and $AgSbF_6$.

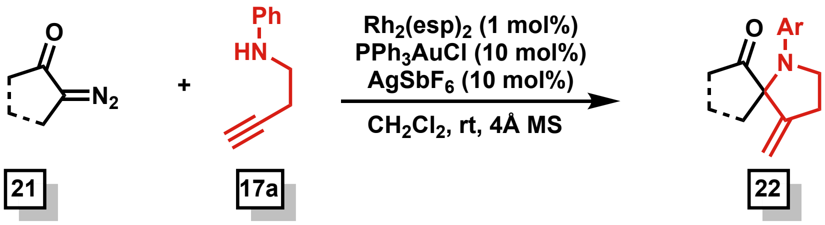

Figure 2.11: Optimized conditions for the synthesis of Spiroalkaloids

Remarkably, this work was tolerable to both donor/acceptor (**22a,22b**) and donor/acceptor (**22c-22e**) diazos (**Figure 2.12**). D/A diazos were able to be decomposed readily to access the spiro systems, including diazos synthesized from 2-tetralone (**22a**) were synthesized in a moderate 60% yield, as well phenanthren-9(10*H*)-one-derived diazo (**22b**) 60%. To synthesize diverse spirocyclic alkaloids, the diazos were added dropwise via syringe pump to a 0.3M CH_2Cl_2 solution of the three-component catalyst cocktail in dichloromethane. More stable A/A diazos were also able to facilitate the desired transformations, albeit with slightly modified conditions.

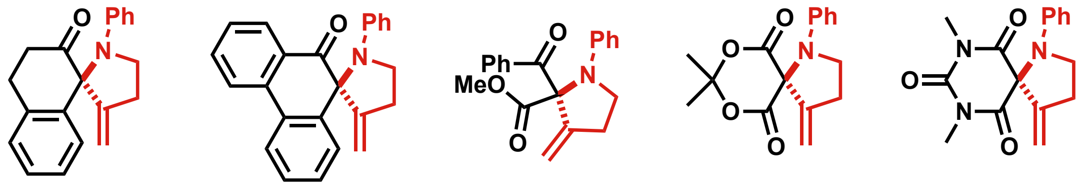

22a, 60% **22b**, 62% **22c**, 62% **22d**, 41% **22e**, 52%

Figure 2.12: Representative Substrate Scope for Spiroalkaloids

The reaction for the substrate **22c** proved initially low yield, due to the competing 5-*endo*-dig cyclization. To further optimize the yield for this reaction, the A/A diazo carbonyl was added to a solution of Rh_2esp_2 alone. After the formation of the desired insertion product via TLC, a solution of PPh_3AuCl (10 mol%) and $AgSbF_6$ (10 mol%) (0.5M in CH_2Cl_2) was added to the insertion product to yield the desired cyclized product via a stepwise pathway.

For the synthesis of spiro-Meldrum's acids and spiro-barbiturates, refluxing conditions were necessary due to difficulty in the decomposition of the corresponding diazo. As such, the corresponding diazo was added to a solution of the aminoalkyne, Rh_2esp_2, and PPh_3AuCl (10 mol%) and $AgSbF_6$ (10 mol%) and then allowed to reflux until the starting material was consumed via TLC.

2.4.2.1 Proposed Mechanism

Hunter conducted mechanistic insights, and the proposed mechanism has been summarized below. Specifically, Rh(II) decomposes diazo **21** to form Rh-carbenoid **25**. Carbenoid **25** can undergo an N–H insertion into the carbenoid to provide ylide intermediate **26** that can tautomerize to furnish rhodienolate Au acetylide species

27 or gold π complex **28**. This is catalyzed by the gold-activation of the propargyl group, inducing a Conia-ene cyclization to supply the desired cyclized product **29**. Alternatively, the ylide species can participate in a 1,2 proton transfer to yield the undesired insertion product **30** (**Figure 2.13**).

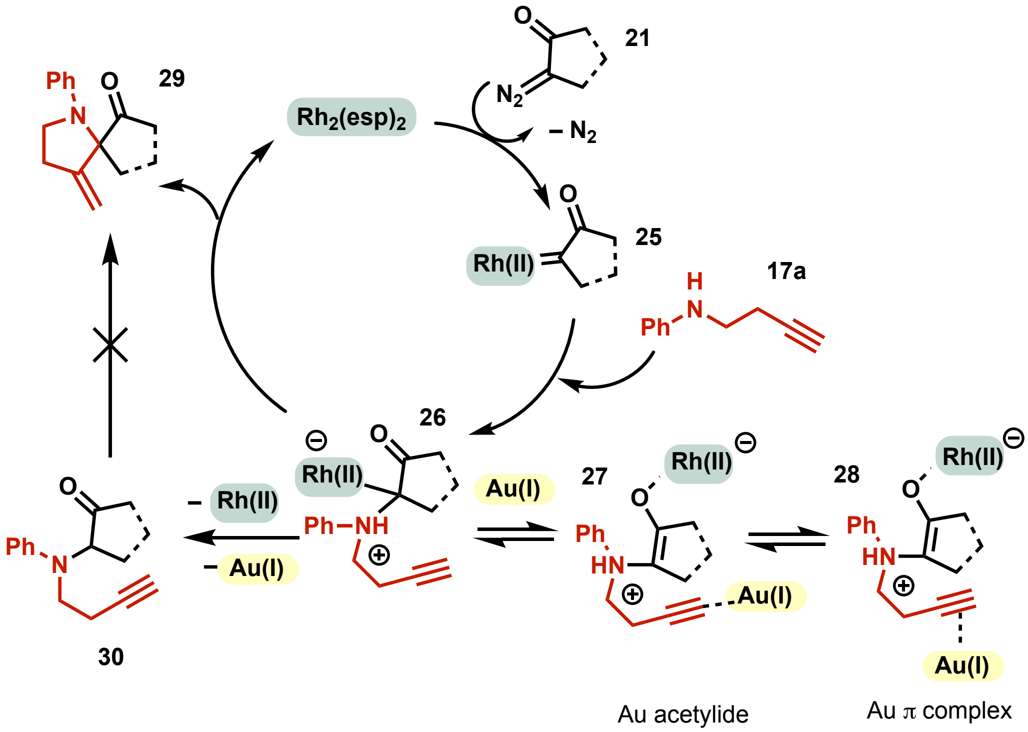
21
N_2
$Rh_2(esp)_2$
$- N_2$
29
Ph
O
N
O
25
Rh(II)
17a
H
N
Ph
26
O
Rh(II)
Ph–NH
Au(I)
27
Rh(II)
O
Ph
HN
Au(I)
28
Rh(II)
O
Ph
HN
Au(I)
– Rh(II)
– Au(I)
O
Ph
N
30
Au acetylide
Au π complex

Figure 2.13: Postulated N–H Insertion/Conia-ene Mechanism

Only A/A diazos will participate in a stepwise mechanism, where the insertion product **30** can be activated by cationic gold. No Conia-ene cyclization is observed with monocarbonyl diazos (pKa~20), as they predominately exist in their ketone form. Dicarbonyl systems, however, typically exist in the enol-form due to their lower pKa (~12).

2.4.2.2 Enantioselective Stepwise N–H Insertion/Conia-ene

We then thought to develop an enantioselective approach to spiroalkaloids, inspired by our previous studies. Our Rh(II)/Au approach did not observe any enantioinduction even when chiral rhodium salts were screened. As our Rh(II)/Au conditions require both substrates' fast and expedient activation, these conditions were not compatible with enantioinduction. We postulated that this is due to our system's poor transmission of ligand chirality. For non-asymmetric Conia-ene transformations, these tend to form purely from the propargyl group's activation. To account for this, we thought to develop a chiral enolate to produce some ee within our system.

Asymmetric reactions attract much attention within the synthetic community –the same is true for Conia-ene reactions. A standard method for asymmetric induction in Conia-ene reactions employs two metals: 1). a hard metal with chiral ligands for enolate activation and 2). a soft carbophilic metal to activate the propargyl group (**Figure 2.14**). The first of these reports was published by Toste in 2005, where the group reported an enantioselective Conia-ene protocol using a Pd(DTBMSegPhos) complex and $Yb(OTf)_3$ co-catalyst.[35c]

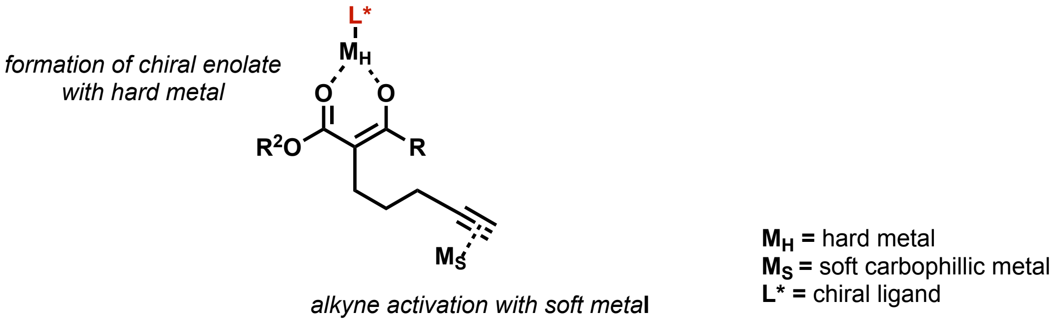
formation of chiral enolate with hard metal
L*
M_H
O
O
R²O
R
M_S
alkyne activation with soft metal
M_H = hard metal
M_S = soft carbophillic metal
L* = chiral ligand

Figure 2.14: Double Metal Activation for Enantioselective Conia-ene

To synthesize a chiral metal center, we turned to readily available bisoxazoline (BOX) ligands. Chiral ligands have served as one of the most dominant platforms for asymmetric catalysis.[39] Exceptionally, C_2 symmetric ligands, such as BOX ligands, have seen great successes in asymmetric transformations and can be synthesized reliably.[40]

In preliminary studies, we attempted a stepwise insertion/Conia-ene from aminoalkyne **17a** and A/A diazo **31**. First, the insertion product **32** was synthesized using Rh_2esp_2 in dichloromethane (**Figure 2.15a**). Once the starting material was consumed via TLC, the insertion product was purified and exposed to a chiral copper BOX complex in chloroform. **L1** was synthesized readily from L-leucine (**Figure 2.15b**).[41] We chose to begin preliminary studies with the Earth-abundant metal copper towards our goal of developing selective transformations with more sustainable methods. Enantioselectives were then measured via HLPC. While we could not induce significant ee, we were able to begin developing more sustainable transformations within the laboratory.

a) Preliminary Studies for Asymmetric Induction

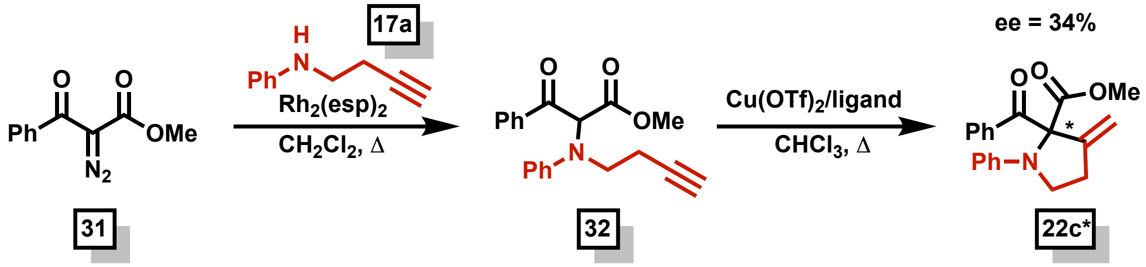
17a
H
Ph
N
Rh$_2$(esp)$_2$
CH$_2$Cl$_2$, Δ
O
O
Ph
OMe
N$_2$
31
Ph
OMe
Ph
N
32
Cu(OTf)$_2$/ligand
CHCl$_3$, Δ
ee = 34%
O
O
OMe
Ph
Ph–N
*
22c*

b) Synthesis of BOX ligand

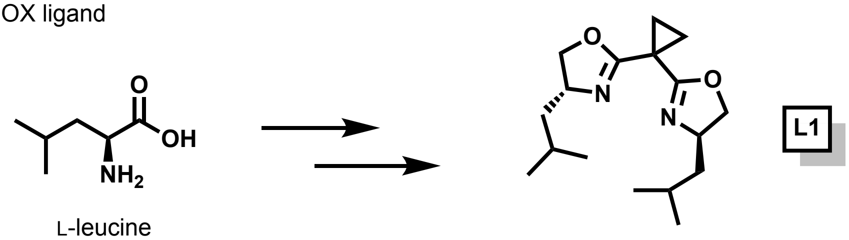
O
OH
NH$_2$
O
N
O
N
L1

L-leucine

Figure 2.15: Copper-catalyzed stepwise asymmetric Conia-ene reaction

2.5 ACCESS TO ALL CARBON SPIROCYCLES

To synthesize spirocarbocycles, we envisioned employing a similar system, utilizing our optimized Rh(II)/Au catalyst cocktail. For our initial investigation, diazo acetacetamide **33** was synthesized and exposed to a Rh(II)/Au catalyst cocktail to synthesize 5-membered spiro-systems. However, via NMR, we observed an undesired exo-glycal **35** due to the disfavoured 5-enolendo-*exo* dig cyclization (**Figure 2.16**).

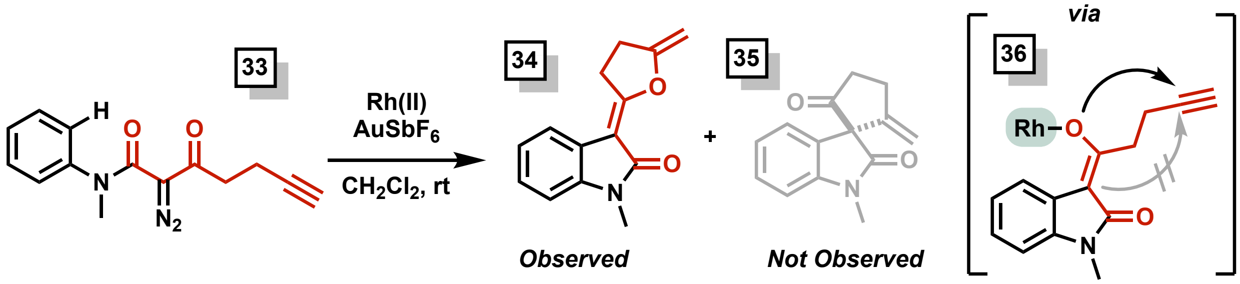

Figure 2.16: Initial Observations for [5,5] Spirocarbocycles

To circumvent this disfavoured cyclization, the carbon skeleton of the diazo precursor was elongated to successfully access 6- and 7-membered spirocycles. Mechanistically, this transformation proceeds through an initial *sp*^{2} C–H insertion into the rhodium-carbenoid, followed by an additional Conia-ene cyclization. A variety of Lewis acids were screened to optimize reaction conditions by Hunter, and a combinatory PPh_3AuCl/CuOTf system was found to be the best reaction condition. Rhodium salts were then screened. $Rh_2(HFB)_4$, a highly electron-deficient dirhodium catalyst, was found to give the most efficient transformation. These conditions were utilized to access both 6- and 7-membered spirocarbocycles (**Figure 2.17**).[18a]

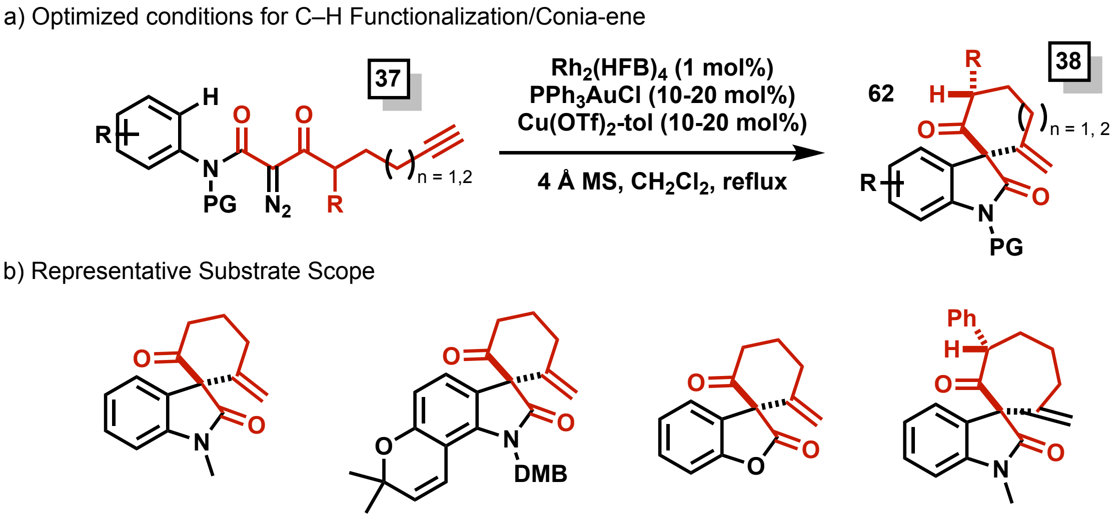
a) Optimized conditions for C–H Functionalization/Conia-ene

b) Representative Substrate Scope

37
Rh$_2$(HFB)$_4$ (1 mol%)
PPh$_3$AuCl (10-20 mol%)
Cu(OTf)$_2$-tol (10-20 mol%)
4 Å MS, CH$_2$Cl$_2$, reflux
38
62
n = 1,2
n = 1, 2
PG
DMB
Ph

38a, 68% **38b,** 87% **38c,** 72% **38d,** 54% dr 98:2

Figure 2.17: Access to [5,6] and [5,7] Spirocarbocycles

2.5.1 SYNTHESIS OF DIAZO ACETAMIDES & CONTRIBUTIONS TO WORK

To synthesize [5,5] spiro-systems, we utilized mono-carbonyl diazos **39** (**Figure 2.18**). As diazos bearing only one electron-withdrawing moiety are less stable, we hypothesized that these diazos could be decomposed without rhodium. As expected, when diazos **39** were subjected to cationic gold, we observed the desired 5-membered spirooxindoles. The parent compound **40a** was synthesized in 67%. Likewise, electron-donating analogue **40b** was synthesized in 69%. Finally, benzopyran fused system **40c** was synthesized in a 54% yield.

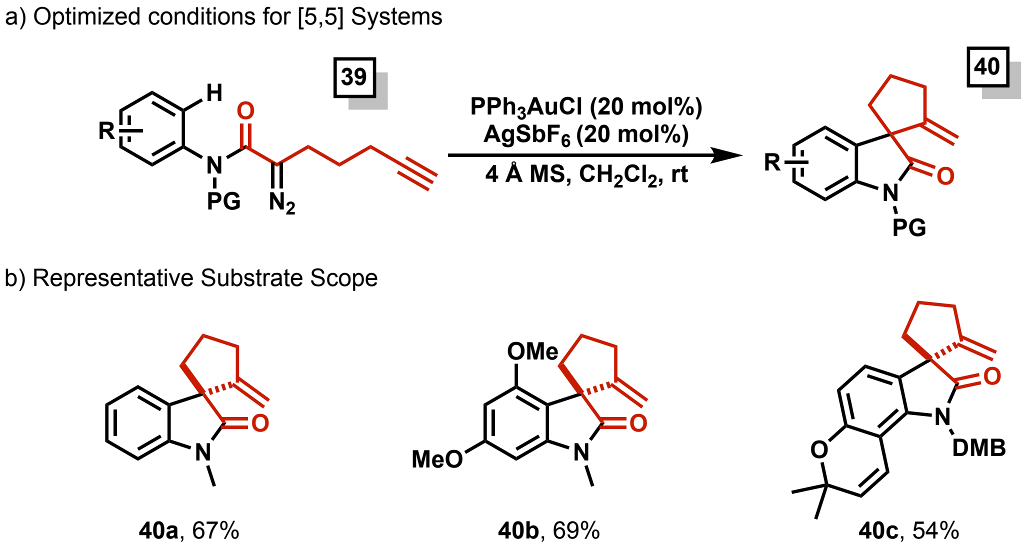
a) Optimized conditions for [5,5] Systems

b) Representative Substrate Scope

40a, 67%

40b, 69%

40c, 54%

Figure 2.18: Access to [5,5] Spirocarbocycles

My independent contributions to this work were the synthesis of monocarbonyl diazos **39b** and **39c**, whose preparation is detailed below. Diazo **39c** was synthesized in seven total steps from 2-methylbut-3-yn-2-ol (**41**).

2-methylbut-3-yn-2-ol (**41**) was coupled to 2-nitrophenol using copper-catalyzed conditions to form alkyne **42**. Alkyne **42** was then heated in xylenes to induce a thermally induced [3,3] sigmatropic rearrangement followed by a rearomatization and cyclization to form an inseparable mixture of regioisomers **43** and **44**,[42] which are then reduced by iron metal. Once reduced, the regioisomers could be separated and the desired aniline is then protected with 2,4 dimethoxybenzaldehyde to synthesize protected aniline **47**. Aniline **47** is then exposed to an acylated Meldrum's acid and subjected to refluxing toluene to open **48**, forming ketoamide **49**. Propargyl iodide **50** can be synthesized readily from the corresponding propargyl alcohol in one step and then exposed to ketoamide **49** to form the propargyl ketoamide **51**. Ketoamide **51** is then exposed to *p*ABSA and DBU to undergo a deacylative diazo transfer to yield the desired diazo **39c** (**Figure 2.19**).

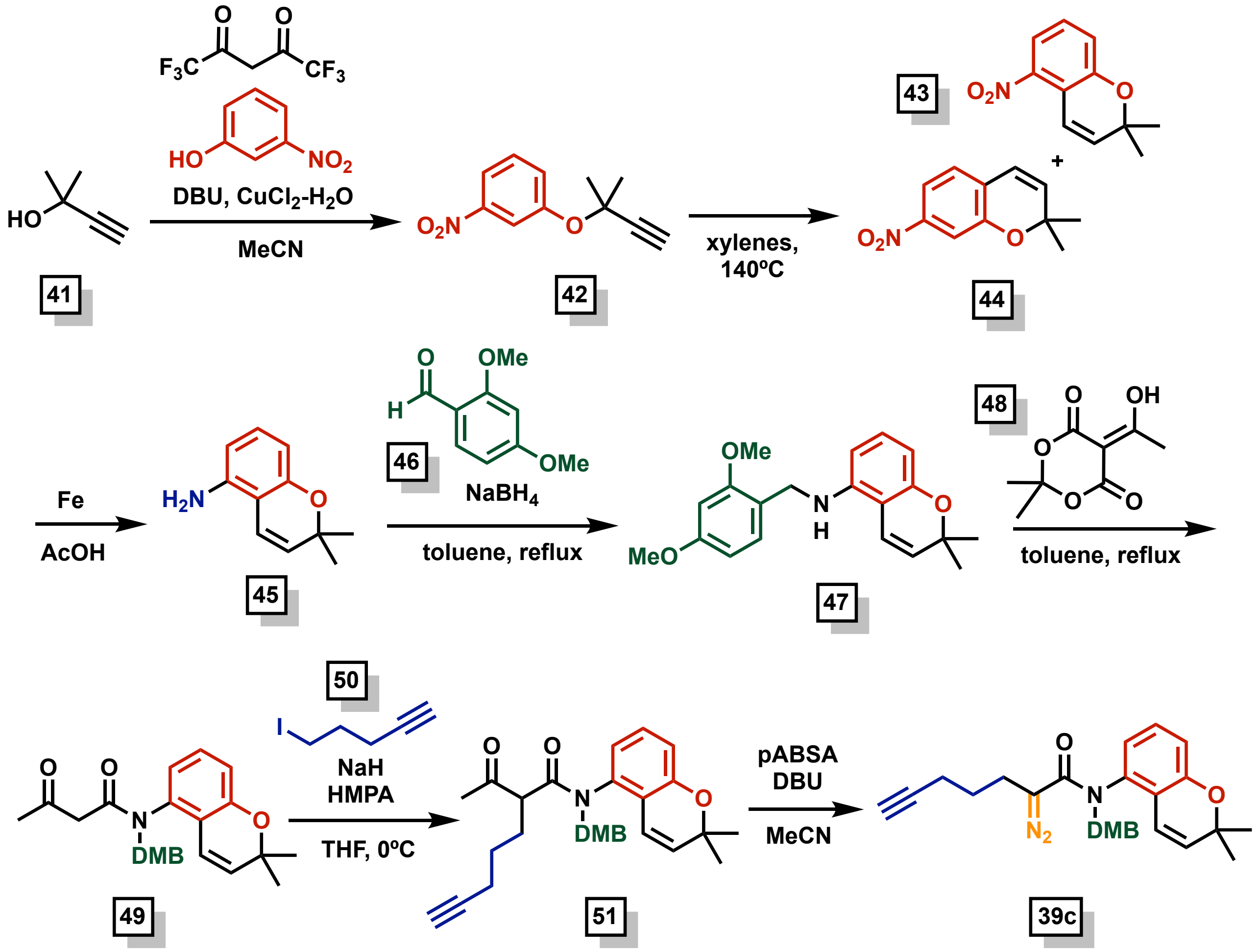
41
HO
F3C
CF3
HO
NO2
DBU, CuCl2-H2O
MeCN
O2N
O
42
xylenes, 140ºC
43
O2N
O
+
O2N
O
44
Fe
AcOH
H2N
O
45
46
H
OMe
OMe
NaBH4
toluene, reflux
MeO
OMe
N
H
O
47
48
O
OH
toluene, reflux
N
DMB
O
49
50
I
NaH
HMPA
THF, 0ºC
N
DMB
O
51
pABSA
DBU
MeCN
N2
N
DMB
O
39c

***Figure 2.19**:* Starting Material Preparation for Spirocarbocycles

Additionally, diazo **39b** was synthesized in a similar protocol from 1-(2,4-dimethoxyphenyl)-*N*-methylmethanamine (**52**) (**Figure 2.20**).

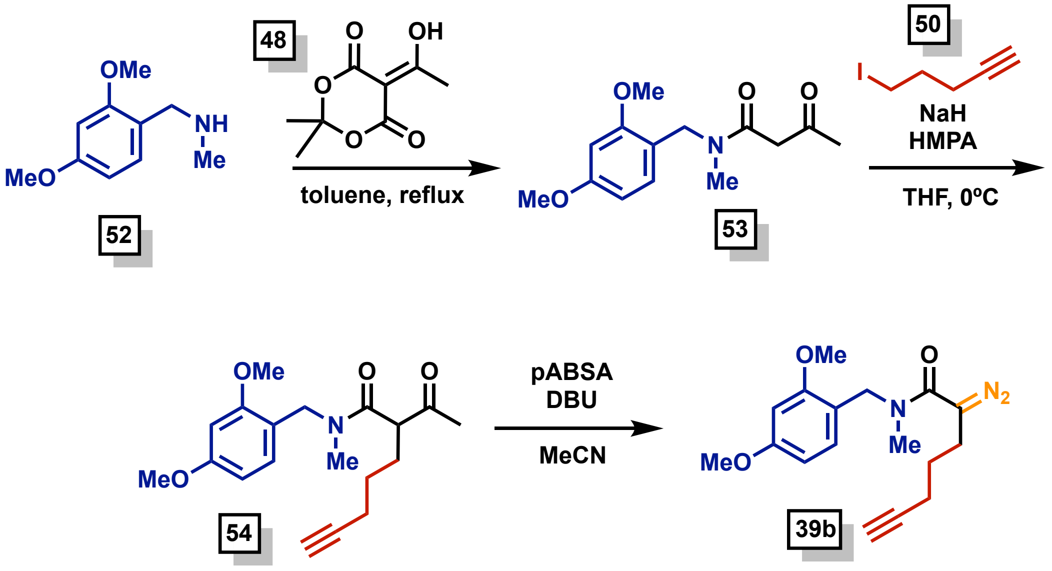

Figure 2.20: Synthesis and Preparation of Diazo **39b**

2.6 ACCESS TO SPIROETHERS: O–H INSERTION/ALDOL CASCADE

2.6.1 DEVELOPMENT OF EARTH-ABUNDANT CATALYSIS STRATEGIES

There is a dire need to develop greener, less wasteful synthetic methodologies in multistep reactions, particularly in drug development. Synthetic routes for relevant compounds often require several synthetic steps. Multistep (cascade) reactions remove the need to isolate and purify compound intermediates, thereby generating less waste and also negating the use of additional reagents and solvents.

Due to its economic advantages, iron-based catalysis can affect all industries, including agriculture, pharmaceutical manufacturing, and food processing. The limited amounts of precious metals available require extensive efforts to obtain, as opposed to the ease of acquiring Earth-abundant metals such as iron, copper, and zinc.[43] Likewise, today's population surges have led to the increased demand for metals in manufacturing and industrial practices. The utilization of these metals in these capacities can meet these needs while simultaneously offering economic advantages. As the cost of a drug is directly proportional to the cost of reagents, employing cheaper Earth-abundant metals poses a distinct advantage over traditional metal catalysis. Towards these goals, we began screening conditions to develop an O–H/Insertion/aldol cascade that featured Earth-abundant metal catalysts.

Inspired by Moody,[44] who developed an O-H insertion/aldol cascade using rhodium and copper salts, we thought to develop this system further to facilitate other Earth-abundant metals (**Table 2.1**). Due to its abundance, we began screening iron metal salts with an achiral tetramethyl BOX ligand **L2**.

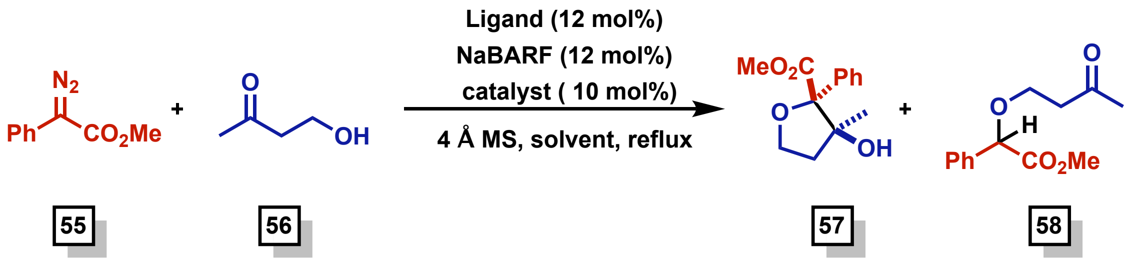

entry	catalyst	solvent	57 : 58	Yield
1	$FeCl_2$	CH_2Cl_2	nd	nd
2	$FeCl_2$	$CHCl_3$	3:1	35%
3	**$Fe(BF_4)_2$-$6H_2O$**	**CH_2Cl_2**	**3:1**	**54%**

*Optimization reactions were completed by dissolving keto alcohol (1 equiv.), ligand (12 mol%), NaBA$_r$F (12 mol%) and catalyst (10 mol%) were dissolved into 2 mL of dry solvent. The catalyst solution was then allowed to stir at room temperature for 1 h and then brought to reflux for an additional hour. Then, the diazo was dissolved into 1mL of the solvent and added to refluxing catalyst solution over 2 h. Once added, the syringe was quantitively washed with1 mL of the transfer solvent. The reaction was allowed to reflux overnight. The following day, the crude solution was filtered over a silica/celite pad and was analyzed via NMR. Compound was purified with silica gel chromatography. Anomeric ratios are based on the integration of crude spectra.

Table 2.1: Iron Metal Screening for O–H Insertion/Aldol Cascade

Iron is one of the most abundant metals in the Earth's crust and possesses "minimal safety concern" as 1,300-ppm residual iron is deemed acceptable in drug substances. This status represents a distinct advantage compared with the ≤ 10 ppm prescribed for most other transition metals, including rhodium.[43, 45] Preliminary screens led to the identification of $Fe(BF_4)_2$-$6H_2O$ in dichloromethane as optimal conditions for the desired transformation, with 3:1 ratio of the desired aldol to insertion product. Additionally, the aldol product was isolated in a 54% yield. With these conditions in hand, we then hypothesized that different BOX ligands may be able to induce a greater aldol:insertion ratio. As such, four ligands were synthesized (**L3-L6**), including three chiral ligands (**L4-L6**).

Bisoxazoline (BOX) ligands are commonly used in asymmetric catalysis as they can form highly ordered coordination complexes with metal salts. These ligands can be synthesized easily, as depicted. Suitable amino alcohols can be exposed to a dinitrile moiety and zinc salt to form the desired ligand in one step. As the chirality of the amino alcohol is retained in the BOX ligand, this method serves as a general and convenient route to access both chiral and achiral BOX ligands. Ligands **L2-L6** were synthesized in two steps from malononitrile **59** (**Figure 2.21a**). Malononitrile **59** was first dialkylated with

a) Synthesis of various BOX Ligands

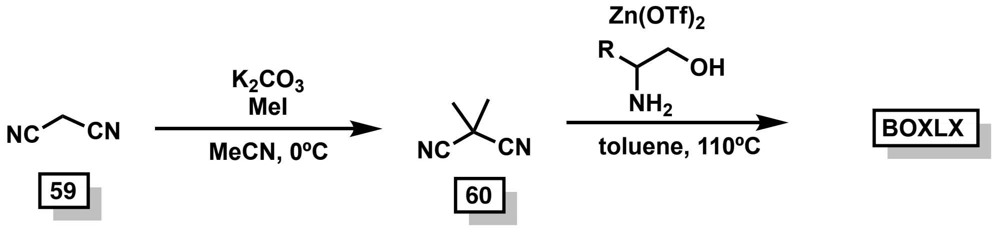

b). BOX Ligands synthesized and studied:

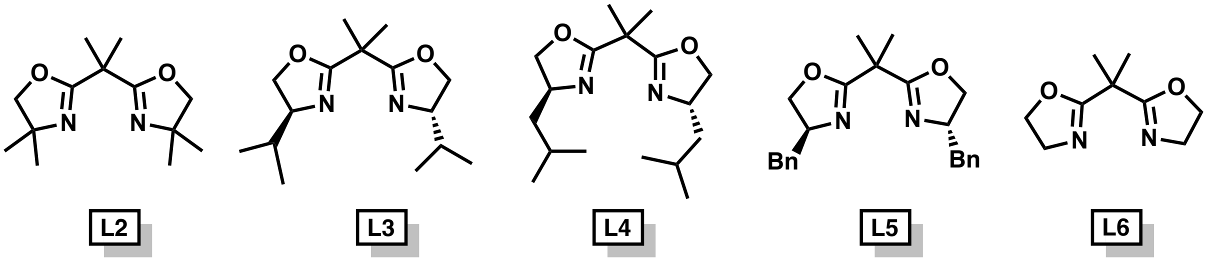

Figure 2.21: Synthesis of BOX Ligands screened

iodomethane, followed by refluxing in toluene with zinc (II) triflate to reliably synthesize the desired ligands (**Figure 2.21b**). Once synthesized, each ligand was exposed to the initial conditions; however, no significant increase in yields or ratios was observed. Additionally, ee was not measured for chiral ligands.

As no considerable aldol was observed in any condition, we then turned to oxindole diazo **61** for continued screening (**Table 2.2**). As we did not observe any increased aldol formation by screening ligands, this screening was completed without the addition of BOX ligands.

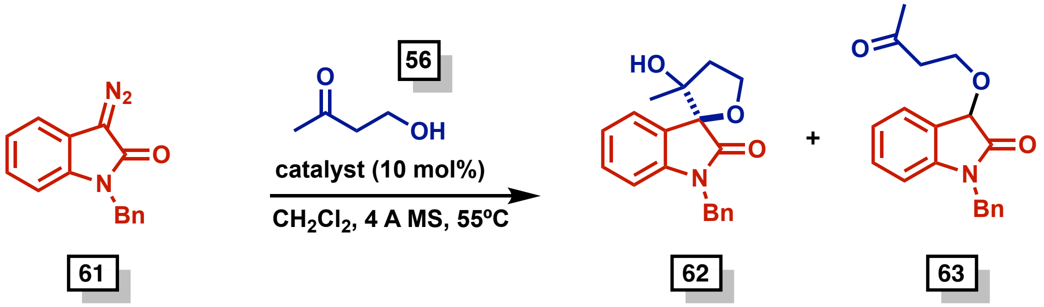

entry	catalyst	62 : 63	Yield
1	$FeCl_3$	63 only	nd
2	$Fe(ClO_4)XH_2O$	63 only	nd
3	$Fe(BF_4)_2$-$6H_2O$	63 only	nd
4	**$Zn(OTf)_2$**	**1 :19**	**93%**
5	$ZnCl_2$	1:4	nd
6	ZnI_2	1:5	nd
7	$In(OTf)_3$	63 only	nd

*Optimization reactions were completed by dissolving keto alcohol (1 equiv.) and catalyst (10 mol%) in 2 mL of dry CH_2Cl_2. The diazo was dissolved into 1mL of the solvent and added to refluxing catalyst solution over 1h. Once added, the syringe was quantitively washed with1 mL of the transfer solvent. The reaction was allowed to reflux overnight. The following day, the crude solution was filtered over a silica/celite pad and was analyzed via NMR. The compound was purified with silica gel chromatography. Anomeric ratios are based on the integration of crude spectra.

Table 2.2: Catalyst Screening with Oxindole Diazo

We continued screening Earth-abundant catalysts for the O–H insertion/aldol cascade with diazo oxindole diazo **61**. Iron-metal catalysts resulted in the exclusive formation of the insertion product **62** (**entries 1-3**). We then turned to zinc salts as iron could not perform the desired transformation. Zinc is the 24th most abundant element in the Earth's crust. Additionally, zinc is a dietary requirement, and most adults intake several milligrams daily. Surprisingly, when Zn(OTf)$_2$ was screened, it resulted in 1:19 (insertion: aldol) reaction. Further, the aldol product was isolated via a silica gel column at a 93% yield. To further probe the reaction with zinc salts, we subjected both zinc chloride and zinc iodide to the reaction conditions; however, these trials resulted in a higher ratio of the undesired insertion product (**entries 5**,**6**).

2.7 CONCLUSIONS AND SUMMARIES

We have developed a synergistic cascade utilizing diazo-derived metal carbenoids to access privileged spirocyclic motifs. Notably, we utilized Hunter's Rh(II)/Au catalyst combination to access spirocyclic alkaloids and spirocarbocycles. To expand upon this methodology and access enantioselective transformations, we conducted preliminary studies to access spiroalkaloids via a stepwise N–H insertion/Conia-ene sequences using chiral copper BOX complexes to induce moderate 34% ee. Further, we continued the development of our X–H insertion cascade sequences to access spirooxindoles, utilizing an O–H insertion/aldol tandem sequence. With these studies, we have identified zinc (II) triflate as a suitable catalyst and isolated the desired spirooxindole in a 93% yield.

Here, we have disclosed metal-carbenoid based methods to synthesize diverse spirocyclic motifs –one of the *least studied* moieties in drug discovery. The following chapters will discuss our attempts to access the *most abundant* natural product scaffold, carbohydrates, using metal carbenoid systems.

2.8 REFERENCES FOR CHAPTER 2

[1] E. Chupakhin, O. Babich, A. Prosekov, L. Asyakina, M. Krasavin, *Molecules* **2019**, *24*, 4165.

[2] K. Hiesinger, D. Dar'in, E. Proschak, M. Krasavin, *Journal of Medicinal Chemistry* **2021**, *64*, 150-183.

[3] C. Sabbadin, L. A. Calò, D. Armanini, *G Ital Nefrol* **2016**, *33 Suppl 66*, 33.S66.12.

[4] a). D. A. Sica, *Methodist Debakey Cardiovasc J* **2015**, *11*, 235-239; b). I. Dams, A. Białońska, P. Cmoch, M. Krupa, A. Pietraszek, A. Ostaszewska, M. Chodyński, *Molecules* **2017**, *22*, 1354.

[5] W. Wan, G. Ma, W. Gao, J. Wang, L. Li, S. Rao, C. Zheng, H. Jiang, H. Deng, J. Hao, *Organic & Biomolecular Chemistry* **2013**, *11*, 6597-6603.

[6] Y. Zheng, C. M. Tice, S. B. Singh, *Bioorganic & Medicinal Chemistry Letters* **2014**, *24*, 3673-3682.

[7] S. P. Green, K. M. Wheelhouse, A. D. Payne, J. P. Hallett, P. W. Miller, J. A. Bull, *Organic Process Research & Development* **2020**, *24*, 67-84.

[8] a). M. Jia, S. Ma, *Angewandte Chemie International Edition* **2016**, *55*, 9134-9166; b). J. R. Fulton, V. K. Aggarwal, J. de Vicente, *European Journal of Organic Chemistry* **2005**, *2005*, 1479-1492; c). S. Xie, Z. Yan, Y. Li, Q. Song, M. Ma, *The Journal of Organic Chemistry* **2018**, *83*, 10916-10921; d). D. Dar'in, G. Kantin, M. Krasavin, *Chemical Communications* **2019**, *55*, 5239-5242.

[9] in *Comprehensive Organic Name Reactions and Reagents*, pp. 2322-2325.

[10] A. Ford, H. Miel, A. Ring, C. N. Slattery, A. R. Maguire, M. A. McKervey, *Chem Rev* **2015**, *115*, 9981-10080.

[11] a). D. Zhu, L. Chen, H. Fan, Q. Yao, S. Zhu, *Chemical Society Reviews* **2020**, *49*, 908-950; b). B. D. Bergstrom, L. A. Nickerson, J. T. Shaw, L. W. Souza, *Angewandte Chemie International Edition* **2021**, *60*, 6864-6878.

[12] a). A. Padwa, M. D. Weingarten, *Chem. Rev. (Washington, D. C.)* **1996**, *96*, 223-269; b). M. P. Doyle, M. A. McKervey, T. Ye, *Modern Catalytic Methods for Organic Synthesis with Diazo Compounds: From Cyclopropanes to Ylides*; c). M. P. Doyle, D. C. Forbes, *Chemical Reviews* **1998**, *98*, 911-936; d). H. M. L. Davies, J. R. Denton, *Chemical Society Reviews* **2009**, *38*, 3061-3071; e). K. Liao, S. Negretti, D. G. Musaev, J. Bacsa, H. M. Davies, *Nature* **2016**, *533*, 230-234; f). H. M. L. Davies, K. Liao, *Nature Reviews Chemistry* **2019**, *3*, 347-360.

[13] a). C. J. Moody, R. J. Taylor, *Tetrahedron Lett.* **1987**, *28*, 5351-5352; b). G. G. Cox, D. J. Miller, C. J. Moody, E.-R. H. B. Sie, J. J. Kulagowski, *Tetrahedron* **1994**, *50*, 3195-3212.

[14] a). R. R. Nani, S. E. Reisman, *J. Am. Chem. Soc.* **2013**, *135*, 7304-7311; b). S. Zhu, J. A. Perman, X. P. Zhang, *Angew. Chem., Int. Ed.* **2008**, *47*, 8460-8463; c). S. Zhu, X. Xu, J. A. Perman, X. P. Zhang, *J. Am. Chem. Soc.* **2010**, *132*, 12796-12799.

[15] a). J. F. Briones, H. M. L. Davies, *Org. Lett.* **2011**, *13*, 3984-3987; b). X. Cui, X. Xu, H. Lu, S. Zhu, L. Wojtas, X. P. Zhang, *J. Am. Chem. Soc.* **2011**, *133*, 3304-3307; c). M. Uehara, H. Suematsu, Y. Yasutomi, T. Katsuki, *J. Am. Chem. Soc.* **2011**, *133*, 170-171.

[16] a). Y. Jie, P. Livant, H. Li, M. Yang, W. Zhu, V. Cammarata, P. Almond, T. Sullens, Y. Qin, E. Bakker, *J. Org. Chem.* **2010**, *75*, 4472-4479; b). X. Li, D. P. Curran, *J. Am. Chem. Soc.* **2013**, *135*, 12076-12081; c). J. T. Malinowski, R. J. Sharpe, J. S. Johnson, *Science (Washington, DC, U. S.)* **2013**, *340*, 180-182; d). C. S. Shanahan, P. Truong, S. M. Mason, J. S. Leszczynski, M. P. Doyle, *Org. Lett.* **2013**, *15*, 3642-3645.

[17] a). M. Hu, C. Ni, J. Hu, *J. Am. Chem. Soc.* **2012**, *134*, 15257-15260; b). Y. Liu, X. Shao, P. Zhang, L. Lu, Q. Shen, *Org. Lett.* **2015**, *17*, 2752-2755.

[18] a). A. C. Hunter, K. Chinthapally, A. I. Bain, J. C. Stevens, I. Sharma, *Advanced Synthesis & Catalysis* **2019**, *361*, 2951-2958; b). Y. Dong, B. Mei, X.-P. Zhang, H. Xu, *The Journal of Organic Chemistry* **2021**, *86*, 11660-11672; c). F. Xie, Z. Zhang, X. Yu, G. Tang, X. Li, *Angew. Chem., Int. Ed.* **2015**, *54*, 7405; d). C. Qin, H. M. L. Davies, *Journal of the American Chemical Society* **2014**, *136*, 9792-9796; e). Z. Yu, B. Ma, M. Chen, H.-H. Wu, L. Liu, J. Zhang, *Journal of the American Chemical Society* **2014**, *136*, 6904-6907.

[19] A. Padwa, S. F. Hornbuckle, *Chem. Rev.* **1991**, *91*, 263–309.

[20] a). K. C. Nicolaou, J. S. Chen, *Chemical Society Reviews* **2009**, *38*, 2993-3009; b). A. C. Hunter, B. Almutwalli, A. I. Bain, I. Sharma, *Tetrahedron* **2018**, *74*, 5451-5457.

[21] a). V. V. Pagar, A. M. Jadhav, R.-S. Liu, *Journal of the American Chemical Society* **2011**, *133*, 20728-20731; b). S. K. Pawar, C. D. Wang, S. Bhunia, A. M. Jadhav, R. S. Liu, *Angew Chem Int Ed Engl* **2013**, *52*, 7559-7563; c). F. Urabe, S. Miyamoto, K. Takahashi, J. Ishihara, S. Hatakeyama, *Organic Letters* **2014**, *16*, 1004-1007; d). C. Qin, H. M. L. Davies, *Journal of the American Chemical Society* **2013**, *135*, 14516-14519; e). Q.-Q. Cheng, Y. Deng, M. Lankelma, M. P. Doyle, *Chemical Society Reviews* **2017**, *46*, 5425-5443; f). K. O. Marichev, M. P. Doyle, *Organic & Biomolecular Chemistry* **2019**, *17*, 4183-4195; g). X. Xu, M. P. Doyle, *Acc Chem Res* **2014**, *47*, 1396-1405.

[22] A. Padwa, *Top. Curr. Chem.* **1997**, *189*, 121-158.

[23] a). Y. Jiang, R. E. McNamee, P. J. Smith, A. Sozanschi, Z. Tong, E. A. Anderson, *Chemical Society Reviews* **2021**, *50*, 58-71; b). L. F. Tietze, U. Beifuss, *Angewandte Chemie International Edition in English* **1993**, *32*, 131-163; c). K. C. Nicolaou, D. J. Edmonds, P. G. Bulger, *Angewandte Chemie International Edition* **2006**, *45*, 7134-7186.

[24] a). A. C. Jones, J. A. May, R. Sarpong, B. M. Stoltz, *Angewandte Chemie International Edition* **2014**, *53*, 2556-2591; b). H. Yorimitsu, *The Chemical Record* **2017**, *17*, 1156-1167.

[25] a). J. Liao, X. Yang, L. Ouyang, Y. Lai, J. Huang, R. Luo, *Organic Chemistry Frontiers* **2021**, *8*, 1345-1363; b). K. Sun, Q.-Y. Lv, Y.-W. Lin, B. Yu, W.-M. He, *Organic Chemistry Frontiers* **2021**, *8*, 445-465; c). W.-C. Yang, M.-M. Zhang, J.-G. Feng, *Advanced Synthesis & Catalysis* **2020**, *362*, 4446-4461; d). E. Godineau, Y. Landais, *Chemistry – A European Journal* **2009**, *15*, 3044-3055.

[26] a). Y. Xia, Y. Zhang, J. Wang, *ACS Catalysis* **2013**, *3*, 2586-2598; b). D. Qian, J. Zhang, *Chem Rec* **2014**, *14*, 280-302; c). A. Padwa, *Chemical Society Reviews* **2009**, *38*, 3072-3081; d). J. Xiao, X. Li, *Angewandte Chemie International Edition* **2011**, *50*, 7226-7236.

[27] I. V. Alabugin, B. Gold, *The Journal of Organic Chemistry* **2013**, *78*, 7777-7784.

[28] A.-H. Li, L.-X. Dai, *Chem. Rev.* **1997**, *97*, 2341–2372.

[29] a). A. C. Hunter, S. C. Schlitzer, J. C. Stevens, B. Almutwalli, I. Sharma, *The Journal of Organic Chemistry* **2018**, *83*, 2744-2752.; b). Hunter, A. C.; Schlitzer, S. C.; Sharma, I. *Chem. Eur. J.* **2016**, *22*, 16062–16065.

[30] A. E. Allen, D. W. Macmillan, *Chem. Sci.* **2012**, *2012*, 633–658.

[31] a). H. Noda, K. Motokura, W.-J. Chun, A. Miyaji, S. Yamaguchi, T. Baba, *Catalysis Science & Technology* **2015**, *5*, 2714-2727; b). Z.-X. Wang, Z. Zhou, W. Xiao, Q. Ouyang, W. Du, Y.-C. Chen, *Chemistry – A European Journal* **2017**, *23*, 10678-10682.

[32] a). P.-S. Wang, D.-F. Chen, L.-Z. Gong, *Topics in Current Chemistry* **2019**, *378*, 9; b). C. Song, J. Wang, Z. Xu, *Organic & Biomolecular Chemistry* **2014**, *12*, 5802-5806; c). S. Martínez, L. Veth, B. Lainer, P. Dydio, *ACS Catalysis* **2021**, *11*, 3891-3915.

[33] a). A. C. Hunter, K. Chinthapally, I. Sharma, *European Journal of Organic Chemistry* **2016**, *2016*, 2260-2263; b). A. I. Bain, K. Chinthapally, A. C. Hunter, I. Sharma, *European Journal of Organic Chemistry* **2022**, *n/a*, e202101419.

[34] D. Hack, M. Blümel, P. Chauhan, A. R. Philipps, D. Enders, *Chemical Society Reviews* **2015**, *44*, 6059-6093.

[35] a). B. K. Corkey, F. D. Toste, *Journal of the American Chemical Society* **2007**, *129*, 2764-2765; b). J. J. Kennedy-Smith, S. T. Staben, F. D. Toste, *Journal of the American Chemical Society* **2004**, *126*, 4526-4527; c). B. K. Corkey, F. D. Toste, *Journal of the American Chemical Society* **2005**, *127*, 17168-17169.

[36] M. Blümel, D. Hack, L. Ronkartz, C. Vermeeren, D. Enders, *Chemical Communications* **2017**, *53*, 3956-3959.

[37] X.-L. Yu, L. Kuang, S. Chen, X.-L. Zhu, Z.-L. Li, B. Tan, X.-Y. Liu, *ACS Catalysis* **2016**, *6*, 6182-6190.

[38] S. W. Youn, S. R. Lee, *Organic & Biomolecular Chemistry* **2015**, *13*, 4652-4656.

[39] A. Pfaltz, W. J. Drury, *Proceedings of the National Academy of Sciences* **2004**, *101*, 5723-5726.

[40] a). D. A. Evans, S. J. Miller, T. Lectka, P. von Matt, *Journal of the American Chemical Society* **1999**, *121*, 7559-7573; b). J. M. Fraile, P. López-Ram-de-Viu, J. A. Mayoral, M. Roldán, J. Santafé-Valero, *Organic & Biomolecular Chemistry* **2011**, *9*, 6075-6081; c). G. Desimoni, G. Faita, K. A. Jørgensen, *Chemical Reviews* **2011**, *111*, PR284-PR437.

[41] Y. Yamashita, A. Noguchi, S. Fushimi, M. Hatanaka, S. Kobayashi, *Journal of the American Chemical Society* **2021**, *143*, 5598-5604.

[42] K. K. Gruner, H.-J. Knölker, *Organic & Biomolecular Chemistry* **2008**, *6*, 3902-3904.
[43] A. Fürstner, *ACS Central Science* **2016**, *2*, 778-789.
[44] S. M. Nicolle, W. Lewis, C. J. Hayes, C. J. Moody, *Angewandte Chemie International Edition* **2015**, *54*, 8485-8489.
[45] E. B. Bauer, *Top. Organomet. Chem.* **2015**, *50*, 1-18.

2.9 EXPERIMENTAL SECTION FOR CHAPTER 2

MATERIALS AND METHODS

Reagents

Reagents and solvents were obtained from Sigma-Aldrich, Chem-Impex, VWR International, and Acros Organics and used without further purification unless otherwise indicated. Dichloromethane and Acetonitrile were distilled over CaH under N_2 unless stated otherwise. Tetrahydrofuran was distilled over Na under N_2 with benzophenone indicator.

Glassware

All reactions were performed in flame-dried glassware under positive N_2 pressure with magnetic stirring unless otherwise noted.

Chromatography

Thin layer chromatography (TLC) was performed on 0.25 mm E. Merck silica gel 60 F254 plates and visualized under UV light (254 nm) or by staining with potassium permanganate ($KMnO_4$), cerium ammonium molybdate (CAM), phosphomolybdic acid

(PMA), and ninhydrin. Silica flash chromatography was performed on Sorbtech 230-400 mesh silica gel 60.

Analytical Instrumentation

NMR spectra were recorded on a Varian VNMRS 300, 400, 500, and 600 MHz NMR spectrometer at 20 ºC in $CDCl_3$ unless otherwise indicated. Chemical shifts are expressed in ppm relative to solvent signals: $CDCl_3$ (1H, 7.26 ppm, 13C, 77.0 ppm); coupling constants are expressed in Hz. IR spectra were recorded on a Cary 760 FTIR spectrometer with peaks reported in cm^{-1}. Mass spectra were obtained on an Advion Expression CMS TLC Mass Spectrometer

Nomenclature

Chemical structure named in accordance with IUPAC guidelines, automatically generated using ChemDraw 20.1

Additional Information and Considerations

Syringe pump addition reactions were conducted using a Harvard Apparatus (Model: 55-1111) or a New Era Pump Systems, Inc. (Model: NE-300) syringe pump. Sonication was performed using a Bransonic Ultrasonic Cleaner (Model: M5800H).

PUBLICATION AND CONTRIBUTIONS STATEMENT

The research presented in this chapter was published in *Tetrahedron* **2018**, *74*, 5451–5457. **DOI:** 10.1016/j.tet.2018.06.042 and *Adv. Synth. Catal.* **2019**, *361*, 2951–2958. **DOI:** 10.1002/adsc.201900079 as third and second author respectively. Only materials synthesized by Bain will be reported within.

2.9.1 Synthesis of Spirocyclic Alkaloids

2.9.1.1 Synthesis of Aminoalkynes

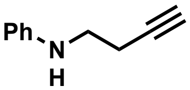

***N*-(but-3-yn-1-yl)aniline (17a):** Compound was prepared from a literature-reported procedure from aniline. The values of the NMR spectra are in accordance with reported literature data [1]

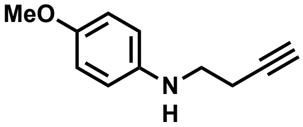

***N*-(but-3-yn-1-yl)-4-methoxyaniline (17b):** Compound was prepared from a literature-reported procedure from aniline. The values of the NMR spectra are in accordance with reported literature data [1]

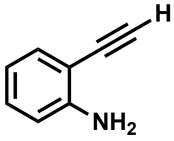

2-ethynylaniline (20): Compound was prepared from a literature-reported procedure from 2-iodoaniline. The values of the NMR spectra are in accordance with reported literature data [2]

2.9.1.2 Synthesis of Diazo Compounds

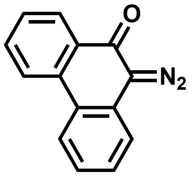

10-diazophenanthren-9(10*H*)-one (21a): Compound was prepared from a literature-reported procedure. The values of the NMR spectra are in accordance with reported literature data [3]

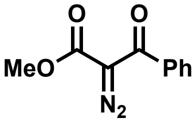

methyl 2-diazo-3-oxo-3-phenylpropanoate (21c): Compound was prepared from a literature-reported procedure. The values of the NMR spectra are in accordance with reported literature data [4]

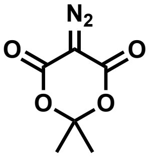

5-diazo-2,2-dimethyl-1,3-dioxane-4,6-dione (21d): Compound was prepared from a literature-reported procedure. The values of the NMR spectra are in accordance with reported literature data [5]

2.9.1.3 N-H Insertion/Cona-ene Reactions

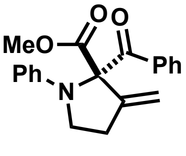

methyl-2-benzoyl-3-methylene-1-phenylpyrrolidine-2-carboxylate (22c): To a 4.0 mL vial equipped with a magnetic stir bar was added $Rh_2(esp)_2$ (1 mol %) and a solution of (but-3-yn-1-yl)-aniline (1.1 equiv.). The diazo (1.0 equiv.) in dichloromethane (0.3 M) was added, and the reaction vessel was sealed and allowed to stir at reflux until bubbling ceased and the diazo was consumed via TLC in 20 minutes. (Take caution when opening reaction flask as the evolution of N_2 gas creates a pressurized system.) Once the insertion product had formed PPh_3AuCl (10 mol %), and $AgSbF_6$ (10 mol %) was added directly into the reaction vessel and this solution was allowed to stir an additional 30 min until the insertion product was no longer visible on TLC and a new, more polar spot had formed (the cyclization product). Once the reaction was complete, the crude reaction mixture was filtered through a slurry of celite/silica gel, concentrated, and analyzed via crude 1H NMR. The crude mixture was then purified via flash chromatography (10% EtOAc/ 90% Hexanes) to furnish **22c** as a yellow oil.

IR (NaCl): 3059, 2949, 2916, 2849, 2320, 1740,1678.

^{1}H NMR (600 MHz, $CDCl_3$) d 7.68 (dd, J ¼ 8.4, 1.4 Hz, 2H), 7.35 (ddt, J ¼ 8.8, 7.3, 1.3 Hz, 1H), 7.24e7.19 (m, 2H), 7.11e7.05 (m, 2H),6.67 (td, J ¼ 7.3, 1.0 Hz, 1H), 6.61 (dq, J ¼ 7.3, 1.5, 1.0 Hz, 2H), (m, 2H), 3.87 (dt, J ¼ 8.9, 7.5 Hz, 1H), 3.73 (s, 3H), 3.64 (dt, J ¼ 8.7, 7.2 Hz, 1H), 2.98 (tt, J ¼ 7.3, 2.3 Hz, 2H).

^{13}C NMR (151 MHz, $CDCl_3$) d 197.2, 169.2, 146.4, 145.1, 136.0, 132.2, 128.8 (2C), 128.7 (2C),127.9 (2C), 118.2, 113.7, 112.8, 80.3, 74.8, 52.7, 47.8, 30.0.

HRMS (ESI) m/z calcd for $C_{20}H_{19}NO_3Na+$ 344.1263; found 344.1272.

2.9.2 Synthesis of Spirocarbocycles

2.9.2.1 Synthesis of Propargyl Keto Diazos

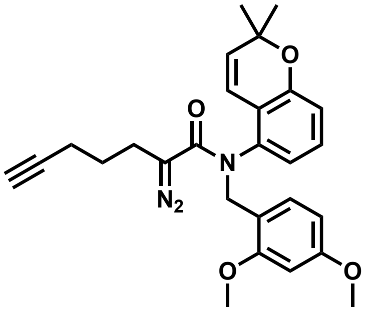

2-diazo-N-(2,4-dimethoxybenzyl)-N-(2,2-dimethyl-2H-chromen-5-yl)hept-6-ynamide (39c): Synthesized in aforementioned protocol (pg 42) Yellow oil (89 mg, 37%).

R$_f$ 0.54 (30% EtOAc in Hexanes).

IR (NaCl): 3435, 3318, 3059, 3028, 2378, 2311, 2218, 1647, 1618, 1570, 1545, 1489, 1449, 1423, 1362, 1335, 1302, 1275, 1227, 1173, 1013, 978, 858, 827, 777, 743, 698, 679, 635.

^{1}H NMR (600 MHz, Chloroform-d) δ 7.30 (d, J = 8.3 Hz, 1H), 6.98 (t, J = 8.0 Hz, 1H), 6.72 (d, J = 8.1 Hz, 1H), 6.50 (dd, J = 7.9, 1.0 Hz, 1H), 6.40 (dd, J = 8.3, 2.4 Hz, 1H), 5.59 (d, J = 10.0 Hz, 1H), 4.99 (d, J = 14.2 Hz, 1H), 4.72–4.66 (d, J = 14.2 Hz, 1H), 3.77 (s, 3H), 3.48 (s, 3H), 2.38 (dh, J = 28.7, 7.4 Hz, 2H), 2.19 (td, J = 7.1, 2.6 Hz, 2H), 1.92 (t, J = 2.6 Hz, 1H), 1.65 (p, J = 7.3 Hz, 2H), 1.39 (s, 6H).

^{13}C NMR (151 MHz, Chloroform-d) δ 166.0, 160.3, 158.7, 153.5, 137.9, 132.1, 132.0, 128.7, 121.3, 120.0, 117.8, 117.6, 116.3, 103.9, 98.1, 83.4, 75.8, 68.8, 60.4, 55.3, 55.0, 48.0, 27.1, 27.7, 26.5, 24.9, 17.6.

HRMS (ESI) m/z calcd for $C_{27}H_{29}NO_4Na$ ([M+Na-N2] +) 454.1995; found 454.1976.

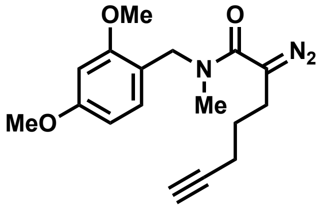

2-diazo-*N*-(2,4-dimethoxybenzyl)-*N*-methylhept-6-ynamide (39b): Synthesized in aforementioned protocol (pg 43) in three steps from 1-(2,4-dimethoxyphenyl)-*N*-methylmethanamine.

R$_f$ = 0.42 (30% EtOAc in Hex).

IR (NaCl): 3296, 2937, 2107, 2067, 1708.

^{1}H NMR (500 MHz, Chloroform-d) δ 6.41–6.38 (m, 1H), 6.36 (d, J = 1.6 Hz, 2H), 3.79 (s, 6H), 3.31 (s, 3H), 2.39 (t, J = 7.4 Hz, 2H), 2.22 (td, J = 7.0, 2.4 Hz, 2H), 1.95 (t, J = 2.5 Hz, 1H), 1.71 (p, J = 7.1 Hz, 2H).

^{13}C NMR (126 MHz, Chloroform-d) δ 161.6, 145.7 (2C), 131.6, 104.8 (2C), 99.1 (2C), 83.3, 69.0, 55.5 (2C), 38.8, 26.4, 24.4, 17.7.

HRMS (ESI) m/z calcd for C16H19N3O3Na ([M+Na]+) 324.1324; found 324.1307

2.9.3 O–H Insertion/Aldol Cascade

2.9.3.1 Synthesis of BOX Ligands

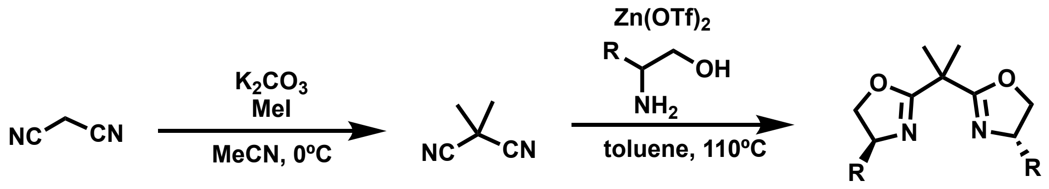
NC CN
K2CO3
MeI
MeCN, 0ºC
NC CN
Zn(OTf)2
R OH
NH2
toluene, 110ºC
O N
R

BOX Ligands L1-L6 were synthesized from the following two-step protocol, from malononitrile and the corresponding amino alcohol.

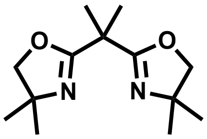

2,2'-(propane-2,2-diyl)bis(4,4-dimethyl-4,5-dihydrooxazole) (L2): Synthesized from the aforementioned protocol using 2-amino-2-methylpropan-1-ol. The values of the NMR spectra are in accordance with reported literature data.[6]

^{1}H NMR (500 MHz, $CDCl_3$) δ 3.91 (s, *J* = 1.4 Hz, 4H), 1.48 (s, *J* = 1.3 Hz, 6H), 1.26 (s, *J* = 1.8 Hz, 12H).

^{13}C NMR (101 MHz, $CDCl_3$) δ 167.62, 79.37, 66.95, 38.20, 28.01, 24.35.

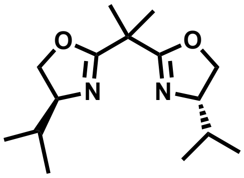

(4*S*,4'*S*)-2,2'-(propane-2,2-diyl)bis(4-isopropyl-4,5-dihydrooxazole) (L3): Synthesized from the aforementioned protocol using L-valinol. The values of the NMR spectra are in accordance with reported literature data.[7]

^{1}H NMR (400 MHz, $CDCl_3$) δ 4.19 (td, *J* = 7.5, 1.4 Hz, 2H), 4.03 – 3.92 (m, 4H), 1.85 – 1.75 (m,2H), 1.50 (d, *J* = 1.8 Hz, 6H), 0.89 (d, 6H), 0.84 (d, *J* = 6.8 Hz, 6H).

^{13}C NMR (101 MHz, $CDCl_3$) δ 168.78, 71.46, 69.91, 38.56, 32.18, 24.45, 18.55, 17.32.

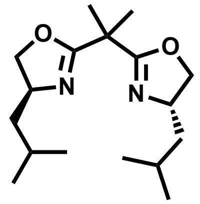

(4*S*,4'*S*)-2,2'-(propane-2,2-diyl)bis(4-isobutyl-4,5-dihydrooxazole) (L4): Synthesized from the aforementioned protocol using L-leucinol. The values of the NMR spectra are in accordance with reported literature data.[8]

^{1}H NMR (400 MHz, $CDCl_3$) δ 4.32 (dd, *J* = 9.3, 8.0 Hz, 2H), 4.20 – 4.08 (m, 2H), 3.85 (m, *J* = 7.8 Hz, 2H), 1.56 (s, 6H), 1.50 (s, 6H), 1.29 (dd, *J* = 6.6, 1.9 Hz, 1H), 0.92 (t, *J* = 6.5 Hz, 12H).

^{13}C NMR (101 MHz, $CDCl_3$) δ 168.65, 73.34, 64.52, 45.24, 38.43, 25.31, 24.35, 23.18, 22.40.

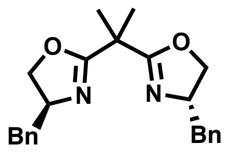

(4*S*,4'*S*)-2,2'-(propane-2,2-diyl)bis(4-benzyl-4,5-dihydrooxazole) (L5): Synthesized from the aforementioned protocol using L-phenylalaninol. The values of the NMR spectra are in accordance with reported literature data.[8]

^{1}H NMR (400 MHz, $CDCl_3$) δ 7.32 – 7.25 (m, 5H), 7.26 – 7.14 (m, 6H), 4.41 (m, *J* = 14.4, 8.5 Hz, 2H), 4.17 (ddd, *J* = 9.3, 7.7, 1.1 Hz, 2H), 4.01 (ddd, *J* = 8.2, 6.8, 1.1 Hz, 2H), 3.09 (dd, *J* = 13.8, 4.7 Hz, 2H), 2.66 (dd, *J* = 13.7, 8.6 Hz, 2H), 1.46 (d, *J* = 1.1 Hz, 6H).

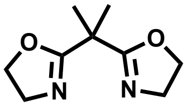

2,2'-(propane-2,2-diyl)bis(4,5-dihydrooxazole) (L6): Synthesized from the aforementioned protocol using 2-amino-ethanol. The values of the NMR spectra are in accordance with reported literature data.[6]

^{1}H NMR (500 MHz, $CDCl_3$) δ 4.30 (t, *J* = 9.5 Hz, 4H), 3.89 (t, *J* = 9.5 Hz, 4H), 1.53 (s, 6H).

2.9.3.2 Data for O–H Insertion/Aldol Cascade

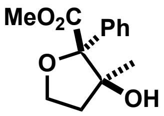

Methyl-3-hydroxy-3-methyl-2-phenyltetrahydrofuran-2-carboxylate (57): Keto alcohol (1 equiv.), ligand (12 mol%), NaBA$_r$F (12 mol%) and catalyst (10 mol%) were dissolved into 2 mL of dry solvent. The catalyst solution was then allowed to stir at room temperature for 1 h and then brought to reflux for an additional hour. Then, the diazo was dissolved into 1mL of the solvent and added to refluxing catalyst solution over 2 h. Once added, the syringe was quantitively washed with1 mL of the transfer solvent. The reaction was allowed to reflux overnight. The following day, the crude solution was filtered over a silica/celite pad and was analyzed via NMR. Compound was purified with silica gel chromatography to yield inseparable mixture of insertion + aldol products. Anomeric ratios are based on the integration of crude spectra

R$_f$ = 0.42 (30% EtOAc in Hex).

^{1} H NMR (500 MHz, Chloroform-d) δ 7.61 – 7.49 (m, 2H), 7.49 – 7.28 (m, 7H), 4.91 (s, 1H), 4.38 – 4.13 (m, 3H), 2.79 (t, *J* = 6.4 Hz, 2H), 2.20 (d, *J* = 1.5 Hz, 3H), 2.14 – 1.97 (m, 3H), 1.16 (s, 4H).

^{13}C NMR (mixer of isomers) (126 MHz, $CDCl_3$) δ 206.97, 171.18, 137.84, 136.20, 130.10, 128.76, 128.63, 128.14, 128.07, 127.20, 125.37, 89.48, 81.83, 81.38, 66.25, 64.79, 52.83, 52.26, 43.58, 38.70, 30.48, 23.99.

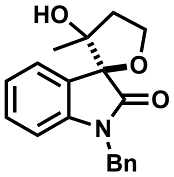

1'-benzyl-3-hydroxy-3-methyl-4,5-dihydro-3*H*-spiro[furan-2,3'-indolin]-2'-one (62): Keto alcohol (1 equiv.), $NaBA_rF$ (12 mol%) and catalyst (10 mol%) were dissolved into 2 mL of dry solvent.

^{1}H NMR (500 MHz, $cdcl_3$) δ 7.45 – 7.24 (m, 5H), 7.22 (td, *J* = 7.8, 1.3 Hz, 1H), 7.06 (td, *J* = 7.5, 1.0 Hz, 1H), 6.75 (dt, *J* = 7.8, 0.8 Hz, 1H), 5.10 (d, *J* = 15.7 Hz, 1H), 4.76 (d, *J* = 15.7 Hz, 1H), 4.51 (td, *J* = 8.5, 7.3 Hz, 1H), 4.30 (td, *J* = 8.4, 3.8 Hz, 1H), 4.22 (s, 1H), 2.58 (ddd, *J* = 12.5, 7.2, 3.8 Hz, 1H), 2.37 (dt, *J* = 12.4, 8.5 Hz, 1H), 1.18 (s, 3H).

^{13}C NMR (101 MHz, $CDCl_3$) δ 176.77, 142.69, 135.15, 129.74, 128.89, 127.80, 127.20, 124.81, 123.23, 109.81, 86.99, 81.74, 67.88, 43.93, 39.89, 23.37.

2.10 APPENDIX 1

Spectra Relevant to Chapter 2

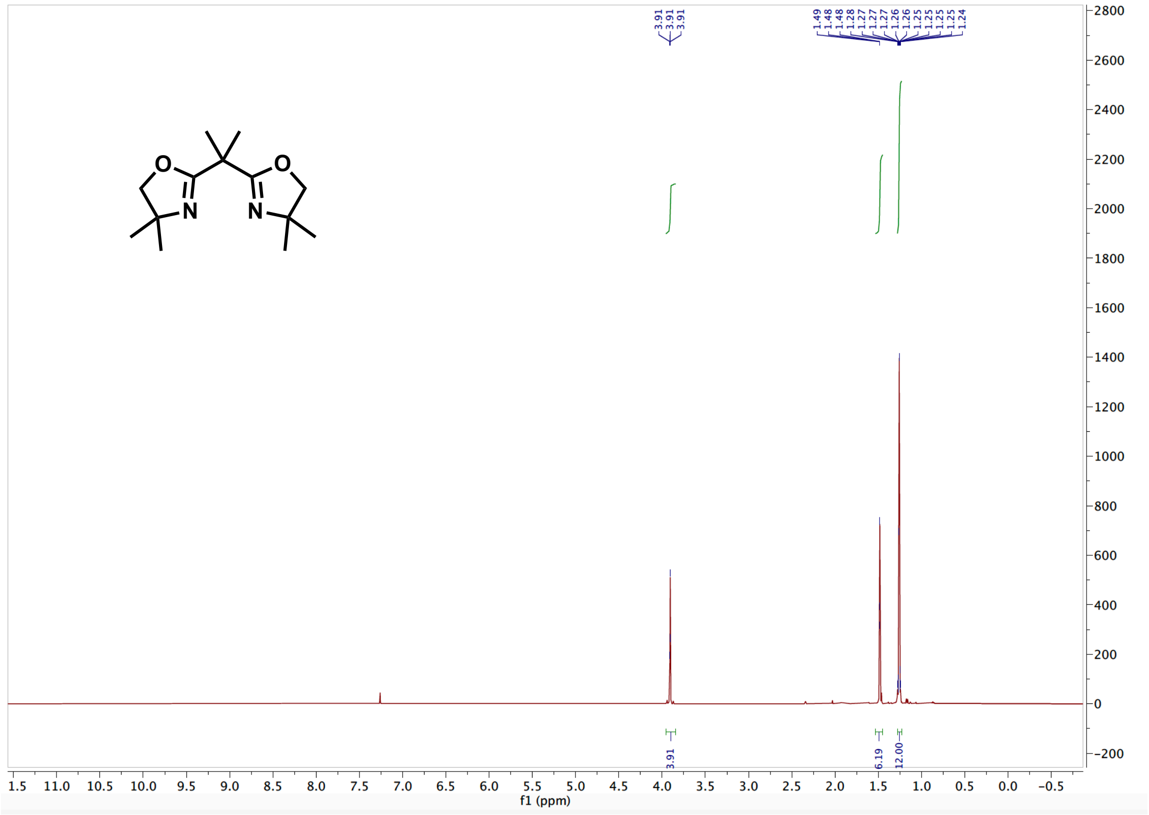
3.91
3.91
3.91
1.49
1.48
1.48
1.28
1.27
1.27
1.27
1.26
1.25
1.25
1.25
1.25
1.24
O
N
O
N
3.91
6.19
12.00
f1 (ppm)

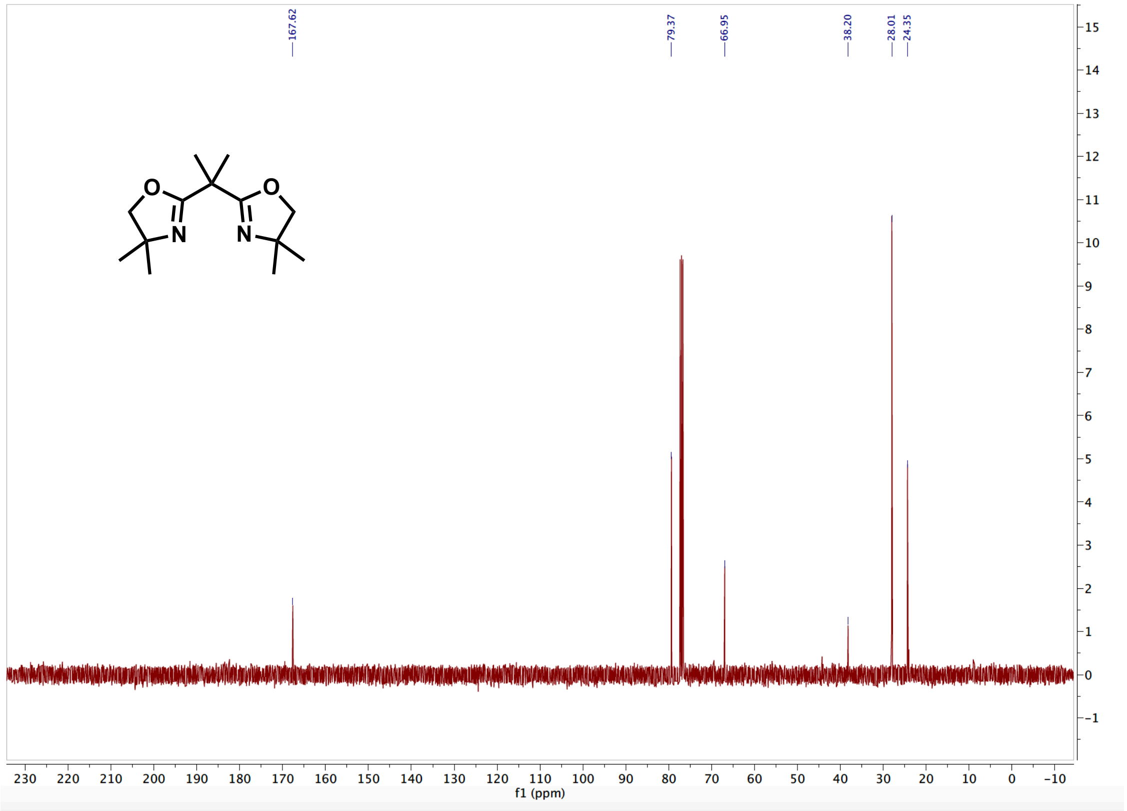
167.62
79.37
66.95
38.20
28.01
24.35
O
N
O
N
f1 (ppm)

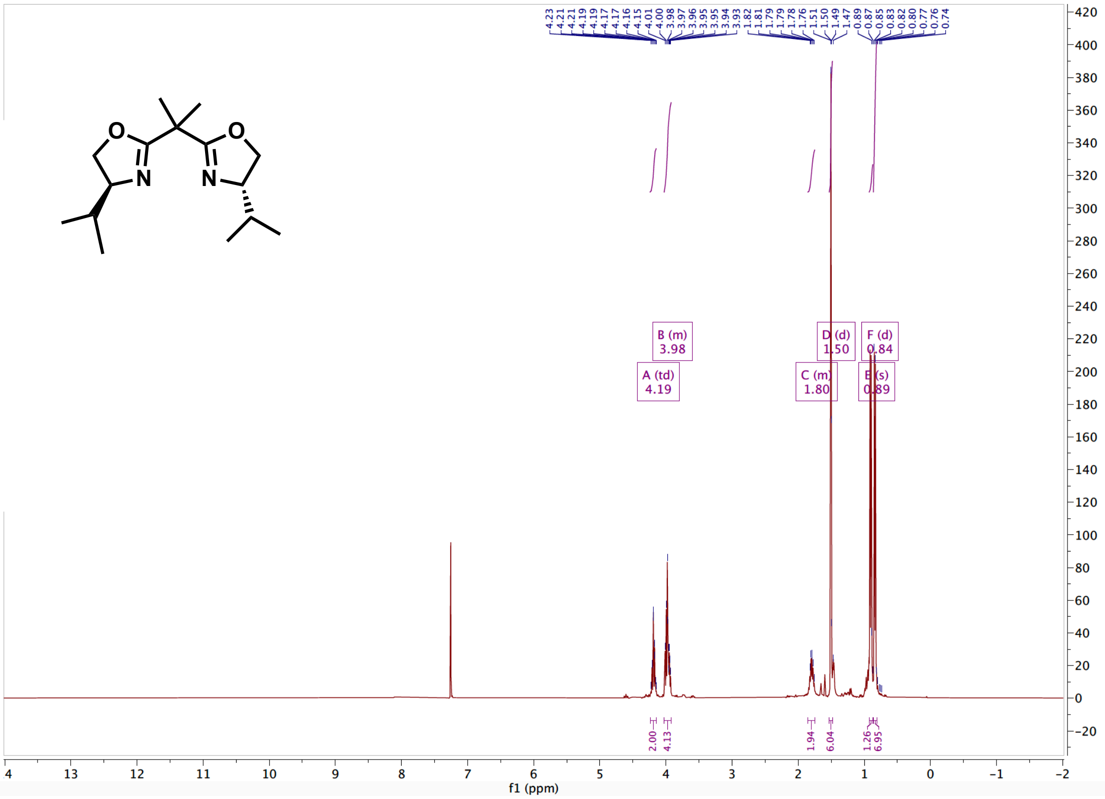
4.23
4.21
4.21
4.19
4.19
4.17
4.17
4.16
4.15
4.01
4.00
3.98
3.97
3.96
3.95
3.95
3.94
3.93
1.82
1.81
1.79
1.79
1.78
1.76
1.51
1.50
1.49
1.47
0.89
0.87
0.85
0.83
0.82
0.80
0.77
0.76
0.74
O
N
O
N
B (m) 3.98
A (td) 4.19
D (d) 1.50
C (m) 1.80
F (d) 0.84
E (s) 0.89
2.00
4.13
1.94
6.04
1.26
6.95
f1 (ppm)

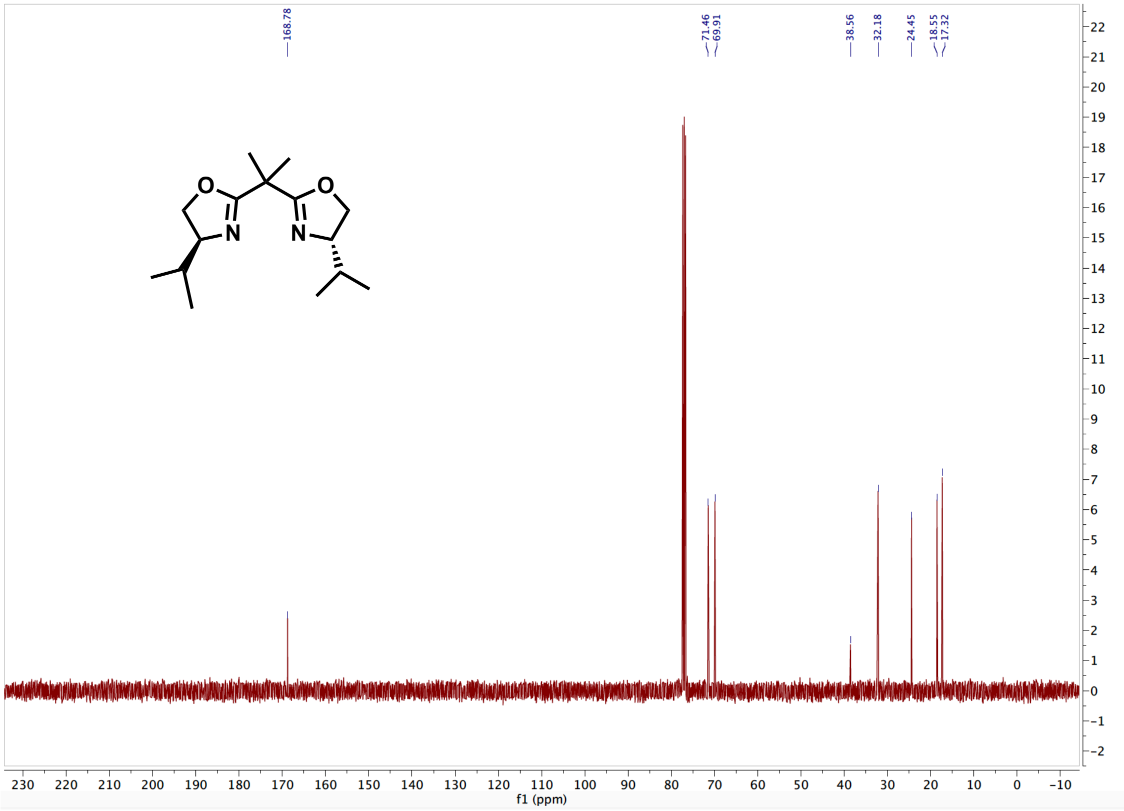
168.78
71.46
69.91
38.56
32.18
24.45
18.55
17.32
O
N
O
N
f1 (ppm)

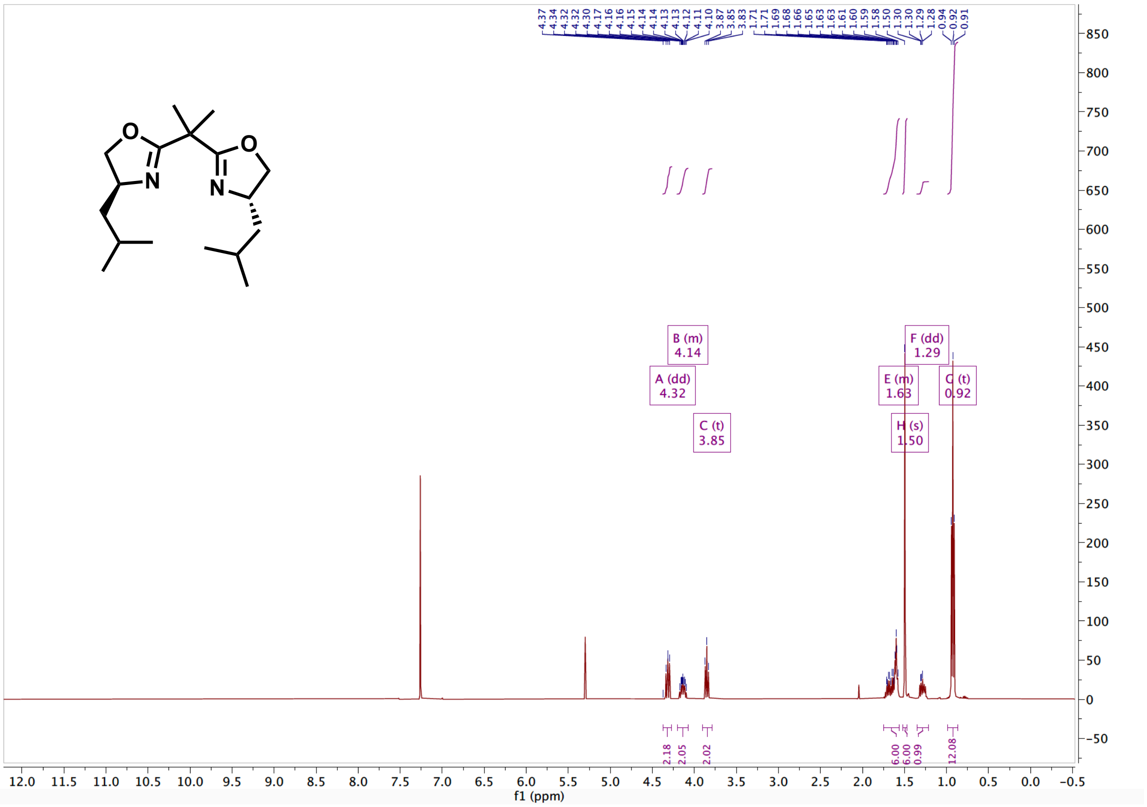
4.37
4.34
4.32
4.32
4.30
4.17
4.16
4.16
4.15
4.14
4.14
4.13
4.13
4.12
4.11
4.10
3.87
3.85
3.83
1.71
1.71
1.69
1.68
1.66
1.65
1.63
1.63
1.61
1.60
1.59
1.58
1.50
1.30
1.30
1.29
1.28
0.94
0.92
0.91
O
N
O
N
B (m) 4.14
A (dd) 4.32
C (t) 3.85
F (dd) 1.29
E (m) 1.63
G (t) 0.92
H (s) 1.50
2.18
2.05
2.02
6.00
6.00
0.99
12.08
12.0 11.5 11.0 10.5 10.0 9.5 9.0 8.5 8.0 7.5 7.0 6.5 6.0 5.5 5.0 4.5 4.0 3.5 3.0 2.5 2.0 1.5 1.0 0.5 0.0 −0.5
f1 (ppm)
850 800 750 700 650 600 550 500 450 400 350 300 250 200 150 100 50 0 −50

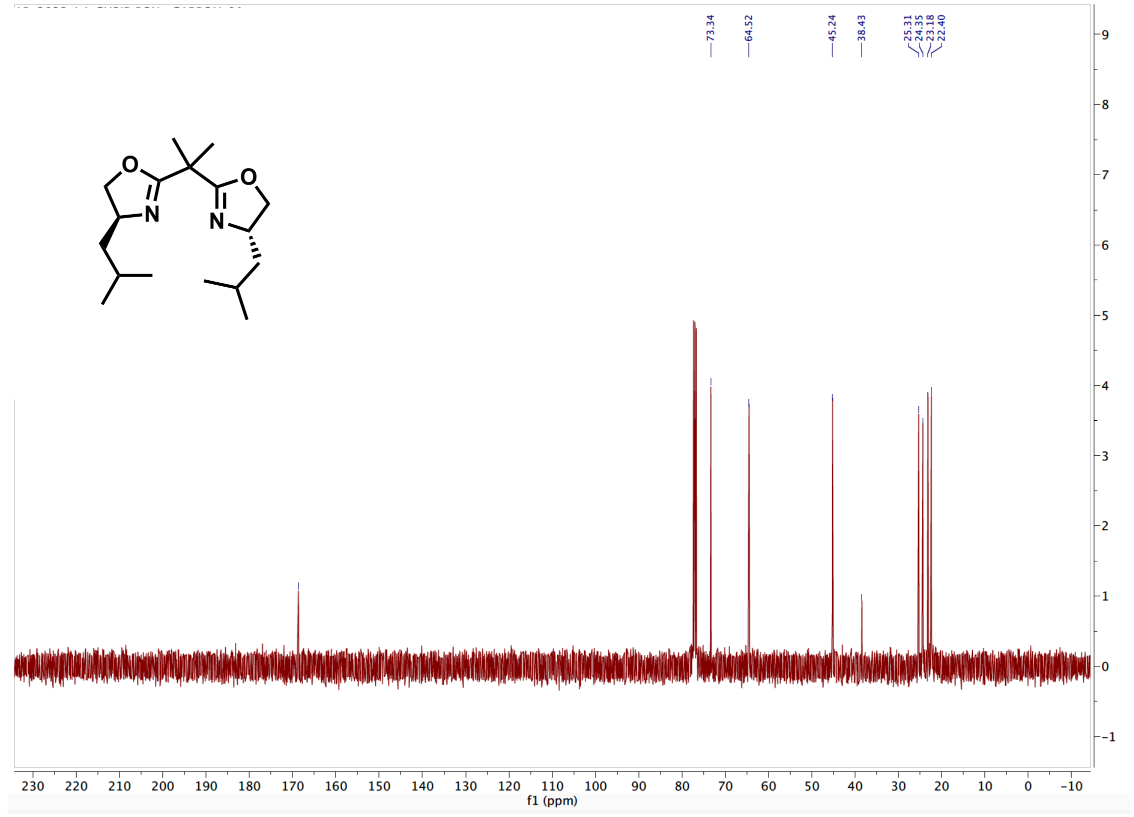
73.34
64.52
45.24
38.43
25.31
24.35
23.18
22.40
O
N
O
N
230 220 210 200 190 180 170 160 150 140 130 120 110 100 90 80 70 60 50 40 30 20 10 0 −10
f1 (ppm)
9 8 7 6 5 4 3 2 1 0 −1

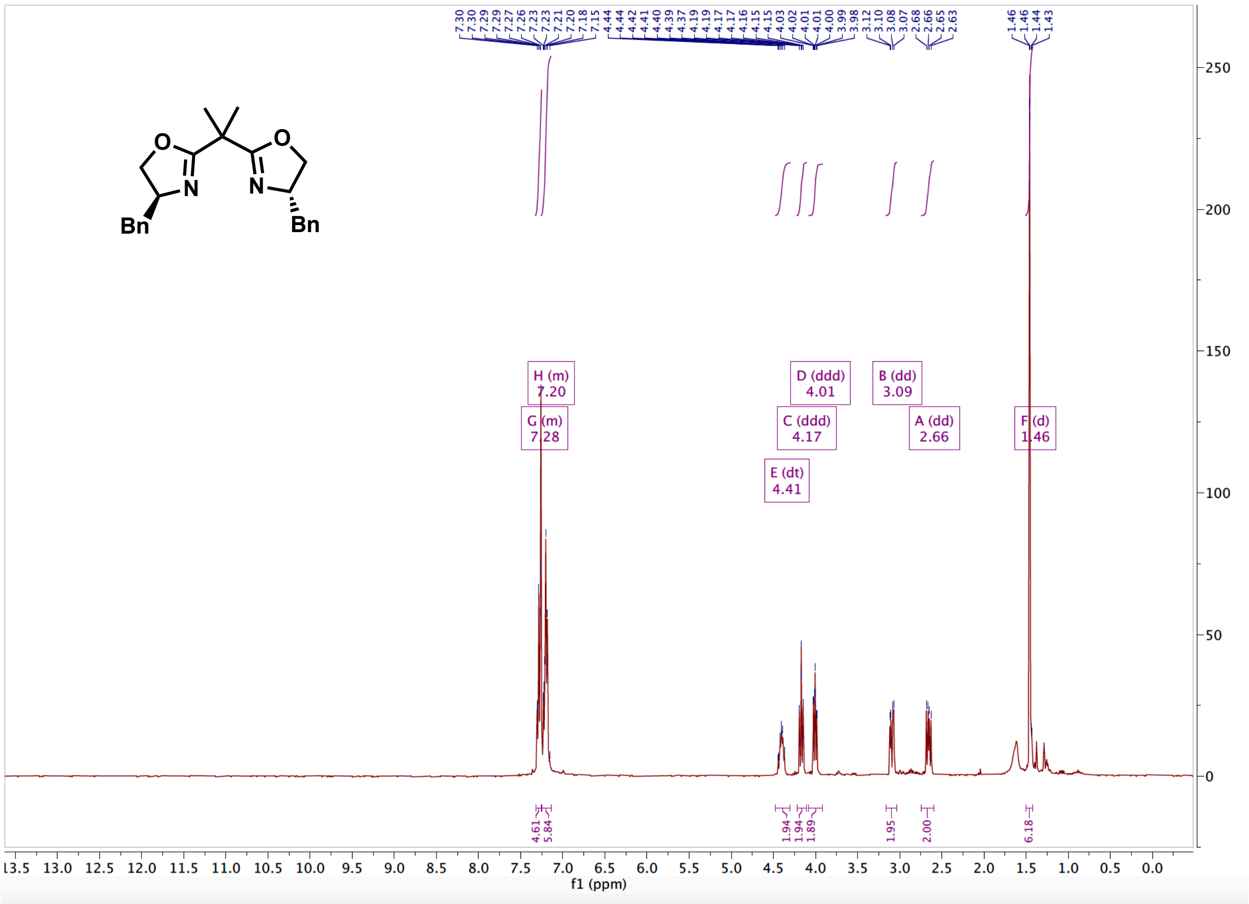
7.30
7.30
7.29
7.29
7.27
7.26
7.23
7.23
7.21
7.20
7.18
7.15
4.44
4.44
4.42
4.41
4.40
4.39
4.37
4.19
4.19
4.17
4.17
4.16
4.15
4.15
4.03
4.02
4.01
4.01
4.00
3.99
3.98
3.12
3.10
3.08
3.07
2.68
2.66
2.65
2.63
1.46
1.46
1.44
1.43
O
N
O
N
Bn
Bn
H (m)
7.20
G (m)
7.28
D (ddd)
4.01
C (ddd)
4.17
E (dt)
4.41
B (dd)
3.09
A (dd)
2.66
F (d)
1.46
4.61
5.84
1.94
1.94
1.89
1.95
2.00
6.18
250
200
150
100
50
0
13.5
13.0
12.5
12.0
11.5
11.0
10.5
10.0
9.5
9.0
8.5
8.0
7.5
7.0
6.5
6.0
5.5
5.0
4.5
4.0
3.5
3.0
2.5
2.0
1.5
1.0
0.5
0.0
f1 (ppm)

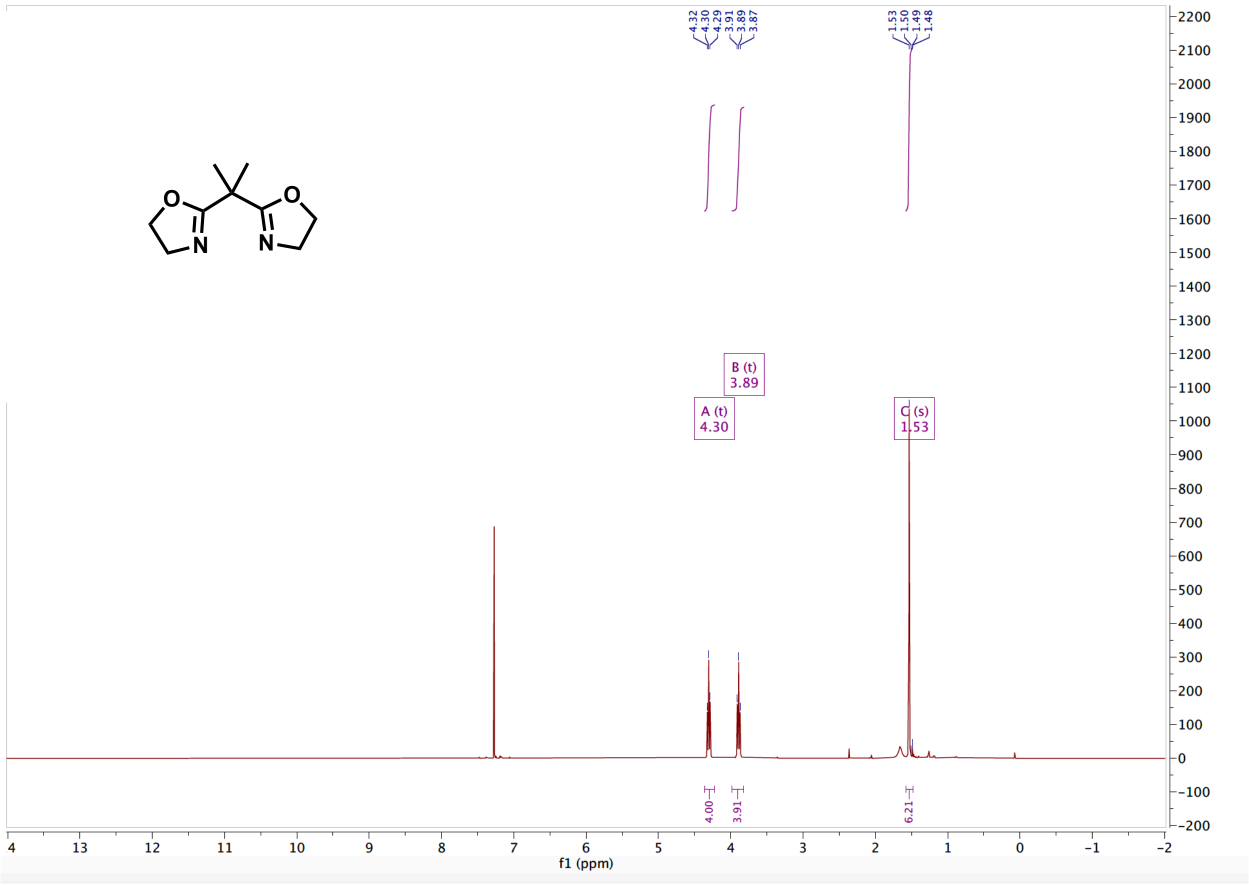
O
N
O
N
4.32
4.30
4.29
3.91
3.89
3.87
1.53
1.50
1.49
1.48
B (t)
3.89
A (t)
4.30
C (s)
1.53
4.00
3.91
6.21
2200
2100
2000
1900
1800
1700
1600
1500
1400
1300
1200
1100
1000
900
800
700
600
500
400
300
200
100
0
−100
−200
4
13
12
11
10
9
8
7
6
5
4
3
2
1
0
−1
−2
f1 (ppm)

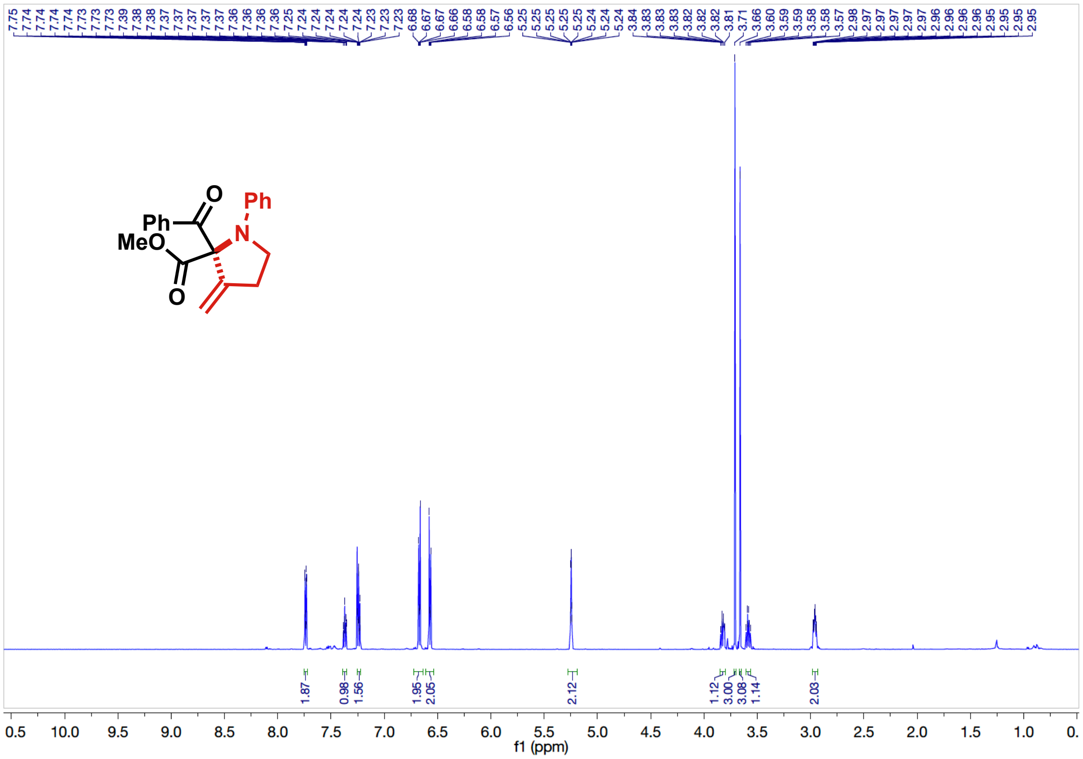
7.75
7.74
7.74
7.74
7.74
7.73
7.73
7.73
7.39
7.38
7.38
7.37
7.37
7.37
7.37
7.36
7.36
7.36
7.36
7.25
7.24
7.24
7.24
7.24
7.24
7.23
7.23
7.23
6.68
6.67
6.67
6.66
6.58
6.58
6.57
6.56
5.25
5.25
5.25
5.25
5.25
5.24
5.24
5.24
3.84
3.83
3.83
3.82
3.82
3.82
3.81
3.71
3.66
3.60
3.59
3.59
3.58
3.58
3.57
2.98
2.97
2.97
2.97
2.97
2.97
2.96
2.96
2.96
2.96
2.95
2.95
2.95
O
Ph
Ph
N
MeO
O
1.87
0.98
1.56
1.95
2.05
2.12
1.12
3.00
3.08
1.14
2.03
0.5
10.0
9.5
9.0
8.5
8.0
7.5
7.0
6.5
6.0
5.5
5.0
4.5
4.0
3.5
3.0
2.5
2.0
1.5
1.0
0.
f1 (ppm)

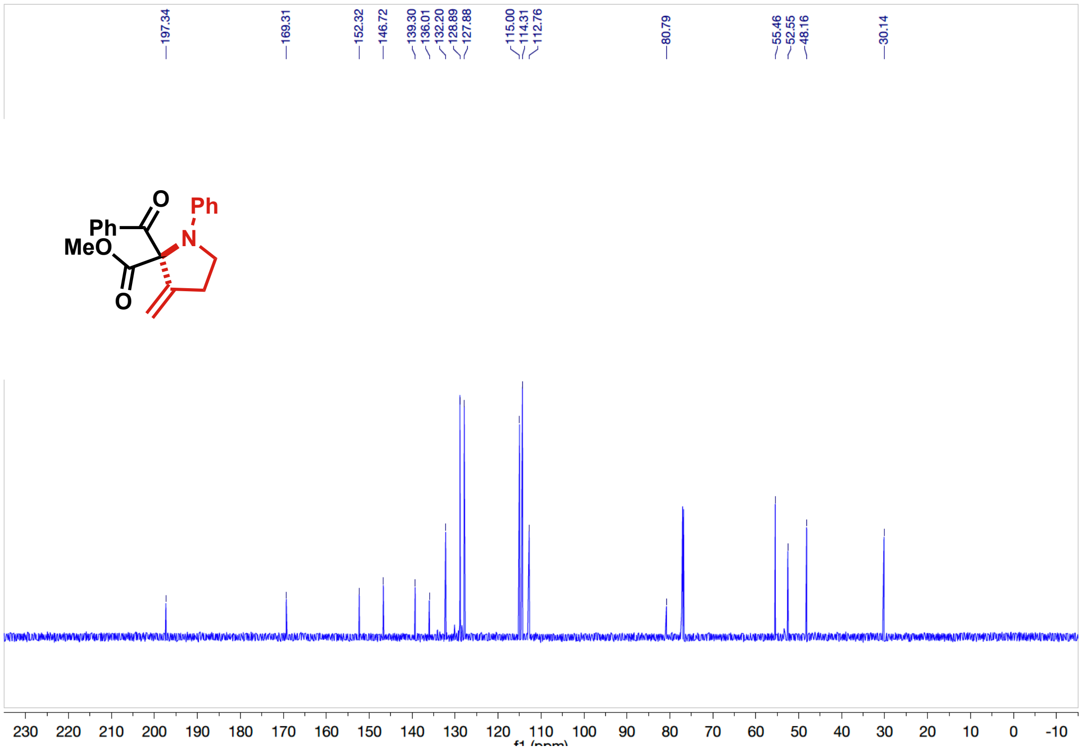
197.34
169.31
152.32
146.72
139.30
136.01
132.20
128.89
127.88
115.00
114.31
112.76
80.79
55.46
52.55
48.16
30.14
O
Ph
Ph
N
MeO
O
230
220
210
200
190
180
170
160
150
140
130
120
110
100
90
80
70
60
50
40
30
20
10
0
-10

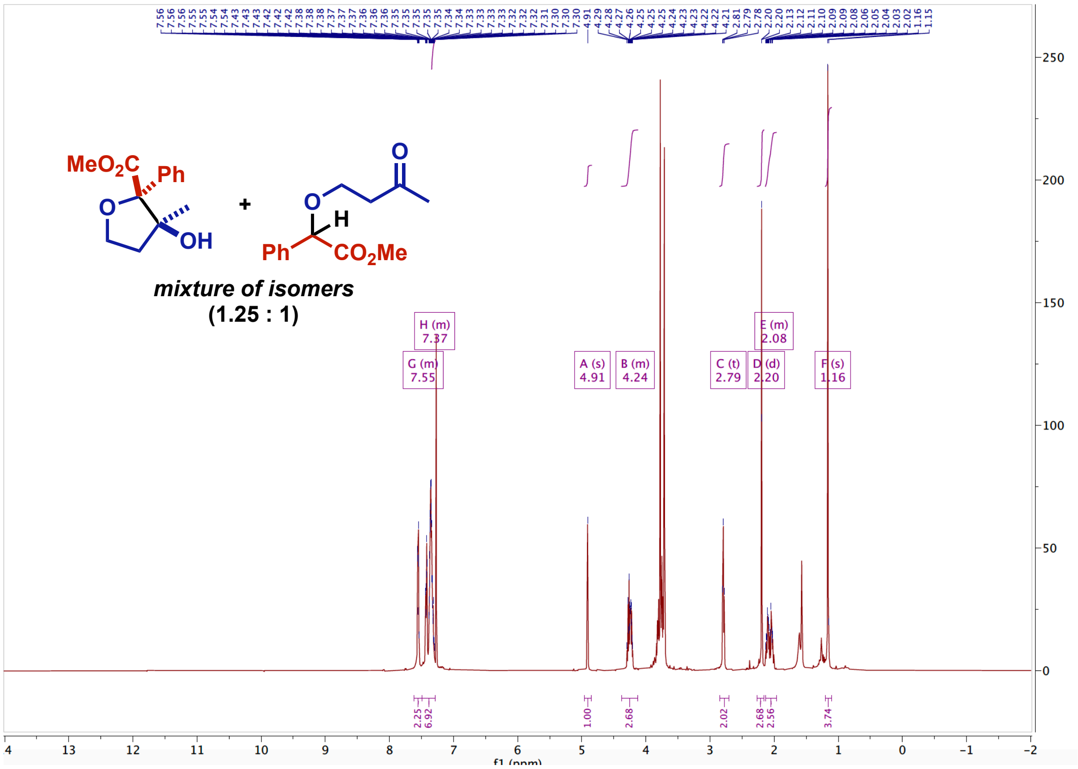
7.56
7.56
7.56
7.55
7.55
7.54
7.54
7.43
7.43
7.43
7.42
7.42
7.42
7.38
7.38
7.38
7.37
7.37
7.37
7.36
7.36
7.36
7.35
7.35
7.35
7.35
7.35
7.34
7.34
7.33
7.33
7.33
7.33
7.32
7.32
7.32
7.31
7.30
7.30
7.30
4.91
4.29
4.28
4.27
4.26
4.25
4.25
4.25
4.24
4.23
4.23
4.22
4.22
4.21
2.81
2.79
2.78
2.20
2.20
2.13
2.12
2.11
2.10
2.09
2.09
2.08
2.06
2.05
2.04
2.03
2.02
1.16
1.15
MeO2C
Ph
O
OH
+
O
O
H
Ph
CO2Me
mixture of isomers
(1.25 : 1)
H (m)
7.37
G (m)
7.55
A (s)
4.91
B (m)
4.24
C (t)
2.79
D (d)
2.20
E (m)
2.08
F (s)
1.16
2.25
6.92
1.00
2.68
2.02
2.68
2.56
3.74
250
200
150
100
50
0
4
13
12
11
10
9
8
7
6
5
4
3
2
1
0
-1
-2
f1 (ppm)

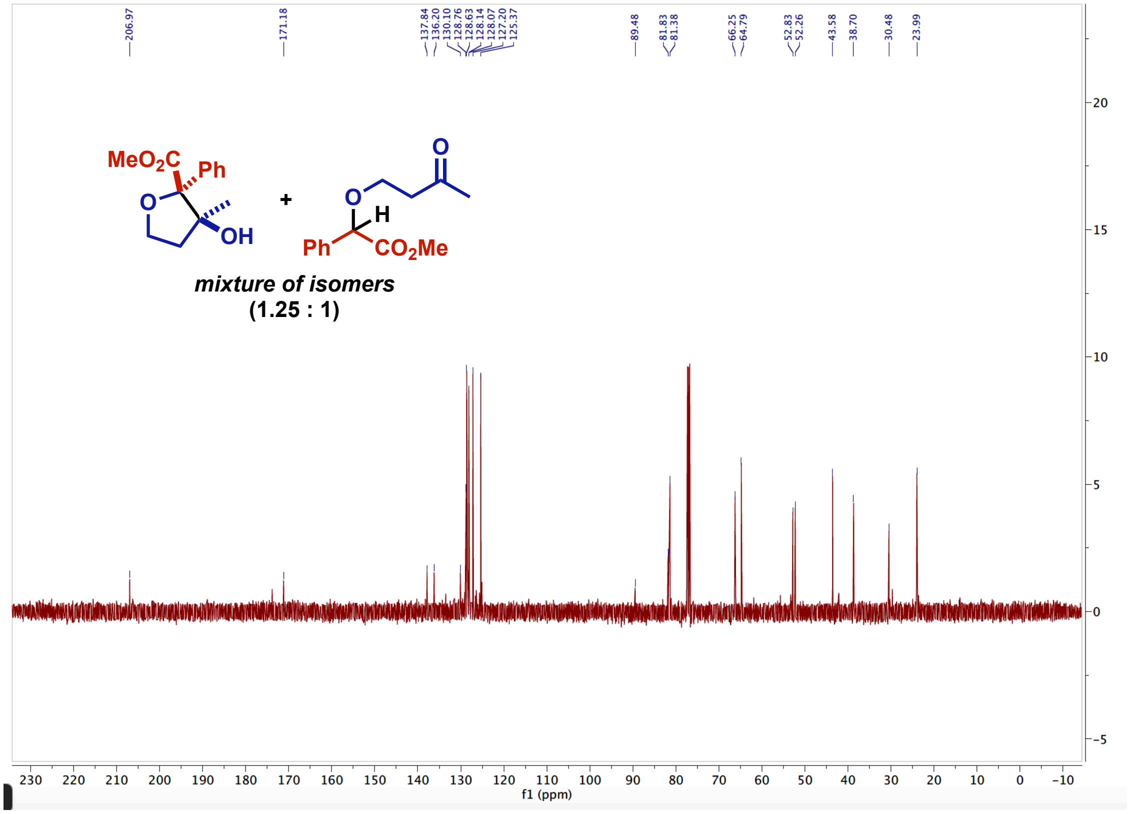
206.97
171.18
137.84
136.20
130.10
128.76
128.63
128.14
128.07
127.20
125.37
89.48
81.83
81.38
66.25
64.79
52.83
52.26
43.58
38.70
30.48
23.99
MeO2C
Ph
O
OH
+
O
O
H
Ph
CO2Me
mixture of isomers
(1.25 : 1)
20
15
10
5
0
-5
230
220
210
200
190
180
170
160
150
140
130
120
110
100
90
80
70
60
50
40
30
20
10
0
-10
f1 (ppm)

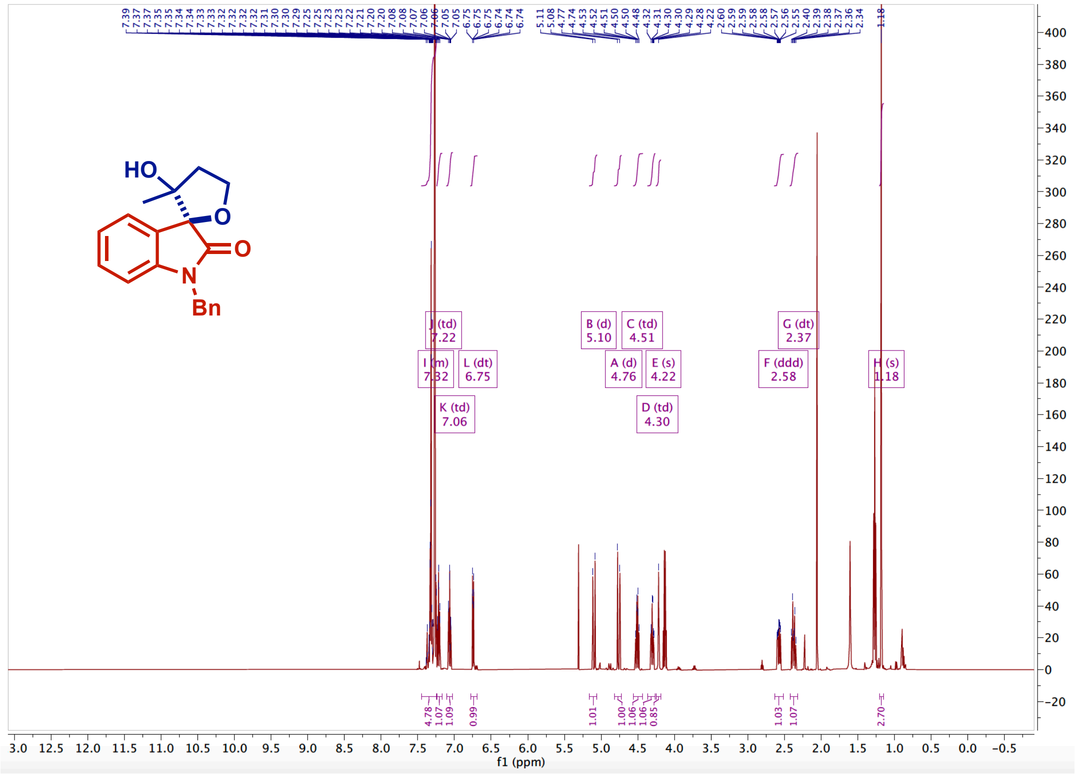
HO
O
O
N
Bn
J (td) 7.22
I (m) 7.32
L (dt) 6.75
K (td) 7.06
B (d) 5.10
C (td) 4.51
A (d) 4.76
E (s) 4.22
D (td) 4.30
G (dt) 2.37
F (ddd) 2.58
H (s) 1.18
4.78
1.07
1.09
0.99
1.01
1.00
1.06
1.06
0.85
1.03
1.07
2.70
f1 (ppm)

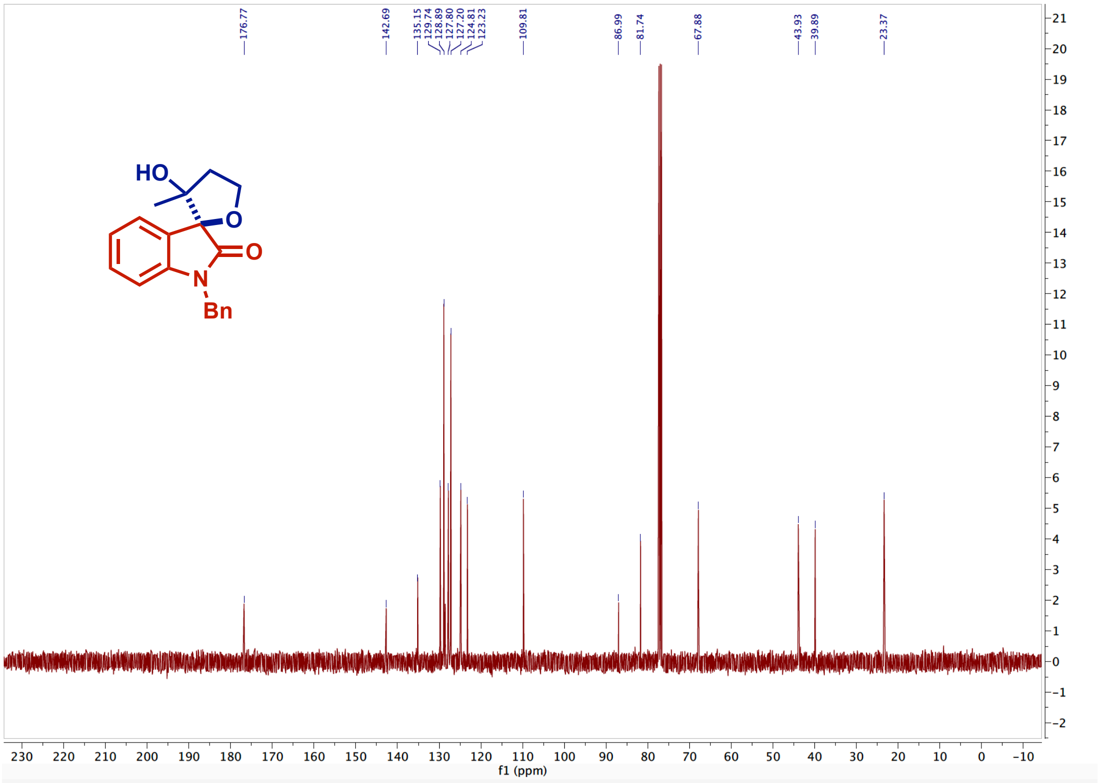
176.77
142.69
135.15
129.74
128.89
127.80
127.20
124.81
123.23
109.81
86.99
81.74
67.88
43.93
39.89
23.37
HO
O
O
N
Bn
f1 (ppm)

2.11 REFERENCES FOR CHAPTER 2 EXPERIMENTALS

[1] X.-L. Yu, L. Kuang, S. Chen, X.-L. Zhu, Z.-L. Li, B. Tan, X.-Y. Liu, *ACS Catalysis* **2016**, *6*, 6182-6190.

[2] S. W. Youn, S. R. Lee, *Organic & Biomolecular Chemistry* **2015**, *13*, 4652-4656.

[3] M. Kitamura, R. Fujimura, T. Nishimura, S. Takahashi, H. Shimooka, T. Okauchi, *European Journal of Organic Chemistry* **2020**, *2020*, 5319-5322.

[4] K. E. Coffey, G. K. Murphy, *Synlett* **2015**, *26*, 1003-1007.

[5] P. Patel, G. Borah, *Chemical Communications* **2017**, *53*, 443-446.

[6] G. Pisella, A. Gagnebin, J. Waser, *Organic Letters* **2020**, *22*, 3884-3889.

[7] Y. Guan, J. W. Attard, A. E. Mattson, *Chemistry – A European Journal* **2020**, *26*, 1742-1747.

[8] J. Mao, F. Liu, M. Wang, L. Wu, B. Zheng, S. Liu, J. Zhong, Q. Bian, P. J. Walsh, *Journal of the American Chemical Society* **2014**, *136*, 17662-17668.

CHAPTER 3

Glycal Carbenes –A Novel Glycosyl Donor for Stereoselective Glycosylation

3.1 INTRODUCTION TO STEREOSELECTIVE GLYCOSYLATION

Extraordinary progress has been achieved pertaining to the construction of glycosidic bonds. Stereoselective glycosylation, however, has remained one of the most significant unresolved challenges within glycoscience and organic chemistry.[1]

There are several critical gaps within carbohydrate chemistry. The most apparent challenge is the lack of general, stereoselective glycosylation approaches for assembling carbohydrates.[2] Most glycosylation methods proceed through either S_N1 or S_N2-type reactivity at the anomeric carbon (**Figure 3.1a/b**).[3] The stereoselectivity of these reactions is typically dominated by the anomeric effect and protecting group manipulations.[3a] To date, the significant factors influencing anomeric selectivity are neighboring group participation of 2-*O*-acyl protecting groups,[4] concentration, and solvent effects (**Figure 3.1c**).[1a]

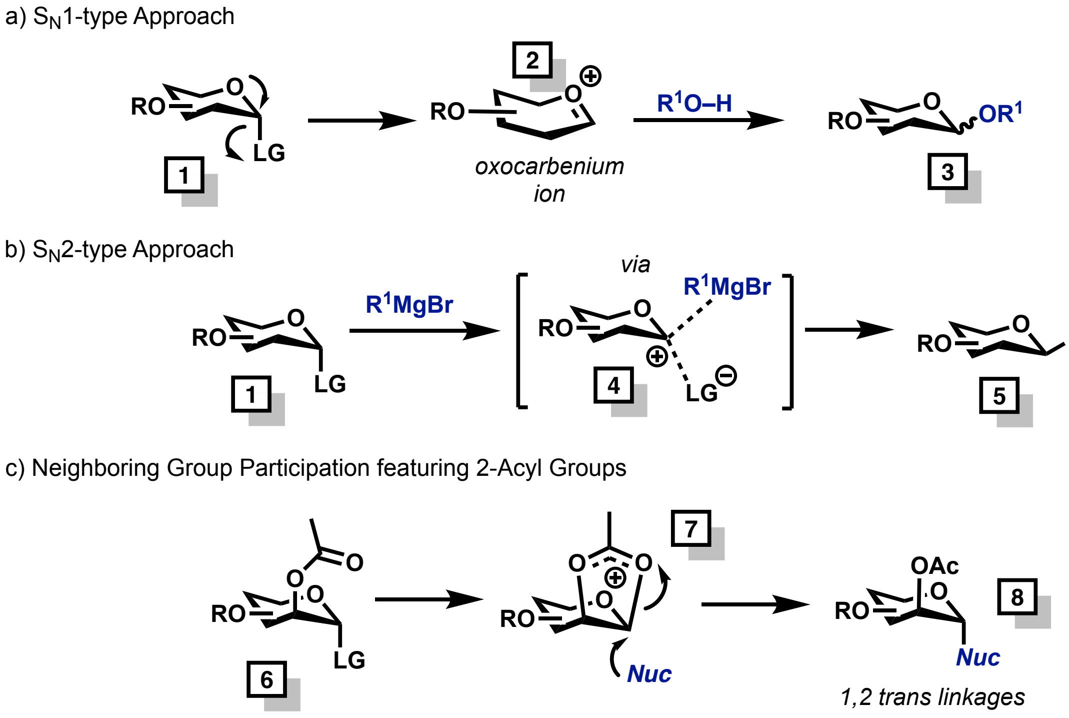
a) S$_N$1-type Approach
RO
O
LG
1
2
RO
O
oxocarbenium ion
R^{1}O–H
RO
O
OR^1
3
b) S$_N$2-type Approach
RO
O
LG
1
R^{1}MgBr
via
RO
O
R^{1}MgBr
LG
4
RO
O
R^1
5
c) Neighboring Group Participation featuring 2-Acyl Groups
O
O
RO
O
LG
6
O
O
RO
O
Nuc
7
OAc
RO
O
Nuc
8
1,2 trans linkages

Figure 3.1: Traditional Approaches to Glycosidic Bond Formation

Catalytic methods can serve as a powerful alternative to traditional methods; however, they often require a vast excess of glycosyl donors and acceptors or additional promoters, as observed in modern adaptations of Fischer[5] and Koenigs–Knorr[6] glycosylation protocols. Opposingly, catalytic glycosylation approaches with low catalyst loadings routinely rely on precious metal catalysts, such as rhodium,[7] palladium,[8] platinum,[9] and gold.[10] To address these challenges, the objective of this chapter is fundamental insight for the design of new carbene-mediated glycosyl donors catalytically activated by Earth-abundant metals.

3.1.1 VINYLCARBENOIDS AND OXY-VINYLOGOUS CARBENES

Carbene-assisted strategies are rare opportunities within glycosylation. To utilize a carbene-mediated strategy, we envisioned harnessing the vinylogous reactivity of metal-carbenoids. Metal carbenoids are versatile synthetic intermediates capable of novel transformations, [11] leading to the rapid generation of molecular complexity with high efficiency, selectivity, and atom economy.[12] Within the class of donor/acceptor diazos is a diazo known as vinyl diazos (**12**) (**Figure 3.2**).

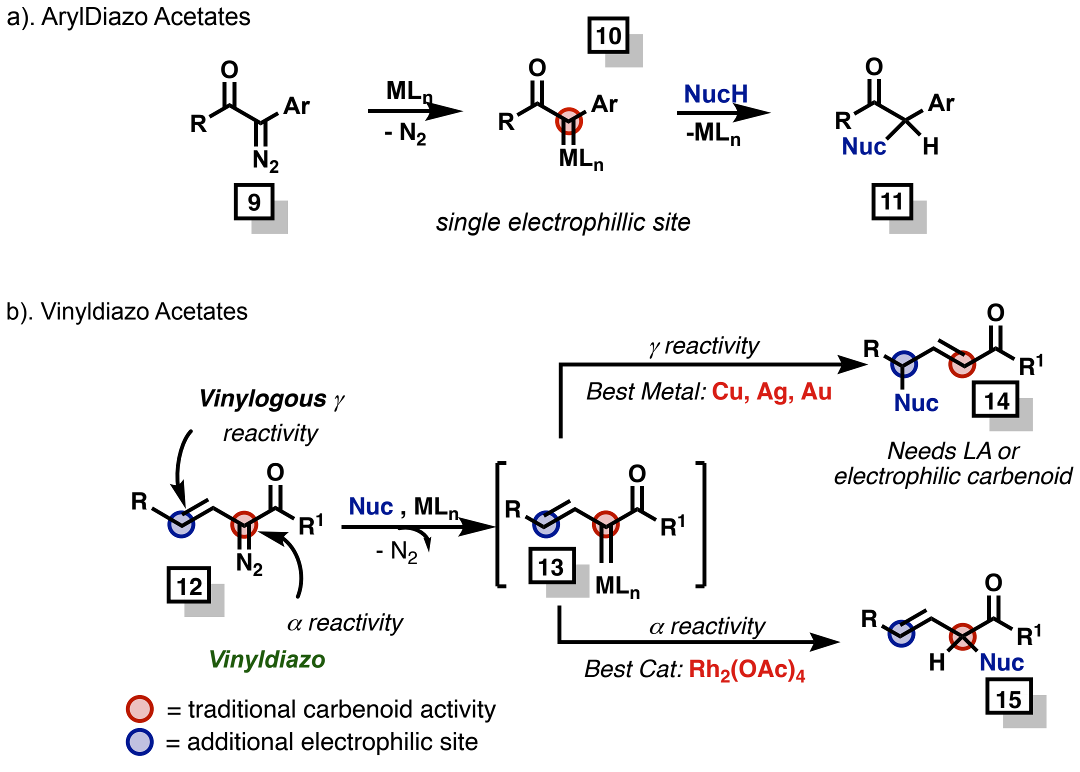
a). ArylDiazo Acetates
O
R
Ar
N2
9
MLn
- N2
10
MLn
NucH
-MLn
Nuc
H
11
single electrophillic site
b). Vinyldiazo Acetates
Vinylogous γ reactivity
R
O
R1
N2
12
α reactivity
Vinyldiazo
Nuc , MLn
- N2
13
MLn
γ reactivity
Best Metal: Cu, Ag, Au
Nuc
14
Needs LA or electrophilic carbenoid
α reactivity
Best Cat: Rh2(OAc)4
H
Nuc
15
= traditional carbenoid activity
= additional electrophilic site

Figure 3.2: Vinylogous Reactivity of Vinyl Metal Carbenoids

Vinyl carbenes are powerful synthetic intermediates as they encompass the traditional ambiphilic α-carbenoid site (red) and an additional electrophilic γ site (blue).[12d, 14] This reactivity is often dictated by choosing an appropriate metal catalyst.[15] These substrates are exceedingly versatile as they possess ambiphilic reactivity at the alpha carbon of the carbenoid center and electrophilic reactivity at the vinylogous position.[13] This dual reactivity provides access to a diverse array of zwitterionic-intermediary cascades. As a result, vinyldiazos possess a distinct advantage over traditional donor/acceptor aryldiazo acetates, which only contain one reactive site.

Various factors can dictate whether the vinylcarbenoids react at the carbenoid terminus or vinylogous terminus. Davies conducted early fundamental studies on α- versus γ- reactivity of Rh(II) carbenoids[13] and demonstrated that judicious choice of solvent, substrate, and catalyst could alter regioselectivity. Namely, bulky carbenoid precursors and electron-deficient catalysts tend to favor reactivity at the vinyl terminus. Since this report, studies have reported the propensity of coinage metal carbenoids such as silver to undergo regioselective γ additions.[15-16]

The first oxy-vinylogous carbene was reported in 1991, were authors observed the vinylogous insertion of methanol into oxy-vinylogous carbenes (**Figure 3.3**).[17] Oxy-vinylogous carbene **17** was synthesized by exposing the corresponding tosylhydrazone to a concentrated NaOMe solution. Following the formation of the oxy-vinyl carbene, the species undergoes an oxygen-assisted vinylic insertion, despite being the more sterically disfavored position to furnish **18.**

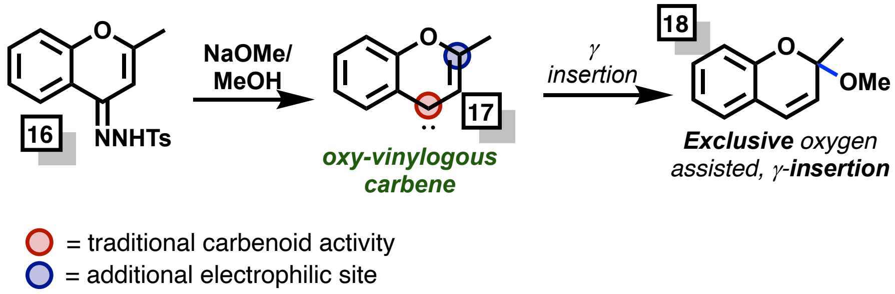
16
NNHTs
NaOMe/
MeOH
17
oxy-vinylogous
carbene
γ
insertion
18
OMe
Exclusive oxygen
assisted, γ-insertion
= traditional carbenoid activity
= additional electrophilic site

Figure 3.3: Oxy-vinylogous Carbene Literature Precedence

Inspired by this work, we thought to construct a parallel system to accommodate our glycosylation strategy. Our proposed glycal system is a near-perfect recreation of the parent system, as the endocyclic oxygen inherent to glycosides can serve analogously to the oxygen of the benzopyran. Electron donation from the anomeric oxygen can increase the electrophilicity at the desired vinylogous position, further accommodating the desired γ insertion.

3.1.2 OBJECTIVE OF CHAPTER

The goal of this chapter is the synthesis and utilization of novel glycosyl donors towards our goal of a highly stereoselective glycosylation approach. This chapter will detail the design, synthesis, and applications of a novel glycosyl donor, *glycal carbenes* (**Figure 3.4b**). Here, we will highlight the completed and ongoing research where glycal carbenes are utilized to promote catalytic, stereoselective anomeric functionalization.

As carbene-assisted glycosylation strategies are rarities within glycoscience, these donors will serve to provide fundamental insight towards carbene-mediated glycosyl donors. Our proposed donors are fundamentally different from traditional donors, such as thioglycoside and trichloroacetimidate donors (**Figures 3.4a**). This approach features a vinylcarbenoid moiety integrated into the carbohydrate scaffold. We intend to harness the electrophilic vinylogous position of the designed glycosyl donors to promote our glycosylation strategy. Additionally, this approach features low catalyst loadings with Earth-abundant metals, and we intend to utilize these donors to access a variety of glycosidic bonds with different glycosyl acceptors.

a) Common Glycosyl Donors

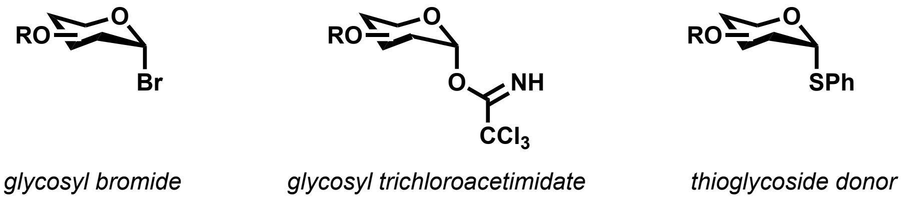
RO
O
Br
glycosyl bromide
RO
O
O
NH
CCl3
glycosyl trichloroacetimidate
RO
O
SPh
thioglycoside donor

b) Proposed Work

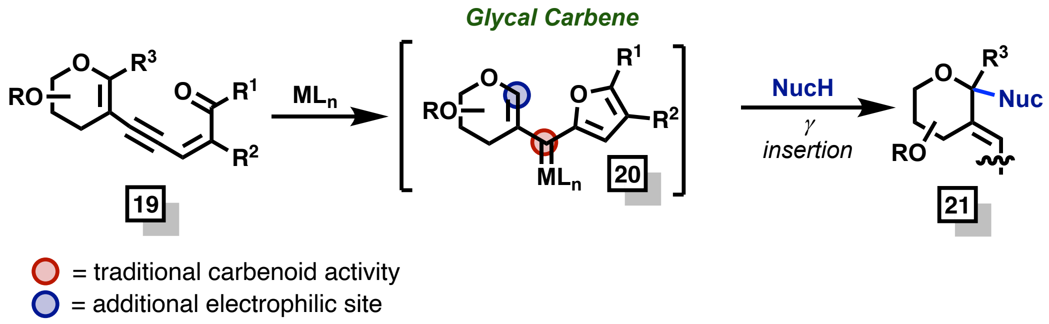
Glycal Carbene
RO
O
R3
O
R1
R2
19
MLn
RO
O
O
R1
R2
MLn
20
NucH
γ
insertion
O
R3
Nuc
RO
21
= traditional carbenoid activity
= additional electrophilic site

Figure 3.4: Overview of Glycosylation Strategy

3.2 DESIGN, SYNTHESIS, AND STUDY OF GLYCAL CARBENES

To harness the vinylogous reactivity of vinyl carbenoids on a sugar system, we thought to implant the vinylcarbenoid motif onto a sugar glycal system. Glycals, sugars with an embedded olefin, are readily available from commercial sources. Initially, we thought to graft a vinyl diazo moiety onto the sugar glycals, given our laboratory's extensive experience in diazo-derived metal carbenoids and vinyl diazo carbonyls.[18] However, we found the synthesis of sugar diazos to be infeasible.

In one route, we synthesized iodoglycal **23** readily.[19] Our goal was to optimize palladium-catalyzed conditions to couple ethyl diazo acetate to the glycal scaffold. However, despite vast screening and literature reports on similar systems,[20] we were unable to develop favorable conditions (**Figure 3.5a**).

a) Initial route to access glycal diazos

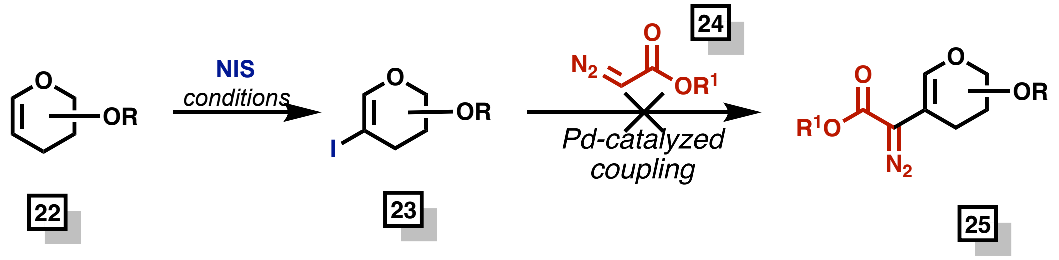
NIS
conditions
O
OR
I
24
N_2
OR^1
Pd-catalyzed
coupling
R^1O
22
23
25

b) Alternative route to access glycal diazos

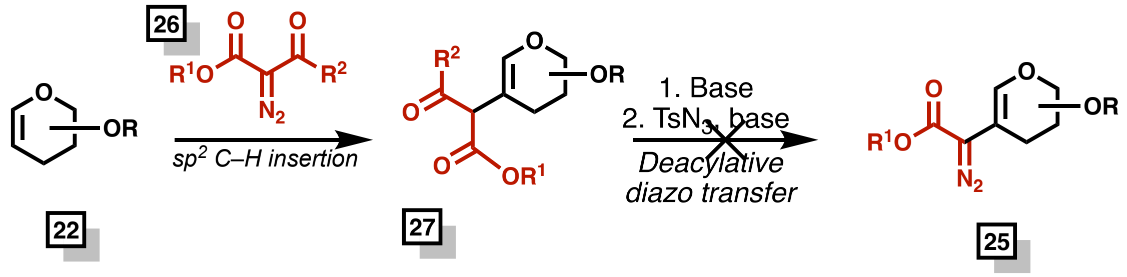
26
R^1O
N_2
R^2
sp² C–H insertion
O
OR
OR^1
1. Base
2. TsN_3, base
Deacylative
diazo transfer
22
27
25

Figure 3.5: Failed Syntheses of Glycal Diazos

Alternatively, we synthesized **27** by allowing glycal **22** to undergo a C3 *sp*^{2} C–H insertion into A/A diazo **26**. Following the isolation of **27**, we then attempted a deacylative diazo transfer to synthesize the diazo glycal. However, the diazo transfer resulted in a complex mixture that was unable to be further utilized (**Figure 3.5b**). After these failures, we hypothesized that diazos were ill-suited for our glycosylation strategy. Additionally, we postulated that diazos, due to their instability and notoriety, would be quite challenging to incorporate into newly developed synthetic practices. Due to this, we turned to other carbene precursors.

Following a literature review, we found that metal carbenes can readily be synthesized from alkynes precursors.[21] In fact, enynones (**28**) have experienced considerable success in carbene-mediated chemistry.[21-22] Once activated, these precursors share similar reactivity to diazo-derived carbenes (**Figure 3.6**). We hypothesized that installing an additional olefinic moiety alpha to the propargyl group would furnish vinylic metal carbenes. These carbene surrogates host a multitude of advantages over traditional diazo precursors and allow access to carbene species that would be challenging to generate through conventional diazo chemistry.[23]

a). Enynones as a Metal Carbenoid Precursor

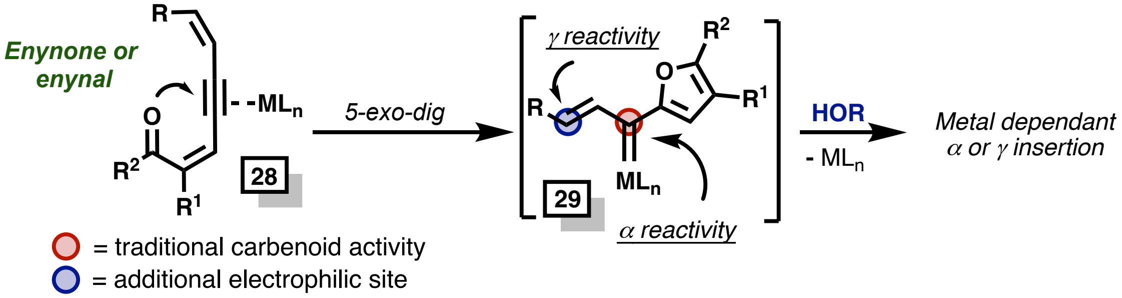
Enynone or enynal
R
O
R2
R1
ML_n
28
5-exo-dig
γ reactivity
R
O
R2
R1
ML_n
29
α reactivity
HOR
- ML_n
Metal dependant α or γ insertion
= traditional carbenoid activity
= additional electrophilic site

b). Gamma Insertion Precendant: Lopéz, 2013.

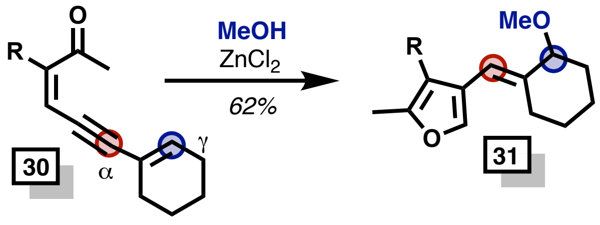
O
R
30
α
γ
MeOH
ZnCl2
62%
R
O
MeO
31

Figure 3.6: Enynones and Enynals as Metal Carbenoid Precursors

Revisiting alkynes, we thought to synthesize glycal carbenes using enynones as a metal carbene precursor. Initially, the free glucose-derived glycal **32** (glucal) was protected with either benzyl or acetate protecting groups, following a literature known protocol. The tri-protected glucal was then exposed to *N*-iodosuccinimide and silver nitrate to form the corresponding iodoglycal **34** .[19]

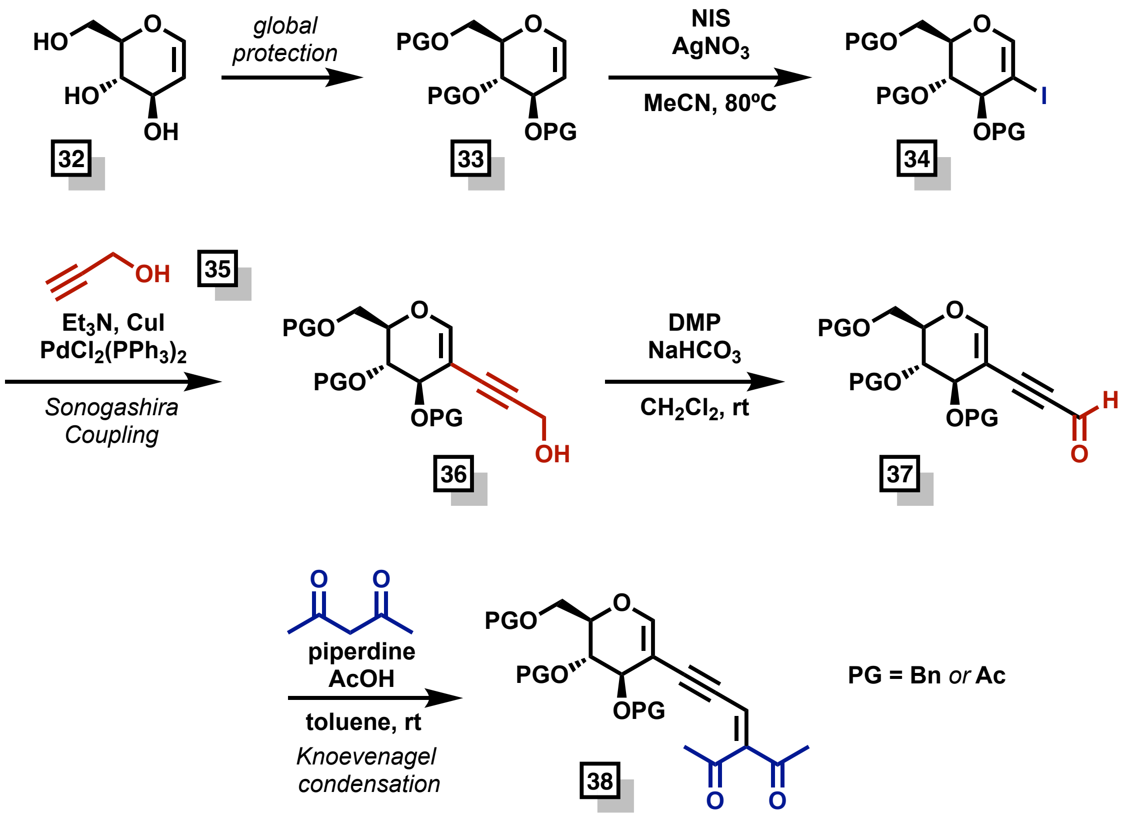
HO
HO
OH
32
global protection
PGO
PGO
OPG
33
NIS
$AgNO_3$
MeCN, 80ºC
PGO
PGO
OPG
I
34
OH
35
Et_3N, CuI
$PdCl_2(PPh_3)_2$
Sonogashira Coupling
PGO
PGO
OPG
OH
36
DMP
$NaHCO_3$
CH_2Cl_2, rt
PGO
PGO
OPG
H
O
37
O
O
piperdine
AcOH
toluene, rt
Knoevenagel condensation
PGO
PGO
OPG
O
O
38
PG = Bn *or* Ac

Figure 3.7: Synthesis of Glycal Carbene from Enynones

Following iodination, the substrate was exposed to palladium-catalyzed, Sonogashira coupling conditions with propargyl alcohol **35** to synthesize the hydroxyl propargyl glycal **36**. This step is extremely low-yielding. We postulate that this is due to the bulk of the C3 groups hindering the oxidative addition of the palladium metal center. Once **36** was synthesized in good amounts, it was exposed to Dess Martin Periodinane to be oxidized to the glycal aldehyde **37**. Following isolation, the aldehyde **37** was exposed to 2,4 pentanedione in toluene to undergo a Knoevenagel condensation to produce the desired tri-protected enynone **38** (**Figure 3.7**).

SCREENING OF CATALYTIC CONDITIONS

With a reproducible route established to synthesize the desired glycal carbenes, we then focused on the optimization of catalytic conditions to promote the desired γ insertion. Encouraged by the disclosed results of Lopéz,[21a] where the authors observed exclusive γ insertion of primary alcohols with enynones bearing an additional alkenyl moiety, we exposed the benzyl-protected glycal **38b** to analogous conditions. Thus, at room temperature, we exposed **38b** to isopropanol with $ZnCl_2$ (10 mol%) in dichloromethane (**Figure 3.8**).

Monitoring this reaction via TLC, we observed consumption of the starting material within one hour. We expected to observe a ratio of regioisomers for both the α and γ insertion of isopropanol. However, extrapolation of NMR data confirmed that neither the α nor γ insertion product was formed. Opposingly, this system resulted in the C–H functionalization of the benzyl C3 methylene group to form product **42**.[24]

a). Initial Observations using Benzyl Protected Glycal Carbenes

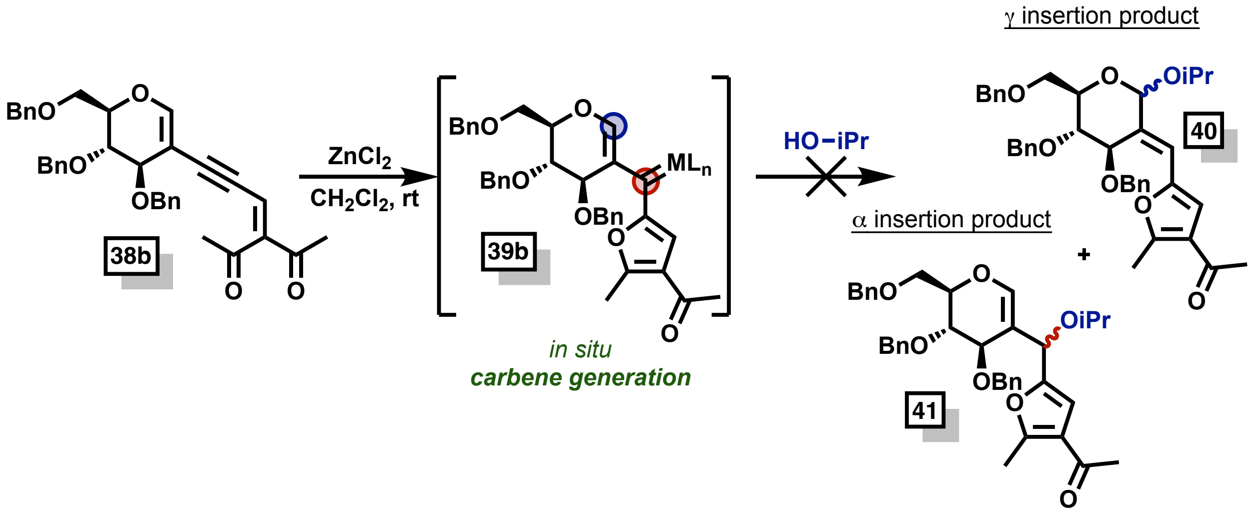
γ insertion product
BnO
BnO
OBn
38b
ZnCl$_2$
CH$_2$Cl$_2$, rt
BnO
BnO
OBn
ML$_n$
39b
in situ
carbene generation
HO−iPr
OiPr
40
α insertion product
+
OiPr
41

Neither regioisomer observed

b). Hypothesized Product Formation

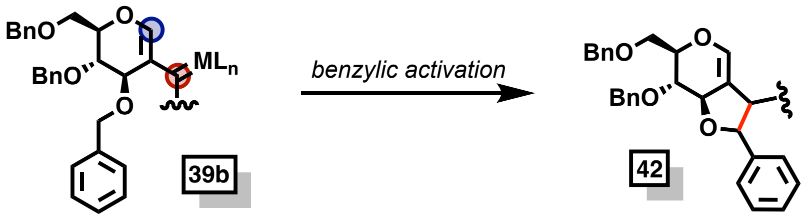
BnO
BnO
ML$_n$
39b
benzylic activation
42

Figure 3.8: Initial Observation with Benzyl-protected Glycal

With these results, we postulated that the arming benzyl protecting group was ill-suited for our designed system. We then synthesized the triacetate-protected analog **38a** and exposed this substrate to analogous conditions to circumvent this. We observed complete consumption of the starting material within one hour via TLC, to our delight. Upon completion, with NMR spectral analysis we observed a single regioisomer –the desired γ insertion adduct **43 (Figure 3.9)**.

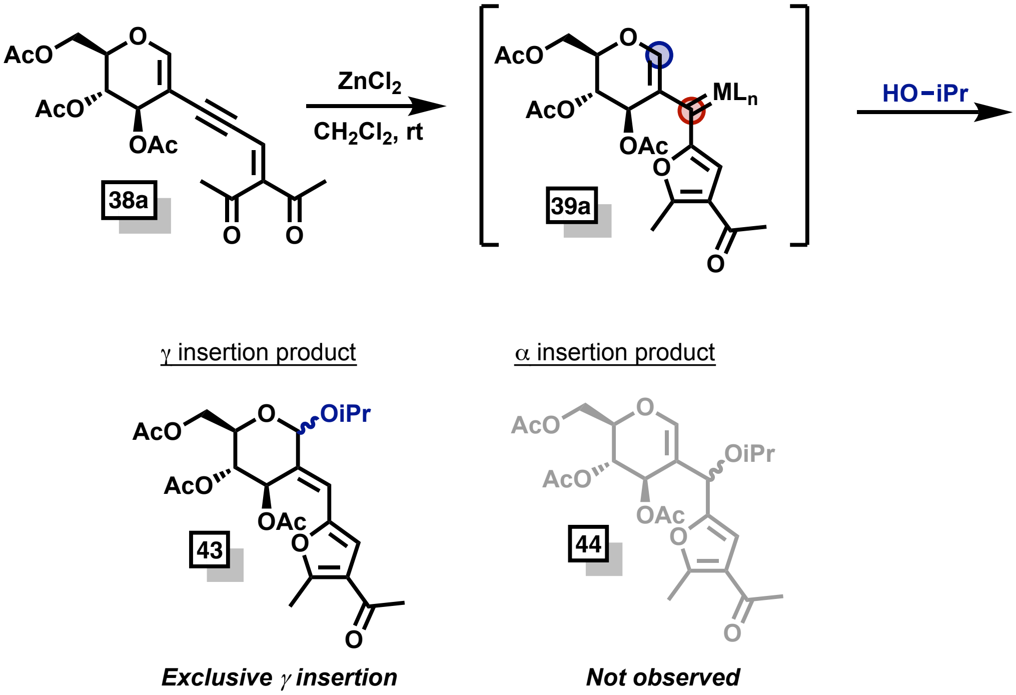
38a
ZnCl2
CH2Cl2, rt
39a
MLn
HO–iPr
γ insertion product
α insertion product
43
44
OiPr
Exclusive γ insertion
Not observed

Figure 3.9: Initial Observations using Triacetate System

We were thrilled to solve the initial question of regioselectivity and then turned our attention to addressing the stereochemical outcome of the reaction. After thorough examination of the crude spectra, we determined the anomeric ratio to be 1:4 (α : β) for the $ZnCl_2$ catalyzed reaction. To solve for stereochemistry, we initially screened a variety of commercially available metal salts using isopropanol as a trapping agent in dichloromethane (**Table 3.1**).

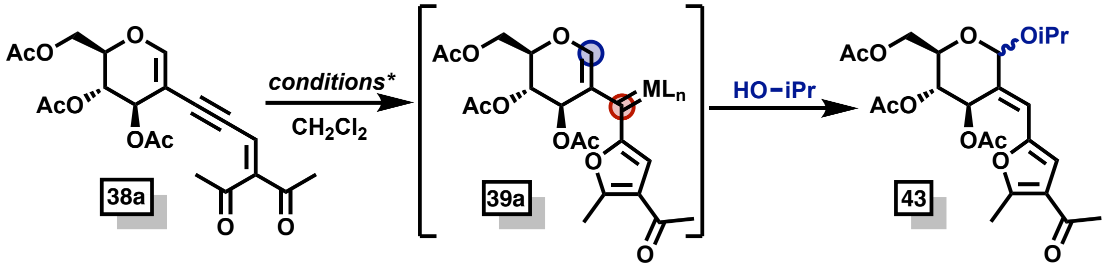

entry	catalyst	temp	time	α : β
1	**$ZnCl_2$**	**-20ºC**	**1 h**	**1:4**
2	$ZnBr_2$	-20ºC	12 h	1:1
3	ZnI_2	-20ºC	12 h	1:1
4	$Zn(OTf)_2$	0ºC	1 h	5:1
5	$(MeCN)_4CuBF_4$	0ºC	4 h	3:1
6	$AgBF_4$	0ºC	2 h	8.5 :1
7	$Fe(BF_4)$-H_2O	0ºC	12 h	n.d
8	$FeCl_3$	0ºC	12 h	n.d
9	$Rh_2(esp)_2$	0ºC	1 h	1:3

*Optimization reactions were completed by dissolving isopropanol (1.2 equiv.) into 500 μL of distilled dichloromethane and cooled to the appropriate temperature. After 10 minutes the catalyst (0.3 equiv.) was added to solution and allowed to stir an additional 5 minutes. Finally, **38a** (0.015g, 1 equiv.) was added to the reaction and monitored via TLC. Once complete, the reaction is diluted in dichloromethane and washed with a saturated $NaHCO_3$ solution. The organics were extracted a total of three times, before drying over Na_2SO_4. Anomeric ratios based on the integration of crude spectra.

Table 3.1: Metal Catalyst Optimization for Anomeric Stereoselectivity

A variety of metal salts were screened. Initially, to observe the effect of other halide anions, both zinc bromide and zinc iodide were studied. However, these experiments resulted in a racemic mixture on anomers (**entries 2**,**3**). To further study the effect of anion substitution, zinc triflate was screened (**entry 4**) and, to our surprise, resulted in a flip of anomeric selectivity. NMR analysis resulted in the observation of a 5:1 (α:β) anomeric ratio. This was contrary to our $ZnCl_2$ results and piqued our scientific interests. We hypothesized that the more liable, less coordinating triflate ligand would produce a more cationic metal center that could be responsible for the stereoselectivity observed. To test this hypothesis, both copper and silver tetrafluoroborate were assessed (**entries 5**,**6**) as the tetrafluoroborate ligand is also a weakly-coordinating complex. This resulted in anomeric selectivity in line with our hypothesis.

We then attempted to screen iron salt complexes, given our goal of developing Earth-abundant metal catalysis protocols. Iron is the second most abundant metal in the Earth's crust, after aluminum, and is considered to possess "minimal safety concern" as in drug substances. However, neither ferric chloride nor iron tetrafluoroborate resulted in a clean reaction (**entries 7**,**8**). Lastly, we screened $Rh_2(esp)_2$, due to its success in the diazo-mediated transformations developed within our research laboratory.[18b]

Catalyst screening led to the identification of $Zn(OTf)_2$ and $AgBF_4$ as optimal catalysts for the predominant formation of the α anomer (thermodynamic product). However, $ZnCl_2$ was the best-screened catalyst for the formation of the β anomer and resulted in the cleanest rection. In line with our goals to identify catalyst systems using Earth-abundant metals, we continued our optimization studies using $ZnCl_2$ as the catalyst of choice. Zinc is the 25thmost abundant metal within the Earth's crust, and most adults intake several milligrams daily. To continue optimizing for the formation of the β anomer, we then turned to solvent screening (**Table 3.2**).

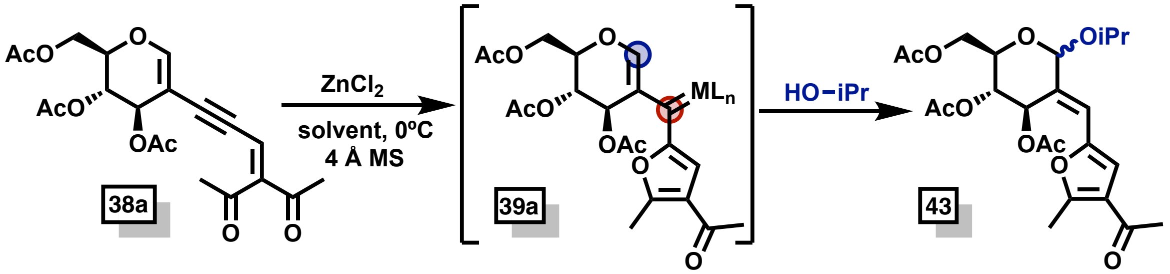

entry	solvent	time	a : b
1	CH_2Cl_2	> 1 h	1 : 3
2	**$PhCF_3$**	**3 h**	**5 : 1**
3	nitromethane	3 h	decomposition
4	$CHCl_3$	overnight	4 :1
5	toluene	0ºC	6 :1
6	MeCN	overnight	1 : 4
7	THF	overnight	nr
8	Heptane: CH_2Cl_2 (6 : 1)	overnight	1 : 2.3

*Optimization reactions were completed by dissolving isopropanol (1.1 equiv., 2 uL, $ZnCl_2$ (20 mol %), and 20 mg of activated 4-angstrom molecular sieves into 500 μL of the desired solvent and cooled to 0ºC. After 10 minutes, **38a** was added to the solution and allowed to stir and warm to room temperature until starting material consumption via TLC. Once complete, the reaction is diluted in dichloromethane and washed with a saturated $NaHCO_3$ solution. The organics were extracted a total of three times, before drying over Na_2SO_4. Anomeric ratios are based on the integration of crude spectra.

Table 3.2: Solvent Optimization Table

After solvent screening, we noticed a profound solvent effect on the anomeric selectivity of the glycosylation reaction. When α,α,α-trifluorotoluene and toluene were screened, both nonpolar solvents, we observed a higher ratio of the α-product was observed. This was also observed with chloroform as a solvent. Seemingly, only dichloromethane furnishes a greater ratio of the β-anomer. Additionally, when a ratio of heptane and DCM (6:1) was used, we observed a 1:2.3 (α:β) ratio. Notably, the Lewis basic solvent THF resulted in no product formation, and nitromethane resulted in severe product decomposition.

With these results, we decided to first pursue the α-anomer using triflourotoulene, as these conditions resulted in the cleanest product formation. Continued optimization led to the identification of finalized reaction conditions, which included the addition of 0.5 equivalents of 2,6-Di-tert-butyl methylpyridine, a non-coordinating Brønsted base, to quench any acid that may be formed *in situ*, as it is known that Lewis acids can serve as a mild source of their corresponding Brønsted acid.[25] These conditions result in an efficient and fast glycosylation strategy, complete within 1 hour (**Figure 3.10**).

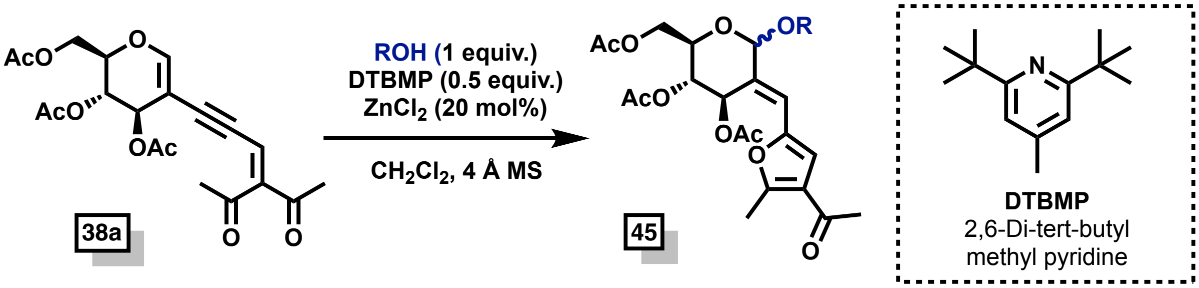

Figure 3.10: Optimization Conditions for α-anomer formation

3.2.1 APPLICABLE SUBSTRATE SCOPE

We then attempted to prepare a substrate scope featuring a variety of *O*-glycosyl acceptors, with optimized conditions in hand. When isopropanol was used as a glycosyl acceptor, we were able to prepare the corresponding glycoside **45a** in a moderate 57% yield. When we exposed the bulky chiral alcohol L-menthol to our glycal carbene system, we observed a profound effect on the diastereoselectivity of our reaction conditions and observed almost exclusive α-anomer formation via NMR. We went on to isolate **45b** in a moderate 48% yield. Additionally, we are currently synthesizing the galactal-derived glycal carbene. Once prepared, we intend to expose it to analogous conditions to determine whether the stereochemistry of the glycosyl donor will affect yields and anomeric selectivity (**Figure 3.11**).

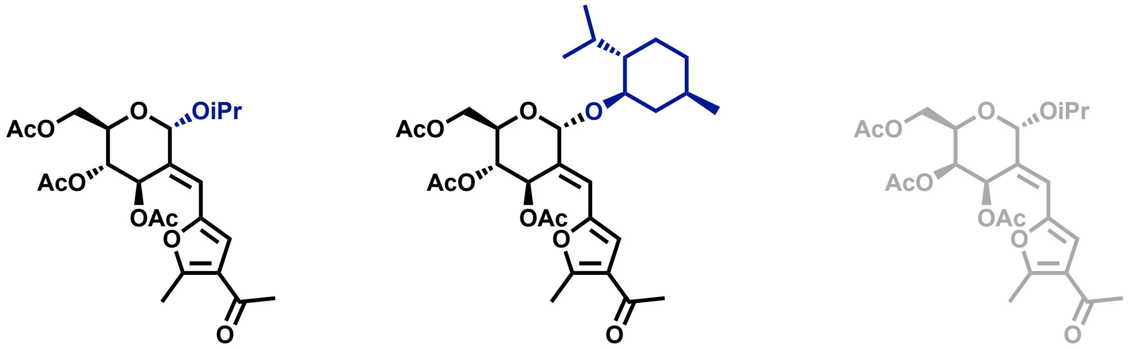

45a, 57%, dr: 5:1 (α:β) **45b,** 48%, dr: 98:2 (α:β) **45c,** *in preparation*

Figure 3.11: Glycosylation Reactions with Simple Alcohols

We then turned our attention to sugar glycosyl acceptors to form disaccharide bonds. In light of this, we synthesized primary sugar alcohol **46** and exposed it to our glycal system. However, despite attempting to optimize conditions with the sugar alcohol (solvent, temperature, catalyst, etc.), we were never able to develop respectable conditions. Additionally, the reaction with the bulkier alcohol was much more sluggish. While reactions with simple alcohols are complete within 1 hour, conditions with the sugar alcohol never reach full consumption of the glycal carbene. Additionally, less than 10% of the desired glycoside **47** was formed via TLC and NMR analysis (**Figure 3.12**).

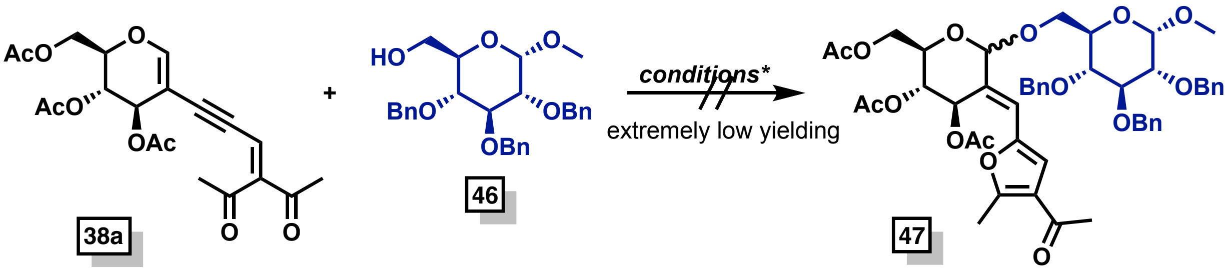

Figure 3.12: Glycosylation Attempts with Sugar Acceptor

These observations concluded that this system was not conducive for disaccharide and oligosaccharide synthesis.

3.2.2 MECHANISTIC INSIGHTS

Mechanistically, we hypothesize the possibility of two major pathways responsible for the regio- and stereo-selectivity observed (**Figure 3.13**). Both mechanisms are initiated through an intramolecular *5-exo*-dig cyclization forming glycal intermediates **48** and **51**.

In **Route I**, back donation from the metal salt will lead to the formation of the $^{4}H_{5}$ intermediate **49**. A bottom facial attack suffers from unfavorable steric interactions between the incoming nucleophile and the C2 and C5 substituents.[3b] Therefore, the nucleophile preferentially attacks from the top face, furnishing the β–anomer. When employing electron-poor metals, we believe that after cyclization, electron donation from the endocyclic oxygen can lead to the formation of glycosyl oxocarbenium **52** (**Route II**). Here, steric restraints favor a top facial attack, leading to the α-anomer.

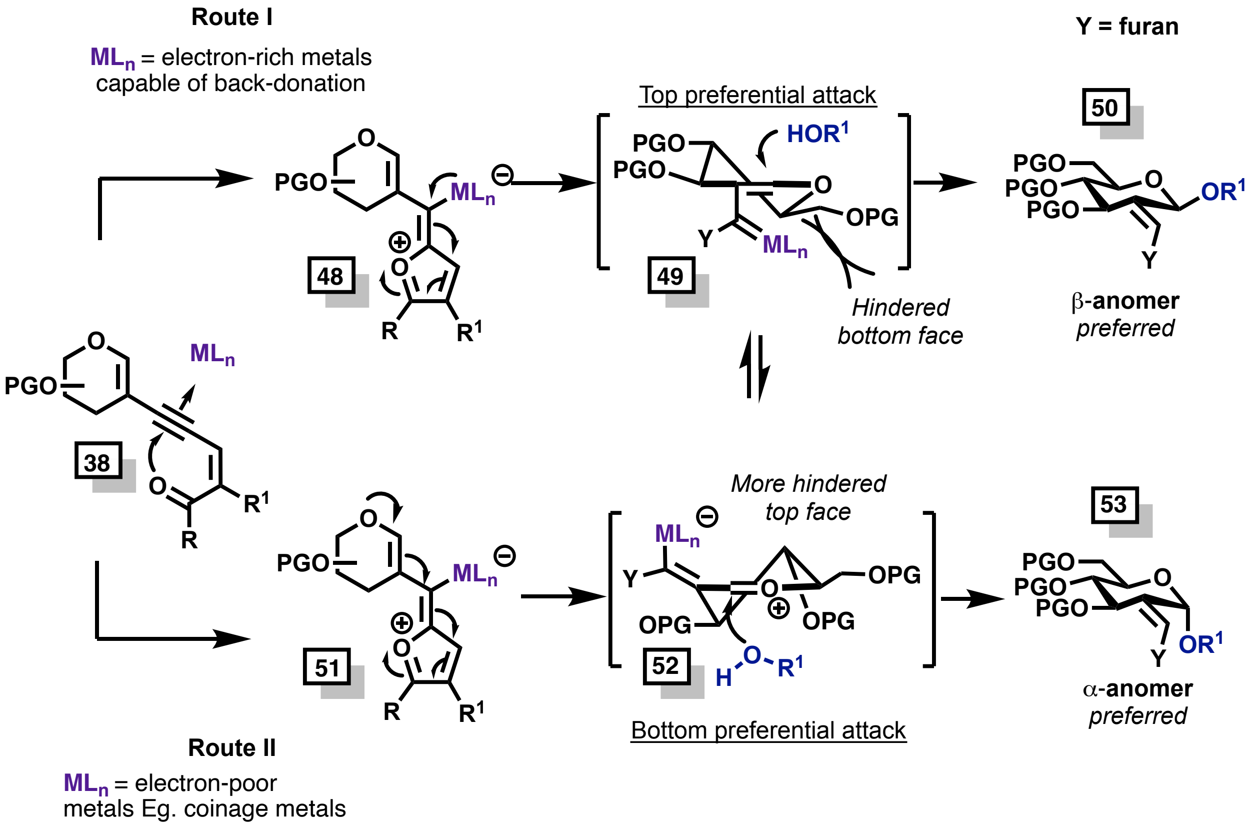
Route I
MLn = electron-rich metals capable of back-donation
Y = furan
Top preferential attack
HOR1
Hindered bottom face
β-anomer preferred
48
49
50
38
51
52
53
More hindered top face
Bottom preferential attack
α-anomer preferred
Route II
MLn = electron-poor metals Eg. coinage metals

Figure 3.13: Mechanistic Rationale for Glycosylation

Another factor that can influence the stereocontrol of the reaction is the role of the counter anion discharged from the metal catalyst,[26] as we have observed. In the event of the formation of glycosyl oxocarbenium intermediate **52**, the intermediate may exist in equilibrium as a solvent-separated ion pair (SSIP) **54**, contact-ion pair (CIP) **55**, or α-covalent species **56** (thermodynamic product), which all can exist in equilibrium. A subsequent S_N2 attack on the α-covalent species would also furnish the β-anomer (**Figure 3.14**).

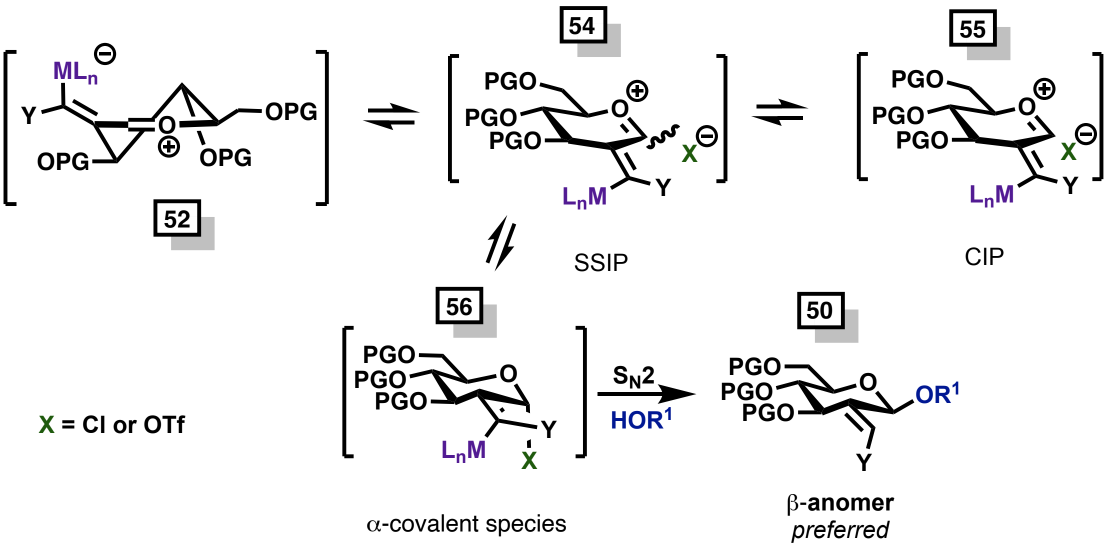
52
54
55
56
50
MLn
Y
OPG
OPG
OPG
PGO
PGO
PGO
X
LnM
Y
SSIP
CIP
X = Cl or OTf
SN2
HOR1
OR1
α-covalent species
β-anomer
preferred

Figure 3.14: Solvent and Counterion Effect on Anomeric Ratio

3.3 FUTURE DIRECTIONS AND LIMITATIONS

With our optimized conditions, we will continue the application of our glycal carbene to a variety of simple alcohols. While the realization of our glycal carbene approach will enhance the fundamental understanding of metal-carbene chemistry in glycosylation reactions, there may be certain limitations for the preparation of simple oligosaccharides due to the additional manipulations required after glycosylation. To address this, we intend to cleave the pendant furan group via an oxidative cleavage yielding 2-oxyglycoside **57**.[27] This will result in a C2 ketone, an excellent diversification handle that can be used to diversify the glycoside (**Figure 3.15a**).

a) Cleavage of pendant furan

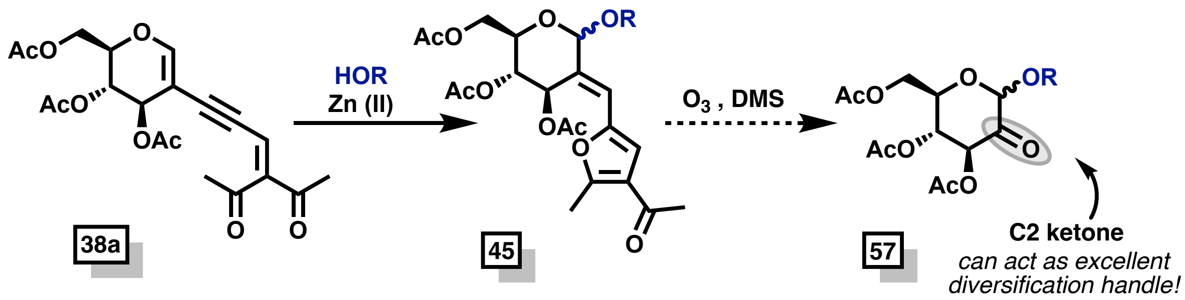
AcO
AcO
OAc
38a
HOR
Zn (II)
OR
45
O_3 , DMS
57
OR
C2 ketone

can act as excellent diversification handle!

b) Diversification of pendant furan

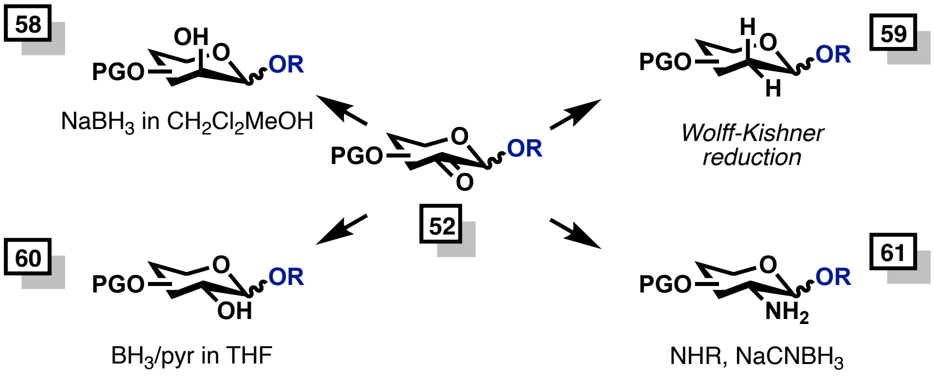
58
PGO
OH
OR
NaBH$_3$ in CH$_2$Cl$_2$MeOH
59
H
H
Wolff-Kishner reduction
52
60
OH
BH$_3$/pyr in THF
61
NH$_2$
NHR, NaCNBH$_3$

Figure 3.15: Diversification of Furan Moiety for Diverse pyranosides

2-Oxyglycoside **57** can undergo a Wolff-Kishner reduction[28] to remove the C2 carbonyl moiety for the synthesis of 2-deoxygenated sugars **59**. Equally, a reductive amination sequence would furnish glycosyl amines **61**.[29] Finally, a reduction sequence would allow the installation of secondary alcohol at the C2 position. Stereoselective reductions can also be implemented to access biologically relevant targets bearing a particular stereochemistry found in either glucose[30] or mannose[31] series (**58**,**60**) (**Figure 3.15b**).

3.4 SUMMARIES

We have successfully synthesized and tested a novel, carbene-based glycosyl donor we have termed *glycal carbenes*. These donors function through the vinylogous addition of nucleophiles at the anomeric position. Through this mechanism, in theory, two regioisomers are possible. In our first successful trial using this system, we were thrilled to have solved the initial question of regioselectivity, thereby effectively harnessing the vinylogous reactivity of glycal carbenes. Further, we have demonstrated that γ-addition leads to the formation of the single geometric (*E*)-isomer of the resulting exo-olefin. This strategy is applicable to simple alcohol glycosyl acceptors and can synthesize glycosides in moderate yields.

This work is extremely novel and in its infancy. We have optimized conditions for both α- and β- anomer formation and have begun synthesizing analogues with these conditions for α-glycosides. With our optimized conditions, we have synthesized sugar analogs in moderate yields with isopropanol (57%). Encouragingly, when the bulky chiral alcohol L-menthol is used, diastereoselectivity increases dramatically (98:2). Unfortunately, while novel and exciting, we are not able to apply this chemistry towards di- and oligosaccharide synthesis. Additionally, we recognize that these donors require post-transformation modifications which decreases the impact of this strategy. The following chapter will discuss the design of another carbene-assisted donor we have developed to overcome these limitations.

3.5 REFERENCES FOR CHAPTER 4

[1] a). A. M. Vibhute, N. Komura, H.-N. Tanaka, A. Imamura, H. Ando, *Chemical record (New York, N.Y.)* **2021**; b). in *Selective Glycosylations: Synthetic Methods and Catalysts*, **2017**, pp. 135-153; c). M. J. McKay, H. M. Nguyen, *ACS catalysis* **2012**, *2*, 1563-1595; d). J. H. Kim, H. Yang, J. Park, G. J. Boons, *J. Am. Chem. Soc.* **2005**, *127*, 12090; e). J.-H. Kim, H. Yang, G.-J. Boons, *Angewandte Chemie International Edition* **2005**, *44*, 947-949; f). Y. Du, R. J. Linhardt, I. R. Vlahov, *Tetrahedron* **1998**, *54*, 9913.

[2] X. Zhu, R. R. Schmidt, *Angew. Chem., Int. Ed.* **2009**, *48*, 1900-1934.

[3] a). P. O. Adero, H. Amarasekara, P. Wen, L. Bohé, D. Crich, *Chemical Reviews* **2018**, *118*, 8242; b). K. Le Mai Hoang, W. L. Leng, Y. J. Tan, X. W. Liu, *Selective Glycosylations: Synthetic Methods and Catalysts*, **2017**.

[4] a). A. I. Tokatly, D. Z. Vinnitskiy, N. E. Ustuzhanina, N. E. Nifantiev, *Russian Journal of Bioorganic Chemistry* **2021**, *47*, 53-70; b). R. Ogasahara, S. Abdullayev, V. A. Sarpe, A. R. Mandhapati, D. Crich, *Carbohydrate Research* **2020**, *496*, 108100; c). B. Ghosh, S. S. Kulkarni, *Chemistry – An Asian Journal* **2020**, *15*, 450-462; d). M. Heuckendorff, L. T. Poulsen, H. H. Jensen, *J. Org. Chem.* **2016**, *81*, 4988.

[5] L. F. Bornaghi, S.-A. Poulsen, *Tetrahedron Letters* **2005**, *46*, 3485-3488.

[6] a). Y. Singh, A. V. Demchenko, *Chemistry – A European Journal* **2019**, *25*, 1461-1465; b). L. Sun, X. Wu, D. C. Xiong, X. S. Ye, *Angew. Chem., Int. Ed.* **2016**, *55*, 8041.

[7] a). S. J. Moons, R. A. Mensink, J. P. J. Bruekers, M. L. A. Vercammen, L. M. Jansen, T. J. Boltje, *J Org Chem* **2019**, *84*, 4486-4500; b). M. Boultadakis-Arapinis, E. Prost, V. Gandon, P. Lemoine, S. Turcaud, L. Micouin, T. Lecourt, *Chem. - Eur. J.* **2013**, *19*, 6052; c). K. Mébarki, M. Gavel, F. Heis, A. Y. P. Joosten, T. Lecourt, *The Journal of Organic Chemistry* **2017**, *82*, 9030-9037.

[8] a). K. K. T. Mong, T. Nokami, N. T. T. Tran, P. B. Nhi, *Selective Glycosylations: Synthetic Methods and Catalysts*, **2017**; b). H. Yao, S. Zhang, W. L. Leng, M. L. Leow, S. Xiang, J. X. He, H. Liao, K. Le Mai Hoang, X. W. Liu, *ACS Catalysis* **2017**, *7*, 5456–5460; c). C. S. Bennett, *Selective Glycosylations: Synthetic Methods and Catalysts: Synthetic Methods and Catalysts*, **2017**.

[9] T. Li, T. Li, H. Zhuang, F. Wang, R. R. Schmidt, P. Peng, *ACS Catalysis* **2021**, *11*, 10279-10287.

[10] X. Ma, Z. Zheng, Y. Fu, X. Zhu, P. Liu, L. Zhang, *Journal of the American Chemical Society* **2021**, *143*, 11908-11913.

[11] a). A. Ford, H. Miel, A. Ring, C. N. Slattery, A. R. Maguire, M. A. McKervey, *Chem. Rev.* **2015**, *115*, 9981–10080; b). G. Maas, *Angew. Chem., Int. Ed.* **2009**, *48*, 8186-8195; c). K. A. Mix, R. T. Raines, *Org. Lett.* **2015**, *17*, 2358-2361; d). Z. Zhang, J. Wang, *Tetrahedron* **2008**, *64*, 6577-6605.

[12] a). R. Ardkhean, D. F. J. Caputo, S. M. Morrow, H. Shi, Y. Xiong, E. A. Anderson, *Chem. Soc. Rev.* **2016**, *45*, 1557-1569; b). A. Padwa, *Prog. Heterocycl. Chem.* **2009**, *20*, 20-46; c). A. Padwa, M. D. Weingarten, *Chem. Rev.* **1996**, *96*, 223–269; d). B. T. Parr, H. M. L. Davies,

Nat. Commun. **2014**, *5*, 4455; e). B. T. Parr, H. M. L. Davies, *Org. Lett.* **2015**, *17*, 794–797; f). S. Jansone-Popova, P. Q. Le, J. A. May, *Tetrahedron* **2014**, *70*, 4118–4127.

[13] H. M. L. Davies, B. Hu, E. Saikali, P. R. Bruzinski, *The Journal of Organic Chemistry* **1994**, *59*, 4535-4541.

[14] a). R. Fang, L. Yang, L. Zhou, A. M. Kirillov, L. Yang, *Organic Letters* **2020**, *22*, 4043-4048; b). B. Zhang, H. M. L. Davies, *Angew Chem Int Ed Engl* **2020**, *59*, 4937-4941; c). P. E. Guzman, Y. Lian, H. M. Davies, *Angew Chem Int Ed Engl* **2014**, *53*, 13083-13087; d). J. F. Briones, H. M. Davies, *Journal of the American Chemical Society* **2013**, *135*, 13314-13317; e). W. Shi, F. Xiao, J. Wang, *The Journal of Organic Chemistry* **2005**, *70*, 4318-4322.

[15] J. H. Hansen, H. M. L. Davies, *Chem. Sci.* **2011**, *2*, 457-461.

[16] E. Lopez, S. Gonzalez-Pelayo, L. A. Lopez, *Chem Rec* **2017**, *17*, 312-325.

[17] E. Fischer, *Berichte der deutschen chemischen Gesellschaft* **1893**, *26*, 2400-2412.

[18] a). K. Chinthapally, N. P. Massaro, I. Sharma, *Org Lett* **2016**, *18*, 6340-6343; b). A. C. Hunter, K. Chinthapally, I. Sharma, *European Journal of Organic Chemistry* **2016**, *2016*, 2260-2263; c). A. C. Hunter, B. Almutwalli, A. I. Bain, I. Sharma, *Tetrahedron* **2018**, *74*, 5451-5457; d). K. Chinthapally, N. P. Massaro, S. Ton, E. D. Gardner, I. Sharma, *Tetrahedron Letters* **2019**, *60*, 151253; e). D. J. Paymode, I. Sharma, *European Journal of Organic Chemistry* **2021**, *2021*, 2034-2040; f). A. I. Bain, K. Chinthapally, A. C. Hunter, I. Sharma, *European Journal of Organic Chemistry* **2022**, *n/a*, e202101419.

[19] S. Dharuman, Y. D. Vankar, *Org Lett* **2014**, *16*, 1172-1175.

[20] a). F. Ye, S. Qu, L. Zhou, C. Peng, C. Wang, J. Cheng, M. L. Hossain, Y. Liu, Y. Zhang, Z.-X. Wang, J. Wang, *Journal of the American Chemical Society* **2015**, *137*, 4435-4444; b). C. Peng, J. Cheng, J. Wang, *Journal of the American Chemical Society* **2007**, *129*, 8708-8709.

[21] a). J. González, J. González, C. Pérez-Calleja, L. A. López, R. Vicente, *Angewandte Chemie International Edition* **2013**, *52*, 5853-5857; b). R. Vicente, J. González, L. Riesgo, J. González, L. A. López, *Angewandte Chemie International Edition* **2012**, *51*, 8063-8067.

[22] D. Zhu, L. Chen, H. Fan, Q. Yao, S. Zhu, *Chemical Society Reviews* **2020**, *49*, 908-950.

[23] a). D. Zhu, L. Chen, H. Fan, Q. Yao, S. Zhu, *Chem Soc Rev* **2020**, *49*, 908-950; b). B. D. Bergstrom, L. A. Nickerson, J. T. Shaw, L. W. Souza, *Angewandte Chemie International Edition* **2021**, *60*, 6864-6878.

[24] H. M. L. Davies, K. Liao, *Nature Reviews Chemistry* **2019**, *3*, 347-360.

[25] a). T. C. Wabnitz, J.-Q. Yu, J. B. Spencer, *Chemistry – A European Journal* **2004**, *10*, 484-493; b). T. T. Dang, F. Boeck, L. Hintermann, *The Journal of Organic Chemistry* **2011**, *76*, 9353-9361.

[26] a). H. Satoh, H. S. Hansen, S. Manabe, W. F. van Gunsteren, P. H. Hunenberger, *J. Chem. Theory Comput.* **2010**, *6*, 1783; b). S. S. Nigudkar, A. V. Demchenko, *Chemical Science* **2015**, *6*, 2687–2704.

[27] F. Emery, P. Vogel, *Tetrahedron Letters* **1993**, *34*, 4209-4212.

[28] D. Horton, W. Weckerle, L. Odier, R. J. Sorenson, *Journal of the Chemical Society, Perkin Transactions 1* **1977**, 1564-1574.

[29] T. Yoshida, Y. C. Lee, *Carbohydrate Research* **1994**, *251*, 175-186.

[30] A. Fürstner, I. Konetzki, *Tetrahedron* **1996**, *52*, 15071-15078.

[31] F. W. Lichtenthaler, T. Schneider-Adams, *The Journal of Organic Chemistry* **1994**, *59*, 6728-6734.

3.6 EXPERIMENTAL SECTION FOR SECTION 3

MATERIALS AND METHODS

Reagents

Reagents and solvents were obtained from Sigma-Aldrich, Chem-Impex, VWR International, and Acros Organics and used without further purification unless otherwise indicated. Dichloromethane and Acetonitrile were distilled over CaH under N_2 unless otherwise indicated. Tetrahydrofuran was distilled over Na under N_2 with benzophenone indicator.

Glassware

All reactions were performed in flame-dried glassware under positive N_2 pressure with magnetic stirring unless otherwise noted.

Chromatography

Thin layer chromatography (TLC) was performed on 0.25 mm E. Merck silica gel 60 F254 plates and visualized under UV light (254 nm) or by staining with potassium permanganate ($KMnO_4$), cerium ammonium molybdate (CAM), phosphomolybdic acid (PMA), and ninhydrin. Silica flash chromatography was performed on Sorbtech 230-400 mesh silica gel 60.

Analytical Instrumentation

NMR spectra were recorded on a Varian VNMRS 400 and 500 MHz NMR spectrometer at 20 ºC in $CDCl_3$ unless otherwise indicated. Chemical shifts are expressed in ppm relative to solvent signals: $CDCl_3$ (1H, 7.26 ppm, 13C, 77.0 ppm); coupling constants are expressed in Hz. IR spectra were recorded on a Cary 760 FTIR spectrometer with peaks reported in cm^{-1}. Mass spectra were obtained on an Advion Expression CMS TLC Mass Spectrometer

Nomenclature

Chemical structure named in accordance with IUPAC guidelines, automatically generated using ChemDraw 20.1

Additional Information and Considerations

Syringe pump addition reactions were conducted using a Harvard Apparatus (Model: 55-1111) or a New Era Pump Systems, Inc. (Model: NE-300) syringe pump. Sonication was performed using a Bransonic Ultrasonic Cleaner (Model: M5800H).

PUBLICATION AND CONTRIBUTIONS STATEMENT

The research within this section is unpublished. All materials and procedures are contributions by A. Bain solely.

3.6.1 Synthesis of Glycal Carbene

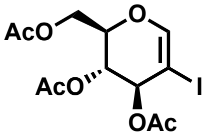

(2*R*,3*R*,4*S*)-2-(acetoxymethyl)-5-iodo-3,4-dihydro-2*H*-pyran-3,4-diyl diacetate (34a): Compound was prepared from a literature-reported procedure from D-glucal.[1]

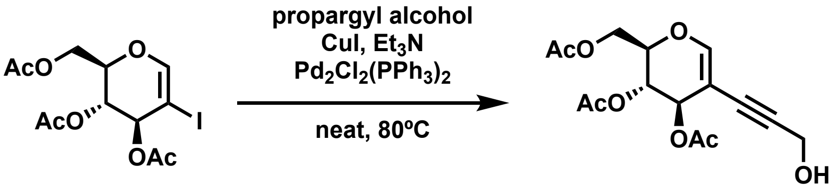

(2*R*,3*S*,4*R*)-2-(acetoxymethyl)-5-(3-hydroxyprop-1-yn-1-yl)-3,4-dihydro-2*H*-pyran-3,4-diyl diacetate (36a): 34a (1 equiv.), $PdCl_2(PPh_3)_2$ (20 mol%) and CuI (20 mol%) was suspended into 0.2 M solution of Et_3N in a Teflon coated 20 mL vial. The solution was degrassed N_2 for 15 minutes with a 6 inch needle, before propargyl alcohol (5 equiv.) was added to reaction. The flask was then sealed and heated to 80ºC. After two hours, the starting material was consumed via TLC. The crude reaction was filter over celite with EtOAc and washed twice with brine. The organics were extracted three times before drying over Na_2SO_4. The crude compound was purified via a silica gel chromatography at a 20% EtOAc / 80% Hexanes to 50% EtOAc / 50% Hexanes gradient as a yellow oil.

R_f = 0.22, 50% EtOAc/ 50% Hexanes

^{1}H NMR (500 MHz, $CDCl_3$) δ 6.88 (s, 1H), 5.50 (dt, *J* = 5.2, 0.9 Hz, 1H), 5.19 (dd, *J* = 6.6, 5.2 Hz, 1H), 4.41 (dd, *J* = 12.1, 6.3 Hz, 1H), 4.35 (dd, *J* = 6.4, 3.4 Hz, 4H), 4.20 (dd, *J* = 12.1, 3.3 Hz, 1H), 2.15 – 2.06 (m, 13H).

^{13}C NMR (126 MHz, $CDCl_3$) δ 170.40 (d, *J* = 25.8 Hz), 169.43, 151.27, 96.15, 88.09, 79.90, 74.23, 66.96, 66.29, 61.01, 51.43, 21.55 – 19.82 (m).

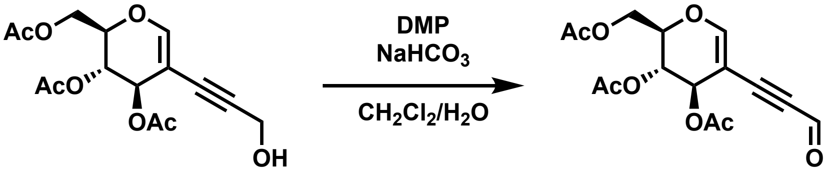

(2*R*,3*S*,4*R*)-2-(acetoxymethyl)-5-(3-oxoprop-1-yn-1-yl)-3,4-dihydro-2*H*-pyran-3,4-diyl diacetate (37a): 36a (1 equiv) was dissolved in wet 0.15M of dichloromethane (50:1 DCM:H_2O) in a round bottom flask. Sodium bicarbonate (10 equiv) was added to the reaction flask and the reaction was allowed to stir at room temperature overnight. After 12 hours, the reaction was complete via TLC. The reaction was diluted with DCM and washed with sodium bicarbonate. The organics were extracted three times before drying over sodium sulfate. The crude compound was purified via isocratic 40% EtOAc/60% Hexanes eluent system.

R_f = 0.25, 30% EtOAc in Hexanes

^{1}H NMR (500 MHz, CDCl$_3$) δ 9.25 (d, *J* = 1.5 Hz, 1H), 7.22 (s, 1H), 5.58 – 5.50 (m, 1H), 5.22 (t, *J* = 5.6 Hz, 1H), 4.52 – 4.39 (m, 2H), 4.23 (dd, *J* = 11.9, 3.0 Hz, 1H), 2.17 – 2.06 (m, 11H).

^{13}C NMR (101 MHz, CDCl$_3$) δ 175.91, 170.38, 169.90, 169.28, 157.53, 94.43, 92.27, 91.16, 75.15, 65.67, 65.57, 60.73, 20.72, 20.66.

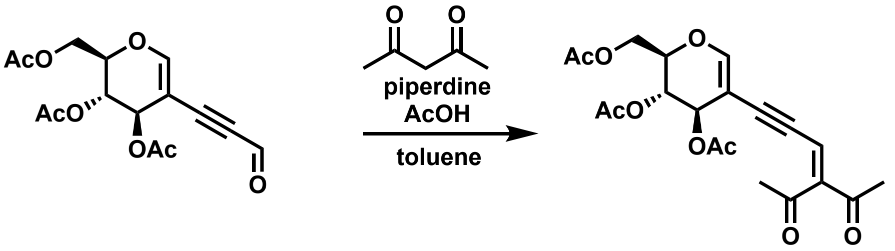

(2*R*,3*S*,4*R*)-2-(acetoxymethyl)-5-(4-acetyl-5-oxohex-3-en-1-yn-1-yl)-3,4-dihydro-2*H*-pyran-3,4-diyl diacetate (38a): 37a (1 equiv) was dissolved in a 0.05M solution of toluene in a flame-dried round bottom flask. In succession, dione (1.2 equiv.), piperidine (10 mol%) and glacial acetic acid (30 mol%), and sodium sulfate (20 mol%) was added to the reaction flask. After reaction completion (1 h), the reaction was diluted with EtOAc and washed twice with brine. The organics were dried over sodium sulfate then purified via a 20% EtOAc in hexanes to 40% EtOAc in hexanes gradient as a yellow powder, Average yield 72%. *Compound must be stored neat at a temperature below -20ºC.*

R$_f$ = 0.15, 30% EtOAc/70% Hexanes

^{1}H NMR (400 MHz, CDCl$_3$) δ 7.03 (d, *J* = 1.0 Hz, 1H), 6.79 (s, 1H), 5.52 (d, *J* = 5.1 Hz, 1H), 5.20 (t, *J* = 5.4 Hz, 1H), 4.48 – 4.37 (m, 2H), 2.43 (s, 3H), 2.32 (s, 3H), 2.16 – 2.06 (m, 12H).

^{13}C NMR (126 MHz, CDCl$_3$) δ 200.63, 195.53, 170.37, 169.93, 169.31, 154.39, 148.15, 122.33, 103.09, 96.59, 87.13, 74.87, 66.12, 66.07, 60.83, 30.88, 27.26, 20.73, 20.71, 20.65.

3.6.2 Synthesis of Sugar Acceptor

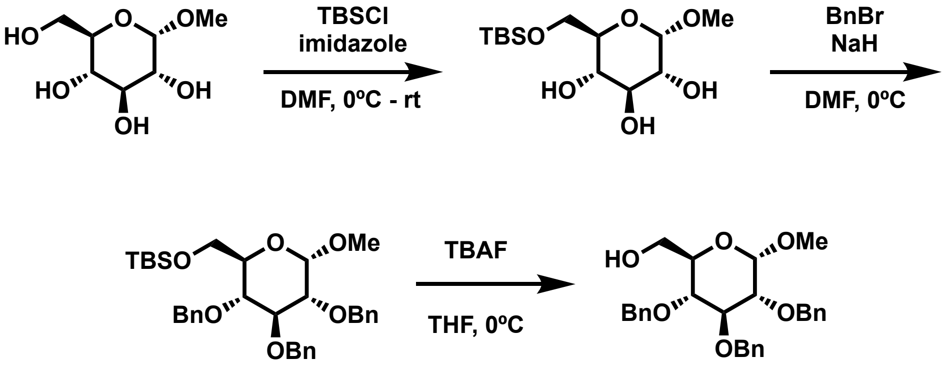

HO
OMe
HO
OH
OH
TBSCl
imidazole
DMF, 0ºC - rt
TBSO
OMe
HO
OH
OH
BnBr
NaH
DMF, 0ºC
TBSO
OMe
BnO
OBn
OBn
TBAF
THF, 0ºC
HO
OMe
BnO
OBn
OBn

((2*R*,3*R*,4*S*,5*R*,6*S*)-3,4,5-tris(benzyloxy)-6-methoxytetrahydro-2*H*-pyran-2-yl)methanol (46): The sugar alcohol **46** was synthesized in three steps from methyl α-D-glucopyranoside, from literature know procedures.[2]

R$_f$: 0.45 (30% EtOAc in Hexanes)

^{1}H: (500 MHz, $CDCl_3$) δ 7.40 – 7.24 (m, 15H), 4.99 (d, *J* = 10.9 Hz, 1H), 4.88 (d, *J* = 11.0 Hz, 1H), 4.86 – 4.77 (m, 2H), 4.65 (t, *J* = 11.6 Hz, 2H), 4.57 (d, *J* = 3.5 Hz, 1H), 4.00 (t, *J* = 9.3 Hz, 1H), 3.77 (ddd, *J* = 11.6, 5.4, 2.6 Hz, 1H), 3.69 (dq, *J* = 7.6, 3.7 Hz, 1H), 3.65 (dt, *J* = 10.0, 3.4 Hz, 1H), 3.54 – 3.47 (m, 2H), 3.37 (s, 3H).

^{13}C NMR (101 MHz, $CDCl_3$) δ 138.68, 138.08, 128.50 (d, *J* = 2.0 Hz), 128.43, 128.15, 128.07, 128.00, 127.97, 127.92, 127.66, 98.16, 81.95, 79.90, 75.79, 75.05, 73.45, 70.61, 61.85, 55.21.

3.6.3 General Procedure for Vinylic O–H Insertion of Glycal Carbenes

General Procedure: Nucleophile (1.2 equiv.), 2,6-Di-tert-butylpyridine (0.5) was dissolved into 500 μL of distilled dichloromethane with 20 mg 4 Å MS and allowed to stir. After 10 minutes the catalyst (0.3 equiv.) was added to solution and allowed to stir an additional 5 minutes. Finally, the glycal carbene (0.040g, 1 equiv.) was added to the reaction and monitored via TLC. Once complete, the reaction is diluted in dichloromethane and washed with a saturated $NaHCO_3$ solution. The organics were extracted a total of three times, before drying over Na_2SO_4 and purifying.

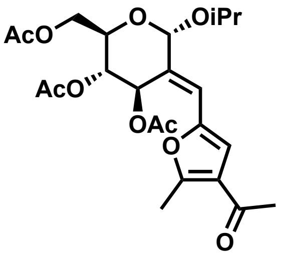

(2*R*,3*S*,4*R*,6*S*,*E*)-2-(acetoxymethyl)-5-((4-acetyl-5-methylfuran-2-yl)methylene)-6-isopropoxytetrahydro-2*H*-pyran-3,4-diyl diacetate (**45a**): Prepared using general protocol. Yellow oil (26 mg, 57%).

R$_f$ = 0.31 (30% EtOAc in Hex).

^{1}H NMR (500 MHz, Chloroform-d) (α-anomer) δ 6.68 (s, 1H), 6.43 (s, 1H), 6.23 – 6.18 (m, 1H), 5.52 (dd, *J* = 7.9, 5.9 Hz, 1H), 5.24 (s, 1H), 4.34 (dd, *J* = 11.8, 5.1 Hz, 1H), 4.26 (d, *J* = 3.9 Hz, 1H), 4.24 – 4.13 (m, 2H), 3.89 (ddd, *J* = 8.5, 5.1, 3.9 Hz, 1H), 2.57 (s, 3H), 2.39 (d, *J* = 1.9 Hz, 5H), 2.13 – 2.03 (m, 17H).

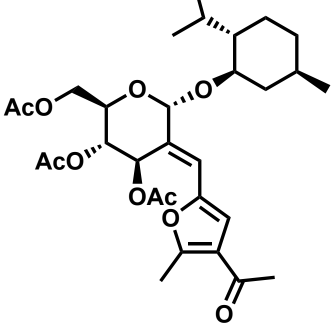

(2*R*,3*S*,4*R*,6*S*,*E*)-2-(acetoxymethyl)-5-((4-acetyl-5-methylfuran-2-yl)methylene)-6-(((1*R*,2*S*,5*R*)-2-isopropyl-5-methylcyclohexyl)oxy)tetrahydro-2*H*-pyran-3,4-diyl diacetate (**45b**): Prepared using general protocol. Yellow oil (26 mg, 48%).

R_f = 0.23, 30% EtOAc/70% Hexanes

^{1}H NMR (500 MHz, Chloroform-d) δ (400 MHz, cdcl$_3$) δ 6.68 (s, 1H), 6.47 (s, 1H), 6.26 – 6.20 (m, 1H), 5.46 (dd, *J* = 9.0, 5.8 Hz, 1H), 5.41 (s, 1H), 4.29 – 4.17 (m, 2H), 3.80 (ddd, *J* = 8.8, 5.2, 3.5 Hz, 1H), 3.70 (td, *J* = 10.6, 4.1 Hz, 1H), 2.57 (s, 3H), 2.39 (s, 6H), 2.18 (d, *J* = 12.2 Hz, 1H), 2.13 – 2.01 (m, 12H), 1.77 – 1.56 (m, 4H), 1.49 – 1.21 (m, 3H), 1.11 – 0.80 (m, 13H)

3.7 APPENDIX 2

Spectra Relevant to Chapter 3

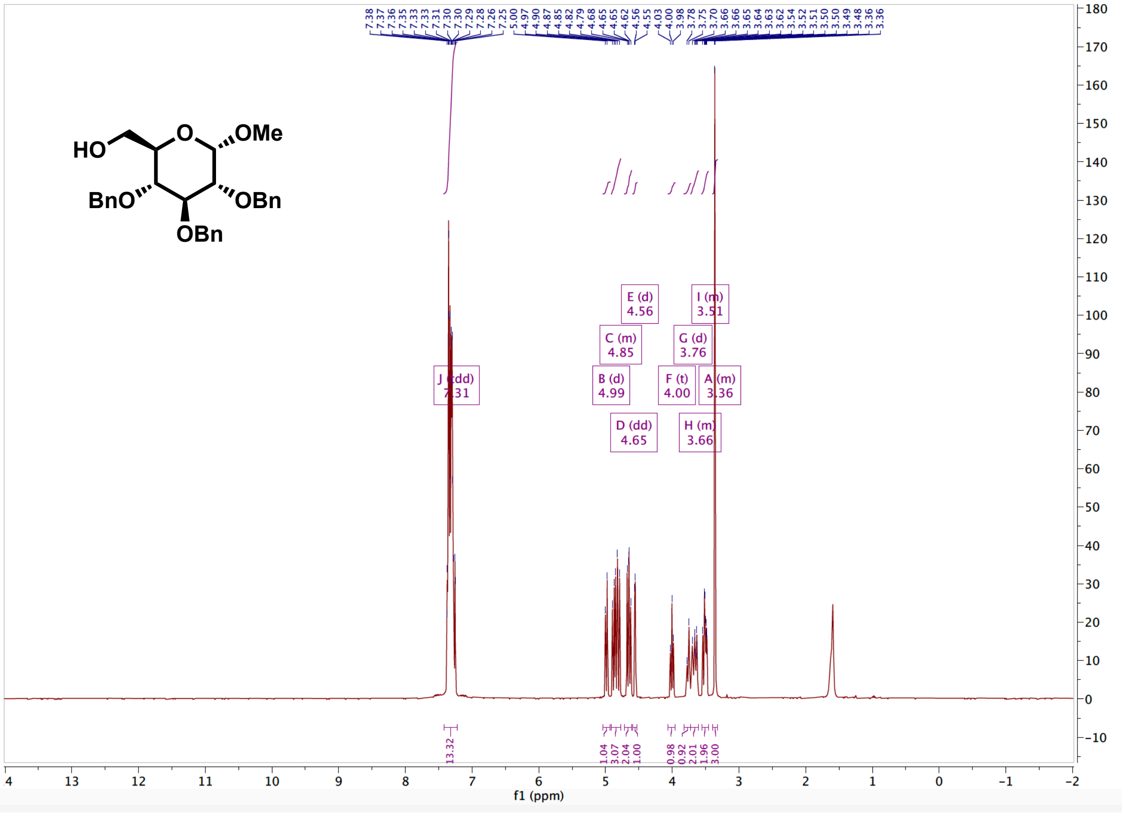
7.38 7.37 7.36 7.35 7.33 7.33 7.31 7.30 7.30 7.29 7.28 7.26 7.25 5.00 4.97 4.90 4.87 4.85 4.82 4.79 4.68 4.65 4.65 4.62 4.56 4.55 4.03 4.00 3.98 3.78 3.75 3.70 3.66 3.65 3.64 3.63 3.62 3.54 3.52 3.51 3.50 3.50 3.49 3.48 3.36 3.36
HO
O
OMe
BnO
OBn
OBn
J (dd) 7.31
B (d) 4.99
C (m) 4.85
D (dd) 4.65
E (d) 4.56
F (t) 4.00
G (d) 3.76
H (m) 3.66
I (m) 3.51
A (m) 3.36
13.32
1.04
3.07
2.04
1.00
0.98
0.92
2.01
1.96
3.00
f1 (ppm)

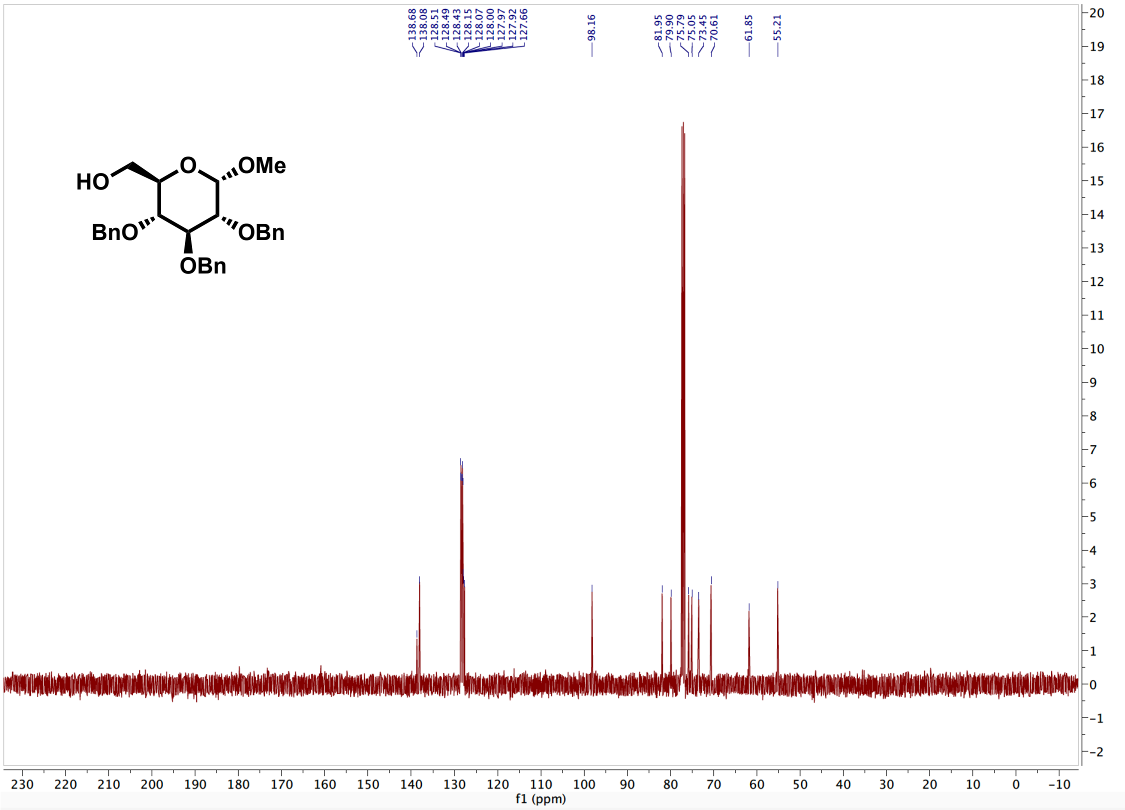
138.68 138.08 128.51 128.49 128.43 128.15 128.07 128.00 127.97 127.92 127.66
98.16
81.95 79.90 75.79 75.05 73.45 70.61
61.85
55.21
HO
O
OMe
BnO
OBn
OBn
f1 (ppm)

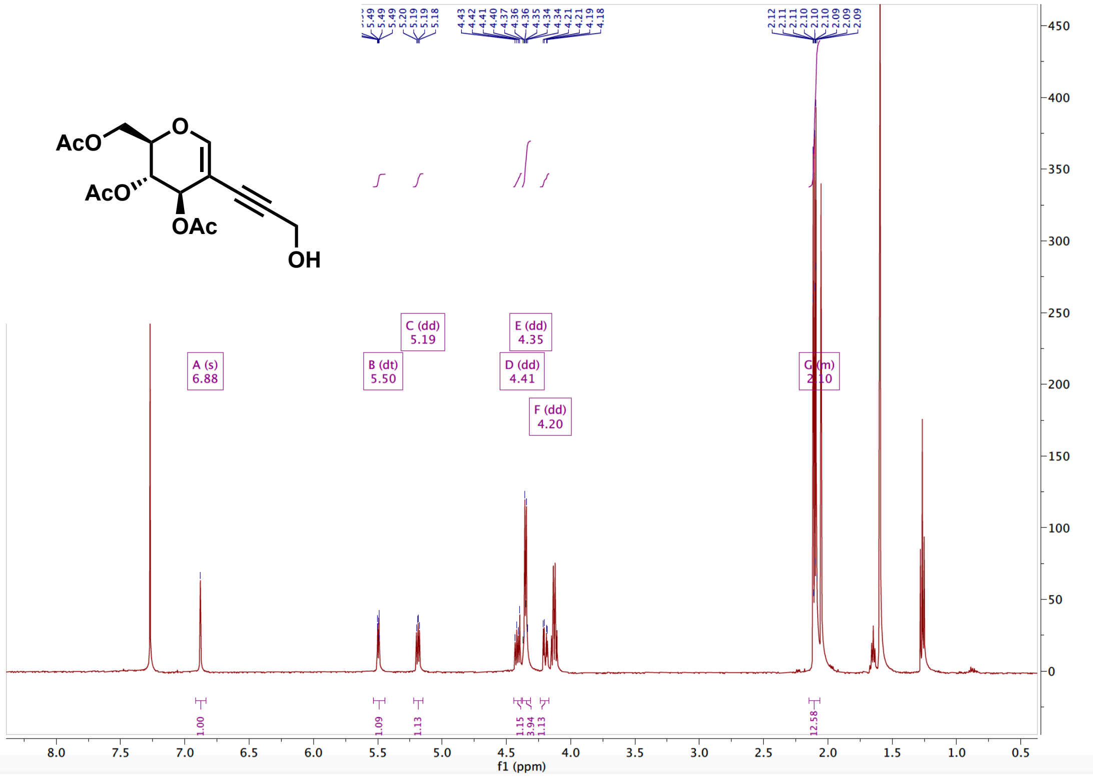
AcO
AcO
OAc
O
OH
5.49
5.49
5.49
5.20
5.19
5.19
5.18
4.43
4.42
4.41
4.40
4.37
4.36
4.35
4.35
4.34
4.34
4.21
4.21
4.19
4.18
2.12
2.11
2.11
2.10
2.10
2.10
2.09
2.09
A (s)
6.88
B (dt)
5.50
C (dd)
5.19
D (dd)
4.41
E (dd)
4.35
F (dd)
4.20
G (m)
2.10
1.00
1.09
1.13
1.15
3.94
1.13
12.58
8.0
7.5
7.0
6.5
6.0
5.5
5.0
4.5
4.0
3.5
3.0
2.5
2.0
1.5
1.0
0.5
f1 (ppm)
450
400
350
300
250
200
150
100
50
0

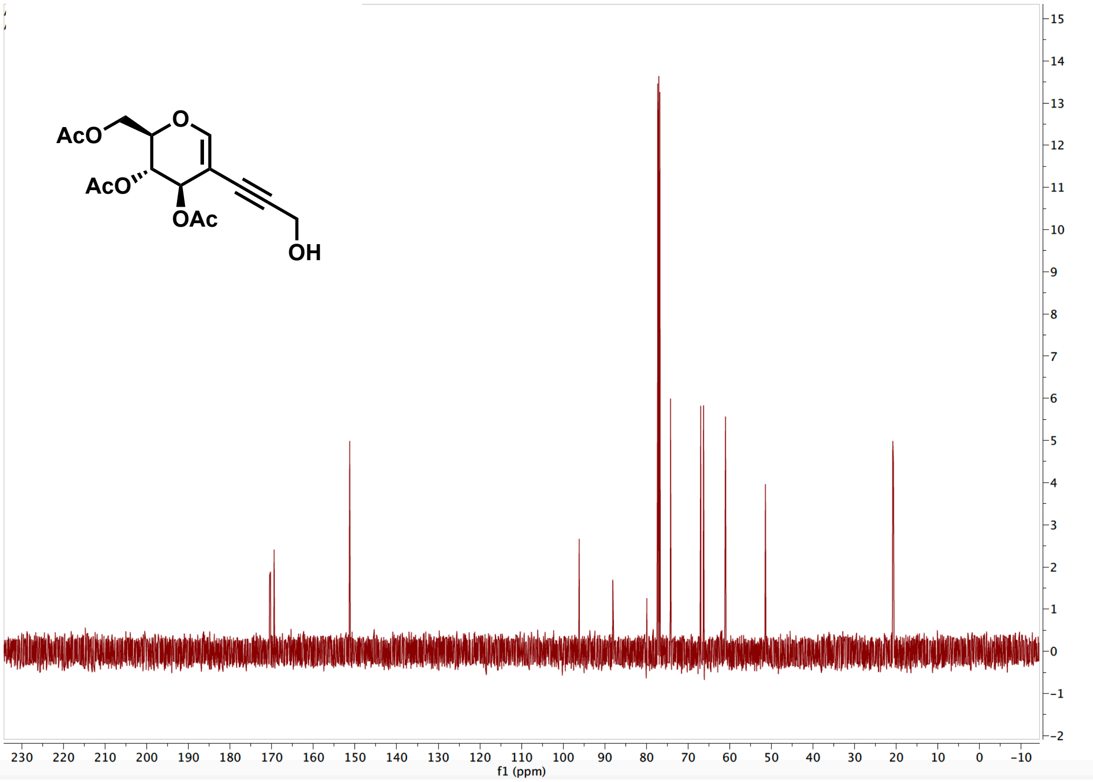
AcO
AcO
OAc
O
OH
230
220
210
200
190
180
170
160
150
140
130
120
110
100
90
80
70
60
50
40
30
20
10
0
−10
f1 (ppm)
15
14
13
12
11
10
9
8
7
6
5
4
3
2
1
0
−1
−2

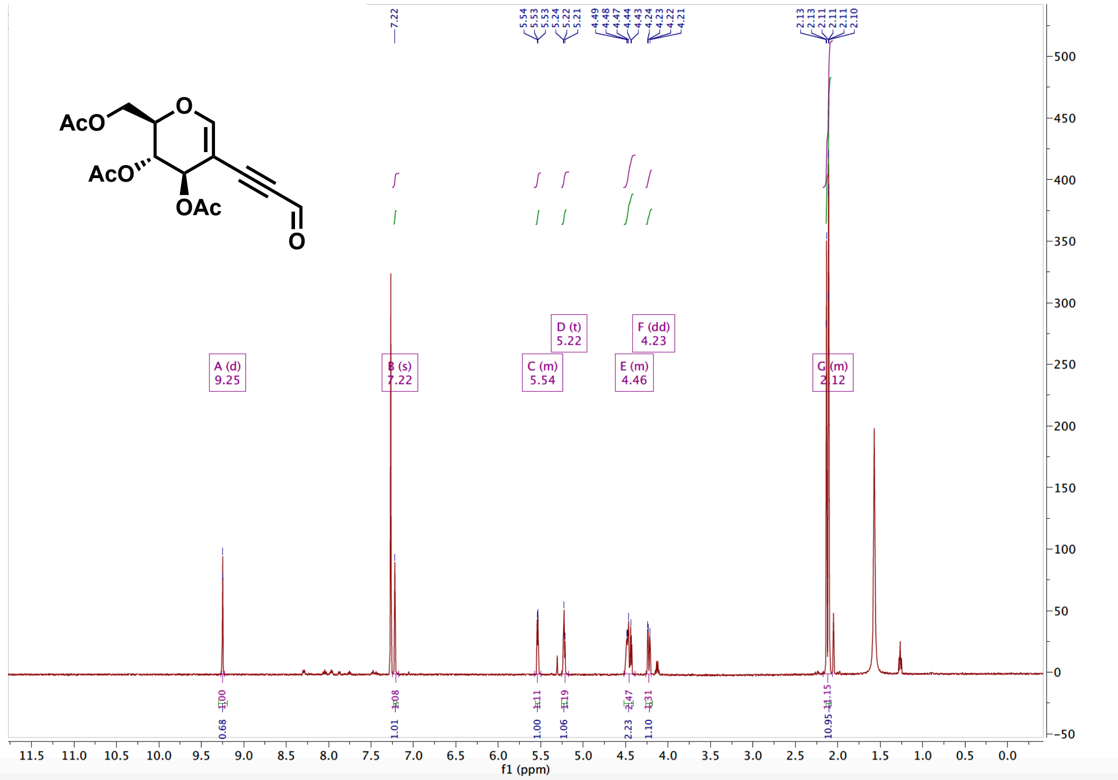
AcO
AcO
OAc
O
O
A (d)
9.25
B (s)
7.22
C (m)
5.54
D (t)
5.22
E (m)
4.46
F (dd)
4.23
G (m)
2.12
f1 (ppm)

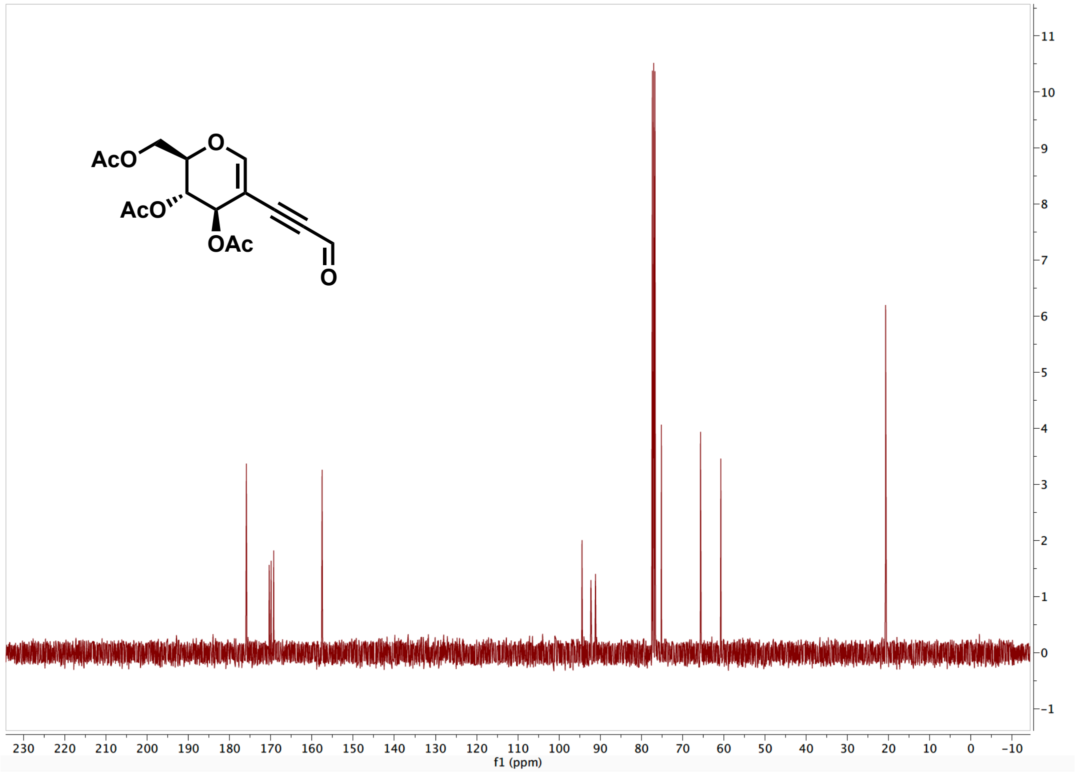
AcO
AcO
OAc
O
O
f1 (ppm)

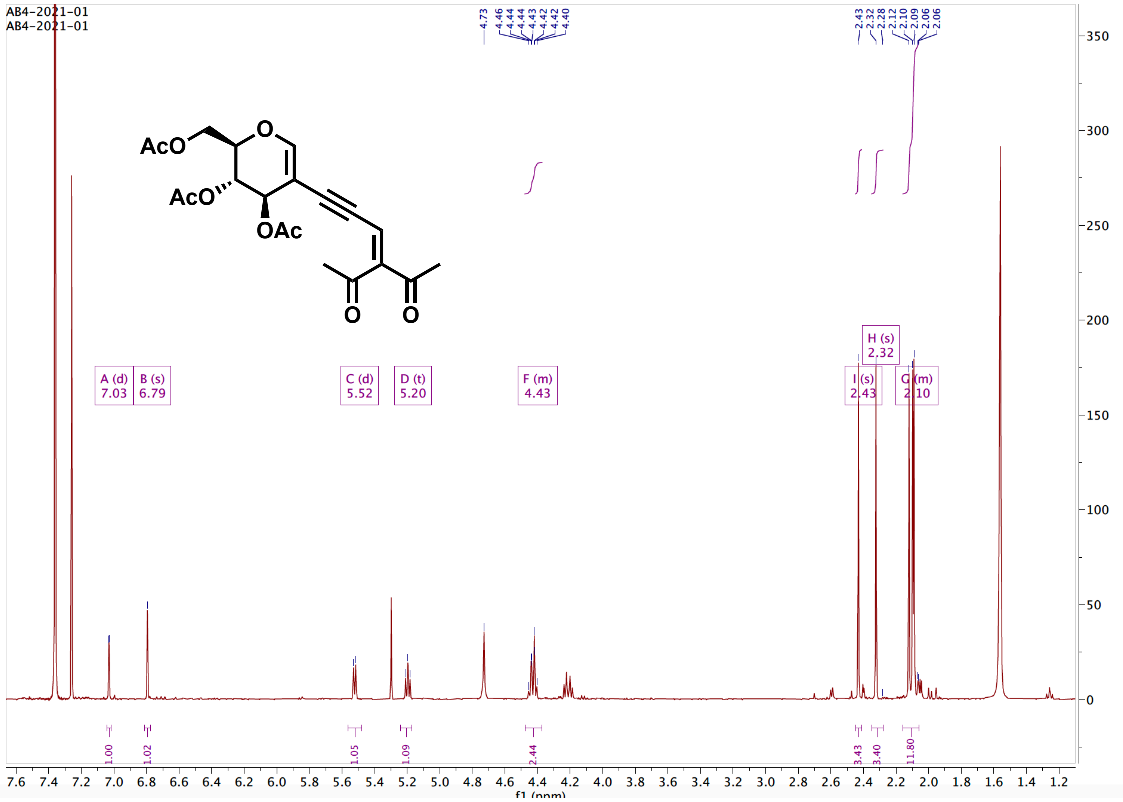
AB4-2021-01
AB4-2021-01
4.73
4.46
4.44
4.44
4.43
4.42
4.42
4.40
2.43
2.32
2.28
2.12
2.10
2.09
2.06
2.06
AcO
AcO
OAc
O
O
O
A (d) 7.03
B (s) 6.79
C (d) 5.52
D (t) 5.20
F (m) 4.43
H (s) 2,32
I (s) 2.43
G (m) 2.10
1.00
1.02
1.05
1.09
2.44
3.43
3.40
11.80
7.6 7.4 7.2 7.0 6.8 6.6 6.4 6.2 6.0 5.8 5.6 5.4 5.2 5.0 4.8 4.6 4.4 4.2 4.0 3.8 3.6 3.4 3.2 3.0 2.8 2.6 2.4 2.2 2.0 1.8 1.6 1.4 1.2
f1 (ppm)
350
300
250
200
150
100
50
0

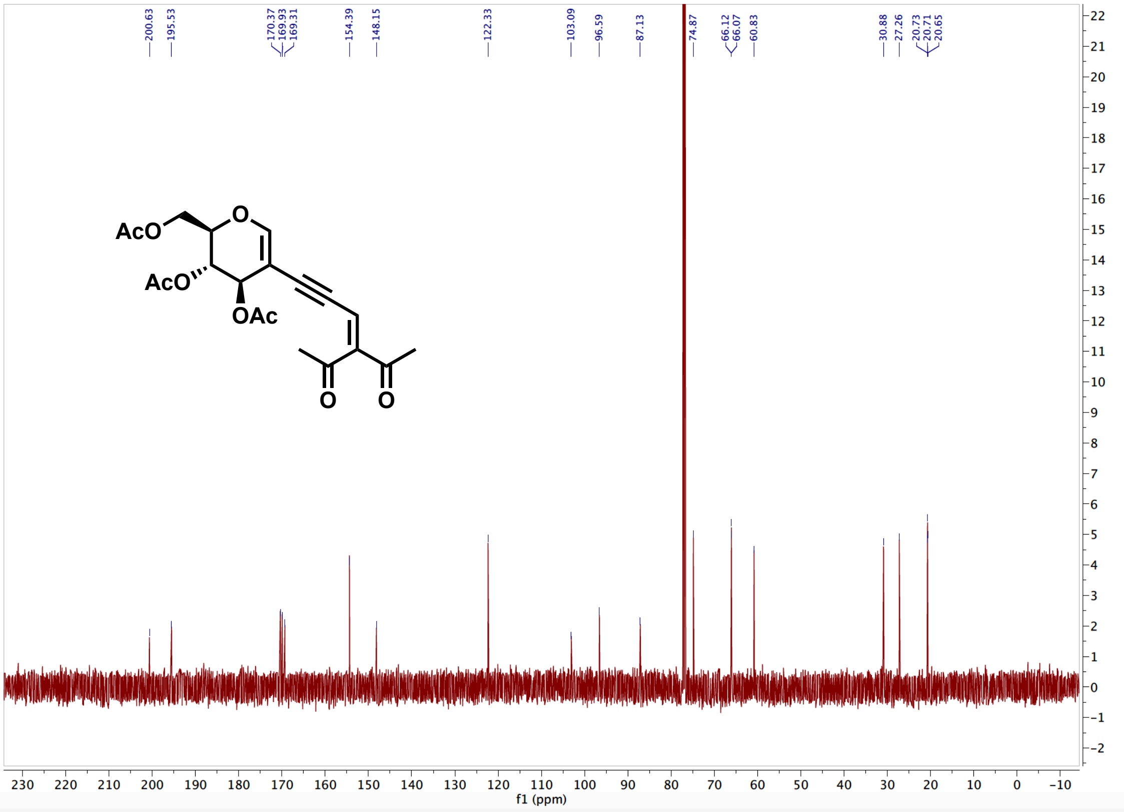
200.63
195.53
170.37
169.93
169.31
154.39
148.15
122.33
103.09
96.59
87.13
74.87
66.12
66.07
60.83
30.88
27.26
20.73
20.71
20.65
AcO
AcO
OAc
O
O
O
230 220 210 200 190 180 170 160 150 140 130 120 110 100 90 80 70 60 50 40 30 20 10 0 -10
f1 (ppm)
22
21
20
19
18
17
16
15
14
13
12
11
10
9
8
7
6
5
4
3
2
1
0
-1
-2

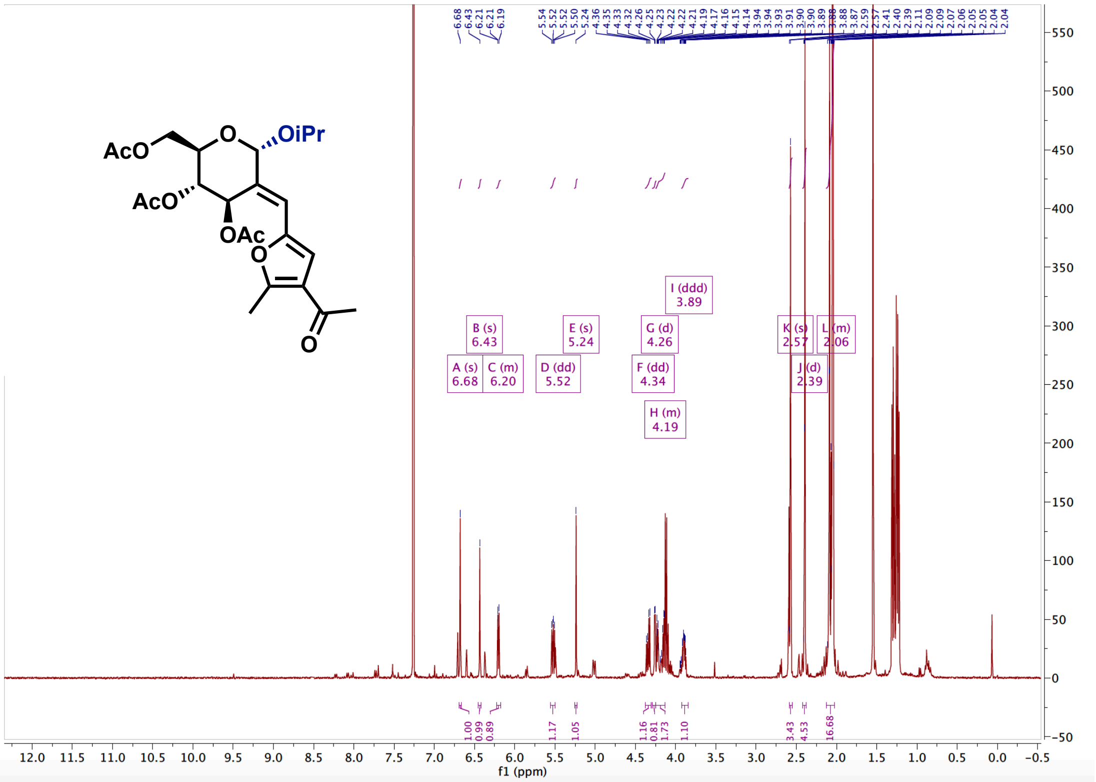

AcO
O
OiPr
AcO
OAc
O
O
A (s) 6.68
B (s) 6.43
C (m) 6.20
D (dd) 5.52
E (s) 5.24
F (dd) 4.34
G (d) 4.26
H (m) 4.19
I (ddd) 3.89
J (d) 2.39
K (s) 2.57
L (m) 2.06
1.00
0.99
0.89
1.17
1.05
1.16
0.81
1.73
1.10
3.43
4.53
16.68
f1 (ppm)
12.0
11.5
11.0
10.5
10.0
9.5
9.0
8.5
8.0
7.5
7.0
6.5
6.0
5.5
5.0
4.5
4.0
3.5
3.0
2.5
2.0
1.5
1.0
0.5
0.0
−0.5
550
500
450
400
350
300
250
200
150
100
50
0
−50

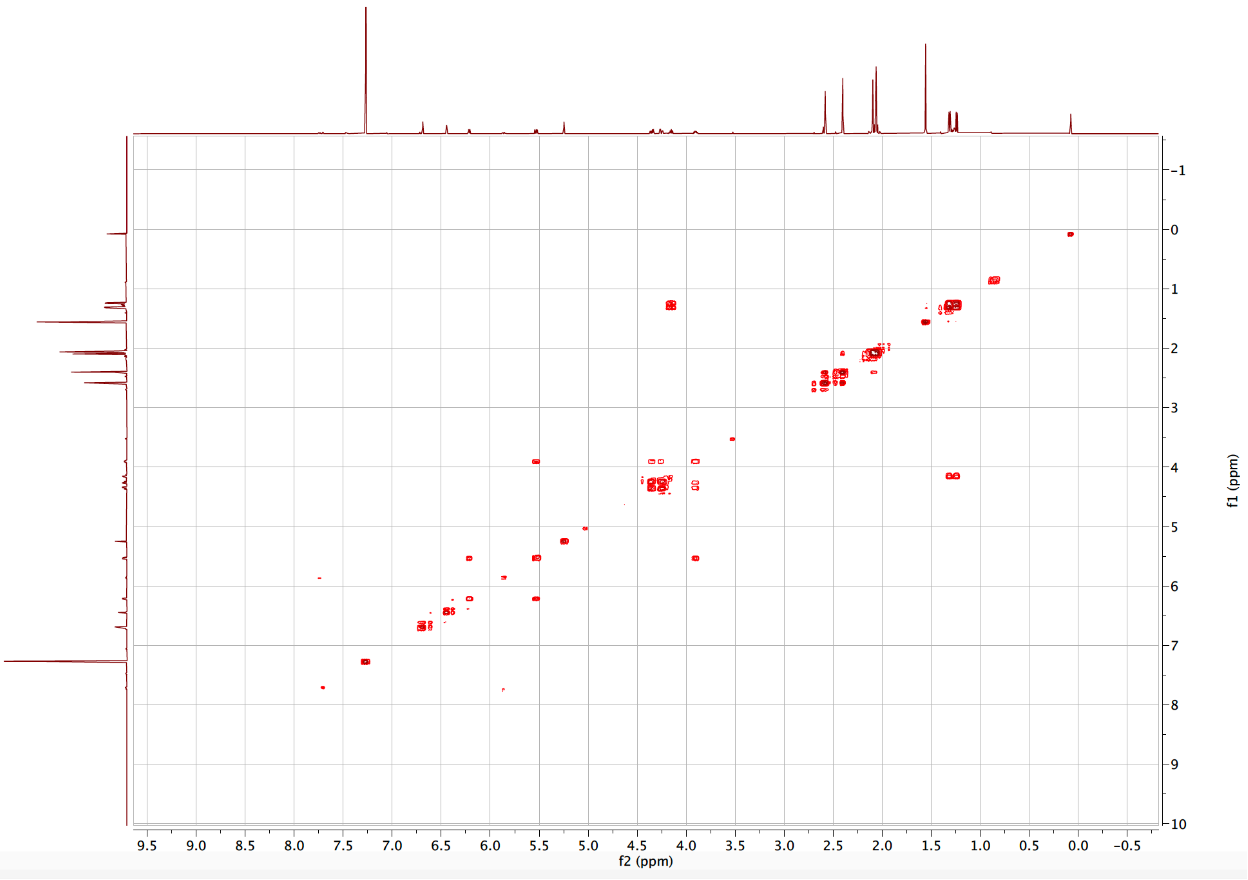
f2 (ppm)
f1 (ppm)
9.5
9.0
8.5
8.0
7.5
7.0
6.5
6.0
5.5
5.0
4.5
4.0
3.5
3.0
2.5
2.0
1.5
1.0
0.5
0.0
−0.5
−1
0
1
2
3
4
5
6
7
8
9
10

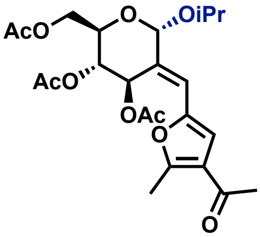
AcO
O
OiPr
AcO
OAc
O
O

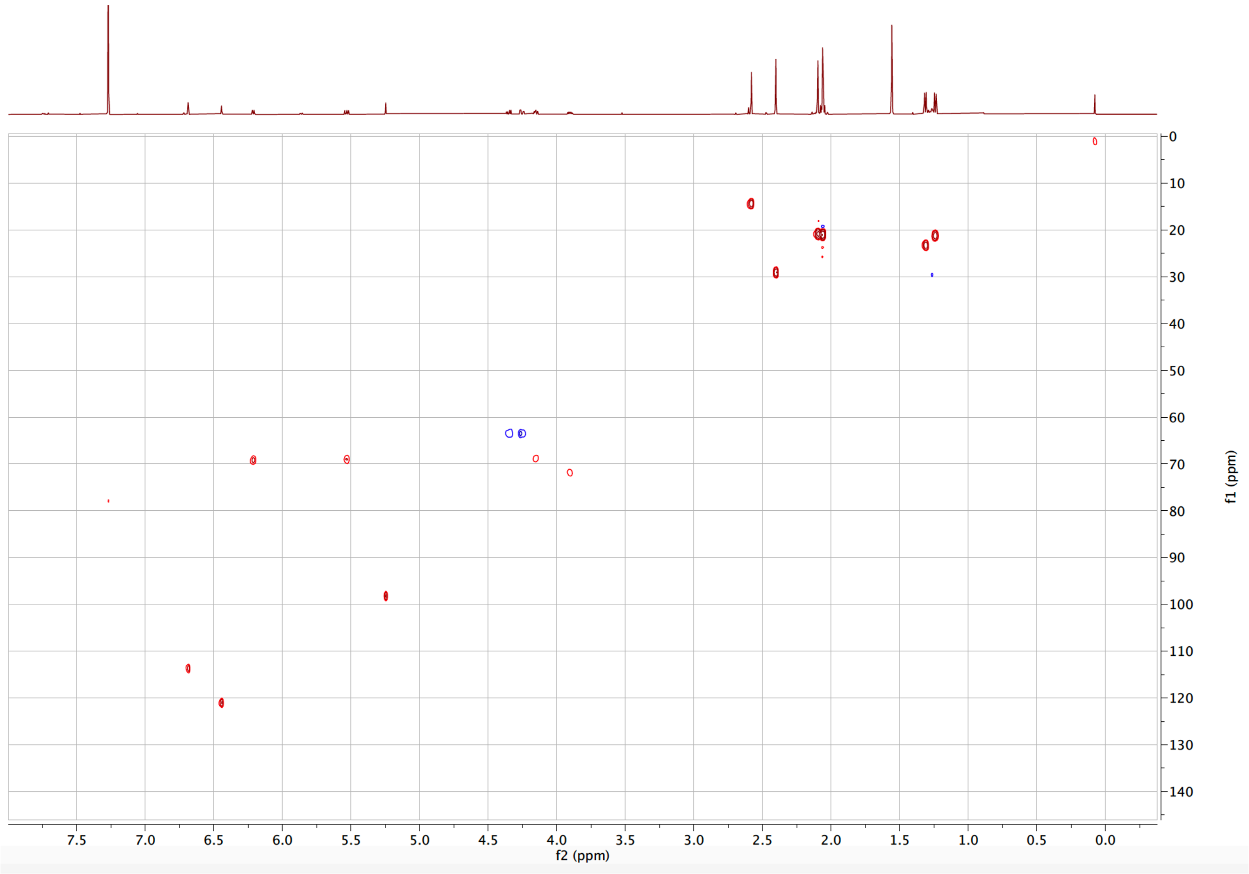
f2 (ppm)
f1 (ppm)
7.5
7.0
6.5
6.0
5.5
5.0
4.5
4.0
3.5
3.0
2.5
2.0
1.5
1.0
0.5
0.0
0
10
20
30
40
50
60
70
80
90
100
110
120
130
140

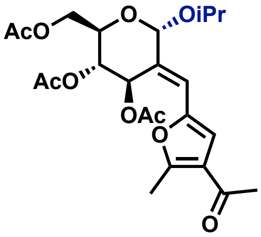
AcO
O
OiPr
AcO
OAc
O
O

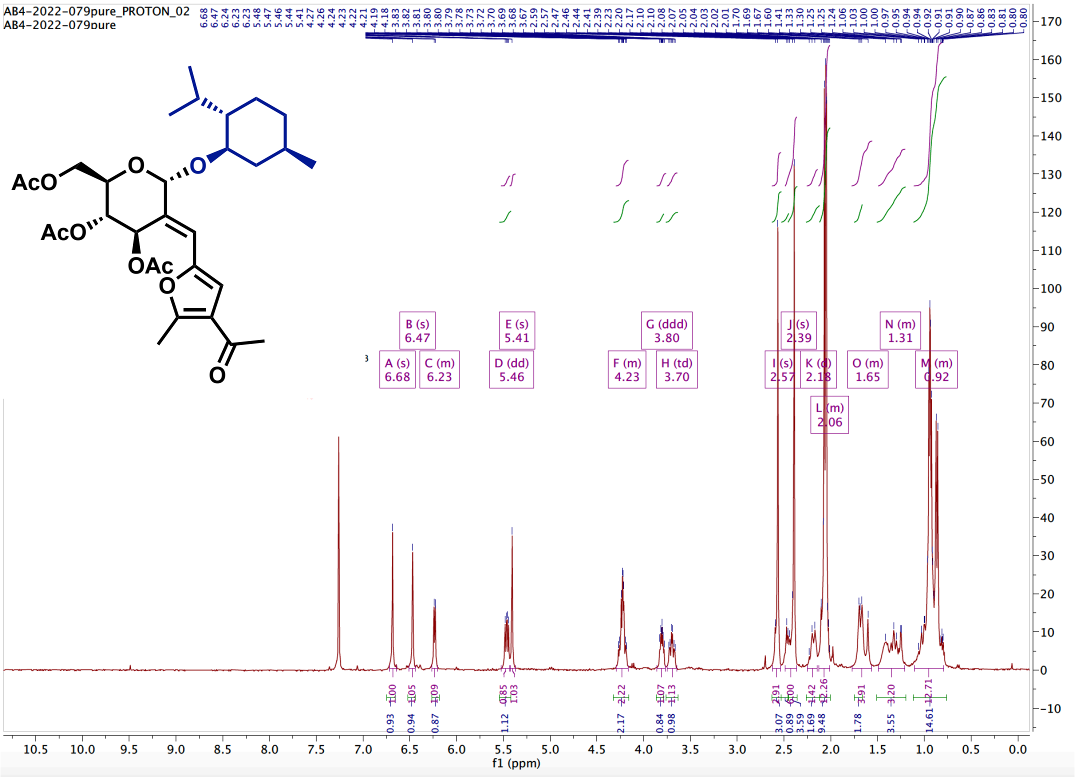
AB4-2022-079pure_PROTON_02
AB4-2022-079pure
AcO
AcO
OAc
O
O
O
O
A (s) 6.68
B (s) 6.47
C (m) 6.23
D (dd) 5.46
E (s) 5.41
F (m) 4.23
G (ddd) 3.80
H (td) 3.70
I (s) 2.57
J (s) 2.39
K (d) 2.18
L (m) 2.06
M (m) 0.92
N (m) 1.31
O (m) 1.65
0.93
0.94
0.87
1.12
2.17
0.84
0.98
3.07
0.89
3.59
1.69
9.48
1.78
3.55
14.61
f1 (ppm)

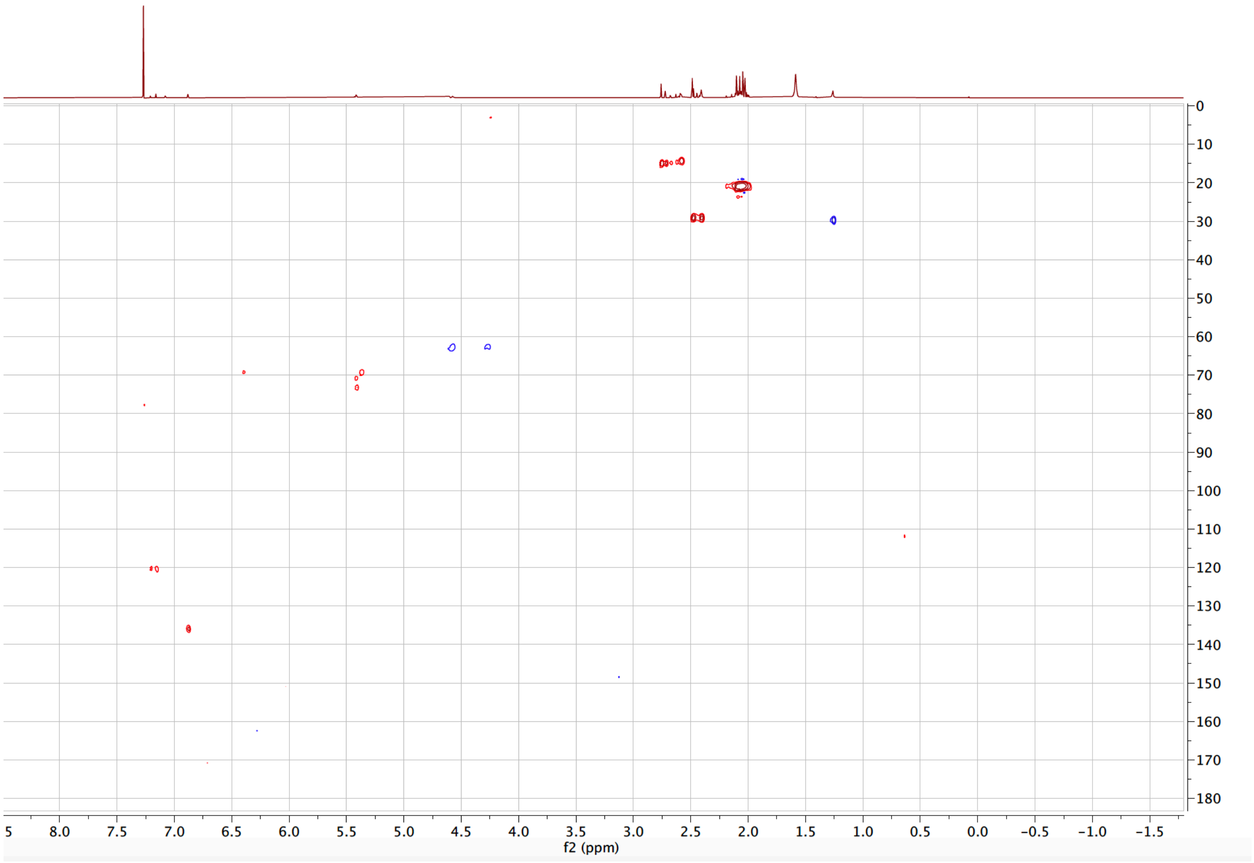
5
8.0
7.5
7.0
6.5
6.0
5.5
5.0
4.5
4.0
3.5
3.0
2.5
2.0
1.5
1.0
0.5
0.0
-0.5
-1.0
-1.5
f2 (ppm)
0
10
20
30
40
50
60
70
80
90
100
110
120
130
140
150
160
170
180

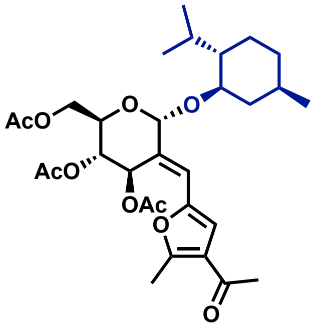
AcO
AcO
OAc
O
O
O
O

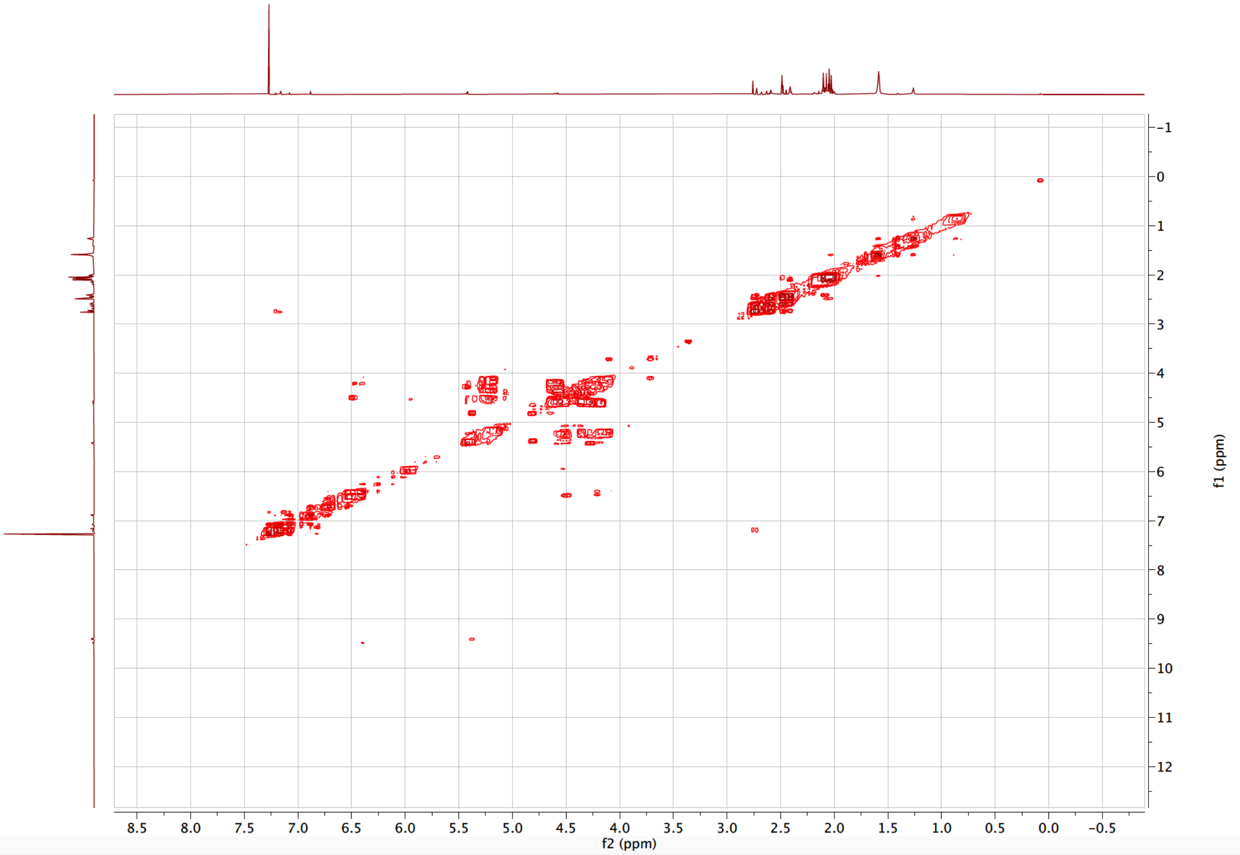

8.5
8.0
7.5
7.0
6.5
6.0
5.5
5.0
4.5
4.0
3.5
3.0
2.5
2.0
1.5
1.0
0.5
0.0
-0.5
f2 (ppm)
-1
0
1
2
3
4
5
6
7
8
9
10
11
12
f1 (ppm)

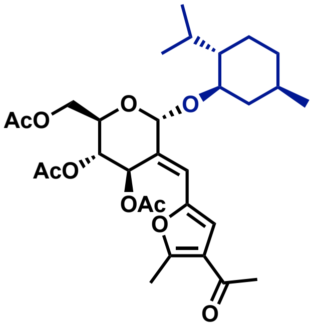

AcO
O
O
AcO
OAc
O
O

3.8 REFERENCES FOR CHAPTER 3 EXPERIMENTALS

[1] S. Dharuman, Y. D. Vankar, *Organic Letters* **2014**, *16*, 1172-1175.

[2] S. Boonyarattanakalin, X. Liu, M. Michieletti, B. Lepenies, P. H. Seeberger, *Journal of the American Chemical Society* **2008**, *130*, 16791-16799.

CHAPTER 4

Carbene-Mediated Glycosyl Donors

4.1 INTRODUCTION TO CARBENE-ASSISTED GLYCOSYLATION

Highly selective transformations involving metal carbenoid synthons are well-studied in organic synthesis.[1] These reactions are well documented, engage in well-understood transformations, and have resulted in libraries of valuable, biologically active scaffolds.[2] Despite this, these synthons are rarely utilized to construct glycosidic bonds. In fact, carbene-mediated transformations are rarities in glycoscience.

Lecourt *et al.* developed an intramolecular glycosylation strategy towards the synthesis of ketopyranosides.[3] This approach relies on the Rh(II) catalyzed functionalization of the anomeric C–H bond to insert into the diazo functionality grafted at the C2 position (**Figure 4.1a**). Further, Tang developed a carbene-assisted alkylation protocol where the authors selectively promoted the Rh(II) catalyzed O–H insertion of either C2 or C3 carbohydrate hydroxyl group (**Figure 4.1b**).[4] Wan and coworkers reported the Rh(II)/Brønsted acid relay strategy to activate thioglycosides. While this transformation proceeds in an S_N1-like manner, the group reported sizeable stereocontrol (**Figure 4.1c**).[5]

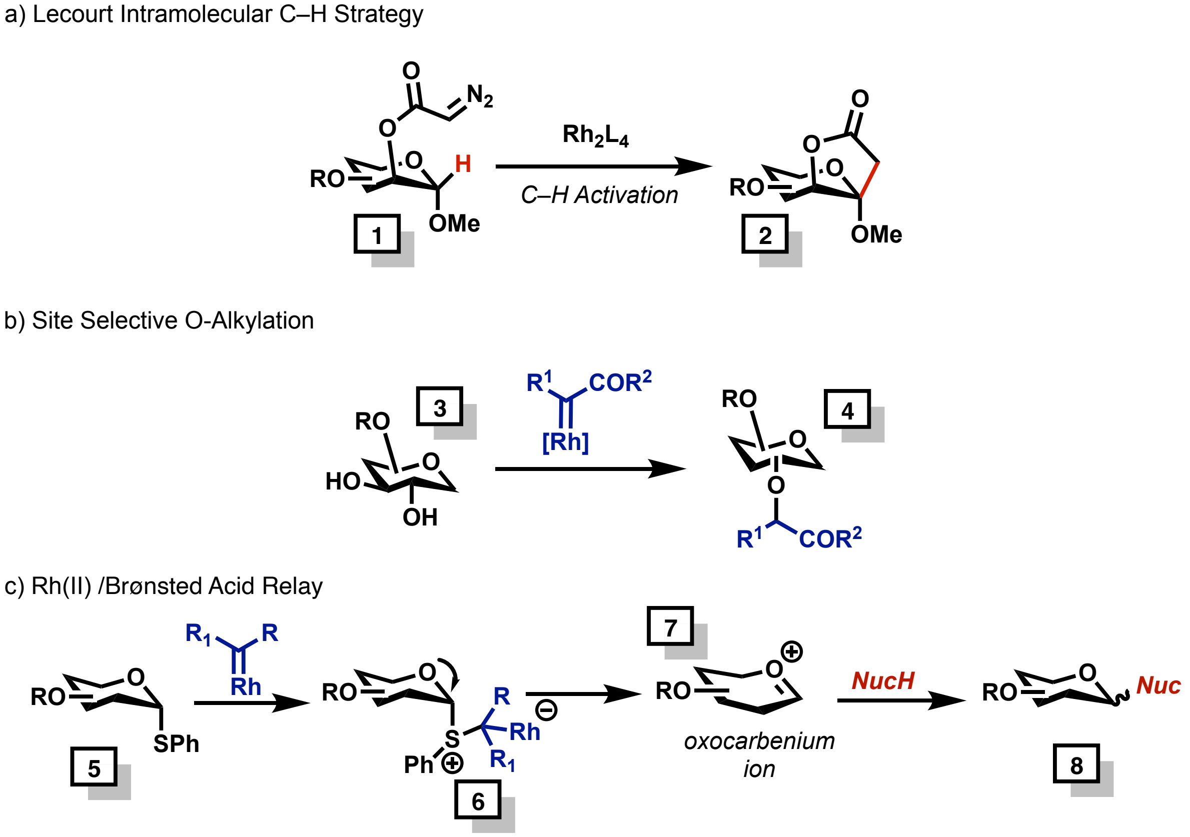
a) Lecourt Intramolecular C–H Strategy

b) Site Selective O-Alkylation

c) Rh(II) /Brønsted Acid Relay

Figure 4.1: Reported Carbene-Assisted Glycosylation Strategies

While unique, these strategies all employ rhodium, an expensive precious metal catalyst, to synthesize the diazo-derived metal carbenoid species. The research highlighted within this chapter will disclose a carbene-mediated glycosylation protocol featuring the use of readily available Earth-abundant metal catalysts to facilitate the proposed transformations. Additionally, we have designed an alkynyl-based system to furnish metal-carbenoids *in situ*, a significant advantage over unstable diazo-derived carbenoid systems.

4.1.1 GOLD-ASSISTED GLYCOSYLATIONS

One of the most critical challenges within carbohydrate chemistry is the lack of general approaches for assembling carbohydrates tolerant to various glycosyl acceptors.[6] Recently, the design of alkynyl-embedded glycosyl donors has emerged as an elegant approach to construct valuable and diverse glycosidic bonds.

Gold activation of alkynes is a powerful tool that scientists have utilized to catalyze synthetically valuable transformations.[7] However, catalytic glycosylations are still relatively new to glycoscience. A new class of gold-activated glycosylations was first reported in 2006; Hotha and Kashyab synthesized C3-O propargyl protected glucal **9**, which was exposed to catalytic amounts of Au(III) to undergo a Ferrier-like reaction with various aglycones (aliphatic, aromatic, alicyclic, and monosaccharide) to synthesize α-glucosides stereoselectively (**Figure 4.2a**).[8] This work was expanded that same year, and the group installed a propargyl leaving group at the anomeric position to synthesize the donor **11**. This report was tolerant to a range of simple glycosyl O-H acceptors, however, with low anomeric selectivities (**Figure 4.2b**).[9] Both of these reports were limited to benzyl-protected glucal-based donors.

a) Au(III) mediated Ferrier-Type Mechanism

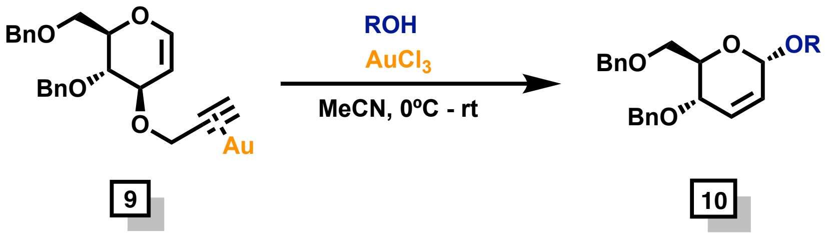

b) First Report of Anomeric Propargyl Glycosides as Glycosyl Donor

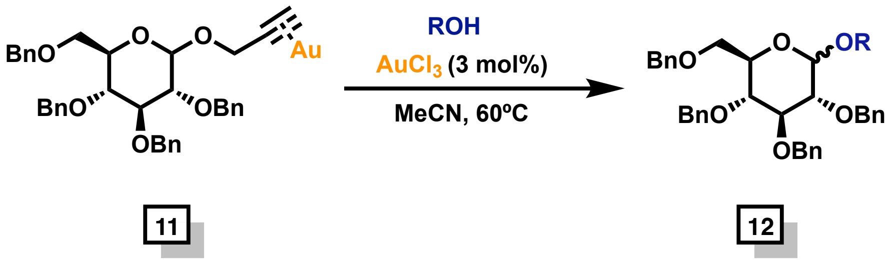

Figure 4.2: Early Reports of Au-Mediated Glycosylations

Following these reports, *ortho*-alkynylbenzoates and *ortho*-alkynyl arylthioglycosides emerged as highly stereoselective glycosyl donors. Both donors typically employ Au(I), and these reactions' mechanisms are summarized below (**Figure 4.3**).[10] Gold activation of the propargyl moiety of the glycosyl donor results in the formation of gold-π-complex **13**. This activation increases the electrophilicity of the propargyl species, resulting in the intramolecular attack of the nucleophilic species (either a *sp*^{2} CO or S) via an *endo*-dig cyclization to form intermediate **14**. Electron donation of the endocyclic oxygen results in the formation of oxocarbenium ion and promotion of the leaving group species **16**. Hydrolysis of species **16** regenerates the gold catalyst to form species **17**. Once produced, the oxocarbenium ion **7** is intercepted by an appropriate glycosyl acceptor, resulting in the desired glycosidic linkage **18**.

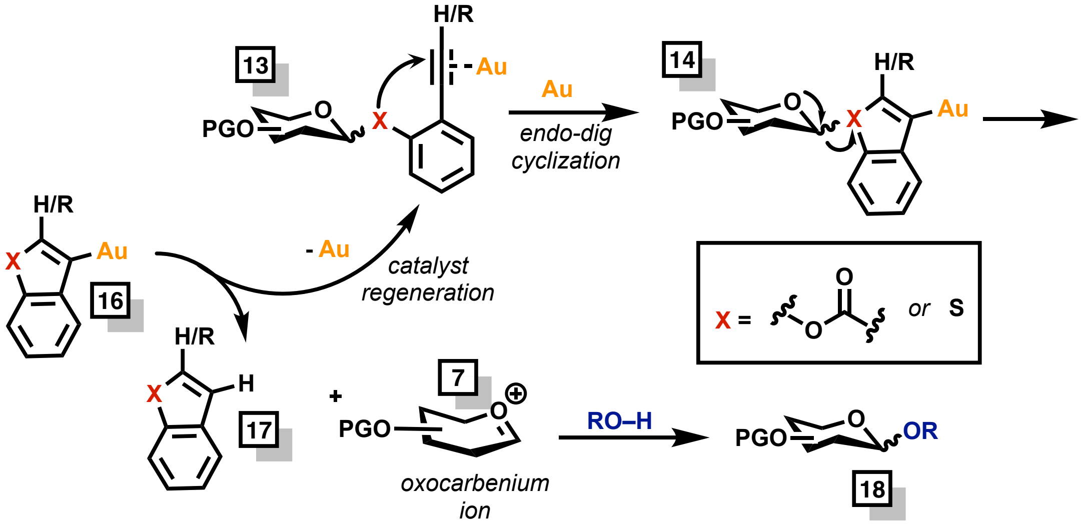
13
PGO
O
X
H/R
Au
endo-dig
cyclization
14
H/R
Au
16
X
- Au
catalyst
regeneration
X = O or S
17
H
+
7
PGO
oxocarbenium
ion
RO–H
18
OR

Figure 4.3: Gold-Assisted Alkyne Activations for Glycosylations

The design of these propargyl-embedded donors can play a significant role in the stereoselectivity observed. In 2021, Zhang designed a donor bearing sterically hindered oxazole to function as a directing group and base (**Figure 4.4**).[10a] These donors function via an S_N2 pathway, and the group reported outstanding selectivities and high yields.

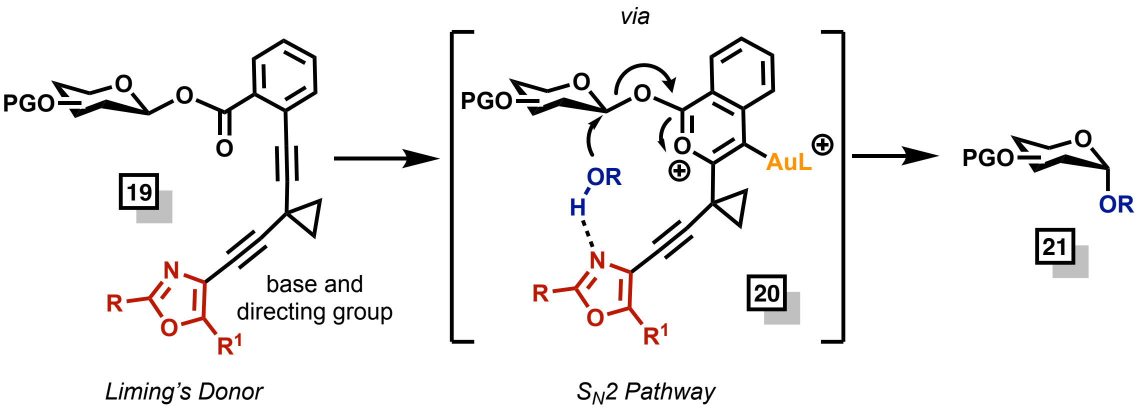
via
PGO
O
19
base and
directing group
N
R
O
R^1
Liming's Donor
OR
H
AuL
⊕
20
S_N2 Pathway
21
OR

Figure 4.4: Liming Zhang's oxazole based Glycosyl Donor

4.1.2 OBJECTIVES OF CHAPTER

This chapter will detail the design, synthesis, and applications of a new variety of carbene-mediated glycosyl donors. These donors are fundamentally distinct from other propargyl-embedded or diazo-embedded donors reported and can be activated with Earth-abundant metal salts.

Mechanistically, this system is designed to undergo an intramolecular cyclization once exposed to a suitable metal salt to form a metal-carbenoid *in situ* (**Figure 4.5**). Following this cyclization, a nucleophile can attack the anomeric position, thus promoting the elimination of the latent benzofuranone functionality in either an S_N1-like or S_N2-like fashion.

The glycosylation strategy entailed is unique and fundamentally innovative. In addition to synthesizing an unprecedented variety of glycosyl donors, we have demonstrated its utility using Earth-abundant catalysis –namely copper salts. Our goal is to utilize these donors to target challenging glycosidic linkages, particularly 1,2 *cis* glycosides. The synthesis of 1,2 *cis*-glycosides is a considerable challenge within glycoscience. There are several convenient and eloquent strategies to access 1,2 *trans*-linkages. These strategies often employ techniques involving neighboring group participation.[11] Contrastingly, the vicinal C2 group that aids and is responsible for stereospecific *trans* linkages inhibits the formation of the *cis* counterpart.

Previous Literature: **Gold/Alkyne Activation for glycosylations**

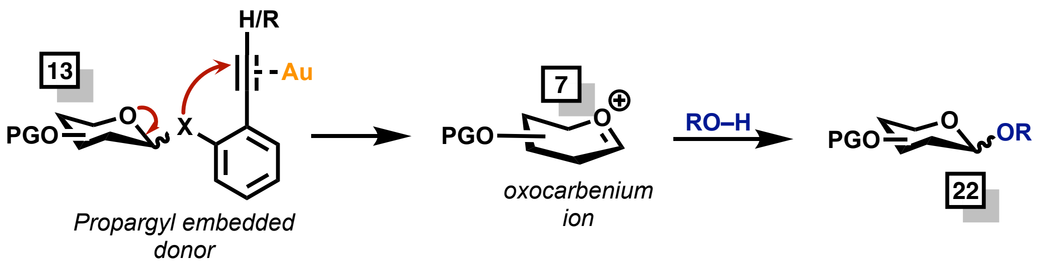
H/R
13
Au
PGO
O
X
Propargyl embedded donor
7
PGO
O
oxocarbenium ion
RO–H
PGO
O
OR
22

This Work: **Enynone-based, carbene-mediated glycosylation**

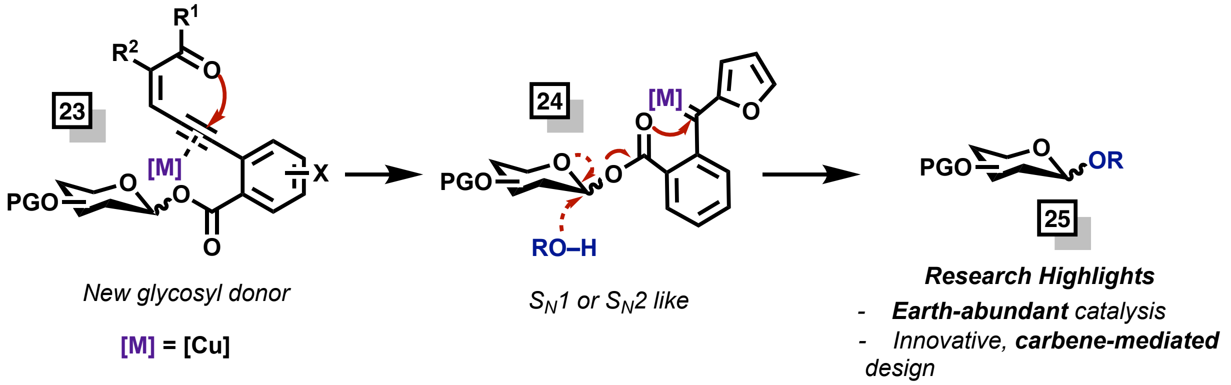
R1
R2
O
23
[M]
X
PGO
O
O
O
New glycosyl donor
[M] = [Cu]
24
[M]
O
O
PGO
O
O
RO–H
SN1 or SN2 like
PGO
O
OR
25
Research Highlights
- Earth-abundant catalysis
- Innovative, carbene-mediated design

Figure 4.5: Overview of Glycosylation Strategy

This work complements and enhances the glycal carbenes encountered in *Chapter 3* of this dissertation. Glycal carbenes are a rare example of carbene-mediated glycosylation. While innovative, we recognize that they require post-glycosylation transformations to cleave the pendant furan moiety. In this new system, we have grafted the carbene at the anomeric position, which is then cleaved during the glycosylation. Additionally, this system is currently being optimized for the synthesis of di- and oligosaccharides –a feat that was low-yielding in our glycal carbene system.

4.2 DESIGN, SYNTHESIS, AND APPLICATIONS OF CARBENE-MEDIATED DONOR

To study our envisioned carbene-mediated donor, we thought to design an enynone-derived, metal carbenoid system. Based on our design of glycal carbene donors (*Chapter 3*) and the instability associated with diazo compounds, we envisioned an enynone-based system to access metal carbenoids.

Diazos are not industrially utilized due to their explosive behavior and toxicity, despite serving as historically useful carbenoid precursors.[12] This instability regularly requires low-temperature storage. Likewise, their highly reactive nature necessitates low concentration reaction pots or slow diazo addition to prevent dimerization, a significant side reaction typically observed in carbene chemistry.[13] The incorporation of alternative alkyne-derived, carbene precursors will significantly impact the scope of these reactions and can pave a pathway to industrially convenient carbene-based protocols.

4.2.1 OVERCOMING LIMITATIONS OF GLYCAL CARBENES

The major setback with our initial glycal carbene donor (*Chapter 3*) is the cleavage of the pendant furan system tethered at the C2 position. To rectify this impediment, we thought to cleave the furan with an ozonolysis step furnishing a C2 ketone. Carbonyls can serve as an excellent diversification handle and could aid in pyranose diversification. However, we acknowledge these this additional step would weaken the impact of our donor due to the required post-glycosylation transformations. To account for this, we thought to develop a new donor, where the furan moiety would be grafted at the anomeric position; and therefore, would be cleaved during the glycosylation step. Another limitation that we observed during optimization was that our glycal carbene systems were not applicable to disaccharide systems. The construction of this newly designed donor was meant to overcome both limitations.

Both donors are designed with an embedded alkynyl-group, designed to undergo an *in situ* carbene formation once exposed to an appropriate Lewis acid. Glycal carbenes, as observed in *Chapter 3* of this dissertation, following carbene formation can undergo a regioselective vinyl addition at the anomeric position (**Figure 4.6a**). Contrastingly, our newly designed donor can be intercepted at the anomeric position following carbene formation via a carbene-assisted strategy (**Figure 4.6b**).

a). *In situ* carbene formation from glycal carbenes

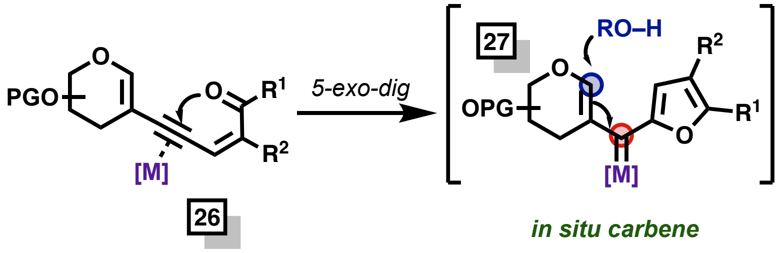
PGO
O
O
R1
R2
[M]
26
5-exo-dig
27
RO–H
R2
OPG
O
R1
O
[M]
in situ carbene

b). *In situ* carbene formation from newly designed donor

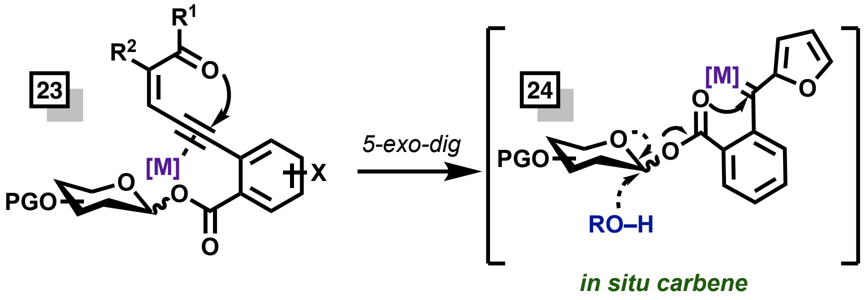
R1
R2
O
23
[M]
X
PGO
O
O
O
5-exo-dig
24
[M]
O
O
PGO
O
O
RO–H
in situ carbene

Figure 4.6: Inspiration behind New Donor Design

4.2.2 EXPERIMENTAL DESIGN

Due to literature-reported high stereoselectivity with sterically hindered protecting groups, we initiated our design featuring a 4,6 *O*-benzylidene protected donor. [14] These protecting groups are known to enhance β-selectivity and fall in line with our goal of synthesizing challenging 1,2 *cis* linkages. To confront the challenge of β-mannosylation, we initiated our studies on a mannose-derived system. First, peracetate-protected pyranmannose sugar **28** was exposed to thiophenol and boron trifluoride diethyl etherate to synthesize the thiophenol-protected sugar **29**. Sugar **29** was exposed to basic conditions to induce a global deprotection to yield **30**, which was exposed to **31** to form the 4,6 *O*-benzylidene protected sugar **32**. Sugar **32** was then di-benzyl protected at the C2 and C3 position, followed by a thiophenol deprotection to yield sugar **34**. Using a well-established carbodiimide coupling strategy, iodobenzoic acids (**35**) were then coupled to the protected sugar to synthesize sugars **36**. Lastly, sugar **36** was exposed to propargyl aldehyde **37** and Sonogashira coupling conditions to yield the desired donor **38** (**Figure 4.7**). Notably, we synthesized the α-anomer almost exclusively with little isomerization to the β-anomer. This is in contrast to the well-reported anomerization of *ortho*-alkynynylbenzoates donors.[10d]

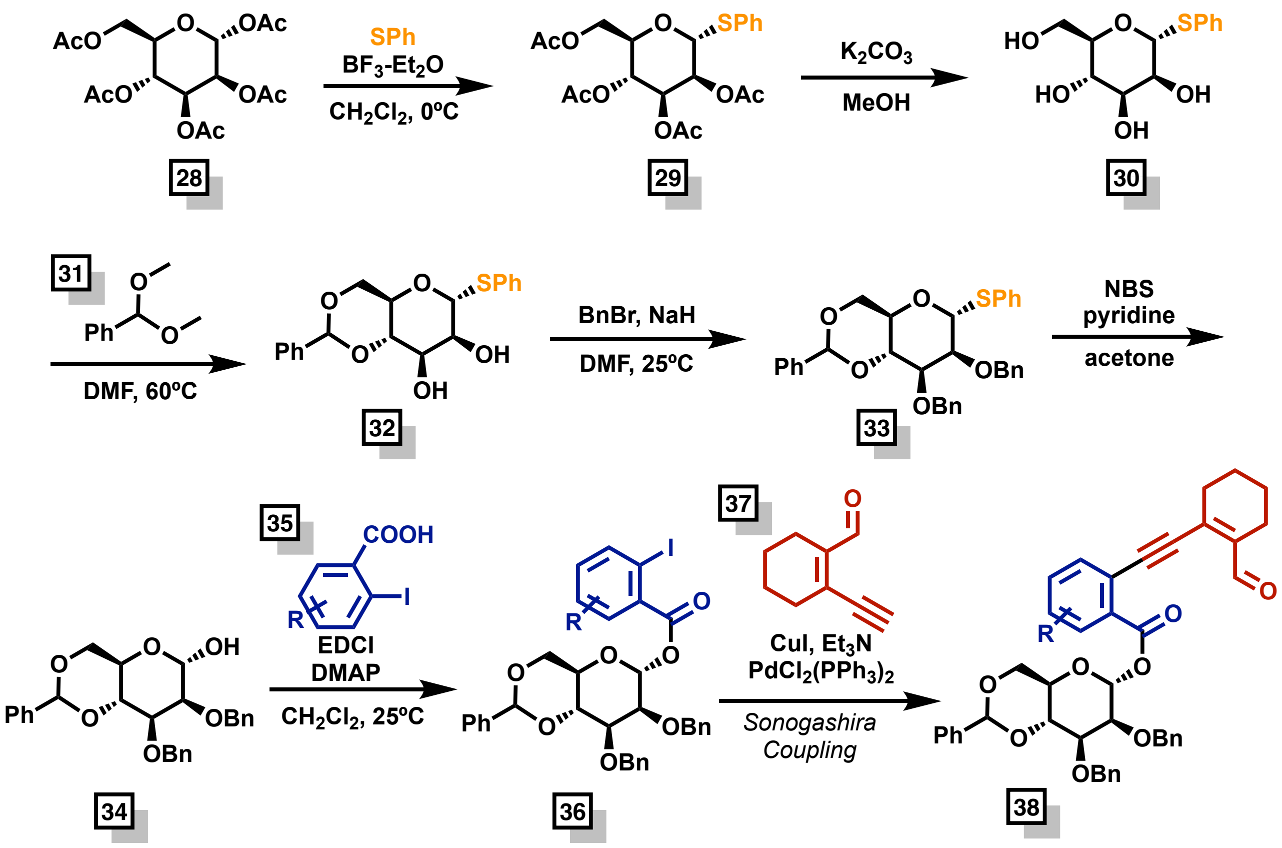
28
SPh
BF3-Et2O
CH2Cl2, 0ºC
29
K2CO3
MeOH
30
31
DMF, 60ºC
32
BnBr, NaH
DMF, 25ºC
33
NBS
pyridine
acetone
34
35
EDCI
DMAP
CH2Cl2, 25ºC
36
37
CuI, Et3N
PdCl2(PPh3)2
Sonogashira
Coupling
38

Figure 4.7: Synthesis of Benzylidene Protected Mannose Donor

4.2.3 PRELIMINARY OPTIMIZATION STUDIES

Based on the success of isopropanol in our glycal carbene system, we initiated our optimization studies, initially using it as a glycosyl acceptor before moving to combat a disaccharide system (**Table 4.1**). Initially, we exposed our donor to zinc (II) chloride, which worked well with our previous glycal carbene system. However, this resulted in low conversion to the desired glycoside (**entry 1**). Copper (I) chloride was also screened and shared similar results (**entry 2**). We then thought to screen more cationic Lewis acids and exposed our system to zinc triflate. This resulted in complete starting material conversion, and we were able to isolate the adduct in a 75% yield. NMR analysis illustrated in a 1:10 α:β ratio (**entry 3**). Lastly, we exposed our donor to Cu(I)OTf and NaBA$_r$F (**entry 4**), and this resulted in the desired product with a shared stereoselectivity 1:10 (α:β), and the product was isolated cleanly in a 79% yield.

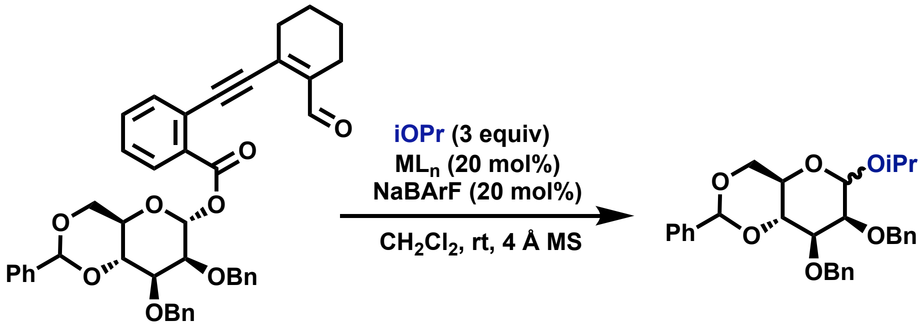

38

39

entry	catalyst	conversion	yield	α:β
1	ZnCl$_2$	40%	nd	n.d
2	Cu(I)Cl	30%	nd	n.d
3	**Zn(OTf)$_2$**	**100%**	**82%**	**1:10**
4	Cu(I)OTf	100%	79%	1:10

*Optimization reactions were completed by dissolving isopropanol (1.1 equiv.), catalyst (20 mol %), NaBArF (20 mol%), and 20 mg of activated 4-angstrom molecular sieves into 500 μL of the dichloromethane. After 10 minutes, **38** was added to the solution and allowed to stir until starting material consumption via TLC. Once complete, the reaction is diluted in dichloromethane and washed with a saturated NaHCO$_3$ solution. The organics were extracted a total of three times before drying over Na$_2$SO$_4$. Percent conversion and anomeric ratios are based on the integration of crude spectra.

***Table 4.1**:* Initial Catalyst Screening of System with Isopropanol

To realize our goal of disaccharide synthesis, we synthesized the sugar acceptor **40** and are currently developing favorable conditions within our lab (**Table 4.2**). Optimization with the sugar donor is currently underway to improve the disaccharide yield using the guidelines for *O*-glycoside formation.[15] In our preliminary experiments, based on our success with zinc triflate in our isopropanol system, it was the first screened catalyst with the sugar acceptor. While the bulky sugar alcohol resulted in the exclusive β-anomer formation, the reaction was extremely low yielding (**entry 1**). Revisiting copper triflate led to a slightly increased 45% yield (**entry 2**). Postulating that this system needed a highly cationic Lewis acid, we increased the amount of NaBA$_r$F to 1 equivalent, increasing the yield to 52% (**entry 3**). To date, we have identified THF as the optimal solvent; however, we are continuing optimization on this system. Additionally, we intend to continue screening catalysts with labile/non-coordinating ligands such as tetrafluoroborate [BF$_4$]$^-$ and hexafluorophosphate [PF$_6$]$^-$.

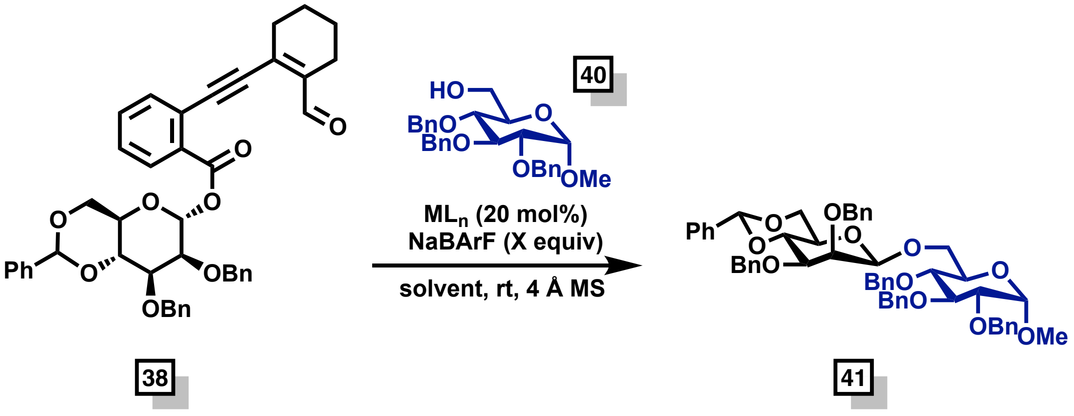

entry	catalyst	solvent	yield	X	α : β
1	Zn(OTf)$_2$	DCM	37%	0.2	β only
2	Cu(I)OTf	DCM	45%	0.2	β only

3	Cu(I)OTf	DCM	52%	1	β only
4	**Cu(I)OTf**	**THF**	**60%**	**1**	**β only**

Optimization reactions were completed by dissolving sugar alcohol (1.1 equiv.), catalyst (20 mol %), NaBArF, and 20 mg of activated 4-angstrom molecular sieves into 500 μL of the desired solvent. After 10 minutes, **38** (0.02 mmol) was added to the solution and allowed to stir until starting material consumption via TLC. Once complete, the reaction is diluted in ethyl acetate and washed with a saturated $NaHCO_3$ solution. The organics were extracted a total of three times before drying over Na_2SO_4. Anomeric ratios are based on the integration of crude spectra.

Table 4.2: Current Optimization with Sugar Acceptor

4.2.4 POSTULATED MECHANISTIC PATHWAY

As mentioned previously, we hypothesize that our system is initiated by the coordination of the metal salt to the alkynyl moiety to induce a *5-exo*-dig cyclization to form sugar furan **38**. Following a *5-exo*-dig cyclization to form sugar furan **42**, the available carbonyl moiety can undergo an sp^2 oxygen insertion into the metal carbenoid to form a latent benzofuranone leaving group. Once species **43** is formed, two pathways are proposed. In one alternative, electron donation from the endocyclic oxygen results in oxocarbenium intermediate, which can be intercepted in an S_N1-like fashion. Contrastingly, the nucleophile can attack in an S_N2-like manner to cleave the pendant benzofuranone functionality (**Figure 4.8a**).

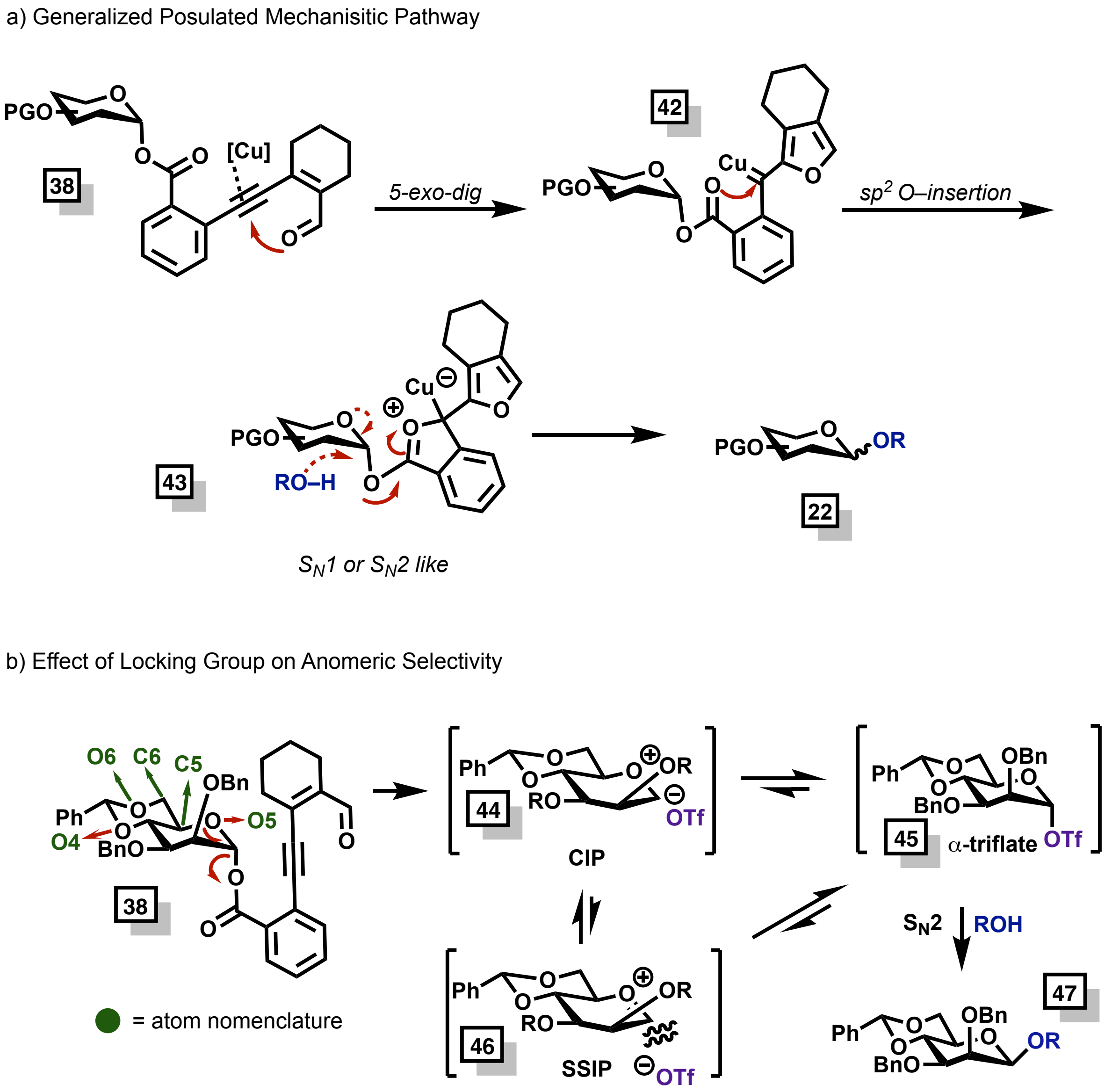
a) Generalized Posulated Mechanisitic Pathway

b) Effect of Locking Group on Anomeric Selectivity

PGO
38
[Cu]
5-exo-dig
42
Cu
sp² O–insertion
43
Cu⊖
⊕
RO–H
S_N1 or S_N2 like
22
OR
O6
C6
C5
OBn
Ph
O4
BnO
O5
● = atom nomenclature
44
RO
⊕OR
⊖OTf
CIP
45
α-triflate
OTf
46
SSIP
S_N2
ROH
47

Figure 4.8: Plausible Mechanistic Pathway

Studies suggest that 4,6 *O*-benzylidene protecting groups restrict the molecule's flexibility by locking the C5-C6 bond (green arrows) in the *trans gauche* conformation, making it more challenging to reach a half-chair transition state from a chair ground state.[16] Apart from this torsional influence, locking the C5-O5 and C6-O6 (green arrows) in an antiperiplanar fashion maximizes their disarming electronic effect, disfavoring oxocarbenium formation.[17] This, in turn, shifts the series of equilibria toward the covalent α-triflate**.** Following the formation of the α-triflate species **45**, the glycosyl acceptor can add onto the sugar via a stereospecific S_N2 to yield the desired β-linkage (**Figure 4.8b**).

4.2.5 HANDICAP OF METHODOLOGY

Optimization of this methodology is currently underway; however, these experiments have highlighted a significant limitation that handicaps the yields of our system. Our glycosylation strategy is competing with an intramolecular rearrangement to yield the benzofuranone adduct **49** (evidenced through ^1H NMR analysis). Additionally, this by-product has an extremely similar, near-identical R_f to the desired glycoside. This results in a decreased yield of the desired glycosides **47** (**Figure 4.9**).

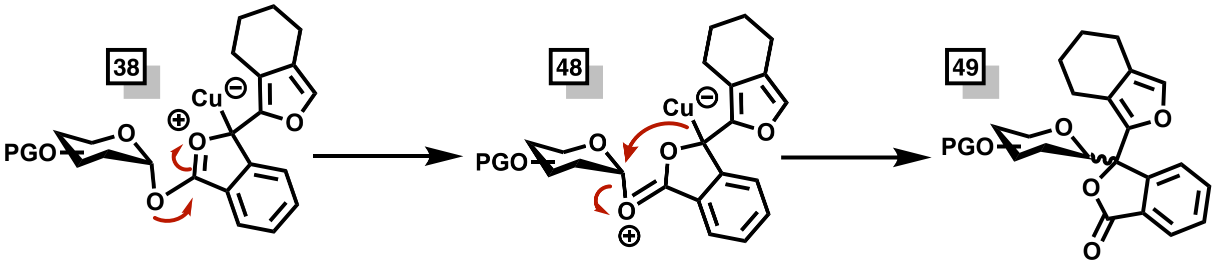

postulated by-product
unable to isolated cleanly

Figure 4.9: Competing Intramolecular Rearrangement

Currently, we are attempting to identify conditions that would hinder the formation of the undesired adduct **49**.

4.3 FUTURE DIRECTIONS AND CONCLUSIONS

This project is still in its infancy, and our research laboratory is currently locating tremendous energy, supplies, and personnel to continue developing this system. We plan to synthesize the β-glycosyl donor **52** to observe the effect of anomeric configuration on selectivity, reaction rates, and yields (**Figure 4.10**). An α-bromo-protected sugar **50** can undergo a stereospecific substitution reaction with iodobenzoic acids **35** to yield the β-sugar benzoate **51**.[10a] A successive Sonogashira coupling can install enynone **37** to generate the corresponding β-glycosyl donor **52**. We will first synthesize the unsubstituted β-mannose derivative to conduct a head-to-head comparison of the two donors. These results will provide fundamental insight into the mechanism (S_N1 or S_N2 type). Additionally, if required, we will develop favorable conditions to induce sizable stereochemical control for β-glycosyl donors.

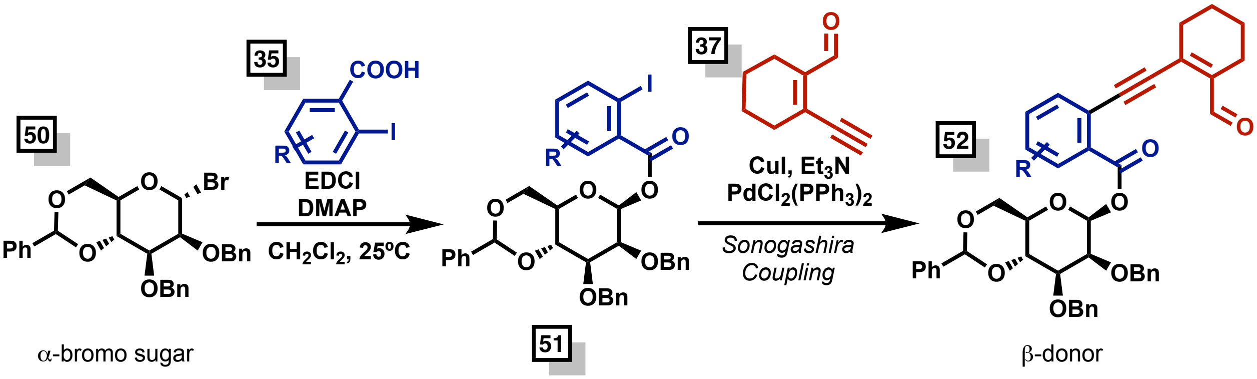
50
35
COOH
I
R
Br
O
Ph
OBn
EDCI
DMAP
CH2Cl2, 25ºC
51
37
CuI, Et3N
PdCl2(PPh3)2
Sonogashira
Coupling
52
α-bromo sugar
β-donor

Figure 4.10: Synthetic Route to β-Sugar Enynone

4.3.1 SYNTHESIS OF O–GLYCOSIDES

Once we have optimized reaction conditions, we intend to prepare a diverse substrate scope featuring a range of oxygen-based acceptors (**Figure 4.11**). We will primarily focus on synthesizing challenging 1,2 *cis*-linkages such as α-glucosides, α-galactosides, and β-mannosides. We have synthesized the β-mannoside **47a** and are currently optimizing conditions to increase the yields for the disaccharide. Additionally, concurrently, we are developing a viable synthetic route to the glucose-derived donor to prepare the β-glucoside **47b**. We expect the glucose system to require further optimization for high selectivity.

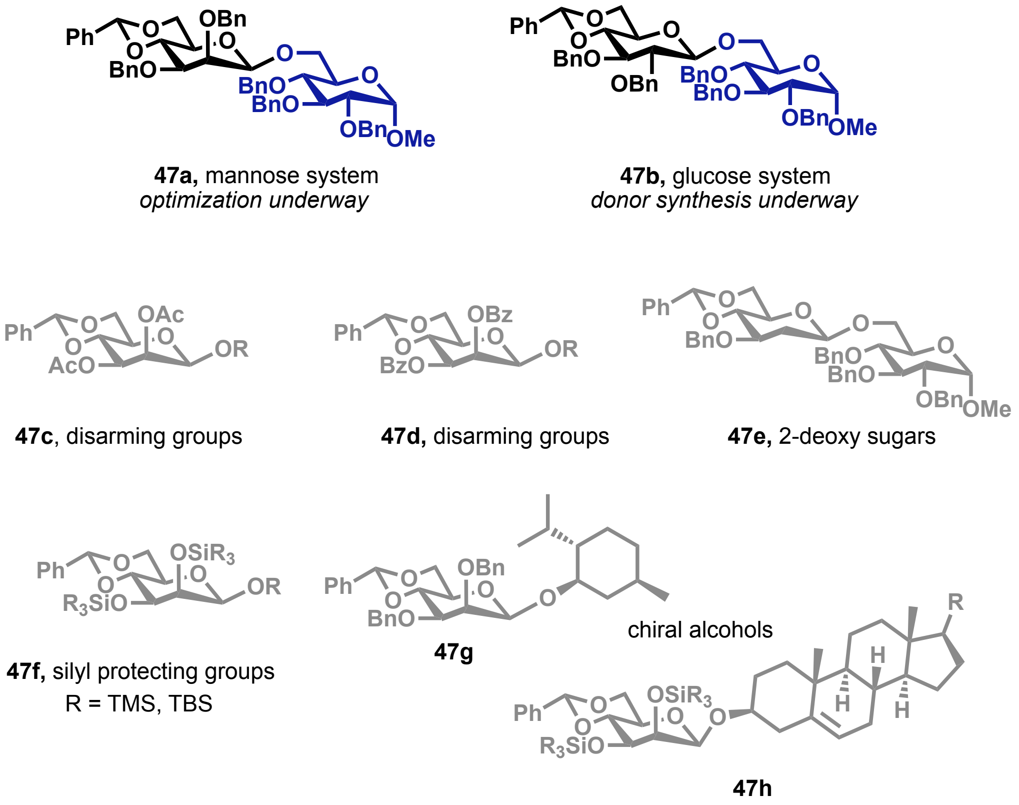
47a, mannose system
optimization underway

47b, glucose system
donor synthesis underway

47c, disarming groups

47d, disarming groups

47e, 2-deoxy sugars

47f, silyl protecting groups
R = TMS, TBS

47g

chiral alcohols

47h

***Figure 4.11**: Access to O–Glycosides*

Following this, we will prepare sugar donors featuring different protecting groups to observe protecting group effects on the system. We will screen disarming protecting groups such as acetate and benzoyl (**47c,47d**). These studies will coincide well, as our parent system is protected with arming (benzyl) groups. Additionally, to observe the effect of the C2 groups, we will synthesize the 2-deoxygenated donor to synthesize **47e**.

Next, we intend to expose our glycosyl donors to chiral alcohols such as L-menthol (**47g**) and cholesterol (**47h**). As previously observed, we expect to achieve sizable selectivity using sterically hindered acceptors.

4.3.2 APPLICATIONS TO N– AND S– GLYCOSIDES AND FURANOSES

Once we have established a diverse library of sugars with oxygen nucleophiles, we will further our methodology by utilizing heteroatom and carbon-based glycosyl acceptors (**Figure 4.12**). Aminoglycosides are particularly attractive linkages due to their potency as bactericidal antibiotics in both gram-positive and gram-negative bacteria.[18] Too, they are commonly involved in the post-synthetic modification of various proteins and can possess antiviral or anticancer activity.[19] By developing a more efficient way to access these privileged glycosides, we can rapidly synthesize libraries of relevant targets that can be screened for their biological activity.

a) Accesss to aminoglycosides

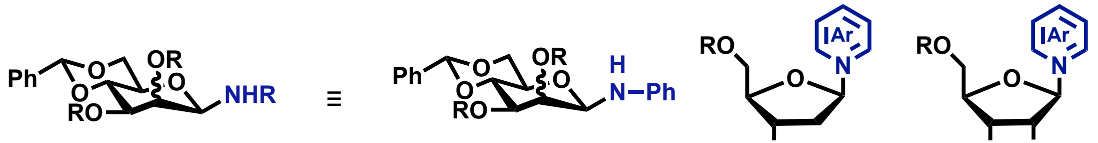

53

53a, aryl aminoglycosides

53b, deoxynucleosides

53c, ribonucleosides

b) Accesss to thioglycosides

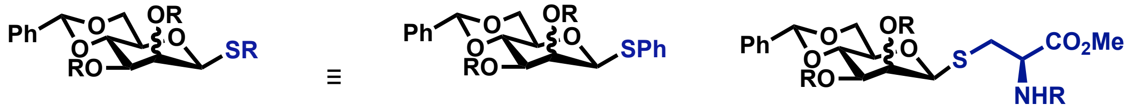

54

54a, glycosyl donors

54b, biological targets

Figure 4.12: Substrate Scope with Non-Oxygen Acceptors

Notably, we hope to synthesize a series of deoxyribonucleosides **53b** and ribonucleosides **53c** using a variety of *N*-nucleophilic aromatic heterocycles. Additionally, we foresee this strategy's compatibility with sulfur nucleophiles to synthesize thioglycosides. This will demonstrate the compatibility of our donors with other glycosyl donors (**54a**), which is helpful for iterative syntheses. Likewise, a library of thioglycosides can be synthesized and evaluated for therapeutic development.

4.3.3 CONCLUSIONS

In summary, in continuation of our interests of carbene-assisted glycosylation strategies, we have developed a novel, alkynyl-embedded donor that can be activated by Earth-abundant metals. This is an extension of our previously disclosed glycal carbene donors (*Chapter 3*).

This donor is a stark contrast to reports of gold-activated alkynyl donors emerging in the literature. We are developing conditions for disaccharide synthesis with sugar acceptors with this donor. We have preliminary conditions using copper (I) triflate as a catalyst to date. We hope to develop these conditions for high-yielding disaccharides and envision expanding this work to access *N*– and *S*– glycosides.

4.4 REFERENCES FOR CHAPTER 4

[1] a). H. M. L. Davies, K. Liao, *Nature Reviews Chemistry* **2019**, *3*, 347-360; b). Y. Xia, D. Qiu, J. Wang, *Chemical Reviews* **2017**, *117*, 13810-13889; c). S. F. Zhu, Q. L. Zhou, *Acc. Chem. Res.* **2012**, *45*, 1365.

[2] a). H. M. L. Davies, J. R. Denton, *Chemical Society Reviews* **2009**, *38*, 3061-3071; b). A. Padwa, *Chemical Society Reviews* **2009**, *38*, 3072-3081.

[3] a). M. Boultadakis-Arapinis, P. Lemoine, S. Turcaud, L. Micouin, T. Lecourt, *Journal of the American Chemical Society* **2010**, *132*, 15477-15479; b). M. Boultadakis-Arapinis, C. Lescot, L. Micouin, T. Lecourt, *Synthesis* **2012**, *44*, 3731-3734; c). M. Boultadakis-Arapinis, E. Prost, V. Gandon, P. Lemoine, S. Turcaud, L. Micouin, T. Lecourt, *Chemistry – A European Journal* **2013**, *19*, 6052-6066.

[4] J. Wu, X. Li, X. Qi, X. Duan, W. L. Cracraft, I. A. Guzei, P. Liu, W. Tang, *Journal of the American Chemical Society* **2019**, *141*, 19902-19910.

[5] L. Meng, P. Wu, J. Fang, Y. Xiao, X. Xiao, G. Tu, X. Ma, S. Teng, J. Zeng, Q. Wan, *Journal of the American Chemical Society* **2019**, *141*, 11775-11780.

[6] a). H. J. Gabius, *The sugar code: fundamentals of glycosciences*, **2011**; b). Z. Györgydeak, I. F. Pelyvas, B. O. Fraser-Reid, K. Tatsuta, J. Thiem, *Glycoscience: Chemistry and Chemical Biology I–III*, **2001**; c). T. Nishikawa, M. Adachi, M. Isobe, B. Fraser-Reid, K. Tatsuta, J. Thiem, *Glycoscience*, **2008**.

[7] Y. Wang, M. E. Muratore, A. M. Echavarren, *Chemistry (Weinheim an der Bergstrasse, Germany)* **2015**, *21*, 7332-7339.

[8] S. Kashyap, S. Hotha, *Tetrahedron Letters* **2006**, *47*, 2021-2023.

[9] S. Hotha, S. Kashyap, *Journal of the American Chemical Society* **2006**, *128*, 9620-9621.

[10] a). X. Ma, Z. Zheng, Y. Fu, X. Zhu, P. Liu, L. Zhang, *Journal of the American Chemical Society* **2021**, *143*, 11908-11913; b). Y. Li, X. Yang, Y. Liu, C. Zhu, Y. Yang, B. Yu, *Chemistry – A European Journal* **2010**, *16*, 1871-1882; c). Y. Zhu, B. Yu, *Chemistry – A European Journal* **2015**, *21*, 8771-8780; d). Y. Tang, J. Li, Y. Zhu, Y. Li, B. Yu, *Journal of the American Chemical Society* **2013**, *135*, 18396-18405.

[11] S. Manabe, Y. Ito, *Current Bioactive Compounds* **2008**, *4*, 258-281.

[12] a). S. P. Green, K. M. Wheelhouse, A. D. Payne, J. P. Hallett, P. W. Miller, J. A. Bull, *Organic Process Research & Development* **2020**, *24*, 67-84; b). M. Jia, S. Ma, *Angewandte Chemie International Edition* **2016**, *55*, 9134-9166.

[13] a). M. Petzold, A. Günther, P. G. Jones, D. B. Werz, *Chemistry – A European Journal* **2020**, *26*, 11119-11123; b). J. Barluenga, D. de Sáa, A. Gómez, A. Ballesteros, J. Santamaría, A. de Prado, M. Tomás, A. L. Suárez-Sobrino, *Angewandte Chemie International Edition* **2008**, *47*, 6225-6228.

[14] a). D. Crich, N. S. Chandrasekera, *Angewandte Chemie International Edition* **2004**, *43*, 5386-5389; b). A. Ishiwata, Y. Ito, in *Glycoscience: Chemistry and Chemical Biology* (Eds.: B. O. Fraser-Reid, K. Tatsuta, J. Thiem), Springer Berlin Heidelberg, Berlin, Heidelberg, **2008**, pp. 1279-1312.

[15] P. R. Andreana, D. Crich, *ACS Central Science* **2021**, *7*, 1454-1462.

[16] H. H. Jensen, L. U. Nordstrøm, M. Bols, *Journal of the American Chemical Society* **2004**, *126*, 9205-9213.

[17] D. Crich, *Acc. Chem. Res.* **2010**, *43*, 1144.

[18] K. M. Krause, A. W. Serio, T. R. Kane, L. E. Connolly, *Cold Spring Harb Perspect Med* **2016**, *6*, a027029.

[19] a). C. M. Galmarini, J. R. Mackey, C. Dumontet, *The Lancet Oncology* **2002**, *3*, 415-424; b). L. Eyer, R. Nencka, E. de Clercq, K. Seley-Radtke, D. Růžek, *Antiviral chemistry & chemotherapy* **2018**, *26*, 2040206618761299-2040206618761299.

4.5 EXPERIMENTAL SECTION FOR SECTION 4

MATERIALS AND METHODS

Reagents

Reagents and solvents were obtained from Sigma-Aldrich, Chem-Impex, VWR International, and Acros Organics and used without further purification unless otherwise indicated. Dichloromethane and Acetonitrile were distilled over CaH under N_2 unless otherwise indicated. Tetrahydrofuran was distilled over Na under N_2 with benzophenone indicator.

Glassware

All reactions were performed in flame-dried glassware under positive N_2 pressure with magnetic stirring unless otherwise noted.

Chromatography

Thin layer chromatography (TLC) was performed on 0.25 mm E. Merck silica gel 60 F254 plates and visualized under UV light (254 nm) or by staining with potassium permanganate ($KMnO_4$), cerium ammonium molybdate (CAM), phosphomolybdic acid (PMA), and ninhydrin. Silica flash chromatography was performed on Sorbtech 230-400 mesh silica gel 60.

Analytical Instrumentation

NMR spectra were recorded on a Varian NMRS 400 and 500MHz NMR spectrometer at 20 ºC in $CDCl_3$ unless otherwise indicated. Chemical shifts are expressed in ppm relative to solvent signals: $CDCl_3$ (^{1}H, 7.26 ppm, ^{13}C, 77.0 ppm); coupling constants are expressed in Hz. IR spectra were recorded on a Cary 760 FTIR spectrometer with peaks reported in cm^{-1}. Mass spectra were obtained on an Advion Expression CMS TLC Mass Spectrometer

Nomenclature

Chemical structure named in accordance with IUPAC guidelines, automatically generated using ChemDraw 20.1

Additional Information and Considerations

Syringe pump addition reactions were conducted using a Harvard Apparatus (Model: 55-1111) or a New Era Pump Systems, Inc. (Model: NE-300) syringe pump. Sonication was performed using a Bransonic Ultrasonic Cleaner (Model: M5800H).

PUBLICATION AND CONTRIBUTIONS STATEMENT

The research within this section is unpublished. All materials and procedures are contributions by A. Bain and Bidhan Ghosh.

4.5.1 Synthesis of Alkynyl Donor

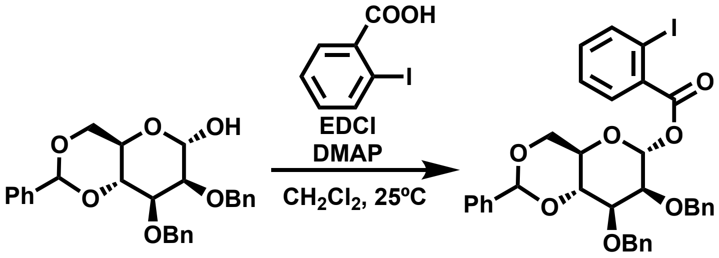

(4a*R*,6*R*,7*S*,8*S*,8a*R*)-7,8-bis(benzyloxy)-2phenylhexahydropyrano[3,2*d*][1,3]dioxin-6-yl 2-iodobenzoate (36): Sugar (1 equiv), iodobenzoic acid (2 equiv), EDC salt (2 equiv) and DMAP (0.3 equiv) were dissolved in distilled dichloromethane (0.2M solution) at room temperature. The reaction was allowed to stir overnight until starting materials were consumed. The following day, the reaction was diluted in DCM and washed with brine. The organics were extracted twice more, then washed with a saturated sodium bicarbonate solution before drying over sodium sulfate. The crude compound was purified via an isocratic 20% EtOAc silica gel column.

R_f: 0.41 (20% EtOAc in Hexanes)

^{1}H: (500 MHz, $CDCl_3$) δ 7.99 (d, *J* = 8.1 Hz, 1H), 7.71 (d, *J* = 7.8 Hz, 1H), 7.52 (d, *J* = 7.3 Hz, 2H), 7.49 – 7.36 (m, 8H), 7.39 – 7.30 (m, 4H), 7.30 (d, *J* = 8.5 Hz, 3H), 7.18 (d, *J* = 15.5 Hz, 1H), 6.40 (s, 1H), 5.68 (s, 1H), 4.87 (s, 2H), 4.83 (d, *J* = 12.5 Hz, 1H), 4.69 (d, *J* = 12.3 Hz, 1H), 4.38 (t, *J* = 9.7 Hz, 1H), 4.30 (dd, *J* = 10.1, 4.6 Hz, 1H), 4.13 (dd, *J* = 10.3, 3.3 Hz, 1H), 4.01 – 3.93 (m, 2H), 3.89 (t, *J* = 10.2 Hz, 1H).

^{13}C NMR (126 MHz, $CDCl_3$) δ 164.38, 141.58, 137.58, 137.46, 134.12, 133.30, 131.60, 128.95, 128.54, 128.45, 128.31, 128.26, 128.08, 128.04, 127.78, 101.53, 94.07, 93.85, 78.56, 75.36, 75.12, 73.68, 72.96, 68.50, 66.92.

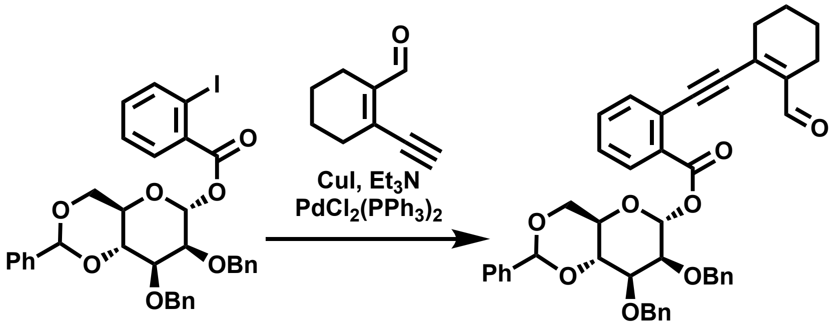

(4a*R*,6*R*,7*S*,8*S*,8a*R*)-7,8-bis(benzyloxy)-2phenylhexahydropyrano[3,2*d*][1,3]dioxin-6-yl-2-((2-formylcyclohex-1-en-1-yl)ethynyl)benzoate (38): Sugar (1 equiv), CuI (30 mol%) and $PdCl_2(PPh_3)_2$ (30 mol%) were dissolved in 0.5M concentration of Et_3N, in a flame-dried round bottom flask fitted with a reflux condenser, then flushed with nitrogen gas for 15 minutes. The enynone was added to the reaction in one portion, and the reaction was heated to 60ºC for 24 hours. After 24 hours, the crude reaction was filter over celite with EtOAc and washed twice with brine. The organics were extracted three times before drying over Na_2SO_4. The crude compound was purified via a silica gel chromatography

R_f: 0.22 (20% EtOAc / 80% Hexanes)

^{1}H (500 MHz, $CDCl_3$) δ 10.38 (s, 1H), 7.83 (d, *J* = 7.9 Hz, 1H), 7.65 – 7.49 (m, 6H), 7.47 – 7.28 (m, 16H), 6.41 (d, *J* = 1.8 Hz, 1H), 5.69 (s, 1H), 4.86 (s, 3H), 4.83 (s, 1H), 4.66 (d, *J* = 12.0 Hz, 2H), 4.39 (t, *J* = 9.7 Hz, 1H), 4.29 (dd, *J* = 10.2, 4.5 Hz, 1H), 4.05 (dd, *J* = 10.0, 3.3 Hz, 1H), 3.97 (d, *J* = 4.6 Hz, 1H), 3.94 – 3.90 (m, 2H), 3.89 (s, 1H), 2.55 (d, *J* = 8.3 Hz, 3H), 2.29 (t, *J* = 6.1 Hz, 3H), 1.74 – 1.60 (m, 6H).

^{13}C NMR (101 MHz, $CDCl_3$) δ 193.38, 162.93, 143.67, 139.61, 138.19, 137.56, 137.35, 134.57, 132.70, 130.73, 130.02, 128.90, 128.73, 128.48, 128.35, 128.22, 128.19, 127.95, 127.70, 127.68, 101.37, 96.59, 93.12, 91.95, 78.49, 75.49, 75.43, 73.48, 73.15, 68.50, 66.88, 32.00, 22.14, 21.82, 20.93.

4.5.2 Synthesis of Sugar Alcohol

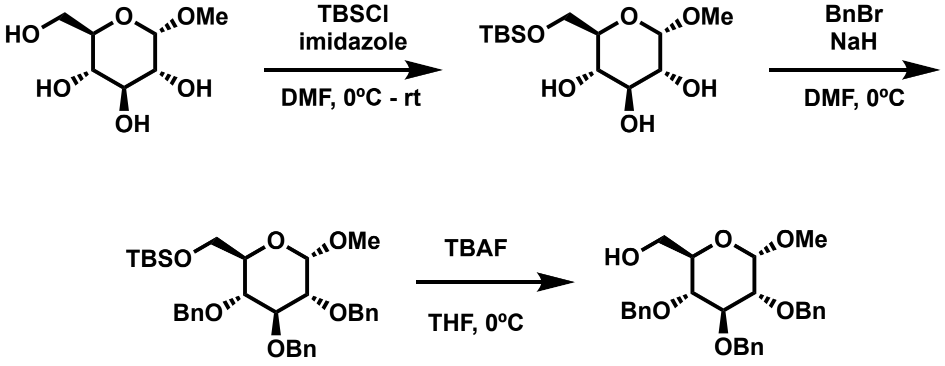
HO
OMe
HO
OH
OH
TBSCl
imidazole
DMF, 0°C - rt
TBSO
OMe
HO
OH
OH
BnBr
NaH
DMF, 0°C
TBSO
OMe
BnO
OBn
OBn
TBAF
THF, 0°C
HO
OMe
BnO
OBn
OBn

((2*R*,3*R*,4*S*,5*R*,6*S*)-3,4,5-tris(benzyloxy)-6-methoxytetrahydro-2*H*-pyran-2-yl)methanol (40): The sugar alcohol **40** was synthesized in three steps from methyl α-D-glucopyranoside, from literature know procedures.[1]

R$_f$: 0.45 (30% EtOAc in Hexanes)

^{1}H: (500 MHz, $CDCl_3$) δ 7.40 – 7.24 (m, 14H), 4.99 (d, *J* = 10.9 Hz, 1H), 4.88 (d, *J* = 11.0 Hz, 1H), 4.86 – 4.77 (m, 2H), 4.65 (t, *J* = 11.6 Hz, 2H), 4.57 (d, *J* = 3.5 Hz, 1H), 4.00 (t, *J* = 9.3 Hz, 1H), 3.77 (ddd, *J* = 11.6, 5.4, 2.6 Hz, 1H), 3.69 (dq, *J* = 7.6, 3.7 Hz, 1H), 3.65 (dt, *J* = 10.0, 3.4 Hz, 1H), 3.54 – 3.47 (m, 2H), 3.37 (s, 3H).

^{13}C NMR (101 MHz, $CDCl_3$) δ 138.68, 138.08, 128.50 (d, *J* = 2.0 Hz), 128.43, 128.15, 128.07, 128.00, 127.97, 127.92, 127.66, 98.16, 81.95, 79.90, 75.79, 75.05, 73.45, 70.61, 61.85, 55.21.

4.5.3 Glycosylation Reactions

Experiments performed by Bidhan Ghosh and A. Bain.

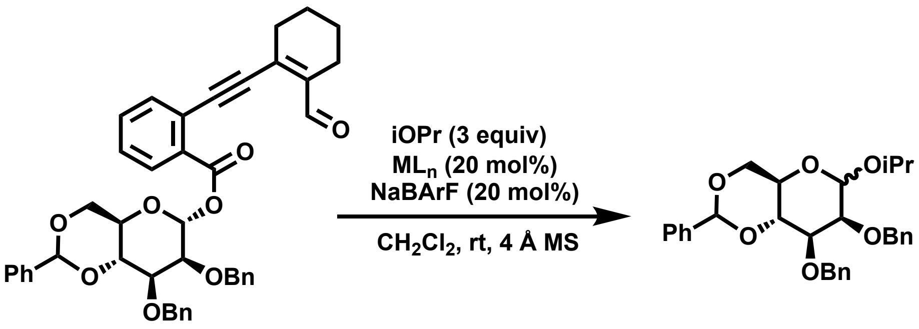

(4a*R*,7*S*,8*S*,8a*R*)-7,8-bis(benzyloxy)-6-isopropoxy-2-phenylhexahydropyrano[3,2*d*][1,3]dioxine (39): Isopropanol (1.1 equiv.), catalyst (20 mol %), NaBA$_r$F (20 mol%), and 20 mg of activated 4-angstrom molecular sieves into 500 μL of the dichloromethane. After 10 minutes, **38** was added to the solution and allowed to stir until starting material consumption via TLC. Once complete, the reaction is diluted in dichloromethane and washed with a saturated $NaHCO_3$ solution. The organics were extracted a total of three times before drying over Na_2SO_4. NMR Spectra was verified by comparison to literature reports.[2]

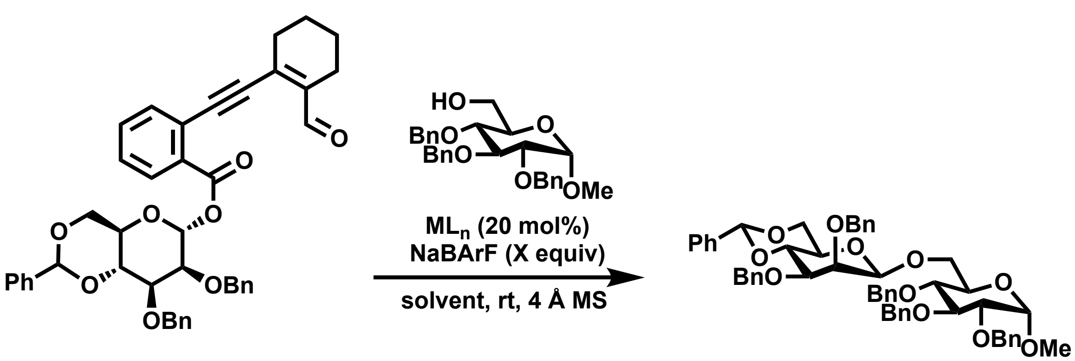

(2*R*,4a*R*,6*R*,7*S*,8*S*,8a*R*)-7,8-bis(benzyloxy)-2-phenyl-6-(((2*R*,3*R*,4*S*,5*R*,6*S*)-3,4,5-tris(benzyloxy)-6-methoxytetrahydro-2*H*-pyran-2yl)methoxy)hexahydropyrano[3,2-*d*][1,3]dioxine (41): Sugar alcohol (1.1 equiv.), catalyst (20 mol %), $NaBA_rF$, and 20 mg of activated 4-angstrom molecular sieves into 500 μL of the desired solvent. After 10 minutes, **38** was added to the solution and allowed to stir until starting material consumption via TLC. Once complete, the reaction is diluted in ethyl acetate and washed with a saturated $NaHCO_3$ solution. The organics were extracted a total of three times before drying over Na_2SO_4. NMR Spectra was verified by comparison to literature reports.[3]

^{1}H NMR (600 MHz, $CDCl_3$) δ 7.51 – 7.46 (m, 2H), 7.41 (d, J = 7.7 Hz, 2H), 7.39 – 7.23 (m, 25H), 7.20 (t, J = 7.2 Hz, 1H), 5.53 (s, 1H), 5.06 (d, J = 10.7 Hz, 1H), 4.86 – 4.78 (m, 3H), 4.78 – 4.73 (m, 2H), 4.67 – 4.57 (m, 4H), 4.38 (s, 1H), 4.30 (d, J = 12.1 Hz, 1H), 4.11 – 4.03 (m, 2H), 3.88 (p, J = 8.9 Hz, 2H), 3.65 (d, J = 3.1 Hz, 1H), 3.61 (dd, J = 9.4, 2.8 Hz, 1H), 3.57 – 3.51 (m, 3H), 3.47 (dd, J = 10.9, 3.0 Hz, 1H), 3.41 (s, 3H), 3.34 (dd, J = 9.9, 3.1 Hz, 1H).

^{13}C NMR (101 MHz, $CDCl_3$) δ 139.38, 138.61, 138.53, 138.30, 137.63, 137.50, 128.80, 128.51, 128.36, 128.35, 128.31, 128.27, 128.14, 128.04, 128.00, 127.77, 127.66, 127.50, 127.44, 127.30, 127.18, 126.05, 101.53, 101.27, 98.37, 80.23, 78.94, 78.68, 78.25, 77.65, 76.96, 75.25, 74.94, 73.61, 73.54, 72.49, 69.54, 68.54, 68.28, 67.21, 55.33

4.6 APPENDIX 3

Spectra Relevant to Chapter 4

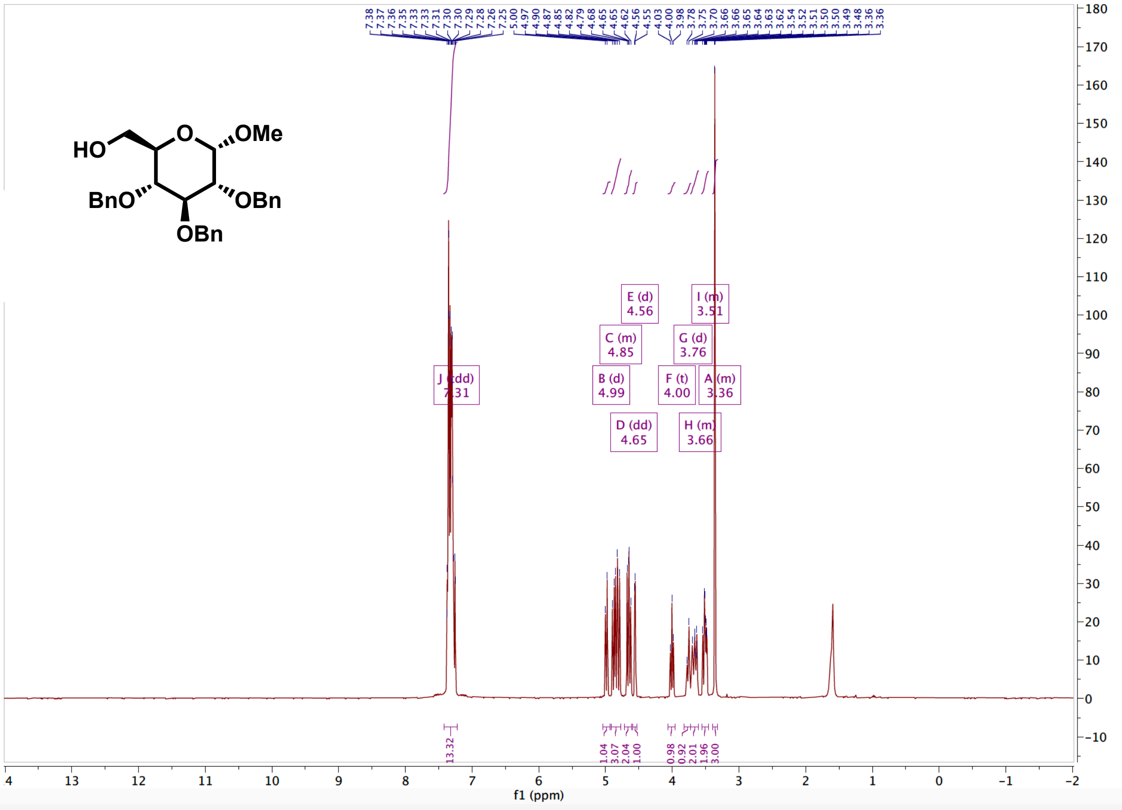
7.38 7.37 7.36 7.35 7.33 7.33 7.31 7.30 7.30 7.29 7.28 7.26 7.25
5.00 4.97 4.90 4.87 4.85 4.82 4.79 4.68 4.65 4.65 4.62 4.56 4.55
4.03 4.00 3.98 3.78 3.75 3.70 3.66 3.65 3.64 3.63 3.62 3.54 3.52 3.51 3.50 3.49 3.48 3.36 3.36
HO
O
OMe
BnO
OBn
OBn
E (d) 4.56
I (m) 3.51
C (m) 4.85
G (d) 3.76
J (dd) 7.31
B (d) 4.99
F (t) 4.00
A (m) 3.36
D (dd) 4.65
H (m) 3.66
13.32
1.04 3.07 2.04 1.00
0.98 0.92 2.01 1.96 3.00
f1 (ppm)

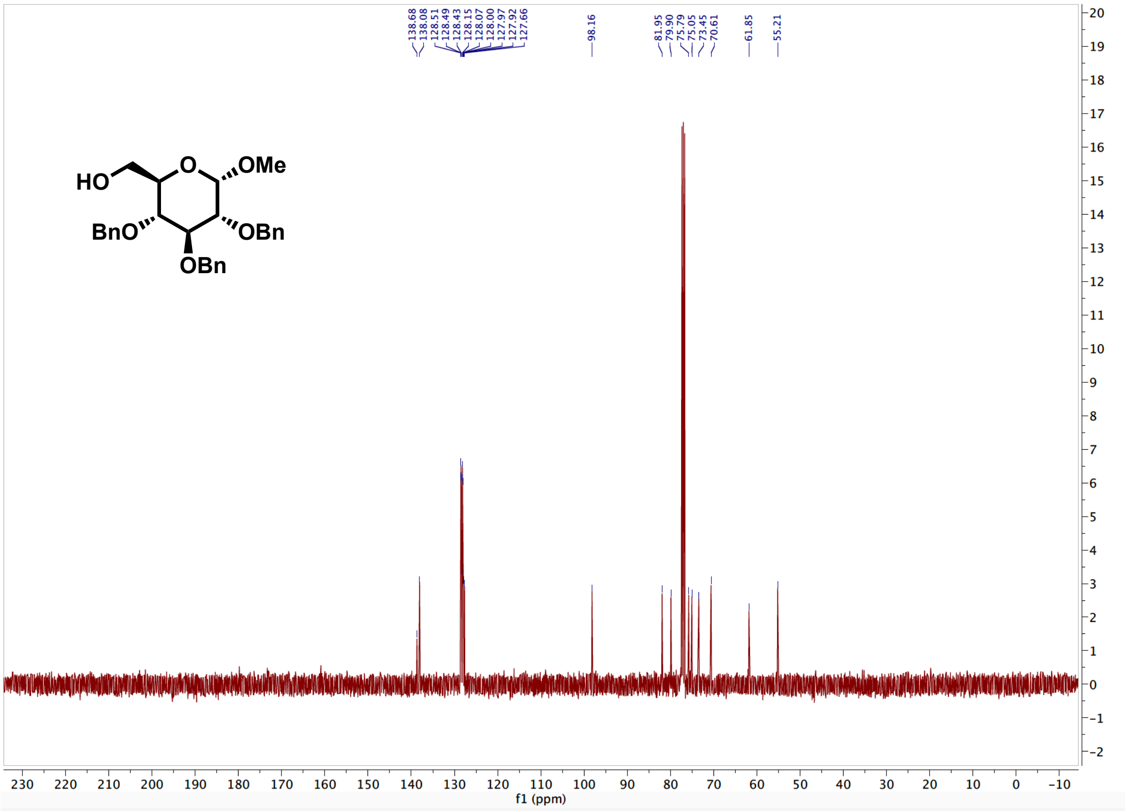
138.68 138.08 128.51 128.49 128.43 128.15 128.07 128.00 127.97 127.92 127.66
98.16
81.95 79.90 75.79 75.05 73.45 70.61
61.85
55.21
HO
O
OMe
BnO
OBn
OBn
f1 (ppm)

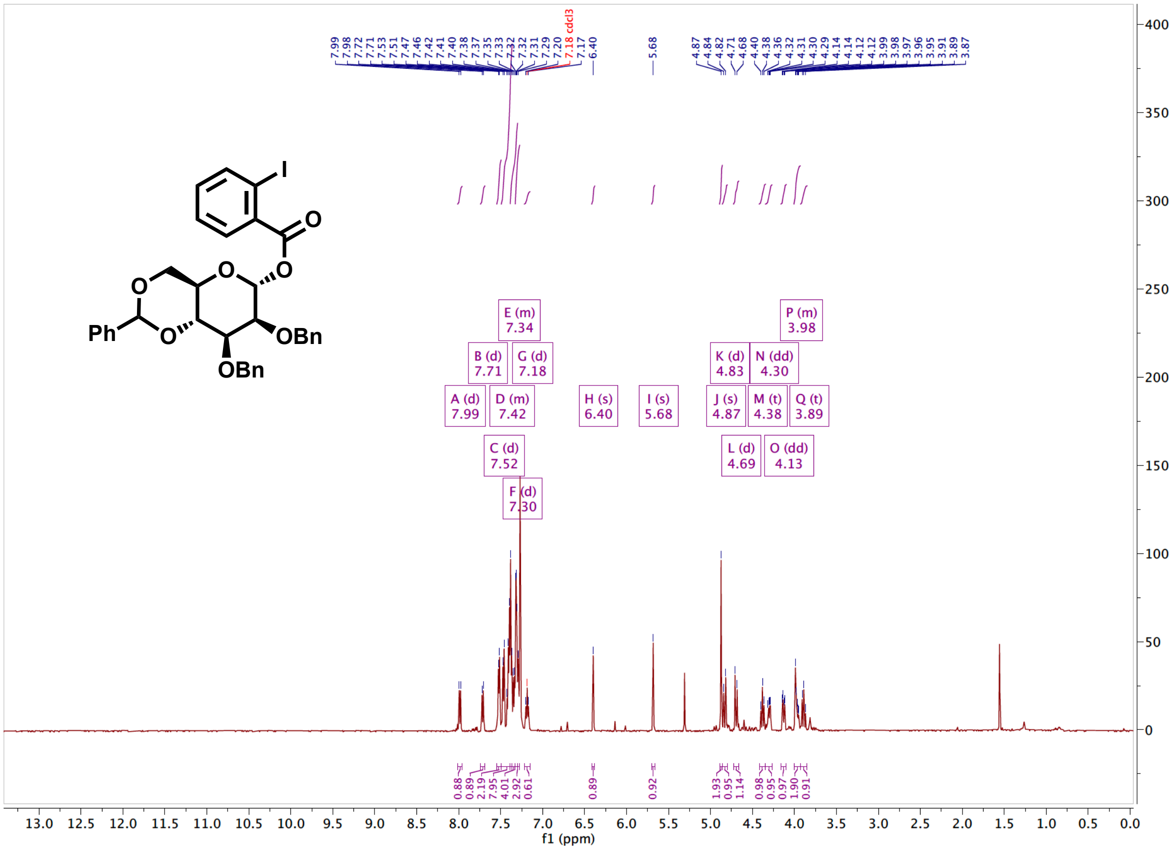
7.99
7.98
7.72
7.71
7.53
7.51
7.47
7.46
7.42
7.41
7.40
7.38
7.37
7.35
7.33
7.32
7.32
7.31
7.29
7.20
7.18 cdcl3
7.17
6.40
5.68
4.87
4.84
4.82
4.71
4.68
4.40
4.38
4.36
4.32
4.31
4.30
4.29
4.14
4.14
4.12
4.12
3.99
3.98
3.97
3.96
3.91
3.89
3.87
I
O
O
O
O
Ph
O
OBn
OBn
E (m) 7.34
B (d) 7.71
G (d) 7.18
A (d) 7.99
D (m) 7.42
C (d) 7.52
F (d) 7.30
H (s) 6.40
I (s) 5.68
P (m) 3.98
K (d) 4.83
N (dd) 4.30
J (s) 4.87
M (t) 4.38
Q (t) 3.89
L (d) 4.69
O (dd) 4.13
0.88
0.89
2.19
7.95
4.01
2.92
0.61
0.89
0.92
1.93
0.95
1.14
0.98
0.95
0.97
1.90
0.91
400
350
300
250
200
150
100
50
0
13.0
12.5
12.0
11.5
11.0
10.5
10.0
9.5
9.0
8.5
8.0
7.5
7.0
6.5
6.0
5.5
5.0
4.5
4.0
3.5
3.0
2.5
2.0
1.5
1.0
0.5
0.0
f1 (ppm)

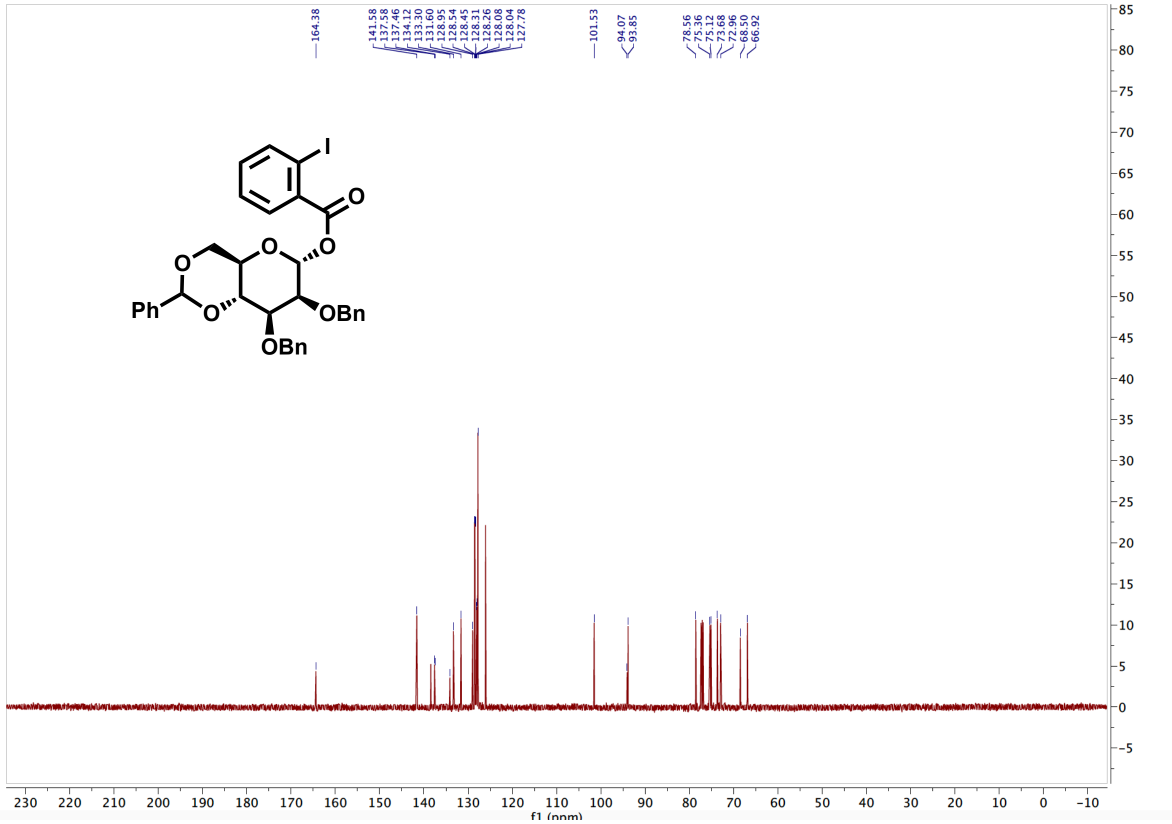
164.38
141.58
137.58
137.46
134.12
133.20
131.60
128.95
128.54
128.45
128.31
128.26
128.08
128.04
127.78
101.53
94.07
93.85
78.56
75.36
75.12
73.68
72.96
68.50
66.92
I
O
O
O
O
Ph
O
OBn
OBn
85
80
75
70
65
60
55
50
45
40
35
30
25
20
15
10
5
0
-5
230
220
210
200
190
180
170
160
150
140
130
120
110
100
90
80
70
60
50
40
30
20
10
0
-10
f1 (ppm)

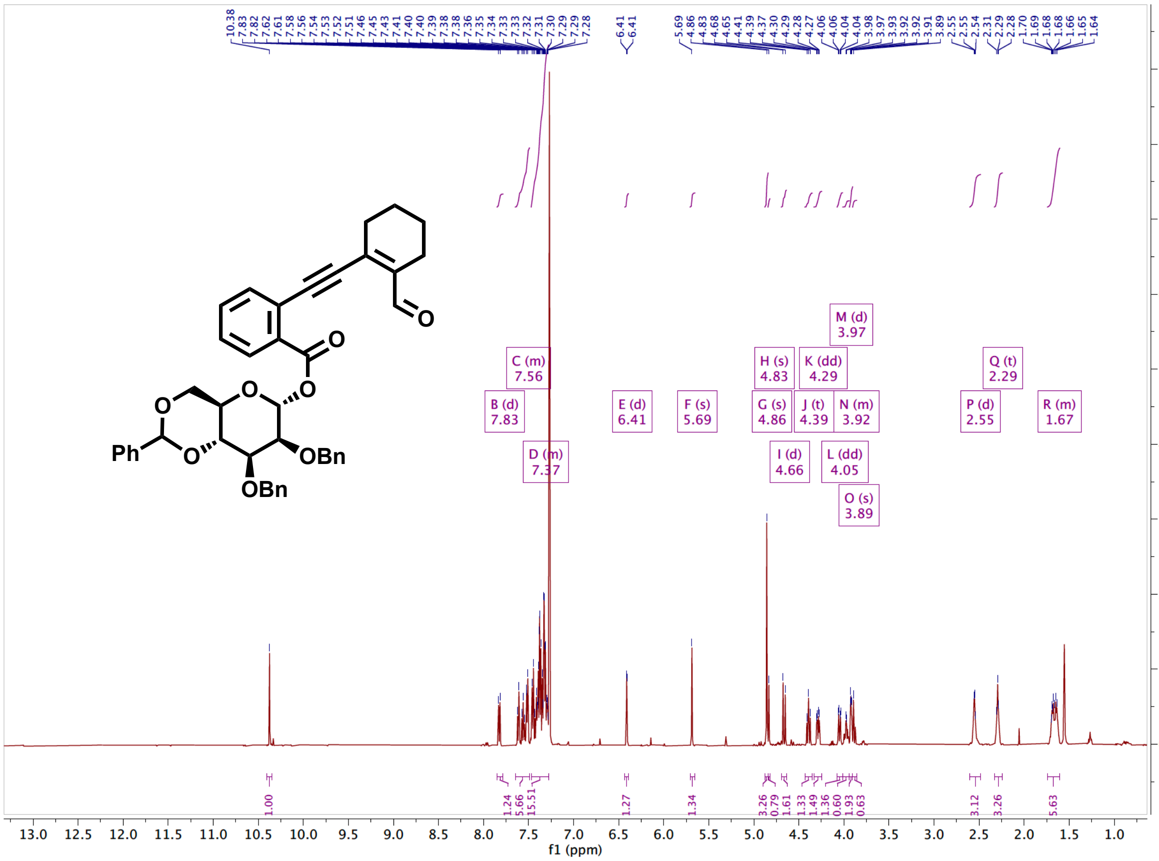
10.38
7.83
7.82
7.62
7.61
7.58
7.56
7.54
7.53
7.52
7.51
7.46
7.45
7.43
7.41
7.40
7.39
7.38
7.38
7.36
7.35
7.34
7.33
7.33
7.32
7.31
7.30
7.29
7.29
7.28
6.41
6.41
5.69
4.86
4.83
4.68
4.65
4.41
4.39
4.37
4.30
4.29
4.28
4.27
4.06
4.06
4.04
4.04
3.98
3.97
3.93
3.92
3.92
3.91
3.89
2.55
2.55
2.54
2.31
2.29
2.28
1.70
1.69
1.68
1.68
1.66
1.65
1.64
O
O
O
O
O
Ph
OBn
OBn
B (d) 7.83
C (m) 7.56
D (m) 7.37
E (d) 6.41
F (s) 5.69
G (s) 4.86
H (s) 4.83
I (d) 4.66
J (t) 4.39
K (dd) 4.29
L (dd) 4.05
M (d) 3.97
N (m) 3.92
O (s) 3.89
P (d) 2.55
Q (t) 2.29
R (m) 1.67
1.00
1.24
5.66
15.51
1.27
1.34
3.26
0.79
1.61
1.33
1.49
1.36
0.60
1.93
0.63
3.12
3.26
5.63
13.0 12.5 12.0 11.5 11.0 10.5 10.0 9.5 9.0 8.5 8.0 7.5 7.0 6.5 6.0 5.5 5.0 4.5 4.0 3.5 3.0 2.5 2.0 1.5 1.0
f1 (ppm)
900 800 700 600 500 400 300 200 100 0

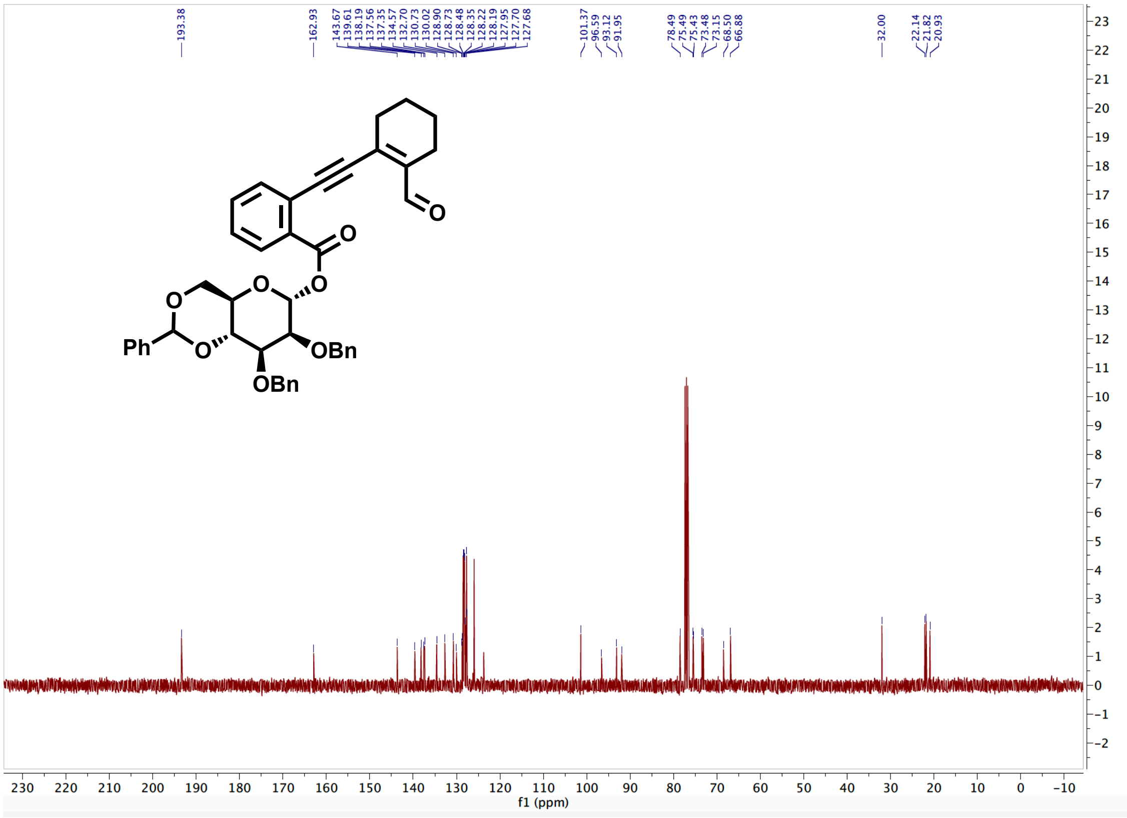
193.38
162.93
143.67
139.61
138.19
137.56
137.35
134.57
132.70
130.73
130.02
128.90
128.73
128.48
128.35
128.22
128.19
127.95
127.70
127.68
101.37
96.59
93.12
91.95
78.49
75.49
75.43
73.48
73.15
68.50
66.88
32.00
22.14
21.82
20.93
O
O
O
O
O
Ph
OBn
OBn
230 220 210 200 190 180 170 160 150 140 130 120 110 100 90 80 70 60 50 40 30 20 10 0 -10
f1 (ppm)
23 22 21 20 19 18 17 16 15 14 13 12 11 10 9 8 7 6 5 4 3 2 1 0 -1 -2

4.7 REFERENCES FOR CHAPTER 4 EXPERIMENTALS

[1] S. Boonyarattanakalin, X. Liu, M. Michieletti, B. Lepenies, P. H. Seeberger, *Journal of the American Chemical Society* **2008**, *130*, 16791-16799.

[2] H. Nagai, K. Sasaki, S. Matsumura, K. Toshima, *Carbohydrate Research* **2005**, *340*, 337-353.

[3] X. Ma, Z. Zheng, Y. Fu, X. Zhu, P. Liu, L. Zhang, *Journal of the American Chemical Society* **2021**, *143*, 11908-11913.

CHAPTER 5

Summaries, Conclusions, And Future Directions

Within this dissertation, we have illustrated the construction of spirocyclic and carbohydrate scaffolds through the utilization of metal-bound carbenoids and alkynes. Building on fundamental metal carbenoid reactivity, these research projects aimed to trap these resourceful synthons in well-designed transformations to construct spirocycles – one of the least explored natural product motifs, and glycosides –the most abundant natural product framework.

5.1 SYNTHESIS OF DIVERSE SPIROCYCLES

Spirocycles are one of the most underrepresented motifs in drug development. Our group has previously developed a synergistic Rh(II)/cationic gold catalyst combination that we were able to extend to these research efforts. To synthesize spirocycles, we initially trapped diazo-derived carbenoids in tandem sequences (*Chapter 2*). Notably, we developed methods to construct spirocyclic alkaloids and spirocarbocycles using an X–H insertion/Conia-ene cascade. We then attempted to access enantioselective alkaloids via a stepwise, copper-catalyzed approach using chiral BOX ligands. However, these conditions did not produce any sizeable enantiocontrol.

Following these studies, we theorized developing a tandem O–H insertion/aldol cascade to synthesize a variety of spiroethers. We became increasingly interested in Earth-abundant catalysis strategies based on our limited success with copper N–H insertion/Conia-ene reactions. We thought to continue our O–H insertion/aldol cascade using readily available, Earth-abundant metals. While we did not find much success with an iron-based system, we observed favorable conditions using $Zn(OTf)_2$ on spirooxindole diazos.

5.2 CARBENE-ASSISTED ACCESS TO GLYCOSIDES

Following the conclusions of our spirocyclization projects, we then set our sights towards one of the most prevalent natural product scaffolds, carbohydrates. The stereoselective glycosylation of carbohydrates remains a significant obstacle in glycoscience. With our background in Rh(II) carbenoid-initiated cyclizations, we thought to develop carbene-assisted strategies to access glycosidic bonds. To achieve this goal, we have designed and synthesized two novel glycosyl donors to address these challenges: glycal carbenes (*Chapter 3*), and carbene-mediated glycosyl donors (*Chapter*

4). Both donors are incredibly innovative and feature carbene-assisted strategies to access glycosides stereoselectively with Earth-abundant metal catalysts.

Utilizing enynones, we first synthesized and tested a novel, carbene-based glycosyl donor: *glycal carbenes*. These donors function through the vinylogous addition of nucleophiles at the anomeric position. We developed favorable conditions and can facilitate the desired transformation using zinc (II) chloride as the optimum catalyst. Unfortunately, we are not able to apply this chemistry towards di- and oligosaccharide synthesis, as bulky sugar acceptors were incompatible with our reaction conditions. Additionally, while innovative, we recognize that they require post-glycosylation transformations to cleave the pendant furan moiety.

To address these shortcomings, we began to design new carbene-based glycosyl donors. Inspired by gold-activated propargyl-embedded glycosyl donors, we designed a new variety of carbene-mediated glycosyl donors. These glycosyl donors function differently and are fundamentally distinct from other alkynyl-embedded or diazo-embedded donors and are activated with Earth-abundant metal salts. We are developing these donors to access *O*–glycosides, and hope to use these donors to access N–, and *S*– glycosides as well. Additionally, we have activated these donors using cheap, readily available copper salts.

5.3 DEVELOPMENT OF EARTH-ABUNDANT CATALYSIS AND SUSTAINABLE STRATEGIES

The initial research presented in this dissertation employed cascade strategies to rapidly access spirocycles in one pot. Additionally, our glycosylation reactions employed cascade sequences. Cascade sequences allow multiple synthetic steps to occur in one pot, thereby negating the use of excess solvents and reagents. These eloquent strategies allow for the rapid generation of structural complexity from relatively simple starting materials thus exhibiting high atom- and step-economy. Thus, using greener reaction conditions to access relevant scaffolds.

As my studies and research progressed within this dissertation, we transitioned to Earth-abundant metal catalysts (Zn/Cu/Fe) to facilitate the proposed transformations as opposed to rhodium. This prompted the development of copper-catalyzed stepwise Conia-ene reactions and iron-catalyzed insertion/aldol strategies.

Iron is one of the most abundant metals in the Earth's crust and possesses "minimal safety concern" as 1,300 ppm residual iron is deemed acceptable in drug substances. This is a distinct advantage compared to the ≤ 10 ppm allowed for most other transition metals, including rhodium and palladium. Likewise, zinc and copper are the 24th and 25th most abundant elements in the Earth's crust. Additionally, zinc and copper are dietary requirements, and most adults intake several milligrams daily. As the cost of a drug is directly proportional to the cost of reagents, employing cheaper Earth-abundant metals poses a distinct advantage over traditional metal catalysis. Therefore, Earth-abundant catalysis promises to empower an efficient, green reaction prototype while simultaneously providing potential economic benefits and safety features.

Despite our strong background in diazo chemistry, we began to consider the drawbacks of using diazos as carbene precursors. While these reagents can be commonly found in the academic lab setting, diazos are not industrially utilized due to their instability and potential explosive behavior. To circumvent these drawbacks, we turned to literature to find safer carbene surrogates. Our literature survey led to the identification of enynones as an industrially friendly carbene precursor. We believe that incorporating alternative, alkyne-based carbene precursors will significantly impact the scope of these reactions, as it can pave a pathway to industrially convenient carbene-based protocols.

5.4 FUTURE DIRECTIONS AND SCOPE OF WORK

The coalition of metal carbenoid chemistry and glycosylation is still in its infancy. Within, we have shared an account of our ongoing research and are excited at the scope and opportunities of this methodology within organic synthesis. There is much knowledge to be uncovered involving metal carbenes in glycosylations. Our ultimate aspiration for the enclosed glycosylation work is to optimize a general, highly selective carbene-mediated donor that is highly tolerant to various nucleophiles for the rapid construction of oligosaccharide libraries.

AUTOBIOGRAPHICAL STATEMENT

Education:

Ph.D., Chemistry *University of Oklahoma, Norman Oklahoma* Advisor: Prof. Indrajeet Sharma	August 2017 - present
B.Sc., Chemistry, *cum laude* *Taylor University, Upland Indiana* Advisor: Prof. Dan Hammond	May 2017

Awards and Honors:

04/2022	**3 Minute Thesis Semifinalist**: As the winner of The University of Oklahoma's 3MT, went on to participate in the regional competition for the Midwestern Association of Graduate Schools (MAGS). Advanced to semifinal round.
02/2022	**3 Minute Thesis 1st Place Winner**: Participated and received first place at the 3MT competition at The University of Oklahoma. Criteria for awards were based on presenting doctoral research in a compelling and engaging manner to a non-specialist audience in three minutes or less.
05/2021	**Jerry J. Zuckerman Scholarship Award**: Awarded to a student in the Chemistry/Biochemistry Department that has made exception advances and findings in the field of Organometallic Chemistry at the University of Oklahoma
05/2020	**Jerry J. Zuckerman Scholarship Award**: Awarded to a student in the Chemistry/Biochemistry Department that has made exception advances and findings in the field of Organometallic Chemistry at the University of Oklahoma.
10/2018	**Student Travel Grant Recipient:** Travel award granted to selected participants and presenters of NOBCChE Orlando conference.

04/2016 **Lab R.A.T Award:** Awarded to an outstanding undergraduate teaching assistant at Taylor University

01/2014 **Governor-General Youth Award Gold Awardee**: Awarded to recipients with 36 months of community service, skill, and completed five-day residential project

Peer-Reviewed Publications:

1. **Bain, A. I**.; Massaro N. P., Chinthapally K. C., "Application of Diazo-Derived Vinyl Metal Carbenes in Cascade Reactions" (Just Submitted)

2. **Bain, A. I**.; Chinthapally, K.; Hunter, A. C.; Sharma, I. "Dual Catalysis in Rhodium (II) Carbenoid Chemistry" *Eur. J. Org. Chem.* **2022**, e202101419 ***Selected as Cover Page***

3. Hunter, A. C.; Chinthapally, K.; **Bain, A. I**.; Steven, J. C.; Sharma, I. "Rh/Au Dual Catalysis in Carbene sp2-CH Functionalization/Conia-ene Cascade to the Stereoselective Synthesis of Diverse Spirocarbocycles" *Adv. Synth. Catal.* **2019**, 361, 2951 – 29.

4. Hunter, A. C.; **Bain, A.** I, Almutwalli B.; Sharma, I. "Trapping Rhodium Carbenoids with Aminoalkynes for the Synthesis of Diverse N-Heterocycles", *Tetrahedron*, **2018**, 74, 5451–5457.

Conferences and Presentations:

1. **Anae I. Bain,** Arianne C. Hunter, Indrajeet Sharma. "*Iron-catalyzed cascade annulations for the synthesis of medium-sized heterocycles*" ACS Spring 2021 Poster Presentation

2. **Anae I. Bain**, Indrajeet Sharma. "*Trapping Rhodium Carbenoids with Aminoalkynes for the Synthesis of Diverse Heterocycles*" 2018, NOBCChE, Orlando, FL.

3. **Anae I. Bain,** Patricia Stan. ***"****Exploring the Usefulness of Ruthenium-based Catalyst* $RuH_2(CO)(PPh_3)_3$ *in Reactions with Aromatic Compounds for Undergraduate Laboratories"* 2017, Butler University: URC, Indianapolis, IN.

Teaching and Leadership Experience:

01/2018-present	**Graduate Research Assistant** with Prof. Indrajeet Sharma at the University of Oklahoma
01/2018-present	**Undergraduate Mentor** with Prof. Indrajeet Sharma at the University of Oklahoma
01/2019-06/2019	**Head Teaching Assistant** for Advanced Inorganic Synthesis course with Prof. Indrajeet Sharma
01/2018-06/2019	**Graduate Teaching Assistant** at the University of Oklahoma. Courses: General Chemistry I & II, Inorganic & Organic Chemistry
08/2016-05/2017	**Undergraduate Teaching Assistant** at Taylor University. Courses: General Chemistry & Organic Chemistry
08/2016-05/2017	**President** for MESA (Multi-Ethnic Student Association); Cabinet Member previous calendar year (August 2015 - May 2016)